A single centre, parallel group pilot study to investigate the effect of opioids on immunomarkers using gene expression profiling

Mary Elizabeth Demopoulos

A thesis submitted in partial fulfilment of the requirements of the Degree of Master of Philosophy.

Queen Mary, University of London

March 2017

William Harvey Research Institute

Statement of originality

I, Mary Elizabeth Demopoulos, confirm that the research included within this thesis is my own work or that where it has been carried out in collaboration with, or supported by others, that this is duly acknowledged below and my contribution indicated. Previously published material is also acknowledged below.

I attest that I have exercised reasonable care to ensure that the work is original, and does not to the best of my knowledge break any UK law, infringe any third party's copyright or other Intellectual Property Right, or contain any confidential material.

I accept that the College has the right to use plagiarism detection software to check the electronic version of the thesis.

I confirm that this thesis has not been previously submitted for the award of a degree by this or any other university.

Signature:

Date:

Details of collaboration and publications:

Patient consent and peripheral blood samples were collected from study patients by anaesthetists at the Pain & Anaesthesia Research Centre, Barts Hospital. The isolation of CD4+, CD8+ and NK cells from peripheral blood, and the extraction of RNA from these cells was performed in collaboration with Dr T Wodehouse. Dr T Wodehouse performed the cytometric bead array and the NK cell degranulation assay.

Abstract

Background: The effects of morphine on immune cells include reduced NK cell cytotoxicity and reduced lymphocyte proliferation but human prospective *in vivo* clinical research has been inconclusive. This study aims to define the changes in intraoperative lymphocyte gene expression in patients receiving morphine.

Methods: mRNA gene expression was analysed in CD4+, CD8+ and NK cells from 40 patients undergoing gynaecological laparotomies, using the 3' Affymetrix microarray. Patients matched by BMI, age, operation duration and pain levels received morphine or control analgesia. Genes demonstrating differential expression (fold change≥±2; p-value≤0.05) following ANOVA were further investigated. Gene expression analysis was confirmed functionally through investigation of serum cytokine concentration (cytometric bead array), serum cortisol concentration (ELISA) and NK cell cytotoxicity (NK cell degranulation assay). Finally, statistical analyses were performed to evaluate the relative importance of individual genes highlighted following analysis.

Results: Microarray analysis identified differential expression of 450 unique genes by morphine at 2 hour and 460 unique genes by oxycodone at 6 hour. Genes were transiently deregulated by morphine and enriched in processes suggestive of lymphocyte anergy. Genes induced by oxycodone were subject to a more sustained deregulation and enriched in processes related to normal immune functioning. Greater increases in IL-6 and IL-10 concentrations were induced by morphine, supportive of a greater TH2 shift. NK cell degranulation results were inconclusive and should be repeated with more samples. Cortisol

concentration did not significantly change between timepoints. Statistical analyses suggested that AGPAT3, TPK1 and TIAM1 might be important in mediating morphine-induced changes.

Conclusion: This study demonstrates altered lymphocyte gene expression in patients receiving intraoperative morphine compared to control analgesia. The greater morphine-induced TH2 shift suggested by gene expression analysis was confirmed functionally, consistent with and extending current knowledge of morphine-induced immunosuppression.

Copyright

Dedication

To Mike, Jimmy and Ismene

You no longer have to hug yourselves, as I think I have finished.

Acknowledgements

The completion of this thesis would not have been possible without the help of a number of people.

Richard Langford conceptualised and designed the study and arranged the funding from Mundipharma. His clinical and academic expertise and experience were pivotal to completion of the project.

John Gribben gave advice relating to the design of the microarray experiments.

Theresa Wodehouse designed the study, arranged regulatory approvals and contributed her invaluable technical expertise and experience as well as giving advice to finalise the thesis.

Rob Petty gave excellent advice throughout relating to microarray experimental design and analysis. His help was invaluable to completion of writing up the thesis. Farideh Miraki-Moud gave technical advice, support and encouragement throughout the project for all assays. Tracy Chapman gave help and advice with microarray experimental design. Ed Wilkes gave excellent advice regarding microarray experimental analysis and helped me with basic statistics.

Finally, the project could not have been completed without the anaesthetists who successfully recruited patients to the study and took blood samples, and the patients who provided their blood.

Table of Contents

List of Figures

List of Tables

Abbreviations

µg	micrograms
µl	microlitre
◦c	degrees centigrade
AUC	area under the curve
Ca^{2+}	calcium
CD	cluster of differentiation
cDNA	complementary deoxyribonucleic acid
DMSO	dimethyl sulfoxide
DNA	deoxyribonucleic acid
EDTA	ethylenediaminetetraacetic acid
ELISA	enzyme-linked immunosorbant assay
FACS	flow assisted cell separation
FCS	foetal calf serum
FDR	false discovery rate
GAPDH	glyceraldehyde 3-phosphate dehydrogenase
HBV	hepatitis B virus
HLA	human leukocyte antigen
HPA	hypothalamic-pituitary-adrenal

IFN-γ	interferon-gamma
Ig	immunoglobulin
IL	interleukin
iv	intravenous
IVT	in vitro transcription
LPS	lipopolysaccaride
MAPK	mitogen activated kinase
M-CSF	macrophage colony-stimulating factor
MHC	major histocompatibility complex
MICB	MHC class I polypeptide-related sequence B
ml	millilitre
MMP9	matrix metallopeptidase 9
mRNA	messenger ribonucleic acid
NFκB	nuclear factor kappa-light-chain-enhancer of activated B cells
NK	natural killer cell
OD	optical density
ORF	open reading frame
PBMC	peripheral blood mononuclear cell
PBS	phosphate buffered saline

PCR	polymerase chain reaction
PE	phycoerythrin
qRT-PCR	quantitative reverse transcription polymerase chain reaction
RIN	RNA integrity number
RNA	ribonucleic acid
RNase	ribonuclease
ROC	receiver operating characteristic
RPM	revolutions per minute
RPMI	Roswell Park Memorial Institute medium
RT	room temperature
RT	reverse transcriptase
SD	standard deviation
SEM	standard error of the mean
SNP	single nucleotide polymorphism
SPSS	Statistical Package for the Social Sciences
Th1	T helper 1 cell
Th17	T helper 17 cell
Th2	T helper 2 cell
TLR	Toll like receptor

TNFα	Tumour necrosis factor alpha
TNFβ	Tumour necrosis factor beta
TURP	Transurethral resection of the prostate
UTR	un-translated region
Wnt	wingless-type MMTV integration site family

Chapter 1
Introduction

1.1 Morphine

1.1.1 Historical use

Opium and the poppy *Papaver somniferum* have been used for thousands of years, for pain relief and 'to bring forgetfulness of every sorrow'. Opium is found in the dried latex of *Papaver somniferum* [1] and its use predates written history; poppy images were found on Sumerian artefacts in modern-day Iraq, dating from 4000BC. Helen, daughter of Zeus, 'cast a drug into the wine of which they drank to lull all pain and anger and bring forgetfulness of every sorrow' in Homer's Odyssey, written around 1000BC; the drug is now thought to be morphine [2]. In the 17th century Thomas Sydenham recommended laudanum, a concoction of opium and sherry, for pain, sleeplessness and diarrhoea. In 1806 the chemist Friedrich Sertürner isolated the active ingredient from opium [3], naming it morphine after Morpheus, god of dreams.

The Opium wars of 1830-1860 were precipitated by the importing of opium to China [4]. In 1852, the modern hypodermic needle and syringe was developed [5], allowing administration of subcutaneous and subsequently intravenous morphine; initially, the benefits of intravenous administration were not appreciated [6].

In 1897, the first evidence to suggest that morphine might be immunosuppressive was published by Coronedi et al, showing that high doses of morphine made dogs unusually susceptible to *Diplococcus lanceolatus* [7]. This was followed shortly after by evidence of altered phagocytosis and

leukocyte trafficking in guinea pigs given morphine, published by Cantacuzene [8, 9]. Within the next decade, clinicians saw links between recreational use of morphine and increased infection rates in humans [9-11], although this was commonly attributed to associated co-morbidities and lifestyle. Further recent research (Section 1.6) has demonstrated conclusively that morphine does indeed suppress the immune system, but the mechanisms, magnitude and clinical relevance are not yet fully described.

Due to the prevalent use of morphine in clinical medicine, it is vital to elicit the mechanisms of immunosuppression to enable its modification or replacement with an alternative, if deemed clinically necessary.

1.1.2 Structure

The structure of morphine was discovered in 1902. It has a modified phenanthrene (three linked benzene rings) structure, of two planar rings and two aliphatic (or non-benzene) rings at right angles to the rest of the molecule [1]. Substitution of either the free hydroxyl on the benzene ring at position C3 or C6 produces other pharmacologically active compounds, for example, diamorphine and oxycodone.

The structure of morphine

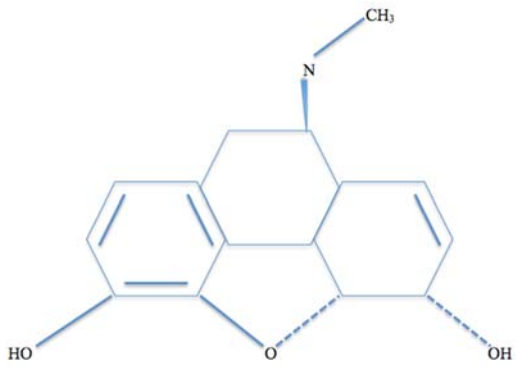

Figure 1.1: the structure of morphine [1]

1.1.3 Pharmacokinetics

Morphine is not very soluble in water so is normally administered as a salt. In this study, morphine sulphate was given intravenously. It has a half-life of 3-4 hours and is converted by UGT2B7 in the liver to 2 metabolites, morphine-3- and morphine-6-glucuronide (M3G and M6G), by a conjugation of glucuronide to the C3 or C6 -OH group position [1]. M6G is an active metabolite that has higher analgesic abilities than morphine, and may be involved in immune suppression [12]. The glucuronides are excreted in urine.

1.1.4 Opioid receptors

Morphine is a ligand for opioid receptors, of which there are four subtypes. Each is named after its first discovered ligand; hence morphine gave its name to the μ opioid peptide receptor (MOR), ketocyclazocine to κ receptor (KOR), mouse *vas deferens* to δ receptor (DOR) and nociceptin to NOR (56). Although other molecules have been postulated as opioid receptors, they have been discounted as they are not blocked by naloxone [13], a pure opioid antagonist.

Opioid receptors were identified over 30 years ago [14-16], then later studies provided the evidence needed to group opioid receptors into at least three types [17]. In any case, it had long been suspected that there were multiple receptor subtypes based on *in vivo* observations that opioids produce a wide range of effects including analgesia, pupillary constriction, respiratory depression and constipation. Morphine binds to all three opioid receptors, with the highest affinity for MOR.

1.1.5 Pharmacodynamics

Morphine is a partial agonist for MOR and also acts on KOR and DOR. It probably produces analgesia via activation of opioid receptors in the CNS: morphine injection into specific brain nuclei produces analgesia. Supraspinal analgesia may involve endogenous opioid peptide release and, at the spinal level, 5-HT release from descending inhibitory fibres may be involved in analgesia as physical disruption of fibres reduces analgesia [1]. Morphine acts both presynaptically, to inhibit neurotransmitter release from primary afferent fibres, and post-synaptically to reduce excitability.

1.2 Structure and function of opioid receptors

The opioid receptors are G protein-coupled receptors (GPCRs): a single polypeptide chain with seven transmembrane α-helices, an intracellular C-terminal domain and an extracellular N-terminal domain that induces intracellular signalling via a G-protein. All opioid receptors are rhodopsin GPCRs, meaning they have a shorter extracellular tail and ligand binds either on this tail or a transmembrane domain. The G protein (subunits α, β, γ and GDP molecule) is attached to the cell membrane and interacts with the guanine nucleotides GDP and GTP [1]. Ligand binding induces a

conformational change in the intracellular domain, giving it high affinity for the αβγ complex. The complex and domain associate and αβγ exchanges GDP for GTP then cleaves into α-GTP and βγ. These activated forms of G protein induce intracellular signalling, ending when GTP is hydrolysed to GDP by the GTPase activity of α subunit [1].

Functional selectivity describes the ability of a ligand to induce a unique combination of intracellular responses most likely through conformational changes in the receptor [18]. In mice, morphine and M6G but not oxycodone induced analgesia that was blocked by a JNK inhibitor, suggesting that opioid analgesic tolerance is induced via a JNK-dependent pathway in morphine and M6G but not oxycodone [19]. Morphine and fentanyl were shown to cause MOR desensitization via 2 different methods, activating JNK either without the need for arrestin, or arrestin-dependently, respectively [20]. It is possible that the immunosuppression induced by morphine but not by oxycodone is reflective of a difference in the intracellular conformation change induced by the ligand.

1.3 Receptor location

There are several variants of MOR which exist both pre- and post-synaptically in the CNS (periaqueductal gray, dorsal horn of the spinal cord, olfactory bulb, nucleus accumbens, cerebral cortex and the amygdala) and in peripheral nerves as part of the ascending pain pathway. It is also found in the gastrointestinal tract, where it causes constipation upon activation. Most importantly to this study, MOR has also been found in immune cells, including T cells, B cells and macrophages [21] [22].

DOR receptors are found in the CNS (pontine nuclei, amygdala, olfactory bulb, deep cortex) and peripherally in sensory neurons. Activation of DOR produces some analgesia, possibly bradypnea and has antidepressant effects.

KOR receptors are found in the CNS (hypothalamus, periaqueductal gray and claustrum), in the substantia gelatinosa in the spinal cord, and peripherally in sensory neurons. Activation causes analgesia, sedation, dysphoria, anticonvulsant and antidepressant effects, dissociative effects, miosis and diuresis.

NOR receptors are found in the cortex, amygdala, hippocampas, septal nuclei, habenula, hypothalamus and spinal cord. Activation results in anxiety, depression and increased appetite. It can also be involved in the development of tolerance to MOR agonists.

1.4 The mechanism of action of morphine

Morphine primarily binds to MOR, causing analgesia, euphoria, sedation, pruritis, bradypnea, nausea, miosis and decreased gut motility [1]. It activates KOR (analgesia, convulsions) and DOR (spinal analgesia, sedation, dysphoria, hallucinations) with a lower affinity.

Following ligand binding, the activated G-protein opens membrane K^+ channels while keeping voltage-gated Ca^{2+} channels closed [1]. The decreased intracellular K^+ causes hyperpolarization and an inability to produce action potentials, reducing neuronal excitability. The decreased intracellular Ca^{2+} also reduces neurotransmitter release [1]. However, MOR activation does increase some neuronal activity, via disinhibiting inhibitory neurons, for example sensory nerve terminals in the periphery.

Activated opioid receptors inhibit adenylyl cyclase and activate MAPK, which phosphorylates serine, threonine and tyrosine, thus directing the cellular response to diverse stimuli – not only mitogens but also osmotic stress and proinflammatory cytokines – via gene expression, proliferation, mitosis and apoptosis.

The varying effects of different opioids are related to the anatomical location of their activated receptors, the variation in their affinity for different receptor sub-types and possibly ligand-directed binding. Morphine predominantly activates MOR in areas related to analgesia: the PAG, RVM and nucleus accumbens in the CNS and the dorsal horn in the spinal cord. The PAG receives input from regions including the cortex; it is the main path that cortical and other information passes through to control the dorsal horn's nociceptive gate [1]. PAG neurones project to the RVM then the dorsal horn as the descending inhibitory pathway; activation of MOR in the PAG both inhibits transmission in the dorsal horn and inhibits discharge of spinothalamic neurones, via pre-synaptic inhibition of 5-HT, enkephalin and GABA [1].

In the nucleus accumbens, activation of MOR increases dopamine release, producing analgesia via the mesolimbic system. Activation of MOR in immune cells is likely to be a factor in morphine-induced immunosuppression, although it is likely that this also happens via a central route [23].

1.5 Immune system

The human innate system responds rapidly to pathogens and involves nonspecific antimicrobial pathways that do not require pathogen pre-exposure [24]. It is also used in the adaptive response. The adaptive system is activated by a particular pathogen and is centred around lymphocytes.

Cells of the immune system

Table 1.1: cells and humoural components of the innate v the adaptive immune systems

	Cells	Other
Innate	Monocytes	Complement
	Neutrophils	Lysozyme
	Basophils	Acute phase proteins
	Macrophages	Cytokines
	Eosinophils	Interferons
	Mast cells	
	NK cells	
Adaptive	B cells	Antibody
	T cells	Cytokines

1.5.1 Innate immune system

The innate immune system consists of three parts: barriers, cells, and serum proteins and the complement system. Barriers are physical or chemical and include tight junctions between epithelial cells and sweat and sebaceous secretions on the skin producing a barrier and a hostile environment [24]. Mucus in gastrointestinal, respiratory and genitourinary tracts traps pathogens while cilia and the cough reflex expel them.

Cells of the innate immune system include monocytes / macrophages, neutrophils, eosinophils, basophils and NK cells. Monocytes are the largest circulating blood cell and differentiate to become macrophages, living for years. They express toll-like receptors (TLRs) whose activation results in

transcription factor phosphorylation and cytokine production, as well as downstream kinase activation. Cytokine production subsequently activates B and T cells of the adaptive immune system (Section 1.5.3). Macrophages also activate the adaptive immune system via antigen fragments on their cell surface.

Natural killer (NK) cells make up 5-10% of circulating lymphocytes and use cell surface receptors to identify and kill tumour cells and cells infected with intracellular pathogens, particularly viruses.

Acute phase proteins (APPs) increase rapidly when the innate immune system is activated. They include lectins which themselves activate complement. Cells produce interferon (IFN) proteins when infected with a virus – IFNα and IFNβ protect nearby cells by inducing expression of genes encoding proteins to attack viral DNA. IFN-γ is produced by activated NK cells and activates additional NK cells and macrophages. The complement system consists of over 20 serum glycoproteins that circulate as pro-enzymes and recruit inflammatory cells to inflammation sites. Activation triggers a cascade resulting in cell lysis, inflammation, opsonization and finally clearance of immune complexes.

1.5.2 Adaptive immune system

Lymphoid cells originate in the bone marrow, where they differentiate into B and NK cells or travel to the thymus to become T cells. The three cell types can be distinguished by receptors and receptor ligands on their cell surfaces. B cells express a B cell receptor (BCR) whereas T cells express a T cell receptor (TCR).

Cell surface ligands of B, T and NK cells

Table 1.2: Typical identifying markers found on lymphocytes. (CD = cluster designation, a membrane-bound molecule)

B cells	T cells	NK cells
B cell receptor	T cell receptor	CD-2
CD-19	CD-2	CD-7
CD-20	CD-3	CD-16
CD-32	CD-4	CD-25
CD-40	CD-8	CD-56
HLA-DR	CD-7	CD-57
	CD-28	

1.5.3 T cells

T cells are characterized by their receptors (TCRs) and their cellular function. TCRs are structurally similar to BCRs as they are made from 110 amino acid domains (α, β, γ and δ) folded seven or eight times with Ig folds. TCRs normally consist of a αβ subunit (95% of T cells) and rarely a γδ subunit, usually found on mucosal surfaces where they recognize antigen without the help of antigen-presenting cells (Section 1.5.3.2).

However, normally TCRs cannot recognize antigen alone, only when presented by Major Histocompatibility Complex (MHC) on Antigen Presenting Cells (APCs). CD3, associated with the TCR, transduces the signal intracellularly. MHC is a general term; in humans the specific antigen is known as Human Leukocyte Antigen (HLA) and is involved in antigen peptide binding, processing and presentation. HLA molecules are present on antigen processing cells (APCs), which include macrophages, B cells and Langerhans cells. The cell processes the antigen then trafficks peptide fragments to MHC molecules on the cell surface. MHCII presents peptide fragments to CD4, and MHCI to CD8: CD4+ T cells respond to MHCII-linked peptide and CD8+ T cells respond to MHCI-linked peptide. T cells are subdivided into several types

include T helper (CD4+), T killer (CD8+), T regulatory (TReg), T memory and Natural Killer T cells.

1.5.3.1 T helper

T helper cells are identified by the presence of a CD4 molecule on their cell surface and activate B cells, cytotoxic T cells and macrophages.

T helper cells are subdivided into T helper 1 (TH1) or T helper 2 (TH2) and T helper 17 (TH17). These subtypes are mutually antagonistic [24] as they each produce cytokines which regulate the opposing population downstream. TH17 cells, which are pro-inflammatory and produce TH17, are mutually antagonistic with TReg cells [25].

TH1 cells produce IL-2, IL-3, IL-10, IFN-γ, TNF, lymphotoxin and GM-CSF and are involved in inflammatory processes and macrophage activation. TH2 cells secrete IL-3, IL-4, IL-5, IL-6, IL-10 and IL-13, TNF and GM-CSF and are involved in synthesis of antibody by B cells. The TH1 response is therefore deemed to be pro-inflammatory, and the TH2 response anti-inflammatory: TH1 response supports a cell-mediated immune response, and TH2 antibody-mediated. Because T helper cells are important in immune functioning and influence cytokine profiles, we looked at gene deregulation in these cells.

1.5.3.2 Cytotoxic T cells

Cytotoxic T cells usually express CD8 on their cell surface and are known as CD8+ cells. They are involved in the killing of virally infected cells and, in their precursor state, can recognize antigen fragments associated with MHCI on APCs. CD8+ cells normally also require a TH cell to kill infected cells; both TH and CD8+ cell will bind to an APC, TH via MHCII and CD8+ via MHCI. IL-2 and IL-6 are then released by TH and stimulate the CD8+ precursor to

differentiate into an antigen-experienced effector CD8+ cell. Once activated, the CD8+ cell delivers cytoxic granules containing perforin and granzymes onto the target cell (APC) at the point of contact between the 2 cells, ensuring killing is specific. Death occurs via induction of apoptosis and also through activation of a nuclease which produces DNA breaks. A second, minor, killing pathway exists via Fas ligand on CD8+ and its receptor on the target cell. Binding of Fas ligand initiates activation of caspase-8 which propagates the death signal [24]. CD8+ cells are subdivided into those that secrete IFNγ and those that secrete IL-4. We also investigated gene deregulation in CD8+ T cells due to their importance in immune functioning.

1.5.4 Antibody-mediated immune response

IL-1, produced by activated macrophages, consists of IL-1α and IL-1β and is a pro-inflammatory cytokine involved in cell proliferation and differentiation. It induces COX2, which is involved in inflammatory pain hypersensitivity. IL-10 is an anti-inflammatory cytokine secreted by cells including monocytes and TH2 cells whose receptor consists of two IL-10R1 and two IL-10R2 subunits [26]. Ligand binding phosphorylates the cytoplasmic tails of the receptor to induce STAT3 signalling, which activates transcription and increases induced TReg differentiation [27].

IL-6 is a pro-inflammatory cytokine, produced by many cell types including T and B cells. As it is rapidly cleared from plasma, its regulation is at the expression level and it is modulated via transcription factors including NF-κB. It induces production of APPs and facilitates neutrophil trafficking to initiate and maintain inflammation [28].

1.5.5 Natural Killer cells

Natural Killer (NK) cells differentiate in the bone marrow and are large granular leukocytes instrumental in death of virus-infected cells via their Killer Activating Receptor (KAR). This receptor is activated by a high molecular weight glycoprotein on the infected cell causing granule movement towards it; granule contents are released into the extracellular space, inducing apoptosis. The Fas-Fas ligand complex can also induce apoptosis via the Fas receptor on the target cell as a minor killing strategy. NK cells also express a Killer Inhibitory Receptor (KIR), which recognizes MHCI (not normally present in virally-infected or tumour cells) and is dominant over KAR, thus avoiding autoimmunity. Tumour cells expressing low or no MHCI are especially susceptible to NK cell killing. NK cells also kill tumour cells via their Fc receptor, which is a receptor for IgG and activated by IL-2 or IFN-γ.

NK cell cytotoxicity (NKCC), or the ability of NK cells to induce apoptosis in target cells, was measured indirectly in this study using NK cell degranulation. This assay uses flow cytometry to measure NK cell surface CD107a, normally found intracellularly in cytolytic granule membranes.

The ability of NK cells to remove tumour cells and the demonstrated reduction in NKCC following morphine administration [29-31] suggests that NK cells should be investigated in this experiment. Reduced NKCC is particularly relevant in the period following surgical resection when tumour cells and their fragments may disseminate in the blood.

1.6 The immunomodulatory effects of morphine

In 1897, the first definitive literature on morphine-associated immune changes was published [7], but despite the wealth of publications since then, the mechanisms remain unconfirmed. Morphine abuse has been linked to immunosuppression and increased infection rates [32], and clinical use to an increase in infection rates in humans [33], immunosuppression [34, 35], and cancer metastases, although some reports have been contradictory [36, 37]. However, it is an important analgesic and recommended on the WHO analgesic ladder as a first-line step three analgesic [38] [39].

As well as observational data, prospective animal and *in vitro* research has confirmed the link between morphine and immune suppression [40], indicating possible mechanisms including NKCC suppression [31, 41]. The influence of the surgery-related stress pathway involving the hypothalamus-pituitary-adrenal (HPA) axis may be important [42, 43]. Prospective human *in vivo* research has been varied and immunosuppression is not always found, possibly due to the presence of confounding factors such as pain, surgical trauma and anaesthesia, which also produce immunosuppression. Non-operative administration of morphine has the advantage of fewer confounding factors but tends to be chronic; tolerance may develop to the immunosuppressive as well as analgesic effects [44].

Nevertheless, despite the equivocal results in some human studies, it is now generally accepted that morphine can suppress immune function.

1.6.1 Opioid structure and immunosuppression

As well as morphine, other opioids are thought to suppress the immune system. Opioids with hydroxyl (-OH) groups at C3 and C6 positions (nalorphine) may be the most immunosuppressive, modification at C3 (codeine) produces some loss of immunosuppression while further C6 modification by substitution with a carbonyl group (oxycodone) may remove immunosuppressive qualities [31]. Following opioid administration in mice, morphine induced a decrease in splenocyte proliferation, IL-2 production and NKCC; codeine induced only a slight decrease in NKCC and IL-2 production; and hydromorphone (a MOR agonist) and oxycodone showed no change. Nalorphine, a mild analgesic, induced a decrease in all parameters, while naloxone and naltrexone both increased proliferation and IL-2 production. The immunosuppressive and analgesic effects do not appear to be correlated [31].

1.6.2 Morphine-linked immunosuppression in humans

PHA is a mitogen that induces calcium mobilisation and proliferation in T cells [45-47]. Patients given morphine post-surgically showed a prolonged suppression of PHA-stimulated proliferation compared to those given tramadol. The tramadol group also showed increased NKCC but there was no change in the morphine group [48]. A healthy volunteer crossover study with fentanyl, buprenorphine, tramadol or morphine showed different intracellular phosphorylation patterns for fentanyl and morphine. Early activation of 55-60 kDa membrane-associated signalling proteins was seen with these analgesics but not seen with buprenorphine or tramadol [49]. Exposure of a separate group of healthy volunteers to continuous morphine for 36 hours

produced suppression of NKCC at 2 hours that lasted until twenty-four hours [29], although no control data was available. In patients undergoing abdominal surgery, the pre-anaesthetic induction addition of noradrenaline to morphine prolonged the NKCC suppression until postoperative day 7, compared to a day 2 recovery in those given morphine alone [50, 51], suggesting a role for the HPA axis.

1.6.3 Tolerance to morphine induced immunosuppression

Tolerance develops to some variables of immune suppression; rats receiving long-term oral saline followed by subcutaneous morphine showed a greater NKCC suppression compared to the long-term oral high dose morphine followed by subcutaneous morphine [41]. However, no tolerance developed to mitogen-stimulated T or B cell proliferation or splenic T cell IFNγ production, suggesting the presence of several morphine-induced immunomodulatory mechanisms [41]. Murine macrophages exposed to *C albicans* in vitro, together with a MOR / DOR / KOR agonist, showed a suppressed dose-dependent capacity to ingest and phagocytose, blocked by the relevant antagonist [52]. PMN cells from Rhesus macaques subjected to repeated increasing morphine doses, showed a maintained ingesting ability but suppressed killing ability, after exposure to yeast blastospores [53]. Morphine suppresses phagocytic function, measured as cell count and index and microbial killing properties, in bone marrow phagocytes of mice exposed to infection; chronic administration increased LD50 almost 2-fold [44]. Higher doses of morphine or nalorphine reduced con-A-stimulated lymphocyte proliferation, NKCC and T cell IL-2 production in mice; the opioid antagonists naloxone and naltrexone had the opposite effects [31].

In advanced cancer patients, those already taking morphine upon study entry showed a possible tolerance to the immunomodulatory effects of morphine. For these patients, no correlation was found between plasma M6G concentrations and PHA-stimulated lymphocyte proliferation or plasma immunoglobulin. However, in those patients not already taking morphine, a negative correlation was found [12]. Conversely, heroin (diacetylmorphine) abusers randomized to either methadone (an acyclic analogue of morphine) or buprenorphine showed an overlapping raised cytokine profile, suggesting that both drugs stimulated the previously suppressed immune system [54] or that they preserve immune function. Rodents showed greater bacterial growth and bacteraemia when given more morphine doses as opposed to fewer [55], suggesting that several mechanisms may be relevant to immunosuppression caused by chronic morphine administration.

In summary, morphine-induced immunosuppression is probably mediated in part via MOR and involves a shift towards a TH2 cytokine profile and cytokine-mediated immunity, thus including suppression of NKCC and decreased phagocytic activity.

1.6.4 Morphine and microglia

Macaques acclimatized to morphine and then exposed to Simian Immunodeficiency Virus (SIV) showed a higher plasma and CSF viral load with increased CNS virus build, compared to saline and SIV animals [56]. Previous work showed that SIV uses the chemokine receptor CCR5 (found on T cells and macrophages), for entry into macrophages. CCR5 was up-regulated by morphine in murine microglia [56], suggesting a possible mechanism for increased SIV viral load in morphine-exposed macaques.

Mice given morphine +/- naltrexone and then infected with bacteria had a higher organ bacterial load and mortality rate than those in the naltrexone only or placebo groups; they also had higher levels of pro-inflammatory cytokines but lower levels of IL-17a. However, a sub-study of IL-17a knock-out mice did not show an increased susceptibility to bacterial infection. [40]. Finally, bovine microglia exposed to morphine then infected with *M bovis* bacteria had a reduced capacity to induce γδ T cell proliferation, compared to the control group [57], suggesting a change in the functioning of microglia may be important.

1.6.5 Immune cell opioid receptors

In 1979 Wybran et al showed the existence of immune cell opioid receptors in humans, following incubation of human PBMCs with morphine [58]. Rosetting, the method used to show receptor existence, has largely been replaced by modern tests, and describes the arrangement of erythrocytes around a central cell, often a lymphocyte, to identify a cell surface receptor. Morphine-treated PBMCs showed reduced rosetting with sheep erythrocytes compared to non-morphine controls, suggesting that morphine modulated a cell surface receptor (now known to be CD2). As rosetting was blocked by pre-incubation with naloxone, a MOR antagonist, it is likely that the changes were mediated via MOR. Unexpectedly, incubation with the endogenous MOR and DOR opioid agonist met-enk showed the opposite effect and increased rosetting [59].

1.6.6 Opioid receptor knockout

Triple opioid receptor knockout (KO) mice showed a differing cytokine profile to wild-type mice [60]. With decreased IL-2 and IFNγ levels, but increased

IL-4 and IL-10 levels, KO mice had a profile more aligned to TH2 than TH1 cytokines compared to wild-type mice. This suggests that KO mice are immune suppressed and that opioid receptors are important in immune modulation. In humans, postoperative (and therefore immune suppressed) patients show a TH2 rather than TH1 profile [61, 62], suggesting that non-suppressed humans may favour a TH1 profile over TH2. These results suggest that modulation of the cytokine profile is an important part of morphine-induced immunomodulation.

1.6.7 Cytokines

IL-4 induces opioid receptor expression in T cells *in vitro* [63]; anti-CD3 and anti-CD28 antibodies induce IL-2 production via activation of the TCR. Healthy human PBMCs and cells from the JURKAT line (an immortal T cell line whose cells produce IL-2) were incubated with IL-4 then anti-CD3 and anti-CD28 antibodies. Those cells exposed to morphine and the MOR and DOR endogenous agonist beta-endorphin showed reduced IL-2 mRNA production [56] compared to controls. This effect was blocked by MOR but not DOR antagonists, confirming the importance of MOR in IL-2 production [64].

Morphine given for post-incisional pain in mice reduced TNFα, G-CSF and KC levels (normally increased post-incision) and reduced wound neutrophil infiltration [65]. These two effects had different mechanisms as mice in the lowest morphine group showed a huge drop in cytokine levels but no concurrent effect on neutrophil numbers [65].

1.7 Intraoperative confounding factors

Acute administration of morphine differs to chronic administration in its immunomodulatory effects. The predominantly post-surgical nature of acute

clinical morphine use involves more confounding factors, which may also influence the immune response post-surgically.

1.7.1 Anaesthesia

Although anaesthetic agents are known to modulate the immune system, this is difficult to quantify in clinical research due to the difficulties of separating analgesic from anaesthetic effects.

For example, the large scale MASTER study in Australasia found no advantage of epidural anaesthesia / analgesia over general anaesthesia (GA) and opioid-induced analgesia, using clinical outcomes as an endpoint, even with analyses of subgroups [37, 66, 67]. However, the epidural group received pethidine and the anaesthetic fentanyl (only 5.6% of patients had a pure epidural infusion) and the opioid group received morphine, pethidine and fentanyl. Fentanyl has been shown to induce NKCC suppression (see below; [68]), possibly preventing the observation of any advantages of epidural administration or disadvantages of morphine administration.

Other studies have delivered a non-opioid group versus a GA + opioid group, but any immunosuppressive effects attributed to the opioid could equally be due to the GA. Patients undergoing breast tumour resection and receiving a levobupivacaine paravertebral block showed a different cytokine profile to those given sevoflurane and morphine PCA [69, 70]. The levobupivacaine group showed lower IL-1β, MMP3, MMP9 and IL-10 levels, indicating a possible protective effect of levobupivacaine compared to GA + morphine in terms of tumour progression [69]. Lower IL-1β can reduce tumour growth in vitro [71] while higher levels of MMPs and IL-10 are associated with tumour expression and metastasis [72-74]. However, it is not known if

levobupivacaine, sevoflurane or morphine caused the difference between groups.

Retrospectively, levobupivacaine given as a paravertebral block alongside GA during mastectomy was shown to have a possible immune-sparing effect, conferring a 94% recurrence free survival at 3 years compared to 77% in the GA only group [75]. This may be due to a reduced need for morphine and GA, a direct effect of the levobupivacaine, or due to reduced pain, as the paravertebral group also had a lower median pain score.

High dose fentanyl caused prolonged NKCC suppression when compared to low dose fentanyl, following abdominal surgery for both malignant and benign indications. This was reversed by IL-2 and partially reversed by IFN-α/β [68], suggesting cells could be re-activated [76]. Rats given ketamine, thiopental or halothane all showed reduced NKCC and increased tumour cell retention and lung metastases, whereas propofol did not produce these effects. Ketamine was associated with the greatest increase in metastases, a finding the authors attributed to its relative NKCC suppressive effects [77]. Patients undergoing spinal (bupivacaine) anaesthesia during TURP (transurethral resection of the prostate) showed a shift to a TH1 profile while total TH cell numbers remained constant, compared to the GA group (propofol + morphine / fentanyl) group [62]. As propofol has not been shown to reduce cell-mediated immunity, the TH1 shift is most likely to due the lack of opioid. TH1 cytokines are involved in cell-mediated immunity and protective against tumour spread and viral infections [62], advantageous in the post-surgical period, when tumour fragments may have disseminated in the circulation.

1.7.2 Surgery & trauma (the neuroendocrine stress response)

The trauma of surgery has immunosuppressive effects via the hypothalamic – pituitary – adrenal (HPA) axis. Cytokines released at the incision site (IFN-γ, TNF, IL-1, -2, -6, β-endorphin) act on the hypothalamus to stimulate corticotropin-releasing hormone and arginine vasopressin release. These then stimulate adrenocorticotropic hormone (ACTH) and glucocorticoid release from the pituitary and adrenal glands respectively. Cytokines also act directly on the pituitary and adrenal gland [61]. Increased levels of glucocorticoids can shift cells to a TH2 profile, seen as a change in cytokine release from stimulated PBMCs [78, 79].

Laparascopic surgery is advantageous over open surgery. Patients undergoing laparoscopic cholecystectomy showed a 2 hour reduction in IL-4 secretion from PHA-stimulated PBMCs and fewer circulating CD23+ B cells (up-regulated by IL-4 *in vivo*), when compared to their age-, sex- and BMI-matched open surgery cohort [61]. This indicates that the surgery-induced immunosuppressive effect is influenced by incision size [61] and may involve a TH2 shift. Cholecystectomy patients given perioperative ibuprofen showed smaller and more transient changes in plasma ACTH, cortisol and glucose compared to the placebo group [80], indicating both a therapeutic use for ibuprofen in surgery and the importance of the neuroendocrine stress response.

However, it may not be a key factor in surgical immunosuppression; rats given experimental surgery showed increased plasma corticosterone, reduced by morphine treatment; the same rats showed a greater lung tumour cell retention in the non-surgical morphine group compared to the surgical

morphine group, concurrently with a 50% drop in corticosterone [81]. It is possible that morphine-induced suppressed NKCC rather than the HPA axis caused tumour cell retention.

1.7.3 Suppression of NK cell cytotoxicity post-surgery

NKCC suppression is seen postoperatively in patients undergoing solid tumour resection [82] and in non-cancer patients undergoing surgery; non-cancer patients also showed suppressed postoperative NKCC following IFNα cell stimulation [83]. It is not always clear if surgery, anaesthesia, analgesia or a combination of factors resulted in reduced NKCC.

1.7.4 Hypothermia

Maintenance of body temperature is important intraoperatively, as general anaesthetics reduce core temperature [84], which can affect drug metabolism: serum morphine levels were elevated in neonatal patients undergoing experimental hypothermia for hypoxic ischaemic encephalopathy compared to the normothermic group [85]. Hypothermia in rats suppresses NKCC and promotes metastases following injection of lung tumour cells; total NK cell numbers were unchanged and the suppressive effects were probably initiated *in vivo*, as NK cells from both groups were cooled and maintained at 23°C prior to functional assay [86].

1.7.5 Pain

Pain has an immunosuppressive effect, but it may be outweighed by that of morphine; rats given intraperitoneal ketamine or morphine following soft tissue injury showed an increased 48 hour mortality rate and reduced LPS-

induced TNF response, compared to the saline group [87]. Conversely, anaesthetised rats undergoing surgery with morphine analgesia showed less NKCC suppression compared to saline surgical controls [88]. Following tumour cell injection, operated animals showed increased tumour cell retention compared to non-surgical controls, attenuated by morphine and suggesting that pain not morphine may be more immunosuppressive. The same group showed an increase in metastases in surgical compared to non-surgical rats following tumour cell injection, possibly a result of suppressed NKCC. This was prevented by morphine, but non-surgical controls were unaffected, suggesting that poorly controlled pain contributes to the spread of metastases [89]. Pre- and postoperative morphine reduced surgery-induced increases in lung metastatic colonization [89, 90] and lung retention of tumour cells [81, 88]. The greatest reduction occurred in the pre-operative morphine only group, although its analgesic duration was the shortest [81].

Indomethacin is a COX inhibitor and therefore prevents conversion of arachidonic acid to prostaglandins by cyclooxygenase (COX); prostaglandins have a role in peripheral and central sensitization. Rats given indomethacin intraoperatively and tumour cells injection post surgery showed a reduction in tumour cell retention compared to placebo, an effect not found seen in the anaesthetized non-surgery group. NKCC was reduced by surgery and increased by indomethacin administration in a sex-dependent way; in females indomethacin prevented surgery-induced suppression of NKCC [91] whereas in males it increased NKCC in both operated and non-operated animals. These results suggest that the pain experienced by rats was important in suppressing NKCC [91].

1.8 Experimental design

1.8.1 Pain model

To attempt to reduce confounding variables, we chose a homogenous surgical group; female patients undergoing open non-cancer gynaecological surgery with a Pfannenstiel incision. Non-cancer surgery was chosen to prevent an influence of cancer-related immune changes. These patients tended to have myomectomies, and therefore a similar level of surgical trauma and surgery duration. Precise surgery was not specified so that recruitment was possible within the required timeframe. A Pfannenstiel incision induces sufficient pain to warrant the use of strong opioid (laparoscopic surgery is unlikely to justify morphine) and also tends to be a uniform length of approximately 8-12 cm [92]. Abdominal surgery is amenable to epidural analgesia, previously used successfully as a control for morphine-induce immunosuppression studies.

1.8.2 Analgesia

Morphine sulphate, oxycodone hydrochloride and epidural bupivacaine were the 3 analgesics used. Morphine was the study drug of interest, oxycodone is a non-immune modulating opioid and epidural bupivacaine is a non-immune modulating non-opioid. Patients were prospectively randomised to receive only 1 of these 3 analgesics.

1.8.2.1 Oxycodone

Oxycodone has a similar modified phenanthrene basic structure to morphine [1]; the C6 hydroxyl group moves to C3 on the same ring, with a new O atom at the C6 position. The hydroxyl group at C3 on the second benzene ring is replaced with H_3CO.

Structure of oxycodone

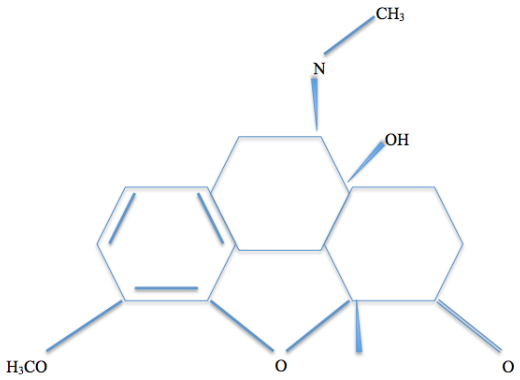

Figure 1.2: the structure of oxycodone [1]

Although oxycodone was traditionally believed to be primarily a MOR agonist with a lower affinity than morphine, it may have a different receptor binding profile. Oxycodone and morphine showed unique activity profiles of analgesia, respiratory depression and constipation following intracerebroventricular administration in rats [93] and radioligand binding studies suggest that oxycodone is mainly a κ-opioid receptor (KOR) agonist with a weak affinity for MOR [94]. Oxycodone crosses the blood brain barrier more efficiently than morphine accounting for its more potent analgesia [95]. Activation of KOR mediates analgesia, dysphoria, anticonvulsant and antidepressant effects, dissociative effects, miosis and diuresis [96]. MOR activation in the presynaptic afferent neurons in the dorsal horn of the spinal cord, and in the PAG in the midbrain and rostral ventromedial medulla (RVM) mediates analgesic and sedative effects. Efferent outflow from the PAG and RVM inhibits nociceptive transmission in afferent fibres in the dorsal horn, using noradrenaline and 5-HT [13].

Oxycodone has a half-life of 3-4.5 hours and its metabolites include oxymorphone, produced by the enzyme CYP2D6. Although oxymorphone has

a high affinity for MOR, it is only produced to a small degree in humans and therefore has a limited contribution to analgesia [97].

1.8.2.2 Bupivacaine

Like other local anaesthetics, bupivacaine has the basic structure of an aromatic group and an amine side chain [85] linked by an amide group. Earlier anaesthetics were linked with an ester group; amide groups tend to give the anaesthetic more stability.

Structure of bupivacaine

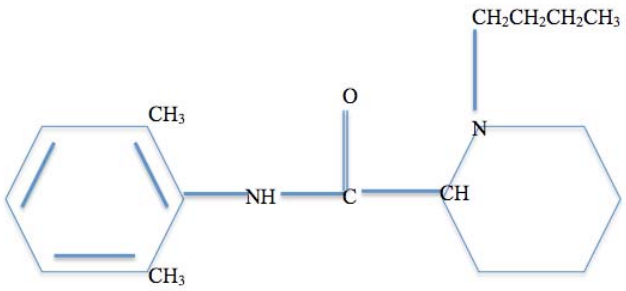

Figure 1.3: the structure of bupivacaine [1]

Bupivacaine binds to sodium channels intracellularly, preventing Na^{2+} influx into the cell and depolarization, particularly of thinner non-myelinated nerve fibres such as nociceptors. Low doses do not completely block depolarization, but reduce the rate of rise of the action potential (AP) due to the reduced intracellular Na^{2+} influx. This increases the duration of the AP and reduces the cell's firing rate. Higher doses completely block APs.

1.8.3 Anaesthesia

A propofol-only anaesthetic protocol was used due to previous work showing propofol to have no immune-modulating properties [77]. Anaesthesia was induced and maintained with propofol only and no other anaesthetics (intravenous or inhalational) were used.

1.8.4 Blood sampling

1.8.4.1 Timepoints

Four sampling timepoints were used: pre-dose, then 2, 6 and 24 hours post-induction. Previous work by this group found changes in phosphorylation patterns of membrane associated signalling proteins as early as 2 hours post-morphine administration [49], and elsewhere, in laparoscopic versus open cholecystectomies, PBMCs showed a difference in secreted IL-4 at 2 hours only [61]. Early changes (probably by 1 hour) were seen in TH1: TH2 ratios in male patients undergoing TURP [62], and surgery-induced cytokines were reduced in the morphine group at 2 hours post incision in mice [65]. Ben-Eliyahu et al found that NKCC remained suppressed at 6 hours post-anaesthesia [86]. Finally, based on experimental practicalities, we chose 24 hours as our last timepoint.

1.8.4.2 Venepuncture and transfusions

Venous blood was taken mainly by repeat venepuncture with a hollow metal hypodermic needle, rather than from in-dwelling catheter, as blood from the catheter route is prone to clotting, causing RNA degradation. No further experimental blood samples were taken from patients who required a blood transfusion, but samples already taken before the point of transfusion were

assayed if at least 3 samples were available. This was due to the unexpectedly large number of transfused study patients.

1.9 Aims

As previous clinical research has produced equivocal results, and due to the wide use of morphine, further investigation of the immunosuppressive effects and mechanisms of morphine is warranted.

We planned to use gene expression analysis to further investigate the previously published immunosuppressive effects of morphine. Our aim was to compare relative gene deregulation in mononuclear cells following morphine, oxycodone or epidural bupivacaine administration intra- and postoperatively in patients undergoing open gynaecological surgery via a standard Pfannenstiel incision. As yet, no clinical study has been published that successfully separates morphine from other analgesia intra- and postoperatively. We therefore aimed to create two non-morphine groups. Further, we aimed to confirm gene deregulation and morphine-induced immunosuppression using functional assays and to identify possible genes that could be used for prognostic tests to identify patients at higher risk of morphine-induced immunosuppression.

Chapter 2

Methods

2.1 Clinical Methods

2.1.1 Study approvals

Ethics approval for the study: A single centre, parallel group, pilot study to investigate the effect of opioids on immunomarkers using gene expression profiling, was obtained from the Royal Marsden Research Ethics Committee, REC reference number 06/Q0801/135.

The initial recruitment target was 45 patients, 15 per treatment group. Following the initial withdrawal of 11 patients, a protocol amendment was submitted to the MREC to increase maximum total patient numbers to 70. This was approved on 26 Sep 2011.

Regulatory approval for the study: A single centre, parallel group, pilot study to investigate the effect of opioids on immunomarkers using gene expression profiling, was obtained from the MHRA and the Joint R&D office of Barts and The London NHS Trust and Queen Mary, University of London (reference number 4757 QM).

2.1.2 Patient recruitment

Patients were selected in advance from elective gynaecological surgery lists, for surgery at Barts and The Royal London hospitals. All patients who met the inclusion and exclusion criteria were consented prior to surgery.

2.1.3 Randomisation and blinding

Prior to study start, 45 slips of paper detailing treatment to be assigned (15 per treatment group) were created and placed in individual envelopes. The

envelopes were mixed and stored in a box in a locked room. To randomize a patient, the consenting investigator chose an envelope from the box at random.

Given a potentially high withdrawal rate (usually transfusion and analgesia-related) and the anticipation that postoperative patient withdrawal would not be evenly spread across treatments, an additional envelope for the same treatment group was created and re-mixed for any patient who withdrew, to ensure sufficient completed patients in each group.

Theatre, ward staff and investigators were unblinded to each patient's treatment. Laboratory assays were conducted by staff blinded to the study group (TW and MD), who remained blinded until sample mRNA was prepared for hybridisation to chips, when unblinding was essential for appropriate stratifying of treatment groups.

2.1.4 Patient population

All patients were female, aged over 18 and recruited from elective non-cancer gynaecological surgery lists, for gynaecological surgery with a Pfannenstiel incision. All patients had surgery at Barts and The London NHS Trust (now Barts Health).

Patients were recruited into the study only if they met all the Inclusion Criteria and none of the Exclusion Criteria (Sections 2.1.5 and 2.1.6).

2.1.5 Inclusion Criteria

- Patients aged 18 years and above with a negative pregnancy test and not lactating
- Patients who are ASA 1-3
- Patients must be inpatients
- Patients who are scheduled for elective gynaecological, non-cancer surgery (via a Pfannenstiel abdominal) incision under general anaesthesia
- Patient has given written informed consent

2.1.6 Exclusion Criteria

1) Patients who are allergic to morphine, oxycodone or bupivacaine
2) Patient with a history of anaesthetic complications
3) Patients with a history of substance abuse
4) Patients who have been on long-term opioid therapy, or have taken opioids within the last one month.
5) Patients taking MAO-I or anti-depressant medications.
6) Patients who have received blood transfusion in the last month
7) Patients who have a history of immune or haematological/bone marrow disorder
8) Known HIV-positive patients
9) Patients with any contra-indications to epidural analgesia (e.g. back surgery, clotting abnormality, local infection or refusal)
10) Patients having laparoscopic surgery
11) Patient who have participated in another study in the past 90 days.
12) Patients who have received an IMP within the last 12 weeks prior to their surgery.

2.1.7 Clinical study design

Patients were treated as per protocol. Potentially suitable patients, scheduled to undergo gynaecological laparotomy, were identified and given the Patient Information Sheet (PIS). If agreeable, their written informed consent to the study was obtained and they were screened and randomised to a treatment group. All pertinent screening and study information was recorded in the CRF. Screening involved ensuring the patient met the inclusion and exclusion criteria.

Upon admission, inclusion and exclusion criteria were rechecked, and medical history, concomitant medication and epidemiological data recorded. A physical examination was performed and vital signs, height and weight recorded. Four blood samples were taken, pre-dose (0 hour), at two hours post-induction (2 hour), six hours post-induction (6 hour) and 24 hours post-induction (24 hour).

Following the pre-dose blood sample, the epidural cannula was sited and the first epidural dose given for those patients assigned to the epidural group. Anaesthesia was then induced and maintained with propofol only, for patients in all three treatment groups. Morphine and oxycodone were given following induction for those patients assigned to these treatment groups respectively, and surgery was performed as normal. During surgery, all medication was recorded in the patient notes, and details for premedication, start and end times of anaesthesia, air flow and propofol dose were all transcribed to the CRF. The duration of surgery and the time of the patient's return to the recovery ward were recorded.

At the time of subsequent blood samples, vital signs, any adverse events and total study drug administered were recorded. If the patient withdrew from the study, the reason for this was recorded.

Except for the use of a propofol-only anaesthetic and analgesia given as per protocol, patients received standard care. Patients with a clinical need for extra analgesia, which could not be covered by their assigned analgesic, were withdrawn from the study and treated. Similarly, patients with a medical need for a blood transfusion were withdrawn from the study, as were patients who themselves chose to withdraw.

2.1.8 Treatment groups

There were 3 treatment groups – morphine, oxycodone and epidural bupivacaine. All three analgesics are licensed for use by the MHRA and were used as licensed. Patients were randomized to one treatment group and doses were as follows:

Morphine sulphate: 0.1mg/kg intravenously intraoperatively then 1mg bolus intravenously as required both intraoperatively and by PCA postoperatively.

Oxycodone hydrochloride: 0.1mg/kg intravenously intraoperatively then 1mg bolus intravenously as required both intraoperatively and by PCA postoperatively

Bupivacaine: 0.25% strength plain bupivacaine (2.5mg/ml) administered as 10ml bolus via the epidural route prior to surgery, with extra bolus doses as necessary, and then continued as a 0.125% epidural infusion postoperatively. This group received no opioid by any route for the 24 hours study period.

2.1.9 Postoperative analgesic administration

Both morphine and oxycodone were administered as PCA postoperatively. The infusion rate of the epidural bupivacaine was continuous with the rate titrated by nursing staff according to pain scores and anaesthetic blockade.

2.1.10 Opioid dose analysis

Cumulative opioid doses were compared between morphine and oxycodone at each timepoint using an independent-samples 2-tailed t test. In addition, non-cumulative doses were also compared separately at each timepoint, again using an independent samples 2-tailed t test. Statistical analyses were performed in SPSS v22.

2.1.11 Pain score analysis

Pain scores were recorded at the same time as each blood sample using an 11-point numerical rating scale (NRS), in which patients were requested to verbally score their pain on a scale of 0-10 (0 = no pain and 10 = the worst pain imaginable). The score was recorded in the patient's Case Report Form (CRF). CRF pain scores were depicted graphically in box plots and analysed across treatment groups using both one-way ANOVA and Kruskal-Wallis (for non-parametric data) in SPSS v22.

2.1.12 Obtaining blood samples

40ml venous peripheral blood was obtained from subjects at each of the four timepoints either through pre-sited cannulae or using standard venepuncture technique. During the initial stages of the study, for the first 5 patients, blood was taken from pre-sited cannulae as well as via venepuncture. As cannula blood had a greater tendency to clot, we moved to a solely venepuncture method. For patients who were withdrawn from the study before their 4th

blood sample (but did not withdraw consent), no further blood was taken but samples that had been taken were analysed.

Blood was taken directly into EDTA-spiked tubes for RNA extraction and cell collection, or gel-containing SST tubes for serum collection. EDTA tubes were inverted to mix then all tubes were stored at 4°C for processing.

2.2 Laboratory methods

2.2.1 Allocation of blood samples

Unclotted blood was collected for microarray and NK cell cytotoxicity assay at each timepoint, while serum from clotted blood was collected for cortisol ELISA and cytokine CBA at 0 and 6 hr.

Table 2.1: Blood taken via venepuncture at each timepoint

Timepoint	Blood taken (mls)	
	EDTA-spiked tubes	Clot-activator tubes
0 hour	35	5
2 hour	40	0
6 hour	35	5
24 hour	40	0

2.2.2 PBMC extraction

PBMCs were extracted from unclotted peripheral blood using the standard Ficoll-Hypaque technique, which involves the use of polysaccharide to grade cells by size; small dense red blood cells pass through the polysaccharide whereas the larger less dense white blood cells do not. Lymphoprep (a combination of sodium diatrizoate and polysaccharide) was used for this. Blood was initially diluted 1:1 with PBS then approximately 20ml diluted blood was layered carefully on top of 15ml Lymphoprep in a 50ml Falcon tube. Samples were centrifuged (1500 revolutions per minute (RPM), room temperature (RT), 25 min) with brakes off to prevent disruption of the layers that formed. Post centrifugation, the PBMC layer (formed as an interface between the plasma and lymphoprep layers) was removed with a pastette; care was taken to avoid removing lymphoprep with the cells, due to its deleterious effects on cells. Cells were washed with approximately 40ml PBS

then each cell pellet diluted in 2ml PBS prior to counting and viability assessment with the Beckman Coulter Vi-cell counter.

Ficoll-hypaque technique

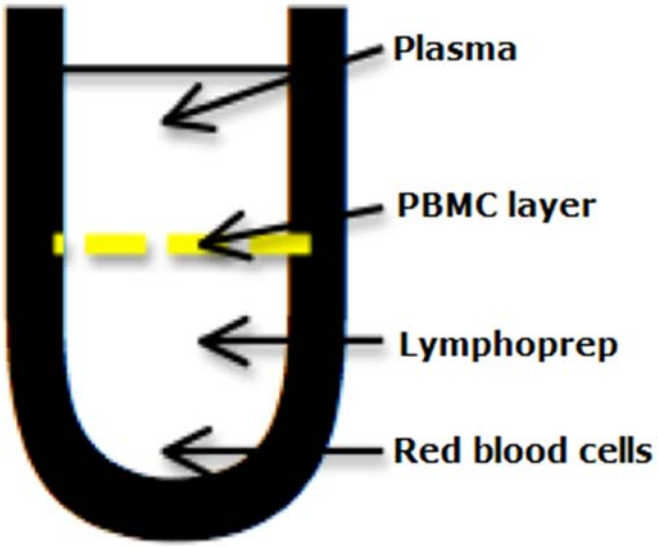

Figure 2.1: layers formed by centrifugation

2.2.3 Cell counting / viability

Cells were counted both pre- and post-separation of PBMC sub-populations. 100µl cell suspension of untouched PBMCs from each sample was mixed with 400µl PBS and cells were counted in an automated cell counter (Figure 2.2) using the trypan blue dye exclusion method. Trypan blue crosses the cell membrane of dead cells causing them to appear blue under a microscope whereas the dye will not cross the membrane of live viable cells, preventing their colouration. 50 separate images of cells were recorded and average number of viable cells and percentage viability of all cells calculated. The

number of viable cells was used to calculate microbead volumes needed during the magnetic separation stage.

Cell counting machine

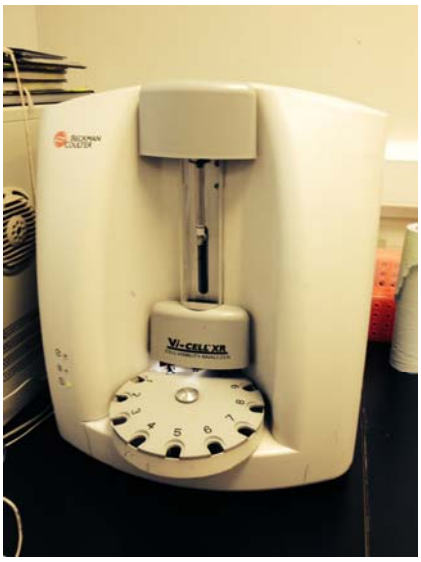

Figure 2.2: the Beckman Coulter Vi-Cell XR counter

2.2.4 Positive magnetic cell separation

2.2.4.1 Incubation stage

PBMCs were isolated and counted as above. CD4+ and CD8+ T cells were separated using positive selection, following binding to anti-human CD4 / CD8 antibodies conjugated to magnetic microbeads. MACS buffer, containing PBS pH 7.2, 0.5% BSA and 2mM EDTA, was made by diluting MACS BSA Stock solution 1:20 with autoMACS Rinsing solution.

Cell suspensions were repelleted post-count (1300 RPM, 4°C, 5 min) then 80μl MACS buffer per 10^7 viable PBMCs added to each aliquot. 20μl CD4 or

CD8 antibody/microbead solution per 10^7 viable PBMCs were added, and cell suspensions vortexed and incubated (4°C, 15 min). Pellets were washed with 2ml MACS buffer and resuspended in 500μl MACS buffer in preparation for passing through magnetic columns.

2.2.4.2 Magnetic separation

MACS LS columns and a QuadroMACS Separator magnet were used to separate magnetically-labelled cells from suspension. LS columns were placed in the QuadroMACS Separator, which contains a powerful permanent magnet. The matrixes of the LS columns are composed of ferromagnetic spheres, which amplify the magnet's field by 10,000 times, inducing a high gradient within the column when in the QuadroMACS' magnetic field. This gradient removes cells less well labelled by MACS microbeads [98].

LS columns (one per aliquot) were placed in the QuadroMACS Separator, activated with 3ml MACS buffer, then cell suspensions were passed through. Following this, 9ml MACS buffer was added to each now-empty Falcon tube to collect any remaining cells and solution then passed through the relevant column. CD4+ and CD8+ T cells were positively selected and therefore captured in the magnetic column. Flushing out columns with 5ml MACS buffer with a plunger eluted cells. The effluent from the columns (ie cells which had passed through columns due to insufficient magnetic labelling) was discarded.

Positively labelled cell suspensions were centrifuged thoroughly to pellet all cells (1500 RPM, 4°C, 20 min) then supernatant removed by inversion and tube blotting, prior to RNA extraction.

2.2.5 Negative magnetic cell separation

NK cells were separated using negative selection, via magnetic labelling of all other cells in suspension (T cells, B cells, stem cells, dendritic cells, monocytes, granulocytes, erythroid cells). All other cells were labelled with a cocktail of biotin-conjugated antibodies and a microbead cocktail then

removed via magnetic separation. This left untouched NK cells in the column effluent, ideal for later assays as no direct labelling of surface molecules had occurred.

2.2.5.1 Incubation stage

As with T cells, cell suspensions were repelleted following cell counting (1300 RPM, 4°C, 5 min), then cells were incubated with 40μl MACS buffer per 10^7 viable cells and 10μl NK Cell Biotin-antibody cocktail per 10^7 viable cells. Cell suspensions were vortexed to mix and incubated (4°C, 10 min). This stage labelled all the non-NK cells with a biotinylated antibody. 30μl MACS buffer per 10^7 viable cells and 20μl NK cell microbead cocktail per 10^7 viable cells was then added, to add a magnetic label to cells. After vortexing, suspensions were incubated again (4°C, 15 min). Cell suspensions were washed with 2ml MACS buffer then pellets resuspended in 500μl MACS buffer in preparation for passing through the magnetic columns.

2.2.5.2 Magnetic separation

Columns were prepared for NK cell separation as for T cells, and cell suspensions passed through the magnetic columns in the same way as CD4+ / CD8+ positive selection, again with an extra 9ml buffer to collect any remaining cells. However, this time the flow through was saved as it contained the untouched NK cells. NK cells were centrifuged to pellet all cells (1500 RPM, 4°C, 20 min) and the supernatant removed by inversion and tube blotting prior to RNA extraction.

2.2.6 RNA extraction

RNA was extracted from pelleted cells with the Qiagen RNeasy Mini Kit, using adapted standard procedures.

2.2.6.1 Preparation

Prior to extraction, buffer RLT was prepared in the fume hood by adding β–Mercaptoethanol (β-ME) in a ratio of 1ml buffer RLT to 10μl β-ME, 1050μl per timepoint (β–ME irreversibly denatures RNases). The buffer mixture was vortexed for 1 minute. 70% ethanol was prepared by mixing 100% ethanol with RNase-free water in the fume hood; a total of 1050μl was prepared per timepoint. The laminar flow hood, Gilson pipettes, tube rack, pipette tip boxes and operator's gloves were thoroughly cleaned with RNase Zap to remove any residual RNase.

2.2.6.2 RNA extraction

350μl buffer RLT mixture was added to each sample pellet, then pellets vortexed for 1 minute to lyse cells. Each lysate was pipetted into a labelled QIA shredder column and centrifuged (14000 RPM, RT, 2 min) to homogenize the cells and reduce viscosity. The QIA shredder was discarded and 350μl 70% ethanol added to each sample, pipetted to mix and placed in an RNeasy spin column. Samples were centrifuged (14000 RPM, RT, 15s) and supernatant removed. 700μl buffer RW1 was added to each spin column and samples were spun (14000 RPM, RT, 15s) and supernatant discarded. 500μl buffer RPE was added to each sample, spun (14000 RPM, RT, 15s) and supernatant discarded, then this step repeated with a 2 minute spin. RNeasy spin columns were then placed in new collection tubes and 40μl RNase-free

water was added to each column. Samples were incubated for 5 minutes at room temperature then centrifuged (14000 RPM, RT, 1 min) to elute the RNA.

The RNA quantity and quality of each sample was measured with a Nanodrop ND-1000 spectrophotometer (Section 2.2.7.1) and RNA was stored at -80°C in a clinical trials freezer prior to hybridisation.

2.2.7 RNA quantification

2.2.7.1 Nanodrop

RNA quantity and quality was measured using UV absorption via a Nanodrop ND-1000 spectrophotometer. The spectrophotometer records absorbance of UV light across the spectrum and plots a curve using absorbance by the sample observed at 260 and 280nm. The concentration and therefore amount of RNA is calculated using Beer-Lambert law, which predicts a linear change in absorbance with concentration [99].

1µl RNA per sample was used for measurements. The reading at 260nm is used to determine the RNA concentration, based on the assumption that a reading of 1.0 is equivalent to 40µg/ml of RNA [99]. The absorbance ratio of 260nm: 280 nm indicates quality; the ideal absorbance is 2.0 when the buffer is at pH 8.0, and lower values indicate contamination with protein [100], also shown by unexpected peaks in the curve. The pH of the buffer used to resuspend RNA can affect 260/280 ratios with lower pHs showing lower ratios; RNase free water has a typical pH of 5.2 which tends to lower over time [101]. Attention should therefore be given to the buffer used for RNA resuspension when considering sample quality. Both RNA concentration and quality were recorded.

2.2.7.2 Bioanalyzer

The Agilent 2100 Bioanalyzer measures RNA degradation via a lab-on-a-chip version of gel electrophoresis. Macromolecules are separated based on their size and charge following the application of an electric charge to gel; molecules move by travelling through pores in the gel. The Bioanalyzer chip consists of 16 wells with connecting microchannels into which a gel-dye mixture is pushed with a syringe. Sample is inserted in up to 12 wells and a ladder consisting of 6 differently-sized RNA fragments is inserted into the ladder well. The dye binds to the RNA and dye-RNA complexes can be detected later by fluorescence.

The Bioanalyzer measures 18S and 28S subunits in ribosomal ribonucleic acid (rRNA - the main rRNA species in eukaryotes) and displays their abundance via two peaks in an electropherogram, together with that of smaller fragments. 18S and 28S subunits present in a ratio of 2.7: 1 in intact RNA; although the subunits have a 1:1 molecule ratio, their differing size gives a sedimentation coefficient of 2.7:1. A ratio of 2.1 is considered good RNA. RNA Integrity Number (RIN) measures RNA degradation and is calculated from the total area under the graph; intact RNA gives a RIN of 10.

Prior to use, the ladder and samples were denatured in a heat block (70°C, 2 min), reagents equilibrated to RT and the Bioanalyzer cleaned with RNase Zap. 9µl gel-dye mix (made from 65µl filtered gel and 1µl dye) was pipetted into each of 3 wells and pushed through the microchannels. 5µl of Nano marker was pipetted into all 13 wells followed by sample / ladder. The chip was vortexed for 1 minute (IKA Works Vortexer) then analysed in the Bioanalyzer.

RINs were measured after RNA extraction and just prior to amplification for hybridisation (all samples). They were also measured post-amplification and post-fragmentation to confirm that the experiment was progressing satisfactorily (16 amplified and 19 fragmented subjects, at least two timepoints for each subject). All data can be seen in Appendix B.

2.2.7.3 RIN analysis

One-way ANOVAs were performed in SPSS v22 to investigate any differences in RNA integrity at each timepoint between all treatment groups, and in each treatment group, between all timepoints.

2.2.8 Cell freezing

Cells kept for later use were initially frozen at -80ºC. 1ml freeze mix (4.75ml FCS and 0.25ml DMSO) was added to each cell pellet and vortexed. Resulting cell suspensions were placed in a 1.5ml Nalgene cryovial and gradually cooled overnight (-80ºC) in a Nalgene freezing container containing isopropanol. Samples were transferred to liquid nitrogen the following day for storage at -196ºC.

2.2.9 Affymetrix microarray

The Affymetrix GeneScan 3000 7G scanner was used in conjunction with Affymetrix GeneChip 3' IVT Express Kit and U133+2.0 GeneChips for the hybridisation experiment. Each microarray contains 1.3 million oligonucleotide 25-base-pair probes for 47,000 transcripts, covering 33,000 genes. Each probe is unique to a different section of a gene sequence, and as few as 11 probes are repeated to make one probeset.

Total RNA was transcribed to first strand then double-stranded DNA in two separate hybridisations. An overnight incubation produced amplified RNA, which was conjugated with biotin, hybridised to arrays and stained with Streptavidin Phycoerthyrin (SAPE) before scanning. Fluorescence was recorded as an expression value (Figure 2.3).

The capacities of the machine and the core facility operator limited batches to 20 samples. Hybridisation of RNA to microarrays is known to be temperature sensitive, so samples were run in treatment-stratified batches to avoid any temperature-associated batch variation. Financial constraints meant RNA from cell sub-populations was recombined at each timepoint per patient, so a batch of 20 samples equated to 5 patients. Patients were allocated numerically to a batch, ie the lowest 2 subject numbers in morphine group + lowest 2 subject numbers in oxycodone group + lowest number in bupivacaine group made the 1st batch. For technical reasons, occasionally alternative patient samples were substituted, but treatment stratification was adhered to.

The GeneChip 3' IVT Express kit user manual was used for labelling and amplifying the RNA following the protocol recommended by the manufacturer. 50ng RNA from each of the three cell types per patient timepoint was used, to make a total of 150ng RNA per patient timepoint. This was within the recommended range of 50-150ng RNA per sample; we used the maximum amount of RNA advised, as recommended by Affymetrix when RNA quality and RIN is low.

Flowchart of the hybridisation of RNA to arrays

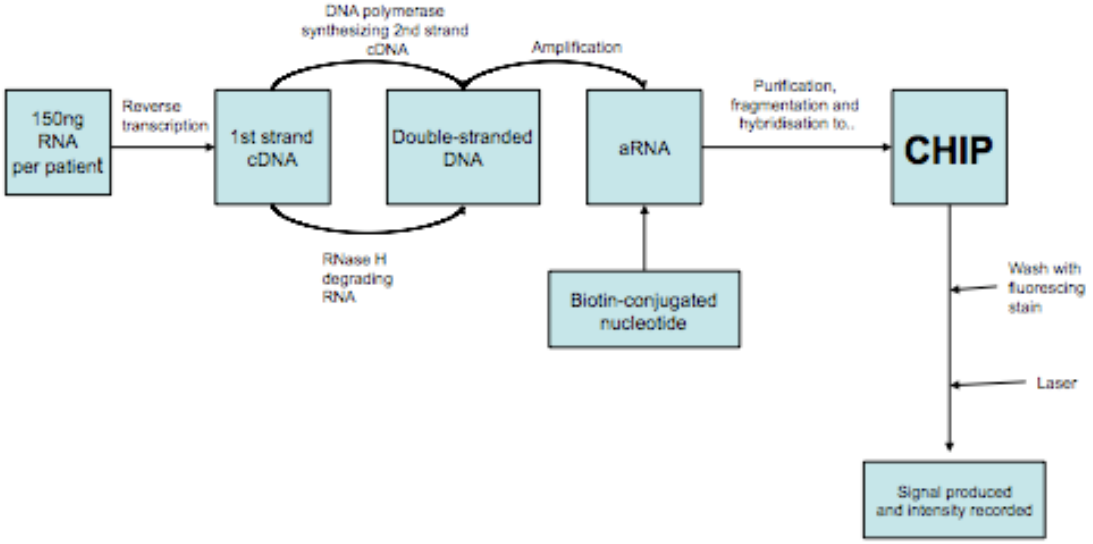

Figure 2.3: Summary of the progression of RNA to raw gene expression data

2.2.9.1 Stratified treatment groups

Eight sample groups were run on separate dates through the GeneChip 3000 Scanner, with 2:2:1 of morphine, oxycodone and bupivacaine samples. Groups 4 and 7 were both run on two consecutive dates, as two samples in each group (52D and 55C in Group 4; 1D and 6B in Group 7) did not load properly into the autoscanner overnight so were rescanned the next day. However, as discussed in Chapter 3 (Section 5.1), no difference was imported by scan date.

2.2.9.2 Preparing RNA for amplification

RNA was defrosted on ice, vortexed and quantified using the Nanodrop spectrophotometer in case degradation had occurred. Sample volume needed to give 50ng RNA was calculated (assuming 40µl volume) and CD4+, CD8+ and NK RNA transferred to a labelled 1.5ml tube. The protocol required RNA

samples to be in a maximum volume of 3µl. Each sample was dehydrated then resuspended in 3µl RNase-free water. Dehydration was performed in a Savant DNA Speed Vac concentrator machine for 15-30 minutes after covering samples with needle-pricked (20-guage) parafilm. Samples were vortexed to mix and placed on ice.

2.2.9.3 Preparing reagents and master mixes

The dilutions table for the Poly-A RNA Control Stock gave dilution ratios based on amount of RNA used; 100ng dilution ratios were chosen as being the closest to our RNA weights of 150ng per sample. Serial dilutions were performed using Poly-A Control Stock and Poly-A Control Dilution Buffer as in the protocol. Master mixes of all solutions were made to achieve enough volume for all samples and to ensure uniformity: mixes were prepared for 21 samples. Tetrad 2 Thermal Cycler was used for all incubations.

2.2.9.4 Reverse transcription

First-strand master mix was prepared on ice with 84µl First-Strand Buffer Mix and 21µl First-Strand Enzyme Mix (master mix for 21 samples). Contents of both the buffer and enzyme mix are proprietary. 2µl of diluted poly-A RNA Controls and 5µl of first-strand master mix were added to each 3µl RNA sample, samples pipetted and placed into an 8-well PCR strip on ice. Samples were vortexed, spun and incubated (42°C, 2 hr). After incubation, samples were spun down then placed on ice ready for the second-strand master mix.

2.2.9.5 Second strand cDNA addition

Second-strand master mix was prepared on ice during the 2-hour first-strand incubation: 273µl RNase-free water, 105µl second-strand buffer mix and 42µl second-strand enzyme mix were vortexed and kept on ice until needed

(master mix for 21 samples). Contents of both the buffer and enzyme mix are proprietary. 20µl second-strand master mix was added to each sample, samples vortexed and spun down, then transferred on ice to incubate in the pre-cooled incubator as failure to pre-cool could reduce the aRNA yield (16°C, 1hr; 65°C, 10min; 4°C, ∞). Following incubation, samples were spun down then placed on ice ready for the amplification stage.

2.2.9.6 Amplification

IVT master mix was prepared during the second-strand cDNA incubation. 84µl IVT biotin label, 420µl IVT labelling buffer and 126µl IVT enzyme mix were added to a nuclease free tube at RT, vortexed then placed on ice. Contents of all reagents are proprietary and were at RT prior to mixing. 30µl IVT master mix was added to each sample, samples were vortexed, spun down and incubated (40°C, 16hr; 4°C, ∞). Post-incubation, RNA from a total of 16 subjects (at least two timepoints) was quantified using the Nanodrop 1000 to ensure amplification had proceeded satisfactorily, both in terms of amount and quality.

2.2.9.7 Purification of amplified RNA

This stage involved removing unincorporated NTPs and salts to leave pure biotin-conjugated amplified RNA (aRNA). Solutions were prepared in advance: 1100µl aRNA elution solution was pre-warmed in a plate warmer (60°C, 30 min) and aRNA Wash Solution Concentrate was diluted with ethanol. aRNA binding mix was prepared by mixing 210µl RNA binding beads and 1050µl aRNA binding buffer concentrate at RT (amounts given are for 21-sample master mix). Again, contents of all reagents are proprietary.

60µl vortexed aRNA binding mix was added to each sample, samples were pipetted then transferred to a U-bottom plate. 120µl 100% ethanol was added to each sample, samples were mixed, plate covered then mixed on a plate shaker (500 RPM, 2min) to allow the aRNA to bind the RNA binding beads. The U-bottom plate was moved to a magnetic plate stand to capture the magnetic beads, seen by the developing translucence of the mixture as the beads formed a ring against the magnets. The supernatant was aspirated carefully without disturbing the beads and discarded; the magnetic beads now contained the aRNA.

The plate was removed from the magnet, 100µl aRNA Wash Solution added to each sample and shaken (700 RPM, 1 min). Magnetic beads were captured and supernatant aspirated and discarded. This was repeated with a second aliquot of 100µl aRNA Wash Solution; following aspiration, the plate was shaken (1000 RPM, 1min) to evaporate leftover ethanol and dry the beads.

50µl aRNA Elution Solution was added to each well to elute aRNA from beads, then the plate was shaken (1000 RPM, 3 min) to disperse beads. Finally, the plate was moved back to the magnet to capture the magnetic beads; the supernatant now contained the aRNA and was aspirated into PCR strips. To check quality and quantity before fragmentation, each aRNA sample was then measured using the Nanodrop 1000 spectrophotometer (see Appendix B).

2.2.9.8 Fragmentation of amplified RNA

At this stage, the protocol required each sample to contain 15µg aRNA but not exceed 32µl in volume. The volume needed was calculated for each sample and samples were either dehydrated (see Section 2.2.9.2) then rehydrated with 32µl RNA-ase free water or the correct volume was taken

from the original sample. Once prepared, samples were transferred to a new 8-well PCR strip for fragmentation. 8µl 5x Array Fragmentation Buffer was added to each sample, samples vortexed and spun down, then fragmented in the incubator (94°C, 35 min). Post-incubation, RNA from 19 subjects (at least two timepoints each) was measured with the Bioanalyzer to ensure successful fragmentation had occurred (see Appendix B).

2.2.9.9 Hybridisation to probe array

262.5µl 20X Hybridisation Control was pre-heated in a heat block (65°C, 5 min) and the hybridisation cocktail master mix prepared in bulk by adding 86.1µl control oligonucleotide, 2625µl 2X Hybridisation Mix, 525µl DMSO and 1050µl Nuclease-free water at RT. (As before, contents of all reagents are proprietary and the master mix was for 21 samples). The cocktail was vortexed and split into 250µl aliquots (one per sample). 33.3µl of each sample was added, vortexed, spun down, then passed to the Affymetrix core facility operator for hybridisation to arrays. If not hybridized immediately, samples were stored at -20°C.

The Affymetrix GeneChip Arrays were brought to RT. Samples in hybridisation cocktail were heated in 2 heat blocks: 99°C, 5 min followed by 45°C, 5 min. Samples were centrifuged (14000 RPM, RT, 5 min) to remove insoluble material from samples. Arrays (one per sample) were wetted with 200µl pre-hybridisation mix through the septum and incubated (45°C, 10 min) while rotating. Pre-hybridisation mix was removed from each array and replaced with 200µl hybridisation cocktail plus sample, avoiding any insoluble material. Arrays were placed into the pre-heated hybridisation oven (60 RPM, 45°C, 16 hr).

2.2.9.10 Washing, staining and scanning arrays

Following hybridisation, arrays were taken from the oven and hybridisation cocktail removed. Each array was washed with wash buffer in the pre-primed automated GeneChip Fluidics station 450/250 to remove un-hybridised probes, then stained with SAPE. SAPE labels the biotinylated aRNA fragments that have hybridized to the array and fluoresces under laser. Arrays were scanned by the GeneChip 3000 Scanner, which can detect as few as 400 phycoerthyrin molecules in a probe site. The GeneChip Command Console software then produces a value correlating to the intensity of each array spot.

2.2.10 Cortisol ELISA

Cortisol ELISA was performed on serum samples at 0 and 6 hour, using the R&D Systems kit KGE008. The ELISA works on the principle of competitive binding, where any cortisol present in patient serum samples competes with horseradish peroxidase-labelled cortisol to bind to a mouse monoclonal antibody. The monoclonal antibody binds to a goat anti-mouse antibody already present on the 96-well plate during the incubation period, after which the plate is washed and substrate solution added. The enzymatic reaction induces a colour change that is stopped after a fixed period then measured via light wave absorbance. The intensity of the colour is inversely proportional to the concentration of cortisol [102].

All kit reagents were brought to room temperature for 30 minutes before use. As saliva contains cortisol, a face mask was worn to avoid accidental contamination. Cortisol was prepared by reconstituting powder with distilled water, then resting for 15 minutes, to produce a stock solution of 100ng/ml. 900µl Calibrator Diluent RD5-43 was pipetted to the 10ng/ml standard tube and 500µl into each subsequent standard tube. Standards were prepared via serial dilution; 100µl stock solution was added to the 10ng/ml standard tube, mixed, then 500µl of this standard pipetted into the 5ng/ml standard tube. The transfer of 500µl of each standard to the next lowest standard was repeated to complete the dilution series. 20ml Wash Buffer Concentrate was diluted with 480ml distilled water to prepare 500ml Wash Buffer. Serum samples were defrosted at room temperature and 30µl sample diluted with 270µl Calibrator Diluent.

150µl Calibrator Diluent RD5-43 was added to each non-specific binding (NSB) wells (wells 1 & 2) followed by 100µl to each zero standard well (wells 3 & 4). 100µl of either standard or sample was added to each well; all assayed in duplicate. 50µl Cortisol Conjugate was added to each well followed by 50µl Primary Antibody Solution to all wells apart from NSB wells. The plate was covered and incubated on a horizontal shaker (500 RPM, RT, 2 hr).

Wells were aspirated in a hood then washed by filling each well with 400µl Wash Buffer. This was repeated three times, ensuring complete removal of supernatant each time. The plate was blotted with a paper towel and Substrate Solution prepared by mixing Colour Reagents A & B together. 200µl substrate solution was added to each well and samples incubated (RT, 30 min). 50µl Stop Solution was added to each well and the plate was read in a BMG Labtech microplate reader with wavelength set to 450nm. Optical densities (ODs) were imported to Fluostar Optima software then copied into Excel for calculation of concentrations.

2.2.11 Cytometric bead array

Serum taken from patients at 0 and 6 hour was used for cytokine analysis. A cytometric bead array (CBA) kit (560484 - BD Biosciences) for TH1, TH2 and TH17 cells was used to measure the concentrations of the following cytokines in serum samples: IL-2, IL-4, IL-6, IL-10, TNFα, IFN-γ and IL-17a. Serum samples were used from patients across all three treatment groups, and both timepoints were used for each patient.

A CBA is preferable to an ELISA as it allows simultaneous quantification of several cytokines, removing experimental variation, saving time and reducing the sample volume needed. Because CBA uses different fluorescing intensities

of a single fluorochrome, specialist equipment is not needed so it can be performed on a clinical flow cytometer. The fluorochrome Phycoerthyrin (PE) is attached to anti-antibodies specific for each cytokine's antibody in varying intensities, giving the ability to perform multiplexing.

Seven bead populations pre-coated with antibodies specific for the seven cytokines above were used. These are known as the capture beads and together form the bead array, which is mixed with sample / standard followed by PE-conjugated anti-antibodies specific for each antibody. Each population of anti-antibodies is incorporated with a different intensity of fluorescing PE, and the resultant sandwich complex, of cytokine conjugated to a bead-bound antibody bound to a fluorescing anti-antibody, was put through a flow cytometer. Fluorescing intensity emitted in red channel FL3/4 was then measured.

2.2.11.1 Preparing standards, samples, bead and tubes

One vial of standard was reconstituted with 2ml Assay Diluent and brought to room temperature. 300µl Assay Diluent added to each of 12 standard tubes. Serial dilutions were performed by transferring 300µl from the Top Standard to the 1:2 tube, mixing then transferring 300µl to the 1:4 tube, and repeating this until the final tube (1:256) was reached. The negative control was created with 300µl Assay Diluent. Samples were prepared by defrosting in a water bath at 37°C.

10µl per bead per sample / standard of each of the seven capture bead suspensions were mixed and spun (200G, RT, 5 min). Supernatant was

removed then replaced with an equal volume of Serum Enhancement Buffer. Bead array were vortexed and incubated (RT, 30 min).

2.2.11.2 Assay

The bead array was vortexed and 50µl added to each standard / sample tube, followed by 50µl of each standard / sample and 50µl PE detection reagent. Tubes were incubated (RT, 3 hr), washed with 1ml wash buffer (200G, RT, 5 min) and resuspended in 300µl wash buffer.

2.2.11.3 Cytometer setup and data acquisition

Cytometer setup procedure was performed during sample incubation. 100µl Cytometer Setup beads and 400µl wash buffer were vortexed together (setup tube) and loaded into the LSR Fortessa (BD Biosciences). The FACSDiva software (BD Biosciences) was set up and the machine set to acquire information. Forward scatter (FSC), side scatter (SSC), PE and fluorescein (FITC) voltages were each adjusted to correct the bead population and settings were saved. Standards and samples were then fed through the LSR Fortessa.

FCAP Array software v3 (BD Biosciences) was used to calculate Mean Fluorescing Intensities (MFIs) of the serially-diluted nine standards for each cytokine, generating a 5-parameter logistic (5PL) dose-response curve. Compared to a 4PL curve, 5PL has an extra parameter enabling the graph to be asymmetrical about the inflexion point. Sample concentrations were interpolated from the dose-response curve to produce MFIs, then averaged to give sample cytokine concentration.

2.2.12 NK cell degranulation assay

Traditionally, the gold-standard assay for measuring NK cell cytotoxicity (NKCC) was the ^{51}Cr release assay. Target cells are labelled with ^{51}Cr then exposed to NK cells; the amount of ^{51}Cr in supernatant indicates the success of target cell killing by NK cells. However, this method is less safe for the operator due to radioactivity. Measuring degranulation is a surrogate marker of NKCC and safe for the operator. Circulating NK cells contain preformed granules in their cytoplasm filled with cytolytic proteins and lined with CD107a. Upon target cell binding, the granules are released at the cell

synapse and contents disgorged; CD107a can then be measured to determine levels of degranulation. NK cells at 0 and 6 hour were used, from all treatment groups (morphine n=7; oxycodone n=7; bupivacaine n=4)

2.2.12.1 Reagent and cell preparation

Staphylococcal enterotoxin B (SEB) was used to stimulate half of each sample and prime cells for degranulation. A stock solution was prepared by mixing 1mg SEB powder with 1ml PBS; stock solution was then prepared for each assay by diluting 1µl in 9µl PBS. Samples were rapidly defrosted in a 37°C waterbath and washed with 10ml Dulbecco's phosphate buffered saline (1500 RPM, RT, 5 min) to remove DMSO from the freezemix. Samples were resuspended in 1ml pre-warmed complete medium (RPMI + 10% FCS + 2% gentamicin).

2.2.12.2 Assay

Samples were transferred to a 96-well plate and incubated overnight in a waterbath (37°C, 24 hr, 5% CO_2). Following incubation, vortexed samples were split into two aliquots: one to be stimulated and one as the unstimulated control. 5µl SEB was added to each stimulated sample to give a concentration of 1µg/ml. 5µl anti-human CD107a-AF647 (clone H4A3) antibody was added to each sample (stimulated and unstimulated) then samples were incubated in a water bath (37°C, 1hr, 5% CO_2). Following incubation, 3.3µl momensin at a concentration of 0.66µl/ml was added to each sample, giving a 1:10 dilution. Samples were mixed then incubated in the waterbath (37ºC, 4hr, 5% CO_2).

Following incubation, samples were aspirated into Falcon tubes and washed with 2-3ml PBS+2% FCS (1500 RPM, RT, 5 min). Following removal of

supernatant, 5µl PE-conjugated anti-CD56 (clone B159) and 5µl FITC-conjugated anti-CD3 (clone UCHT1) were added directly onto each cell pellet. Samples were incubated (RT, 15 min), washed with 4ml PBS+2% FCS (1500 RPM, RT, 5 min) and pellets resuspended in 250µl PBS+2% FCS prior to data acquisition.

2.2.12.3 Compensation cells and data acquisition

Human PBMCs from the National Blood Service (NBS) were used for compensation rather than beads, as their fluorescing intensity was expected to be more closely aligned to that of the experimental cells. Three samples of compensation cells each received PE-conjugated anti-CD56 antibodies, FITC-conjugated anti-CD3 antibodies or APC-conjugated anti-CD107a antibodies. Cells were incubated (RT, 15 min), washed with 4ml PBS+2% FCS (1500 RPM, RT, 5 min) and cell pellets resuspended in 250µl PBS+2% FCS prior to data acquisition.

Samples were run on the LSR Fortessa acquiring 10,000 events per sample / compensation. FACSDiva (BD Biosciences) was used to perform gating and compensation, and data analysed with FloJo v10 (FloJo LLC). NK cells were identified as those cells which were CD3- and CD56+.

2.3 Statistical methods

2.3.1 Affymetrix microarray

2.3.1.1 Background noise removal and data normalization

The volume of data generated in gene expression arrays means experimental variation and background noise will always exist, as a result of pipetting error, operator variation or experimental design. To eliminate background noise, Affymetrix arrays use a probe pairing system. Each perfect match (PM) 25 base pair probe is paired with a mis-match (MM) probe, usually by changing base 13. Background noise can then be calculated by subtracting intensity values for mis-match binding, a result of non-specific background probe binding, from perfect match binding. This method can remove noise but lose information, as only up to 1/3 of MM values are below PM values and can be negative. Instead, robust multi-array average background correction was used, which calculates background-adjusted intensity separately per array, using PM values, assuming a strictly positive distribution.

Normalisation aims to rescale the data, producing a similar size normal distribution across each array, thus removing outliers but keeping statistical variation. Quantile normalization was used, which ranks the intensity values for each array from lowest to highest, then calculates the mean value for each rank position across all arrays. Each probeset intensity value is then scaled to the mean value relevant to its rank.

Probe effect describes the increased range of intensities within a probeset in an array, compared to the same probeset across arrays. After log transformation, the probe effect was removed from intensity values using median polish. This produces one intensity value per probeset per array, by

combining values and normalizing each array and each probeset to its median, until all array and probeset medians are identical. All above background correction and normalization was performed in Partek Suite v6.6.

2.3.1.2 Identification of differentially expressed genes via ANOVA

ANOVA was performed on values adjusted as in Section 2.3.1.1 above, with independent variables of RIN, time, treatment, and (time x treatment). Calculation was performed in Partek and genes were further selected based on p-value and fold-change (FC). (Partek bases FC on ratio, when ratio is calculated from the least-squares mean. FC = ratio unless ratio is less than 1, in which case FC = -1/ratio). Genes differentially expressed from baseline at each timepoint by each treatment, with a fold change ≥±2 and p-value≤0.05, were selected for further analysis. The null hypothesis was one of no difference between baseline (0 hour) and later timepoints.

2.3.1.3 False discovery rate

False Discovery Rate (FDR) correction is used in microarray analysis to correct for false positives produced as a result of multiple testing. An ANOVA using a p-value of ≤0.05 would expect to generate 5% false positives simply as a result of multiple testing. Several different tests exist; Benjamini-Hochberg is a less stringent test commonly used in microarray analysis [103]. It involves ranking p-values for each gene from smallest to largest. The largest p-value is multiplied by the number of genes to produce a new p-value; then the 2nd largest is multiplied by (number of genes / rank) again to produce a new p-value and so on until all p-values have been adjusted. A p-value cut-off is then chosen as normal below which genes are considered significant. In this case, FDR-adjusted p-values ≤0.05 were used.

2.3.1.4 RINs / fluorescing intensity correlation

As most samples had RINs below 10 (Chapter 3), they were correlated with fluorescing intensity using Pearson correlation, to examine if degraded RNA (represented by a lower RIN) influenced intensity. Correlation was performed for all transcripts in Mor0-2 group (genes deregulated at 2 hour by morphine), Mor0-6 group (genes deregulated at 6 hour by morphine), Oxy0-6 group (genes deregulated at 6 hour by oxycodone) and Bup0-6 group (genes deregulated at 6 hour by bupivacaine). Although correlating RIN with intensity could have been done prior to ANOVA, due to time constraints and likelihood of user-introduced errors inherent in correlating 47,000 probesets, it was performed as a post-hoc test. Transcripts with r values $\geq \pm 0.7$ demonstrated a correlation between RNA degradation and intensity and were discarded from the lists.

2.3.1.5 Pathway enrichment

Gene lists were entered into DAVID Ontology Software. DAVID is an acronym for Database for Annotation, Visualisation and Integrated Discovery. It was developed by the Laboratory of Immunopathogenesis and Bioinformatics in 2003 and contains gene annotation information from a range of public genomic sources, representing over tens of millions of identifiers from over 65, 000 species. These are grouped into 1.5 million gene records, allowing for the enrichment of information available for any gene. DAVID was used to classify genes by biological function, pathway and cellular function using over-representation analysis (ORA).

DAVID generates a list at random containing the same number of genes as the list of genes imported, then classifies both lists by biological function,

pathway or cellular function. It uses the Fisher test (which calculates the deviation of each list from the null hypothesis) to calculate if pathways or functions are overrepresented in the list of imported genes.

2.3.1.6 Hierarchical clustering

Hierarchical clustering can be used to find similarities between genes and arrays. Clustering was performed in Cluster 3.0. Data was filtered to remove genes that did not have at least 1 observation with absolute value ≥ 5 and those whose maximum – minimum values were less than 2. Genes were centred to the median then both genes and arrays were clustered using Euclidean distance. Average linkage was used to calculate the difference between values, and data produced was visualized in TreeView.

2.3.1.7 Binomial logistic regression

Binomial logistic regression (LR) aims to predict the most likely one of two possible outcomes for a dependent variable, when the independent variable is known. In this case, the outcome / dependent variable (treatment or not, with a specific analgesic) was already known, and the aim was to predict which variables were most strongly correlated with it, using binomial logistic regression. The independent variables used were the genes in each group, with the pertinent values being logged and normalized intensity values. The dependent variable was the use or otherwise of morphine / oxycodone.

LR was performed in SPSS v22 using a forward conditional stepwise method. In this method, the equation begins with no variables, then they are added one by one starting with that most strongly correlated to outcome. Once no further improvements can be made to the R-value, no further variables are added. Each opioid group underwent LR, using the relevant treatment as the

dependent factor. This was done four times per group (once per timepoint) for Mor0-2, Mor0-6 and Oxy0-6 groups.

2.3.1.8 Receiver operating characteristic

Receiver operating characteristic (ROC) curves are used to represent the accuracy of prognostic testing, and show false positives versus true positives. Traditionally used in prognostic testing, drawing a ROC curve involves ranking numerical values from low to high then plotting the fraction of true positives v false positives for each result. In this case, ROC was used to represent the accuracy of genes found to be predictive through LR and to investigate the importance of those that were highly up- or down-regulated in each group.

Logged and normalized intensity values were the ranked numerical results, subjects given morphine were generally patients, and subjects given oxycodone or bupivacaine were generally controls. (If ROC was calculated for a gene deregulated only by oxycodone, then oxycodone was the patient group and the other treatments the controls). ROC curves were generated in GraphPad Prism for all genes significant through LR in Mor0-2, Mor0-6 and Oxy0-6 groups, and all top 10 up- and down-regulated genes in these groups and Bup0-6. Separate curves were generated at each timepoint.

2.3.2 Cortisol ELISA analysis

Mean optical density (OD) was calculated for the two non-specific binding wells then subtracted from each standard / sample value. Adjusted standard values were used to draw a 4-parameter logistic (4-PL) dose-response curve in GraphPad Prism, where x = cortisol concentration and y = optical density. 4PL curves use four parameters; the response at 0 concentration; the steepest gradient of the curve; the inflexion point at which the gradient slows

to change from concave upwards to concave downwards and the response at infinite concentration. The minimum y-value was also constrained to a value of 0 as all values had been blanked by subtracting the mean NSB.

Sample ODs were interpolated from the curve, the mean of duplicate samples was calculated, inverse logged and multiplied by 20 (to take account of initial serum dilution). Data was imported into SPSS v22; 0 and 6 hour samples for each subject were paired and dependent-samples T tests performed per treatment group. One-way ANOVA was performed at 0 and 6 hour for all treatment groups to rule out timepoint differences between treatment groups.

2.3.3 CBA analysis

Cytokine concentrations were imported into SPSS v22 and dependent-samples T tests performed between 0 and 6 hour cytokine per treatment group. One-way ANOVAs were performed separately at 0 and 6 hour per cytokine between treatment groups to rule out timepoint differences between treatment groups. T-tests and ANOVAs were performed for each of the 7 cytokines measured.

2.3.4 NKCC assay analysis

Number of events were imported into SPSS v22 and medians and percentage changes calculated for all samples. Unstimulated cells were the control and stimulated cells were the test group; the most important test was comparing differences between treatments in stimulated cells at 6 hour, for which Kruskall Wallis, a non-parametric test suitable for small datasets and unpaired data, was used. It was also used to investigate initial differences at baseline, and for the same tests in unstimulated cells.

Non-parametric Wilcoxon signed ranks tests were used to compare changes between 2 datasets. Using this test, changes were compared between unstimulated and stimulated cells for each treatment at each timepoint, between unstimulated cells for each treatment between timepoints and between stimulated cells for each treatment between timepoints.

Chapter 3

Gene expression analysis

3.1 Introduction

The history of the use of morphine is long and fascinating; morphine was probably used even in the stone age [7]. Experimental evidence of the immunosuppressive nature of morphine has existed since 1897, when Coronedi et al published work showing that high doses of morphine made dogs unusually susceptible to *Diplococcus lanceolatus* [7]. Research in guinea pigs demonstrated that animals given morphine showed reduced leukocyte trafficking and phagocytosis *in vitro* [9] and a higher fatality rate following TB infection than controls (Tedeschi, 1899; Oppel, 1902; [7]). However, evidence in humans may have been published as early as the mid 16th century following the death of a probable malaria patient after an experimental opium dose [7]. By the end of the 19th century, several physicians (Thomas Whipham 1875, Osler et al 1880, Isham 1882, Petit 1879) described complications of infections linked to morphine use [7].

More recently, *in vivo* animal experiments have shown that morphine reduces phagocyte count and killing properties in mice and rabbits [44], alters gene expression of MCHII molecules and lymphocyte proliferation in rats [104], increases bacterial growth in mice and rats [40, 55] and increases viral load in HIV-infected monkeys [56]. In mice with a bacterial burden from infection, morphine increases cytokine levels of IL-6 and IL-10 in plasma [40], although it has also been shown to decrease IL-6 in mice [65]. Morphine also induced a five-fold increase in TRegs of monkeys following a 12-week program of morphine administration [105].

Human studies show the suppression of lymphocyte proliferation in surgical cancer patients following morphine administration [48] and, in healthy volunteers, both the suppression of NK cell cytotoxicity (NKCC) [29] and possible early activation of membrane-associated signalling proteins [49]. *In vitro* addition of opioids to PBMCs showed oxycodone and diamorphine, but not morphine, decreased IL-6 production from IL-2 stimulated cells. Morphine showed a trend for suppression of phagocytosis and oxidative burst responses to *E coli,* in monocytes and neutrophils [30]. Morphine also inhibited production of IL-2 mRNA from T cells *in vitro* compared to other opioids, reversed by CTAP (a MOR antagonist). This was accompanied by increased intracellular cAMP levels [64], which activated protein kinase A with a subsequent enhancement of the inhibition of LCK, blocking TCR signalling.

Receptor genotype may play a part in the human response to the immunosuppressive effects of morphine. A11G, a SNP present in the MOR gene, results in reduced receptor transcription and reduced response to receptor binding and analgesic response when the G allele is present; the AA allele showed the greatest breast cancer specific mortality [106].

Clinical research has so far been mainly retrospective. A study comparing opioid prescriptions until death / cancer recurrence at the 10-year mark in breast cancer patients found recurrence to be lower in patients receiving highly immunosuppressive opioids; the authors suggest this may have been because other patients were deceased by this point [107]. A study of advanced cancer patients taking morphine but no other opioids showed reduced T cell proliferation with increasing morphine, seen only in those who

were not taking morphine at study enrolment [12], indicating that tolerance may develop to morphine-induced immunosuppression.

Prospectively, the large scale MASTER study in Australasia found no advantage of epidural anaesthesia / analgesia over general anaesthesia (GA) and opioid-induced analgesia, using clinical outcomes as an endpoint [37, 66, 67]. However, the epidural group received pethidine and fentanyl (only 5.6% of patients had a pure epidural infusion) and the opioid group received morphine, pethidine and fentanyl: fentanyl has been shown to induce NKCC suppression (Section 1.7.1 [68]). In patients undergoing TURP, an increase in TH1 percentage was seen with spinal anaesthesia compared to the propofol and morphine treatment group [62]; as propofol has been shown to be non-immunomodulatory [77], this effect is more likely to be attributable to morphine.

The design of this study aimed to compare two controls groups to a morphine group in a non-cancer patient cohort to remove confounding immune-modulating disease processes. Neither control group contained patients who received morphine and the epidural bupivacaine group contained only patients who received no opioid. All patients were given a propofol-only anaesthesia during surgery, as other anaesthetic agents including fentanyl [68] have been shown to be immunosuppressive, whereas propofol has not [77].

3.2 Aims

The main objective of this Results chapter was to identify unique patterns of lymphocyte gene expression following different intra- and postoperative analgesia.

3.3 Methods

3.3.1 Subject recruitment

Subjects were recruited as described in Chapter 2. Sixty patients were recruited in total to the study; patient withdrawals are summarised in Section 3.4.

3.3.2 Cell separation and RNA microarray

Whole blood was taken from patients at timepoints of 0 hour (pre-treatment), and 2, 6 and 24 hour (post-treatment). Mononuclear cells were removed using the Ficoll-Hypaque technique then CD4+, CD8+ and NK cells separated via positive (CD4+, CD8+) and negative (NK) magnetic separation (Miltenyi Biotec). RNA was extracted using Qiagen RNeasy kits and frozen (-80°C) for array hybridisation. At least 3 samples were needed for a patient's samples to be analysed, as the 6 hour timepoint was chosen for serum assays.

150ng of mRNA for each of 40 patients was used at each timepoint for gene expression, with the exception of 24 hour as only 36 patients had a 24 hour sample. Microarray data is susceptible to experimental variation due to the large numbers of samples processed, caused by experimental design, pipetting errors, inconsistent reagent use, varying operators or scanning machine temperature. To minimize variation, the same operator (MD) always prepared RNA for hybridisation to arrays; RNA was then passed to the Affymetrix processing core facility at QMUL for hybridisation to arrays. To control for the effects of machine temperature on hybridisation, samples were grouped into as few batches as practically possible, and treatment groups were evenly stratified across batches, in a 2:2:1 ratio as below. Although slightly more than 40 patients had RNA from at least three timepoints, in order to maintain an even stratification, only 40 patients were used. Patients

were allocated to a processing batch numerically from subject 1; if blood clots had been noted on receipt of samples, RNA was not used. The 156 samples from 40 patients were therefore divided into 8 batches, giving a maximum of 20 samples per batch.

3.3.3 Statistical analysis

3.3.3.1 Data normalization

Array data was imported as CEL files to Partek Genomics Suite v6.6 (Partek Incorporated, Missouri USA). Data was corrected and normalised using full RMA (robust multi-array average) normalisation, which includes correction for background noise, quantile normalization, log to base 2 transformations and probe set summarisation using median polish.

3.3.3.2 Identification of differentially expressed genes

ANOVA was performed on logged and normalized intensity values in Partek, with independent variables of RIN, time, treatment, and time x treatment. Post ANOVA, p-values were adjusted for False Discovery Rate using the Benjamini-Hochberg step-up method, and differentially expressed genes were identified. Those genes taken to be significant were those with an adjusted fold change $\geq \pm 2$ and p-value ≤ 0.05.

Genes that were differentially expressed from baseline in each treatment group were recorded, with the focus of further analysis on the timepoint that showed the maximal effect on gene expression: morphine at 2 hour and oxycodone at 6 hour. The null hypothesis was therefore one of no difference between baseline and later timepoints, in all treatments.

3.3.3.3 Quality control

All samples were measured for quality using the Nanodrop spectrophotometer at 3 points - following RNA extraction, prior to amplification then again prior to fragmentation. 260/280 ratios and RNA quantity were recorded for all samples. About 70% of samples had 260/280 ratios above 1.7, indicating good quality; those with lower 260/280 ratios tended to also have lower RNA concentrations (below 26ng/µl). As there is a lot of variability in nanodrop measurements at RNA concentrations below 50ng/µl, the lower ratio was assumed to be due to the lower RNA concentration and samples were processed regardless. Nanodrop data can be found in Appendix B.

3.3.3.4 RIN and effect on fluorescing intensity

The Agilent Bioanalyzer was used to measure the RNA Integrity Number (RIN) - a measurement of the integrity of RNA. It measures the 18S and 28S ribosomal subunits in RNA and displays their abundance via 2 peaks in an electropherogram; smaller RNA fragments are also represented. RIN is calculated using the total area under the graph; electropherograms showing examples of RNA integrity in our sample cohort are shown in

Figure 3.1. The lack of statistically significant differences in RIN across treatment groups and timepoints is shown in Section 3.5.2. (All data can be seen in Appendix B).

RIN of samples hybridised to arrays ranged from 0 to 9.4 (degraded to intact RNA); due to this data spread, RIN was correlated with fluorescing intensity using Pearson correlation (Excel) for all samples, to examine if degraded RNA was correlated with intensity. This was performed for all deregulated probes in Mor0-2 group (genes deregulated at 2 hour by morphine), Mor0-6 group

(genes deregulated at 6 hour by morphine), Oxy0-6 group (genes deregulated at 6 hour by oxycodone) and Bup0-6 group (genes deregulated at 6 hour by bupivacaine). Groups were compared separately using only relevant samples; for example intensity values for the 583 probes in Mor0-2 group were correlated with RIN for 32 samples only - 16 from morphine 0 hour and 16 from morphine 2 hour. Probes with r-values ≥±0.7 demonstrated correlation between RNA degradation and intensity, and were discarded from future analysis. Examples of a correlated versus a non-correlated gene are shown in

Figure 3.2.

Electropherograms of unamplified RNA

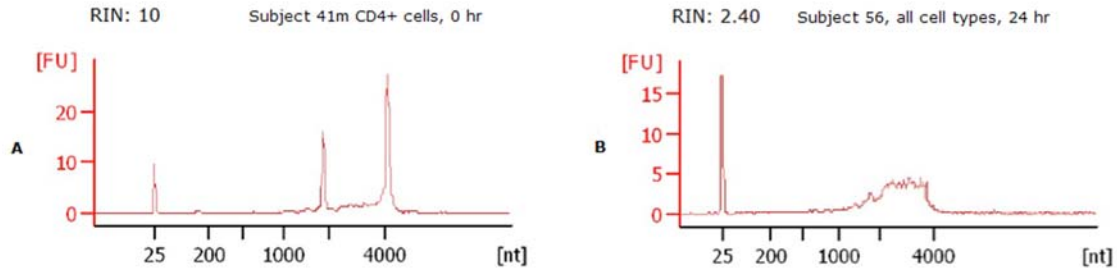

Figure 3.1: electropherograms showing A: unamplified RNA with a perfect RIN, B: degraded RNA.

Correlation of RIN to fluorescing intensity

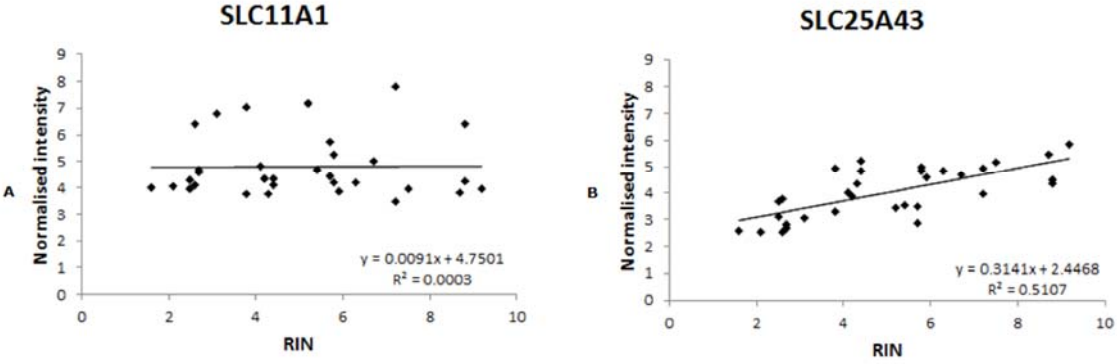

Figure 3.2: Normalised intensity versus RIN for all 0 and 2 hour arrays in the morphine group for two genes showing A (SLC11A1): no correlation and B (SLC25A43) correlation (Pearson correlation coefficient of 0.72).

3.3.4 Analysis of differentially expressed genes

Each group of differentially expressed genes was analysed separately, using several different methods.

Genes were ordered by fold change, and the most highly up- and down-regulated genes were annotated to investigate their relevance to the clinical question of morphine-induced versus oxycodone-induced changes.

Over-representation analysis (ORA) was performed in DAVID v6.7 to identify biological pathways that were enriched. DAVID generates a gene list at random containing the same number of genes as the list of probes imported into the software. It classifies both lists by biological pathway, cellular component or molecular function and uses the Fisher test (which calculates the deviation of each list from the null hypothesis) to calculate which pathways / functions are overrepresented in the list of imported genes.

Clustering of data was performed in Cluster 3.0 (http://bonsai.hgc.jp/~mdehoon/software/cluster/index.html). Data was filtered to include at least 1 observation with absolute value ≥ 5.0 and maximum value – minimum value ≥ 2.0. Filters were applied in all groups. Genes were centred on the median and both genes and arrays were clustered using Euclidean distance. Average linkage was used to draw dendrograms then data was visualized in Treeview v1.6 (http://www.eisenlab.org/eisen/?page_id=42).

3.4 Clinical results

3.4.1 Patient recruitment

The pathway of patients from consent to completion is shown in Figure 3.3. The high level of patient withdrawal necessitated a mid-study increase in patient recruitment targets, to achieve sufficient completed patients. Of 57 patients enrolled, 53 received study drug and 42 completed the study, with 47 patients providing at least 3 blood samples (Figure 3.3).

3.4.2 Sample processing

As discussed in Section 3.3.2, not all patients enrolled were included in the Affymetrix analysis. The numbers of patients initially enrolled to each treatment group compared to those whose RNA was subsequently analysed with Affymetrix arrays can be seen in Table 1. Patient samples were grouped into batches, with all samples for 5 patients in 1 batch. The allocation of patients to batches is shown in Table 3.2.

Patient enrollment and progress pathway

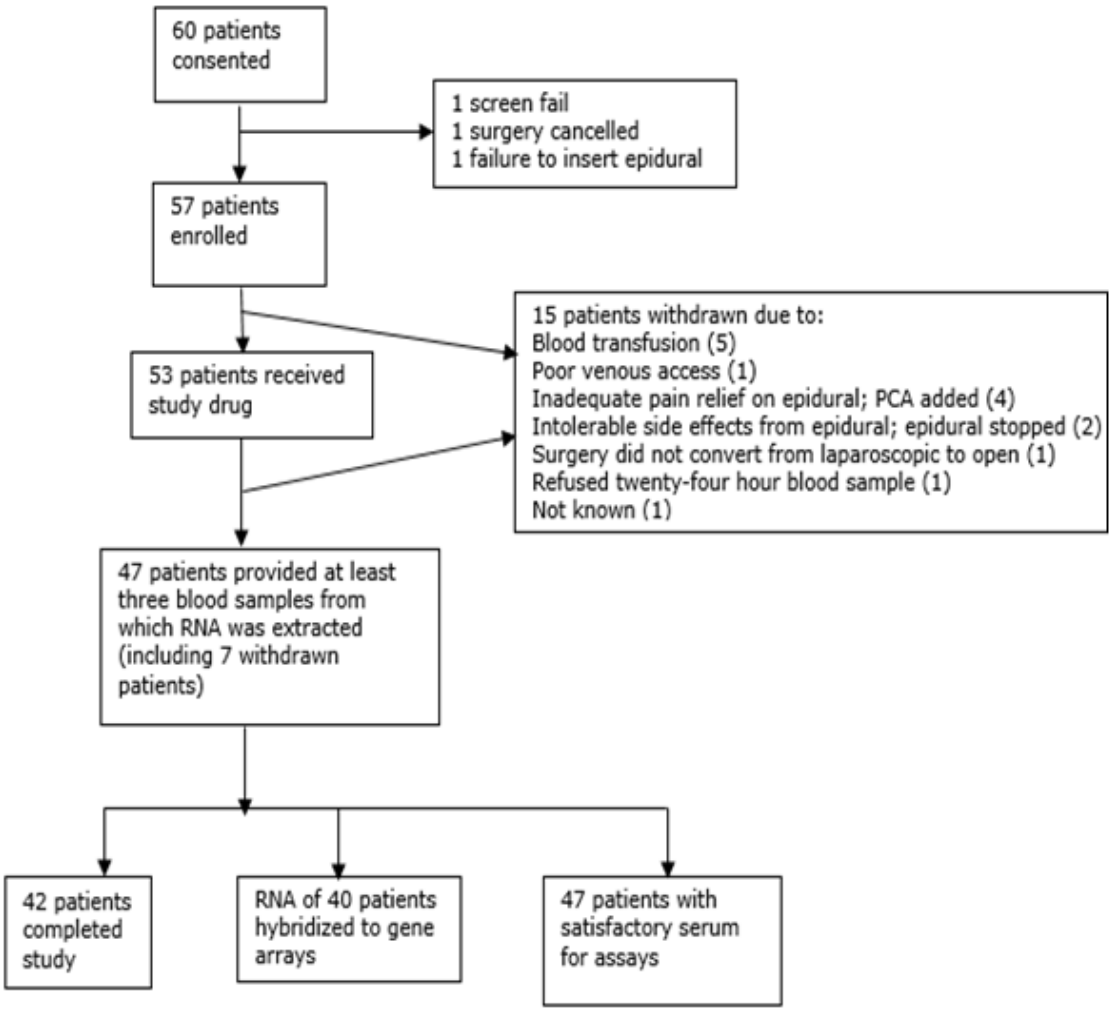

Figure 3.3: The pathway of patients from consent to withdrawal / completion

Table 3.1: Number of patients enrolled per treatment group whose RNA was subsequently analysed by microarray, showing that not all subjects enrolled were used, mainly due to early withdrawals.

Treatment	Patients enrolled (N°)	Patients with at least 3 samples taken (N°)	Patients completed (N°)	Analysed by microarray (N°)
Morphine	22	18	17	16
Oxycodone	19	17	17	16
Epidural	12	12	7	8

Table 3.2: Subjects allocated to each microarray group. Patient samples from each analgesic treatment were spread evenly across groups to avoid batch effect.

Group	Scan date	Morphine	Oxycodone	Bupivacaine
1	4-Sep-12	48, 50	44, 49	51
2	7-Sep-12	31, 35	23, 26	39
3	28-Sep-12	40, 47	9, 34	41
4	23/24-Oct-12	52, 53	55, 56	54
5	30-Oct-12	21, 22	18, 19	36
6	8-Nov-12	45, 57	30, 33	46
7	15/16-Nov-12	1, 2	3, 6	24
8	20-Nov-12	13, 14	15, 29	32

3.4.3 Clinical characteristics of patient cohort used for microarray analysis

Clinical characteristics of those patients allocated to the Affymetrix group were analysed and are displayed in Figure 3.4 and Figure 3.5. (The full set of clinical and statistical data can be found in Appendix A). BMI, age and operation duration were compared between all 3 treatment groups using one-way ANOVA and Kruskal Wallis; no statistically significant differences were seen.

Data was collected for any evidence of varying postoperative infection rates between groups; of 41 sets of patients notes read, 1 bupivacaine and 1 oxycodone patient had postoperative infections that needed treatment with antibiotics.

The modal operation type was open myomectomy (23/40 microarray patients) although this was not represented equally across treatment groups (Figure 3.5); just 1/8 bupivacaine patients underwent open myomectomy compared to 9/16 morphine and 13/16 oxycodone group patients.

Clinical characteristics for microarray patient cohort

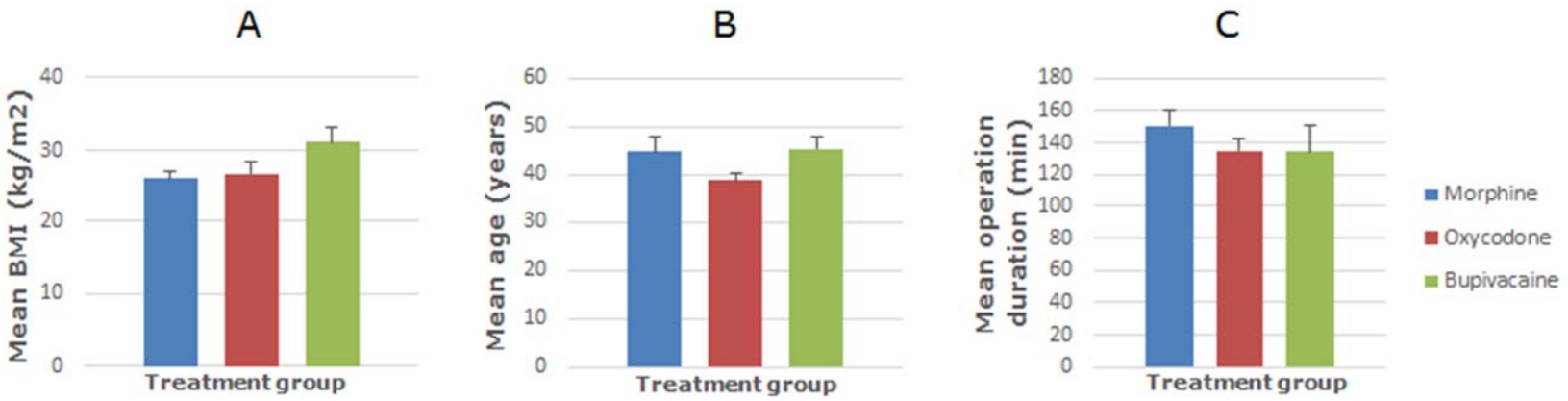

Figure 3.4 showing A: mean BMI, B: mean age and C: mean operation duration for all 3 treatment groups. No statistically significant differences were found between treatment groups for any measurement. Error bars given are SEM.

Operation types for microarray patient cohort

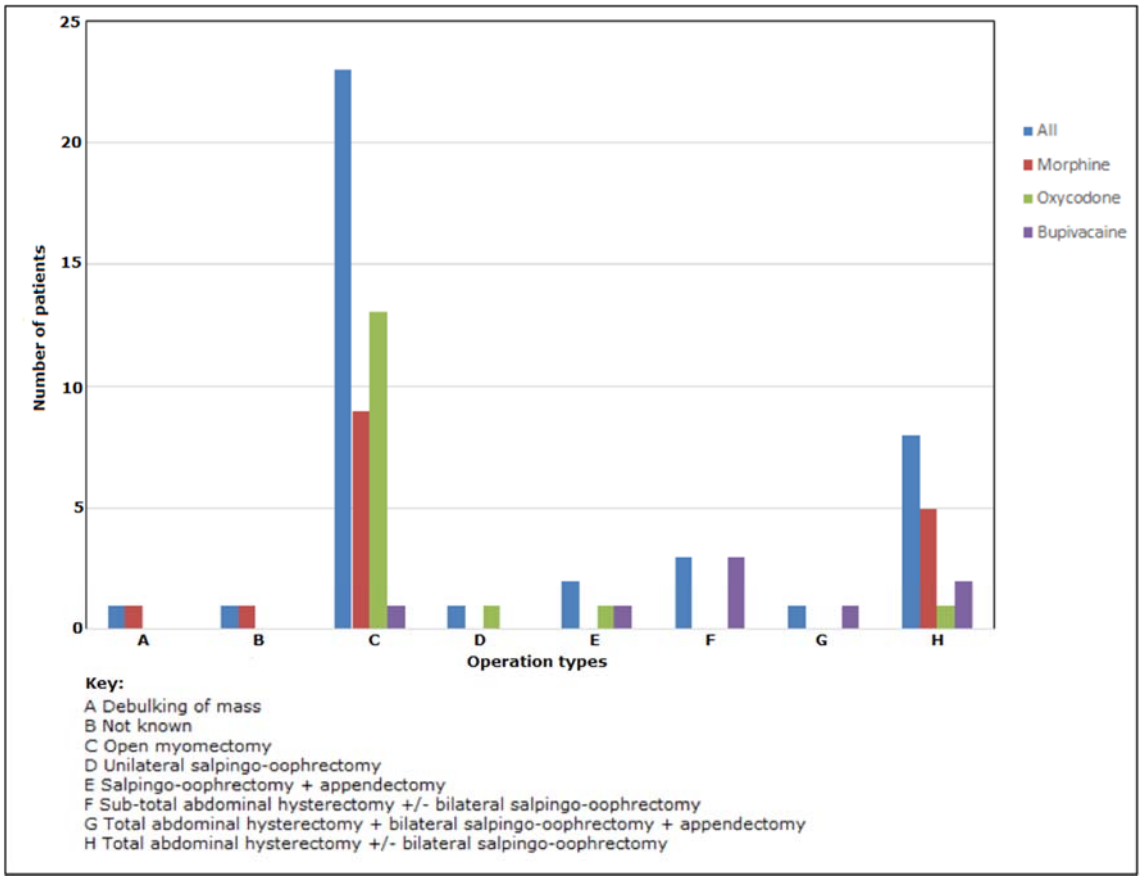

Figure 3.5: Operation types for microarray patient cohort, for all patients and treatment groups, showing the uneven spread of open myomectomy across treatment groups.

3.4.4 Pain scores of microarray patient cohort

Pain scores were recorded for all patients at each timepoint, using the 11-point Numerical Rating Scale (NRS), except where patients were unconscious (frequently the case at 2 hours). Pain scores were compared across treatment groups at each timepoint, using one-way ANOVA and Kruskal Wallis (SPSS v22) for the microarray patient cohort only. No significant difference was found in pain scores between different treatment groups at any timepoint. Data is shown in Appendix A.

The median pain score was 0 in all treatment groups at both baseline and 2 hours with some outliers. As the pre-operative timepoint, no pain was expected at baseline; the pain reported by subject 24 was likely due to their underlying condition or an adverse event. At 2 hours most patients remained unconscious and did not report pain; those six who did report pain were therefore displayed as outliers. Although the number of outliers varied across treatment groups, no statistically significant difference was found at 2 hours between treatment groups. At 6 and 24 hours, the spread of pain scores was more normal, with no outliers and still no statistically significant differences between treatment groups.

Pain scores for microarray patient cohort

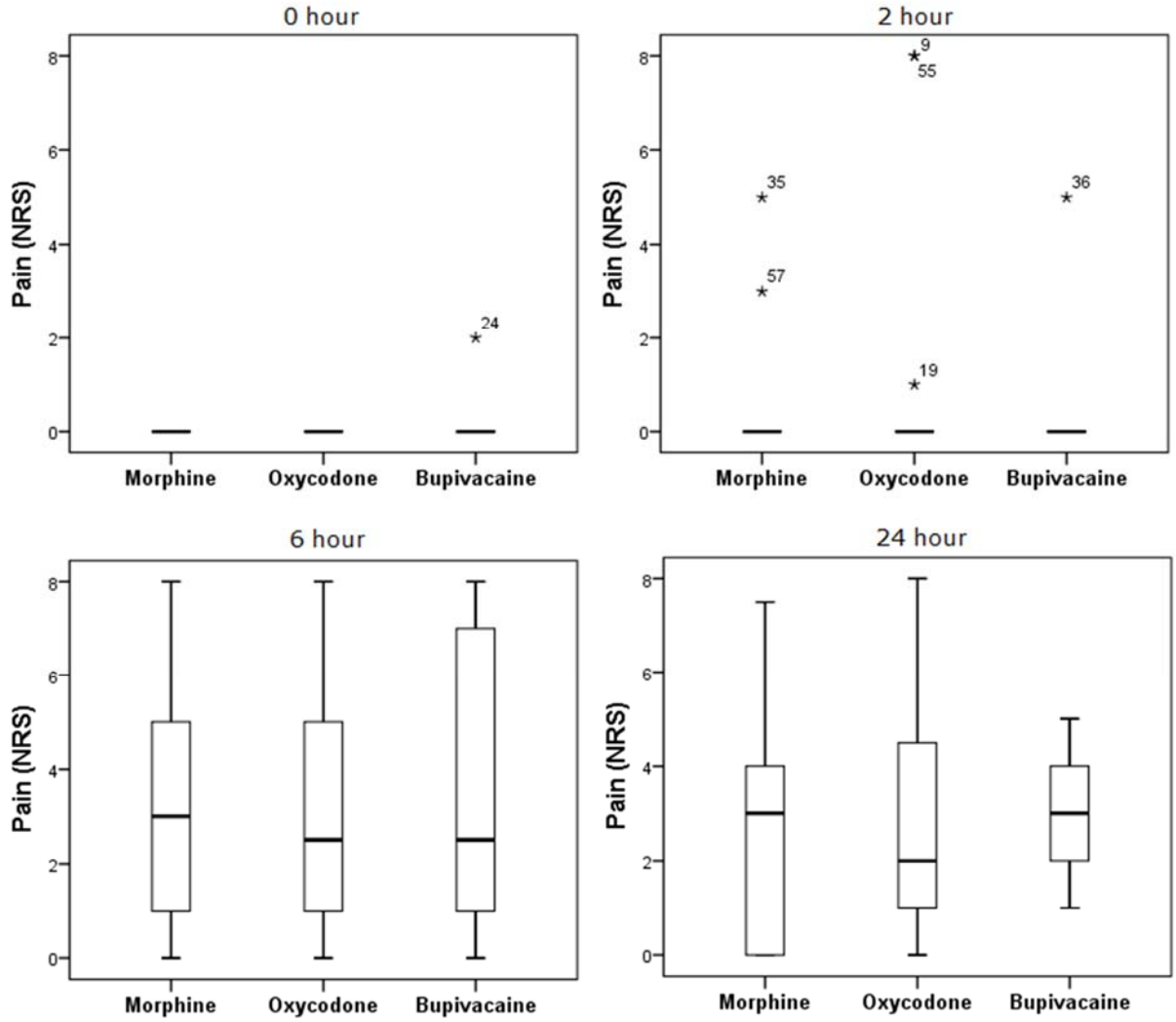

Figure 3.6: Pain scores from the Numerical Rating Scale (NRS) at each timepoint for all 3 treatment groups. The interquartile range is shown; box whiskers show the highest and lowest values not defined as outliers (> 1.5 box lengths outside the box).

3.4.5 Opioid use for microarray patient cohort

Opioid use was recorded in both patient CRFs and hospital notes. In CRFs, cumulative opioid given was recorded at each timepoint. In hospital notes, opioid use was recorded in nursing observational notes with variable frequency. To investigate differences in total opioid use between groups, CRF data was used except where incomplete, when hospital notes were used. Means of cumulative opioid use were compared between the morphine and oxycodone groups at each timepoint, using an independent samples 2-tailed t-test, for the microarray patient cohort only. No statistically significant difference was found in opioid use between opioids at any timepoint, as expected due to their equianalgesic nature on intravenous use. Non-cumulative opioid doses were also calculated and independent samples t-tests performed to compare any difference between treatment groups; again no statistically significant difference was found. Data can be seen in Appendix A.

Mean cumulative opioid doses for microarray patient cohort

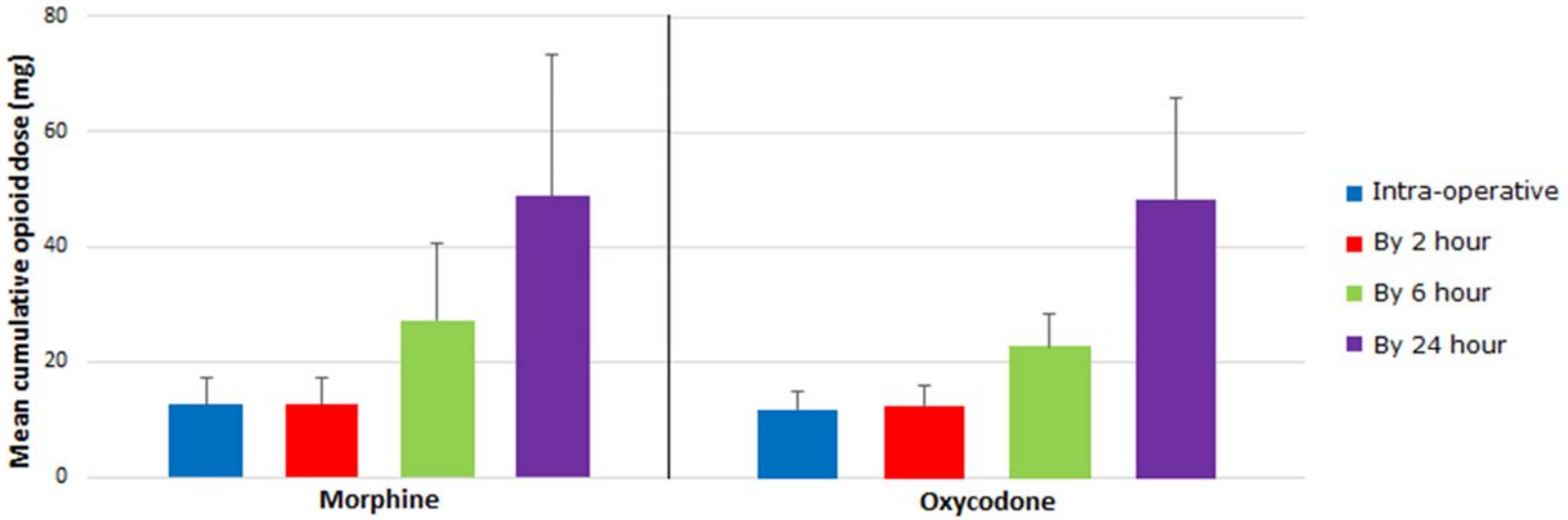

Figure 3.7: Means of cumulative opioid doses of morphine and oxycodone for the microarray patient cohort. Error bars given are SD.

3.5 Affymetrix Results

3.5.1 Normalising and batch effect

Raw intensity values were normalized and summarized in Partek prior to analysis. Pre- and post-normalisation intensities can be seen in Figure 3.8 and Figure 3.9. It can be seen that, post-normalisation, arrays have a similar distribution around the median compared to pre-normalisation; however outliers are now aligned more closely with the main data. Distribution of data is now more consistent across the samples with the median of each sample being equivalent.

A principal component analysis (Figure 3.10) was also performed, confirming that scan date did not import a difference to intensity values.

Fluorescing intensity values pre-normalisation

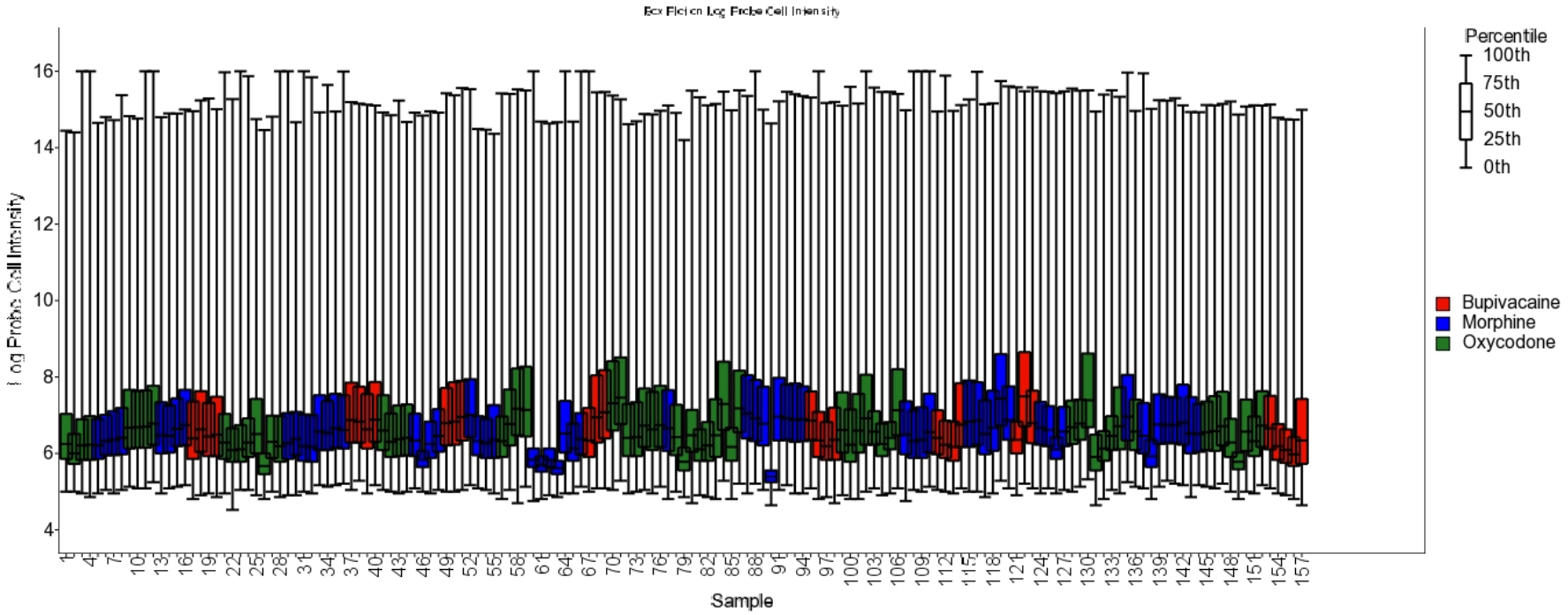

Figure 3.8: Pre-normalisation fluorescing intensity values for all 156 samples that underwent Affymetrix analysis. Figure generated using Partek software. Only 156 samples underwent Affymetrix analysis as 4 subjects did not have a 24 hour sample.

Fluorescing intensity values post-normalisation

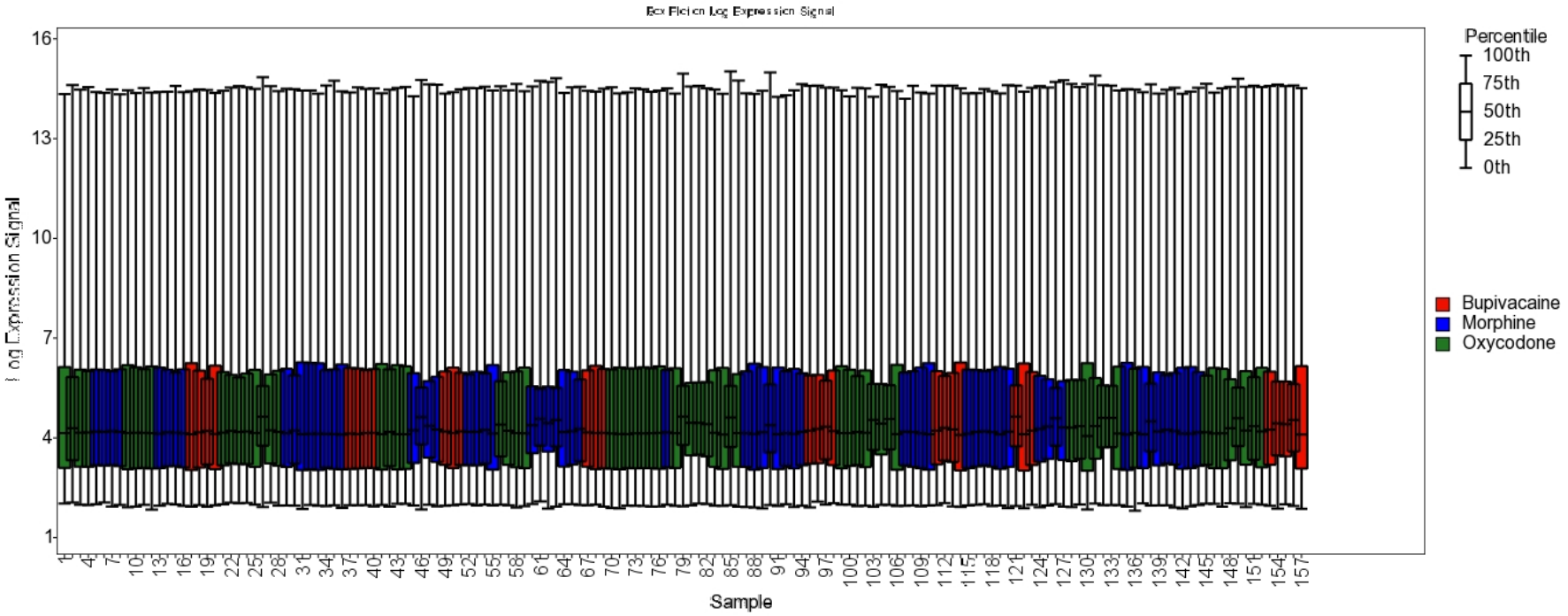

Figure 3.9: Post-normalisation fluorescing intensity values for all 156 samples that underwent Affymetrix analysis. Arrays have undergone RMA; figure generated using Partek software. Only 156 samples underwent Affymetrix analysis as 4 subjects did not have a 24 hour sample.

Principal components analysis showing lack of batch effect

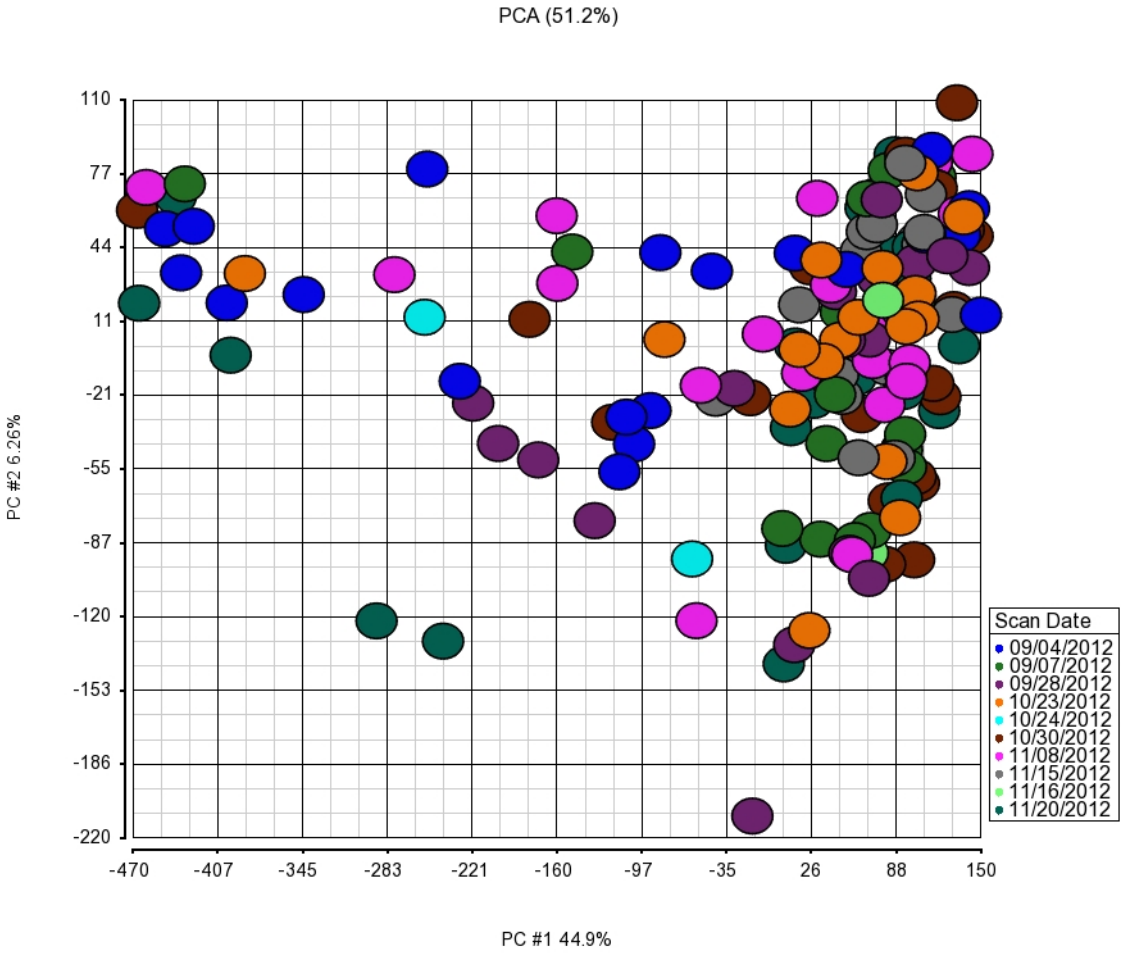

Figure 3.10: Principal components analysis showing absence of batch effect in sample processing.

3.5.2 Variance in RIN

Although somewhat degraded, RNA was not disproportionately degraded in any 1 treatment group or timepoint. One-way ANOVA was performed in SPSS and no statistically significant difference in RINs was found at any timepoint between treatment groups, or between timepoints in any treatment group (see Figure 3.11 and Figure 3.12, and Appendix B for data).

However, lower RINs indicate degraded RNA, which can produce poor hybridisation to arrays, reduced fluorescing intensity and abnormally high 3' 5' ratio in housekeeping genes. cDNA is synthesised from the 3' end of RNA, terminating at the 5' end, so degraded RNA will be underrepresented at the 5' end. Degraded RNA (defined as RNA with a low RIN) also produces more deregulated transcripts following microarray analysis [108]. The removal of probes whose RIN correlated with intensity values (Section 3.3.3.4) was designed to correct for the variable levels of RNA degradation seen across samples. Seven probes were removed from Mor0-2 group and 2 from Bup0-6 group - the resulting numbers of differentially expressed genes for each group are shown in Table 3.3. Numbers given indicate total genes for each treatment group, and therefore include any that were also differentially expressed by other treatments or at other timepoints.

Variance in RIN across treatments and timepoints for microarray patient cohort

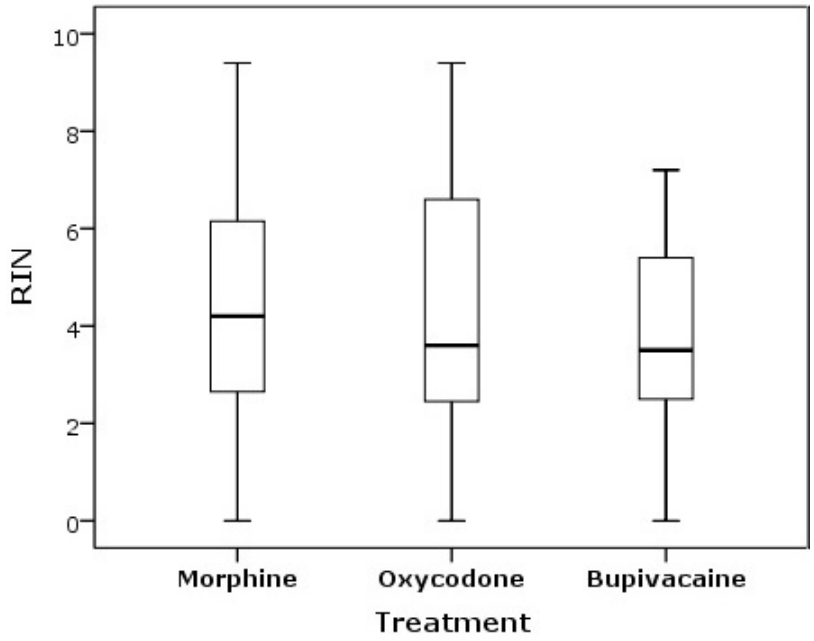

Figure 3.11: The spread of RIN values across treatments. The interquartile range is shown; box whiskers show the highest and lowest values not defined as outliers (> 1.5 box lengths outside the box).

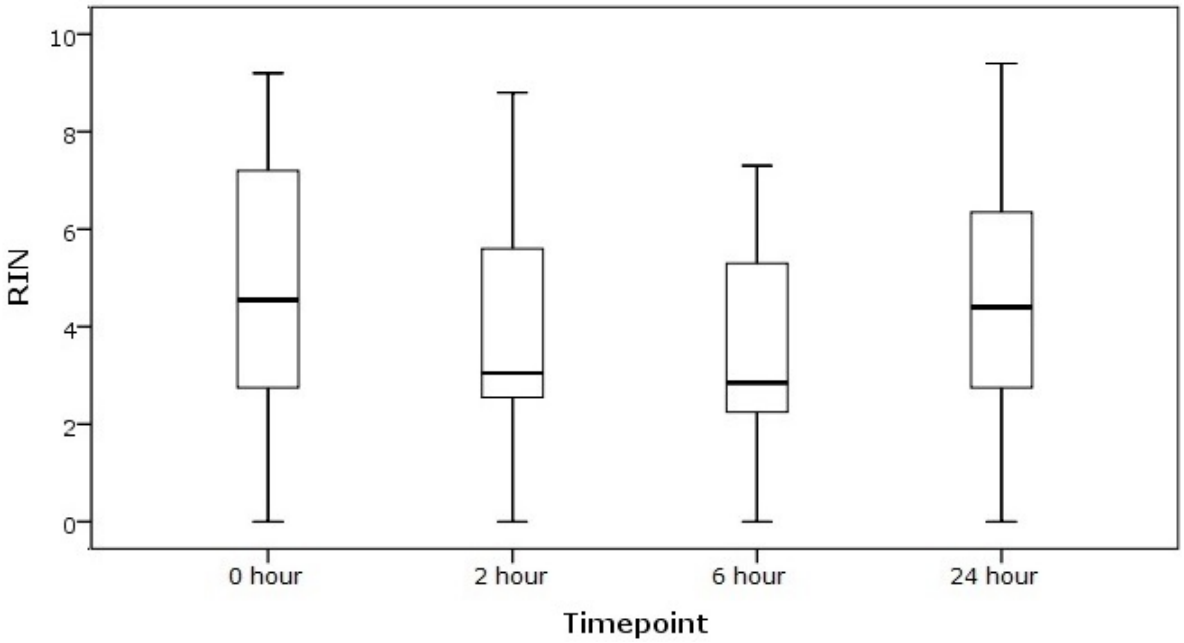

Figure 3.12: The spread of RINS across timepoints. The interquartile range is shown; box whiskers show the highest and lowest values not defined as outliers (> 1.5 lengths outside the box).

3.5.3 Identification of differentially expressed genes

Following ANOVA and removal of probes whose intensity could be correlated with RIN, differentially expressed genes with FC≥2 and FDR-adjusted p-value≤0.05 were identified. Genes were found in most, but not all groups. (For example, no genes were found in Bup0-2 and Bup0-24). Both the numbers of probes and the numbers of genes found in each group are given in Table 3.3 below.

Table 3.3: Numbers of genes identified per group with criteria of FC≥2 and p-value≤0.05.

			Probes deregulated from baseline (Gene totals in parentheses)		
Time-point	**Treatment**	**Group**	**Up-regulated**	**Down-regulated**	**Total**
2 hr	Morphine	Mor0-2	101	475	576 (520)
	Oxycodone	Oxy0-2	3	0	3 (3)
	Bupivacaine	Bup0-2	0	0	0
6 hr	Morphine	Mor0-6	156	2	158 (113)
	Oxycodone	Oxy0-6	790	20	810 (559)
	Bupivacaine	Bup0-6	19	30	49 (44)
24 hr	Morphine	Mor0-24	1	0	1
	Oxycodone	Oxy0-24	1	0	1
	Bupivacaine	Bup0-24	0	0	0

3.5.4 Volcano plots

Volcano plots, generated to visualise genes identified following ANOVA, clearly showed that the maximal effect in gene expression for morphine and oxycodone, at 2 and 6 hours respectively, had opposite directions of change. In both plots (Figure 3.13 and Figure 3.14), all genes with p-value<1 are shown; those genes of significance (FC≥±2; p≤0.05) are in the marked outer sections.

Volcano plot for all deregulated Mor0-2 genes

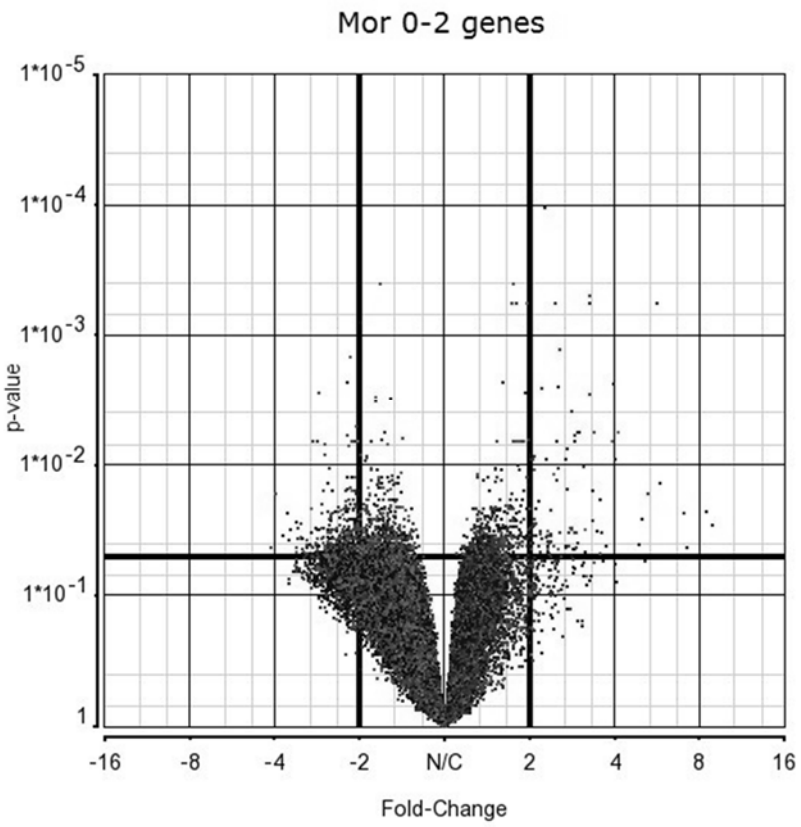

Figure 3.13: Volcano plot of fold-change against p-value for Mor0-2. This is the comparison with the maximal lymphocyte gene expression effect for morphine. All genes are shown; the 583 probes (including the 7 removed after correlation of intensity with RIN) with FC≥±2 and p≤0.05 are in the two outer sections.

Volcano plot for all deregulated Oxy0-6 genes

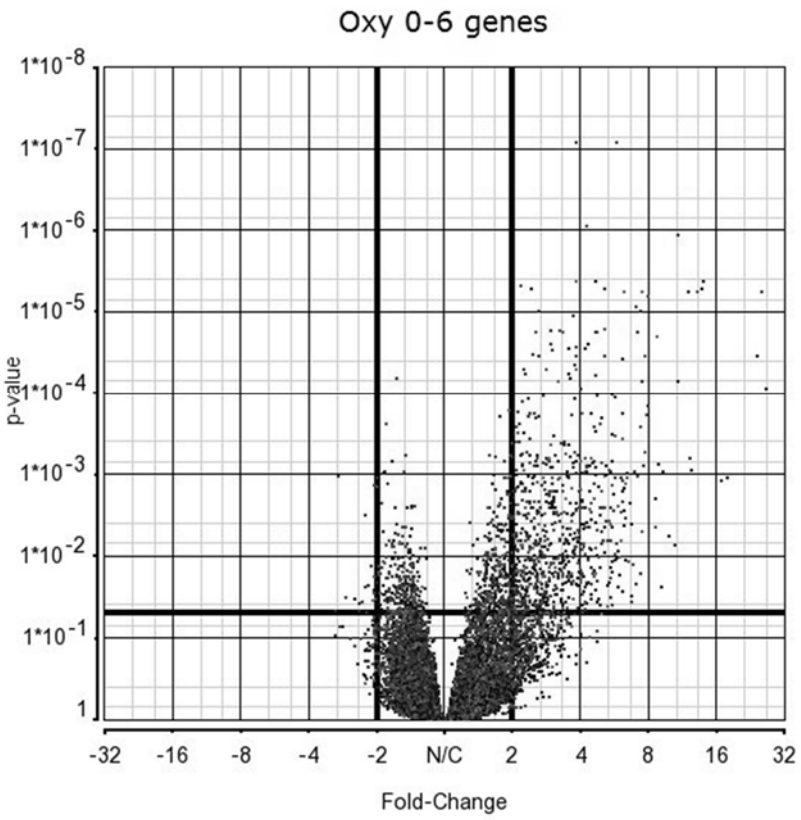

Figure 3.14: Volcano plot of fold-change against p-value for Oxy0-6. This is the comparison with the maximal lymphocyte gene expression effect for oxycodone. All genes are shown; the 810 probes with FC≥±2 and p≤0.05 are in the two outer sections.

3.5.5 Top 10 up- and down-regulated probes

Lists of top up- and down-regulated probes were generated for each group (Table 3.4 - Table 3.7). It can be seen that there is much commonality in highly perturbed genes between treatment groups, as illustrated in the Venn diagram (Figure 3.15). Those genes commonly deregulated always have the same vector of change from baseline, regardless of treatment group. Demonstrating the unique down-regulation of Mor0-2, of all 421 down-regulated genes, only 13 are also deregulated by another treatment, 9 by oxycodone and 4 by bupivacaine. Genes strongly deregulated between *all* treatment groups are up-regulated.

Genes were not deregulated by each treatment at all timepoints; the key groups of deregulated genes, by number of genes perturbed, were Mor0-2 and Oxy0-6, with 520 and 559 genes respectively. These timepoints define the maximal effect of each method of analgesia on lymphocyte gene expression; analysis therefore focused on these groups.

Table 3.4: top 10 up- and down-regulated probes for Mor0-2 gene group.

Mor0-2			
Down-regulated		**Up-regulated**	
Gene	**FC**	**Gene**	**FC**
RCAN3	-4.0978	ARG1	8.9415
AQP3	-3.962	IL1R2	8.4209
CX3CR1	-3.7204	MMP9	7.2341
CREBL2	-3.6165	IL1R2	7.0614
TRAC	-3.5703	CRISP3	5.7943
KLF10	-3.5147	FOXC1	5.6606
BCL11B	-3.3616	ANKRD22	5.242
CD28	-3.3541	SAMSN1	5.0094
NDUFA12	-3.3449	VNN1	4.8867
229629_at	-3.3249	CLEC4E	4.131

Table 3.5: top up- and down-regulated probes for Mor0-6 gene group.

Mor0-6			
Down-regulated		**Up-regulated**	
Gene	**FC**	**Gene**	**FC**
FCER1A	-4.0447	IL1R2	30.1622
FLT3LG	-3.086	IL1R2	26.6013
		CD163	14.5325
		CD163	13.1387
		THBS1	12.0647
		C19orf59	9.0895
		THBS1	8.6255
		MS4A4A	7.4467
		CYP1B1	7.4457
		ACSL1	7.1703

Table 3.6: top 10 up- and down-regulated probes for Oxy0-6 gene group.

Oxy0-6			
Down-regulated		**Up-regulated**	
Gene	**FC**	**Gene**	**FC**
LRRN3	-3.0412	ARG1	26.515
NOG	-2.9491	IL1R2	25.3851
GLYR1 / SEPT6	-2.7426	IL1R2	24.439
NMT2	-2.5123	MMP9	17.9477
GATA3	-2.3973	ANXA3	16.8648
GATA3	-2.3751	CLEC4D	13.9846
VSIG1	-2.3062	CD163	13.8383
TCEA3	-2.259	CD163	13.1508
LFNG	-2.2309	ACSL1	12.4768
BACH2	-2.2279	ACSL1	12.1932

Table 3.7: top 10 up- and down-regulated probes for Bup0-6 gene group.

Bup0-6			
Down-regulated		**Up-regulated**	
Gene	**FC**	**Gene**	**FC**
UBASH3A	-5.2889	IL1R2	32.1056
NOG	-4.4101	IL1R2	28.2915
TCEA3	-4.3265	CD163	17.0523
FLT3LG	-4.1917	CD163	16.7398
SIRPG	-4.0381	C19orf59	9.6065
LMF1	-3.8517	CYP1B1	7.7916
AXIN2	-3.1435	CYP1B1	7.0159
MDS2	-2.8258	IRAK3	6.5001
LOC10050	-2.7875	SLC1A3	5.7867
KLHL3	-2.63	CD163	5.3203

Venn demonstrating similarities in highly perturbed genes between treatment groups

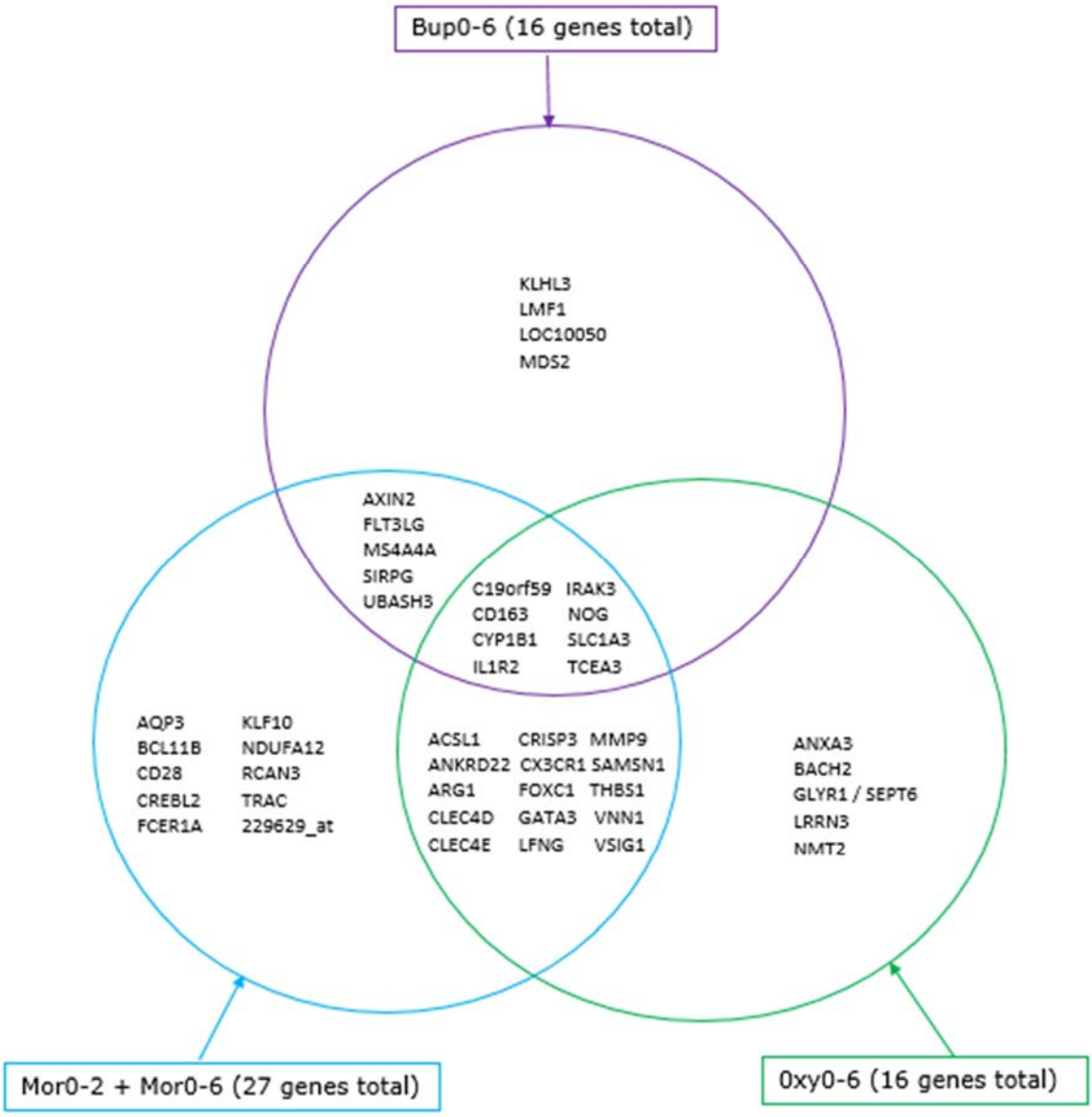

Figure 3.15: Venn showing similarities in top 10 up- and down-regulated genes between treatment groups.

3.5.6 Lymphocyte gene expression perturbed by morphine at 2 hours post treatment initiation

All genes were passed through DAVID ontological software, showing that 56 GO biological processes (p-value ≤ 0.01) were enriched, roughly divided into categories of RNA translation (particularly splicing of pre-mRNA), apoptosis, cell respiration, lymphocyte activation, cell division and enzyme activity (see Appendix B).

Removing probes also deregulated by either oxycodone or bupivacaine removes the general confounding effect of surgery and leaves 494 probes, 32 up-regulated; ORA was also performed on this group. The comparison of processes shown to be enriched following ORA of these 494 probes with those enriched following ORA of Oxy0-6 probes only (633 probes - Table 3.8) demonstrates that the enrichment of pathways related to RNA translation is unique to morphine treatment.

Hierarchical clustering was used to visualise the deregulated genes across 156 arrays (all timepoints and all treatments) in Figure 3.16. Logged and normalized intensity values were clustered in Cluster 3.0, and the results visualized in TreeView. Three gene clusters were seen, with the two end clusters containing up-regulated genes and the middle cluster containing all down-regulated genes. ORA of up-regulated genes produced 21 enriched processes, mostly related to apoptosis (12 similar processes were found in Mor0-2 only). ORA of down-regulated genes only produced enriched processes mainly relating to RNA translation and transcription, and cell respiration.

3.5.7 Lymphocyte gene expression perturbed by oxycodone at 6 hours post treatment initiation

Classification of genes by DAVID ontological software showed 104 processes (p-value ≤ 0.01) to be enriched, which could be divided into response to wounding, apoptosis, lymphocyte activation and cytokine production (Appendix B). Removing genes also deregulated by another treatment removes the general confounding effect of surgery and gives 633 probes, 10 down-regulated. ORA of these probes showed 55 enriched processes (p-value ≤ 0.01). In contrast to Mor0-2, no processes related to RNA translation / transcription were found (see Table 3.8).

A supervised cluster analysis was performed on logged and normalised intensity values for the 810 probes deregulated at 6 hours by oxycodone (Figure 3.17). Arrays are partially separated into treatment groups but do not fully resolve with clustering.

Supervised hierarchical clustering of all genes deregulated by morphine at 2 hours (gene list Mor0-2: 576 probes) for all 156 samples across all 3 treatment groups

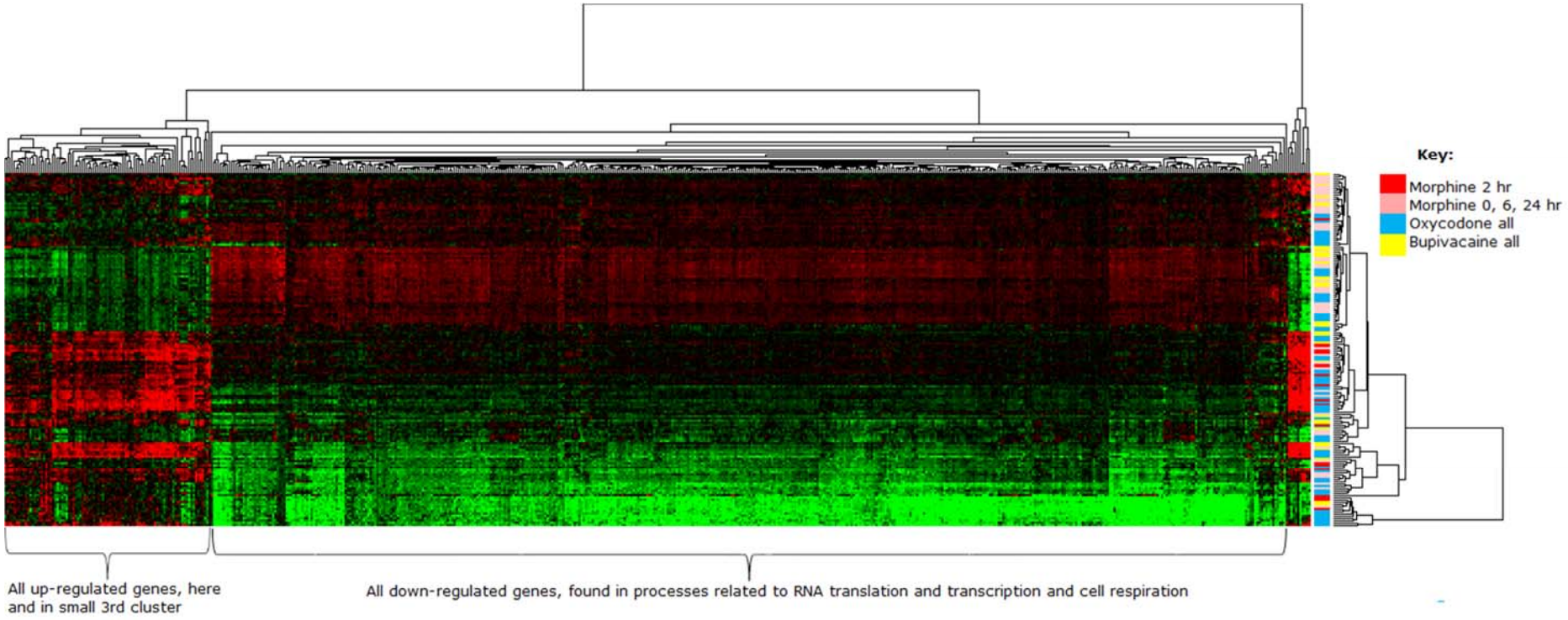

Figure 3.16: Supervised hierarchical cluster analysis for all 576 probes deregulated by morphine at 2 hours for all 156 arrays. 2 hours is the timepoint at which morphine induces its maximal effect on lymphocyte gene expression. Data was correlated by Euclidean distance and average linkage was used to create the linkage tree. Green pixels denote low mRNA expression and red pixels denote high mRNA expression. The key highlights the separation of arrays by treatment group and the separation of morphine 2 hour arrays from morphine arrays at all other timepoints.

Supervised hierarchical clustering of all genes deregulated by oxycodone at 6 hours (gene list Oxy0-6: 810 probes) for all 156 samples across all 3 treatment groups

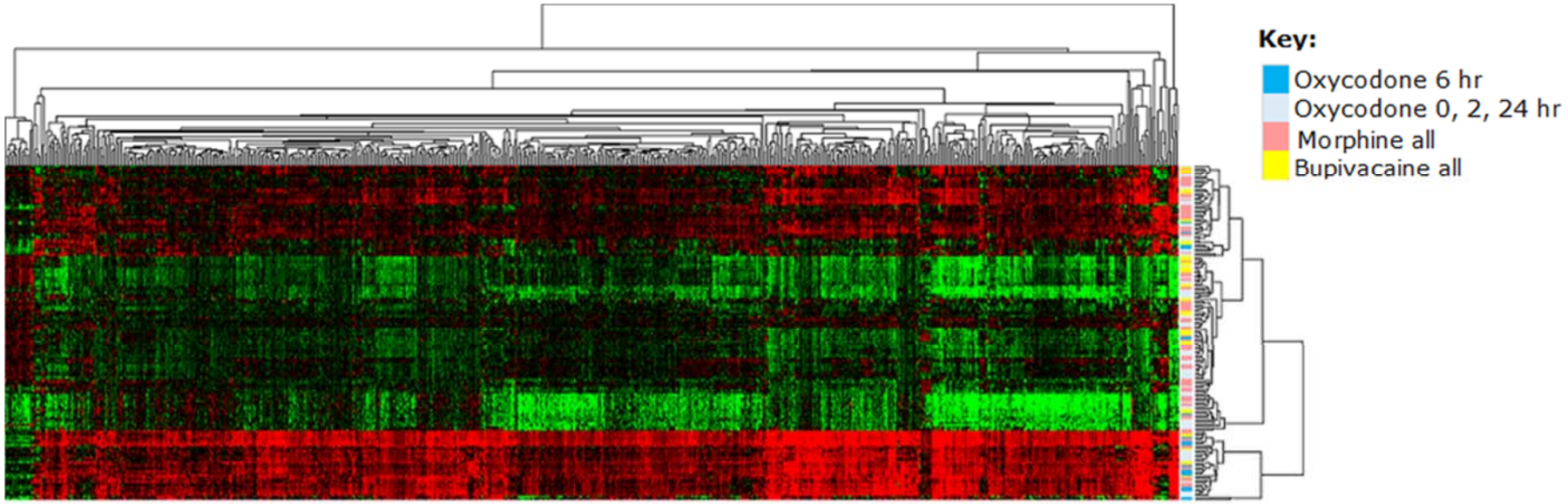

Figure 3.17: Supervised hierarchical cluster analysis for all 810 probes deregulated by oxycodone at 6 hours for all 156 arrays. 6 hours is the timepoint at which oxycodone induces its maximal effect on lymphocyte gene expression. Data was correlated by Euclidean distance and average linkage was used to create the linkage tree. Green pixels denote low mRNA expression and red pixels denote high mRNA expression. The key highlights the separation of arrays by treatment group and the separation of oxycodone 6 hour arrays from oxycodone arrays at all other timepoints.

Table 3.8: Summary of overrepresentation analysis highlighting biological processes enriched in genes significantly deregulated by A: morphine at 2 hours (450 genes / 494 probes) and B: oxycodone at 6 hours (460 genes / 633 probes). Top 20 processes by p-value are shown.

A: Biological processes – Mor0-2 (494 probes)	Genes	% of total input	p-value
translation	28	6.5	4.90E-08
ribonucleoprotein complex biogenesis	18	4.1	2.20E-06
RNA processing	32	7.4	1.40E-05
cellular macromolecular complex assembly	22	5.1	4.10E-05
cellular macromolecular complex subunit organization	23	5.3	7.60E-05
mRNA metabolic process	22	5.1	3.40E-04
RNA splicing, via transesterification reactions	13	3	4.00E-04
RNA splicing, via transesterification reactions with bulged adenosine as nucleophile	13	3	4.00E-04
nuclear mRNA splicing, via spliceosome	13	3	4.00E-04
macromolecular complex assembly	32	7.4	4.90E-04
ncRNA metabolic process	16	3.7	5.80E-04
macromolecular complex subunit organization	33	7.6	7.00E-04
regulation of apoptosis	36	8.3	7.50E-04
ribosome biogenesis	11	2.5	8.60E-04
regulation of programmed cell death	36	8.3	8.80E-04
regulation of cell death	36	8.3	9.20E-04
generation of precursor metabolites and energy	18	4.1	2.00E-03
electron transport chain	10	2.3	2.00E-03
activation of caspase activity	7	1.6	2.00E-03
mitotic cell cycle	20	4.6	2.10E-03

Key:

RNA translation
Apoptosis
Cell respiration

B: Biological processes – Oxy0-6 (633 probes)	Genes	% of total input	p-value
response to wounding	42	10.3	1.10E-11
defense response	43	10.5	3.20E-10
inflammatory response	30	7.4	5.50E-10
positive regulation of cytokine production	12	2.9	7.40E-06
immune response	36	8.8	1.20E-05
detection of biotic stimulus	6	1.5	4.40E-05
adaptive immune response based on somatic recombination of immune receptors built from immunoglobulin superfamily domains	10	2.5	7.20E-05
adaptive immune response	10	2.5	7.20E-05
regulation of cytokine production	15	3.7	8.70E-05
innate immune response	13	3.2	9.10E-05
positive regulation of immune system process	17	4.2	1.50E-04
protein kinase cascade	22	5.4	1.60E-04
leukocyte mediated immunity	10	2.5	1.70E-04
response to bacterium	15	3.7	1.70E-04
positive regulation of multicellular organismal process	17	4.2	1.90E-04
immune effector process	12	2.9	3.00E-04
positive regulation of response to stimulus	16	3.9	4.30E-04
positive regulation of immune response	12	2.9	5.80E-04
regulation of interferon-gamma production	6	1.5	5.90E-04
regulation of erythrocyte differentiation	5	1.2	6.80E-04

Key:

Response to wounding
Lymphocyte activation

3.5.8 Control group – epidural bupivacaine

Patients given epidural bupivacaine were viewed as the control group as they received a non-opioid analgesic not expected to be immune-modulating. Of the 44 genes deregulated by bupivacaine, 21 were down-regulated and 23 up-regulated. Classification of genes by DAVID ontological software showed 3 enriched processes (p-value<0.01; Appendix B) in this group. Removing those genes also deregulated by another treatment removed the general confounding effect of surgery and left 20 genes; ORA of these showed no statistically significant enriched processes (p-value<0.01).

3.6 Discussion

This chapter aimed to determine if morphine influenced lymphocyte gene expression differently to oxycodone or epidural bupivacaine, when given during open gynaecological surgery. RNA was extracted from CD4+, CD8+ and NK cells at 0, 2, 6 and 24 hours following initiation of analgesic treatment.

Non-cancer open gynaecological surgery was chosen as a surgical model providing sufficient pain to warrant opioid use, but for which an epidural was also suitable. This type of surgery is normally a myomectomy, performed in women up to middle age; this younger age group tends to be healthy with few co-morbidities. The study design therefore tended to remove possible confounding factors of co-morbidities and age, while avoiding hindering patient recruitment by restricting eligible surgery. The exclusion of patients with cancer from the study removed the confounding immune-modulating disease processes which have been consistently identified in many cancer types, for example changes in T cell gene expression [109] and features of T cell exhaustion [110].

Importantly, the 3 analgesics were successfully separated, with patients who received more than 1 analgesic due to clinical need withdrawn (Figure 3.3,

Table 3.1). The equal distribution of treatment groups across microarray hybridisation batches avoided batch effect (Figure 3.10). Normalisation was successful, distributing data consistently across samples and aligning outliers, while maintaining the array distribution around the median (Figure 3.8 and Figure 3.9). Although some samples showed degraded RIN, probes whose fluorescing intensity correlated with RIN were removed from the analysis, and

no statistically significant difference in RIN was seen between treatments or timepoints (Figure 3.11 and Figure 3.12).

Clinical characteristics were successfully removed as confounding factors. BMI, age, operation duration, pain and opioid use were not significantly different between treatment groups (Figure 3.4,

Figure 3.6 and Figure 3.7; Sections 3.4.3, 3.4.4 and 3.4.5). Opioid doses given were below those seen previously in similar operations, with 70mg reported as the mean morphine dose over 24 hours [111] compared to 49mg in this study. This difference may be due to variance in operation type, with TAH producing increased tissue damage and pain when compared to the predominantly open myomectomies of this study. In addition, this study used the less invasive Pfannenstiel incision, whereas incision type is not discussed by Stanley et al [111] and may not have been uniform.

Operation type varied across treatment groups: the modal operation across the study was open myomectomy (23/40 microarray patient cohort) but this included only 1/8 bupivacaine patients compared to 9/16 morphine patients and 13/16 oxycodone patients. Protocol required that patients were randomly assigned to analgesic, but clinical need could outweigh this. It is likely that bupivacaine patients both had a more complex presentation (confirmed by the greater range of surgical procedures) and tended to be heavier, although BMI was not significantly increased in this group (Figure 3.4). These patients might therefore have been considered to benefit clinically from an epidural analgesia and its attendant stepped-up care. Although bupivacaine patients were potentially less well and heavier, the scarcity of statistically significant deregulated genes (Table 3.3) and enriched processes induced by

bupivacaine suggests that operation type and clinical presentation did not influence lymphocyte gene deregulation in this study.

Rationale for focusing on genes exclusively deregulated by a treatment can be given by looking at genes deregulated by all treatments. The genes most highly up-regulated in Mor0-2 were also induced by other treatments (Table 3.4, Figure 3.15); 16 of 27 most highly perturbed genes at 2 or 6 hour were also deregulated by other treatments. Two genes, CD163 and IL1R2, were highly up-regulated in *all* treatment groups at six hours. Both the similar degree of fold change (13-14 mean FC for CD163; 25-30 mean FC for IL1R2) and the genes' function suggest a surgery-induced response.

CD163 is an acute phase receptor found on monocytes and macrophages that scavenges haptoglobin / haemoglobin complexes, is shed upon macrophage activation [112] and has been shown to be up-regulated following coronary artery bypass graft surgery [113] and by IL-10 [114]. Its up-regulation could be linked to an increase in cortisol; it was up-regulated in monocytes following high-dose cortisol infusion in healthy volunteers [115]. IL1R2 is a decoy receptor for IL-1, found on immune cells; IL1R1, IL1's functional receptor, is found on almost all cell types [116], suggesting that IL1R2 may protect immune cells against IL1 and modulate inflammation. IRAK3, also up-regulated in all groups, prevents the dissociation of IRAK1 from IRAK4 and its subsequent association with myD88 and TRAF6. This negatively regulates TLR / IL1R signalling, regulating the pro-inflammatory downstream actions of TLR [117], and providing immune homeostasis and further evidence of surgery-induced change.

As well as the deregulation of surgery-induced genes by all treatments, the incomplete clustering of arrays by treatment (Figure 3.16) confirms the importance of focusing on those genes exclusively deregulated by a treatment, and of further investigating genes deregulated by more than 1 treatment.

3.6.1 Morphine genes

The greatest deregulation of lymphocyte gene expression by morphine was identified at two hours, so the focus of analysis for morphine-modulated genes was at this timepoint. This effect is clinically important as almost all patients were still in surgery; mean operation duration was approximately 2-2.5 hours in the 3 treatment groups, with the longest surgery lasting just under 4 hours and only seven less than 2 hours. A meta-analysis of rectal cancer clinical trials across 6 publications found mean operation duration ranged from approximately 2-4.5 hours in laparoscopic surgery and 1.75-3.5 hours in open surgery [118], giving our 2 hour timepoint considerable translational relevance in cancer resection surgery, regardless of surgical approach.

Supervised clustering of Mor0-2 genes (Figure 3.16) sees their separation into down-regulated genes involved with RNA transcription and translation and up-regulated genes involved with apoptosis. The ordering of arrays shows that the analysis does not fully resolve morphine 2 hour arrays, confirming the importance of focusing on the 450 uniquely deregulated genes. Bupivacaine arrays are spread throughout the array group, in keeping with their relative lack of gene deregulation. Enrichment analysis of Mor0-2 450 genes suggests a down-regulation of cell proliferation and T cell

expansion, reduced cytotoxicity killing ability of NK and CD8+ cells and generalised reduced cellular activity.

421 of 434 down-regulated Mor0-2 genes are unique to morphine; those of particular interest include CD28, LCK, TRAC, MICB, HLA-DMB, BCL11B, RCAN3, AQP3, CX3CR1 and KLF10. CD28 (FC -3.4) is a constitutively expressed receptor and co-stimulant for T cell activation found on both CD4+ and CD8+ cells; it has been suggested that the initial signalling scaffold induced by ligand binding forms a structure that intracellular CD28 elements bind to, enhancing TCR effects [119]. CD28-/- mice showed a lack of T cell expansion upon antigen stimulation, reduced TH cell differentiation and increased expression of TH2 cytokines [120]. Blockade of CD28 in CD8+ cells prevented clonal expansion, degranulation and IFN-γ production during the primary and secondary immune response [121, 122]. At levels to mimic physiological cortisol, hydrocortisone inhibited the production of TH1 cytokines in naïve CD4+ cells, but prevented a concurrent TH2 shift by also inhibiting the production of IL-4 during TH2 differentiation; importantly, this was CD28-dependent [123]. Morphine-induced CD28 down-regulation may therefore reduce T cell activation and shift cells to a TH2 profile; a change that could be augmented by the presence of increased cortisol. It would be ideal to investigate any variance in cortisol concentration across treatment groups, to consider its impact on gene deregulation.

LCK and TRAC were also down-regulated by morphine. LCK is a tyrosine kinase that phosphorylates tyrosine in the CD28 cytoplasmic tail [124] and is localised with TCR in the immune synapse [125]. TRAC (T cell receptor α constant) codes for the constant part of TCR's α subunit, an essential part of

the TCR; patients with an inherited immunodeficiency disorder have a mutation impairing TRAC splicing to produce reduced αβ TCR chain expression and immune dysregulation [126]. The down-regulation of CD28, LCK and TRAC by morphine suggests a potential morphine-induced T cell immune synapse dysfunction and a shift to a TH2 profile.

MICB (MHC class 1 polypeptide-related seq B) is an induced self-antigen and transmembrane protein normally expressed only at low levels, but up-regulated in virus-infected and tumour cells [127]. It is a ligand for the NKG2D receptor, found on CD8+, γδ+ and NK cells, whose activation phosphorylates DAP10 and recruits PI3K, inducing target cell killing [128]. The NKG2D receptor is needed for NKCC; MICB down-regulation in mice *in vivo* resulted in a reduced killing ability of NKG2D [129]. The morphine-induced down-regulation in this study suggests a reduced cytotoxic killing ability of CD8+ and NK cells in the morphine group. HLA-DMB (major histocompatibility complex, class 2 DMB) was also down-regulated by morphine and is the β chain of a membrane-bound heterodimer found in intracellular vesicles. In APCs it is involved in peptide loading to MHCII by catalysing the exchange of invariant to pathogenic peptide [130]. A similar role in T cells, a possibility as they can have a role as APCs, suggests that the down-regulation of HLA-DMB by morphine could reduce CD4+ response to pathogen.

BCL11B, down-regulated by morphine, is a zinc finger transcription factor [131] and T cell gene *up*-regulated during T cell transitioning from precursor to double negative state, along with TCF12 [132]. Overexpression of BCL11B induces T helper cell differentiation in mice [133] whereas down-regulation

has been shown to reprogram cells to a NK-like non-specific cell [134]. Both BCL11B and TCF12 were down-regulated, suggesting that morphine may induce a reduced pathogenic response via CD8+ cells and a decrease in cell differentiation in CD4+ cells.

RCAN3 (regulator of calcineurin 3) is the most strongly down-regulated gene by morphine. It inhibits calcineurin, a Ca^{2+}- and calmodulin-dependent serine / threonine phosphatase in the cytoplasm, which activates signalling pathways via activation of NFAT transcription factors and subsequent cytokine gene expression [135, 136]. Calcineurin has been implicated in T cell anergy through prolonged activation of NFAT without its activation partner AP-1, up-regulation of genes including E3 ubiquitin ligases and proteases in murine CD4+ cells (mRNA and protein) and degradation of signalling proteins [137]. Morphine deregulated 2 E3 ubiquitins: HECW2 was up-regulated and WWP1 was down-regulated. The down-regulation of RCAN3 suggests a potential increase in calcineurin activity induced by morphine and possible subsequent T cell anergy.

Aquaporin 3 (AQP3), also strongly down-regulated, is a transmembrane protein involved in the transport of water and glycerol across the cell membrane. Higher levels (mRNA and protein) were shown in TH17 but not TH1 cells following differentiation [138] and AQP3 was expressed in activated but not inactivated T cells from healthy PBMCs [139]. AQP3-mediated H_2O_2 transport is needed for activation of CDC42 in mice, which is essential for T cell migration towards chemokines [140]. The down-regulation of AQP3 by morphine therefore has the potential to disrupt T cell migration and activation and indicates a shift to a TH2 profile.

CX3CR1, aka fractalkine receptor, is a G-protein coupled receptor found on lymphocytes, which binds the chemokine fractalkine. It was up-regulated in human lymphocytes following administration of cortisol to mimic a stressful event [141] and probably caused the adrenalin-induced increase in circulating CD8+ effector cells in humans, opposite to the cortisol-induced, CXCR4-mediated decrease in circulating naïve CD4+ and CD8+ cells [142]. The down-regulation of CX3CR1 by morphine suggests a reduction in circulating CD8+ cells, possibly mediated by a decrease in serum cortisol levels.

Kruppel-like factor 10 (KLF10), down-regulated by morphine, is a zinc finger transcription factor which is pro-apoptotic in association with the down-regulation of oncogene BCL2 [143]. It represses FOXP3, the transcription factor responsible for initiating and maintaining TReg differentiation. Neither FOXP3 nor BCL2 were deregulated, but BNIP3, which antagonises BCL2's actions, was down-regulated. The down-regulation of KLF10 and BNIP3 suggest that cells of the morphine group may display decreased levels of apoptosis and increased TReg differentiation [144].

29 of 86 up-regulated genes are unique to morphine, including DAPK2, PGLYRP1, srGAP2 and srGAP2C. Those present in more than 1 treatment will be discussed in Chapter 6. DAPK2 is a Ca^{2+}-bound calmodulin dependent serine / threonine protein kinase involved in apoptosis and autophagy pathways [145], activating TRAIL-induced apoptosis pathways upon knockdown *in vitro* [146]. Its up-regulation suggests a tendency for decreased apoptosis of T cells by morphine. DAPK2 also appeared in many enriched apoptosis pathways. PGLYRP1 (peptidoglycan recognition protein 1) is a GN / GP bacteria pattern receptor involved in the development of allergic

asthma. PGLYRP1 (-/-) mice showed fewer TH2 and TH17 cells in the lungs following house dust mite sensitisation [147, 148]; a similar effect in human T cells suggests a possible shift to a TH2 profile.

Two probes each for Slit-Robo GTPase-activating protein 2 (srGAP2) and its paralog srGAP2C were *up*-regulated; these proteins are members of the FBAR protein family involved in actin dynamics and membrane trafficking [149]. Overexpression of srGAP2 in neuronal cells induces membrane protrusions rather than the invaginations, decreasing migration [150] with knockdown increasing migration [151]. Again in neuronal cells, srGAP2 couples GTPase signalling to postsynaptic scaffolding proteins Homer and Gephyrin, producing spine morphogenesis, inhibitory synapse formation and the accumulation of GABA and AMPA receptors; all effects were inhibited by srGAP2C [152]. In NIH 3T3 (murine fibroblast) cells, srGAP2 is needed for contact inhibition of locomotion, a repulsion between two fibroblasts [153]. The up-regulation of srGAP proteins by morphine suggests an influence of morphine on immune synapse formation, if the proteins have a similar function in T cells.

3.6.2 Oxycodone genes

The greatest deregulation of lymphocyte gene expression by oxycodone was at six hours, where 559 genes were differentially expressed, 19 down-regulated. As with morphine, clustering of arrays did not fully resolve the treatment group (Figure 3.17) underlining the importance of focusing on the 460 genes uniquely deregulated by oxycodone, rather than the whole dataset. The 460 unique genes were comprised of 450 up-regulated and 10 down-regulated genes.

Several up-regulated genes were of interest including ANXA3, S100A12, S100P, GCA and STAT3. The most highly up-regulated gene was ANXA3 (annexin 3), which binds via phosphatidylserine to dying fibroblast cells; the authors suggest that ANXA3 (and other annexins) may tag dying cells similarly to opsonin [154]. It was expressed more highly in TH1 compared to TH2 cells [155]; its up-regulation by oxycodone therefore suggests that oxycodone may have the potential to shift T cells to a TH1 profile and increase the clearance of apoptotic cells. S100A12 and S100P are Ca^{2+}-binding S100 proteins with a role in cell migration. S100A12 is found in monocytes and lymphocytes and induces migration of monocytes and neutrophils *in vitro* when found outside the cell; its injection into mouse peritoneum induces leucocyte recruitment. S100P induces cellular migration in diseased states [156]. The up-regulation of these genes by oxycodone suggests a possible increase in lymphocyte trafficking.

Grancalcin (GCA) is a Ca^{2+}-binding protein found in neutrophils and macrophages, with a theoretical role in degranulation due to its association with both membrane and granule upon cell activation. Higher levels were found in LPS-stimulated leucocytes [157] although deficient mice did not show a decreased resistance to infection [158]. Its up-regulation by oxycodone may be supportive of increased NK cell degranulation in this group, if its role in NK cells is similar to its role in macrophages.

Signal transducer and activator of transcription 3 (STAT3) is phosphorylated by members of the JAK family following cytokine receptor activation; activated STAT then dimerizes and moves to the nucleus to activate transcription [159]. It is required for TH17 differentiation [160], and ablation

of STAT3 in murine NK cells and dominant negative STAT3 mutations in human NK cells both produced reduced NKG2D expression and reduced responses to IL-10 [161]. The up-regulation of STAT3 by oxycodone suggests a possible increase in TH17 differentiation and an increased killing ability of NK cells.

Only 10 genes were down-regulated uniquely by oxycodone, including NMT2 and BACH2. NMT2 is an enzyme involved in the N-myristoylation (addition of fatty acid myristate) of proteins, resulting in altered protein-protein interactions, enhanced protein / membrane binding and changes in protein stability [162]. Its depletion in murine T cells impaired the TCR signalling cascade; conversely it was expressed more highly in colon cancer tissue than healthy tissue [163]. Its down-regulation by oxycodone suggests a possible impaired T cell signalling, contrary to the general hypothesis of oxycodone-mediated gene deregulation.

BACH2 is a transcriptional regulator that both activates and suppresses transcription: BACH2 -/- mice showed positively regulated TReg development and repressed conventional T cells [164, 165], and repressed lineage-specific genes, including GATA3 [165]. GATA3 was down-regulated by oxycodone and morphine and is a transcription factor needed for notch-mediated differentiation of TH2 murine cells [166]. It has also been called the master driver of TH2 differentiation and its mRNA, protein and activity were repressed by glucocorticoid administration via inhibition of p38MAPK-induced phosphorylation [167]. The down-regulation of BACH2 and GATA3 by oxycodone may increase TReg or TH1 cells; the down-regulation of GATA3 by morphine may increase TH1 cells intraoperatively, opposite to the general

shift hypothesized, and possibly influenced by reduced cortisol. Any variance in cortisol concentration across treatment groups could be investigated, to consider the impact on gene deregulation as discussed in relation to CD28.

3.6.3 Bupivacaine genes

Only 44 genes were differentially expressed at 6 hours by bupivacaine, 21 down-regulated. 20 genes were deregulated uniquely by bupivacaine; those expressed in all treatment groups are discussed in Chapter 6.

3.6.4 Over Representation Analysis (ORA)

ORA was performed in DAVID ontological software to give an overview of the analgesic-induced changes. Processes highlighted were classified into several groups, including RNA transcription and translation, apoptosis, lymphocyte activation, cell respiration, signal transduction and response to wounding. Those genes seen repeatedly in groups of pathways were noted as possibly significant. No statistically significant processes were enriched in genes unique to bupivacaine treatment. This reinforces the merit of using bupivacaine as a control group, as the lymphocyte genes that did experience altered expression from baseline did not seem to function in a coherent manner.

RNA transcription and translation processes were only enriched following morphine treatment: 23 processes, represented by 92 genes (1 up-regulated) were seen, suggesting a global down-regulation of RNA transcription, translation and splicing of pre-mRNA processes. This down-regulation may be due to a reduction in T cell proliferation, seen previously following morphine administration [48]; reduced cellular activity would then result in decreased protein translation [168, 169]. Alternatively, it could be a

direct response to morphine, or an indication of apoptosis, although the down-regulation of apoptosis processes suggests that this is not the case.

Several small nuclear ribonucleoprotein polypeptides (SNRPs D1, E, F and G) appeared repeatedly in these pathways. They form part of the core structural spliceosome ring and are essential for splicing pre-mRNA transcripts [170]; their down-regulation either prevents protein translation or reflects a down-regulation already occurring.

The process grouping apoptosis was enriched by morphine and oxycodone. Morphine showed 12 processes, with 40 of 44 genes down-regulated. In comparison, no processes were enriched by oxycodone at 2 hours, but by 6 hours 3 processes were enriched, represented by 35 up-regulated genes. No apoptosis processes were enriched by bupivacaine. It appears that apoptosis is up-regulated by oxycodone and down-regulated by morphine; the implications of this with regard to T cell anergy will be addressed in Chapter 7.

Several genes were frequently repeated in morphine's enriched apoptosis pathways including DAPK2 and DYRK2. DAPK2's up-regulation may result in decreased apoptosis (see above). DYRK2 is a serine/threonine protein kinase which increased cell proliferation via post-translational modification of c-Jun and c-Myc following knockdown in human osteosarcoma cells, preventing their degradation and shortening the G1 phase of cell cycle [171]. The down-regulation of DYRK2 by morphine suggests a tendency to decreased T cell proliferation.

PTEN and BCL6 were frequently repeated genes in oxycodone's enriched apoptosis pathways. PTEN is a tumour suppressor with a phosphatase

function, through which it inactivates substrate and suppresses tumours [172]. It is involved in T cell differentiation, and was suppressed upon T helper but not TReg induction, in murine CD4+ cells [173]. Its up-regulation by oxycodone is supportive of the hypothesis of oxycodone-induced immunomodulation; the increase in TReg differentiation highlighted in the gene expression data could be the result of a normal resolution of a previous active immune response.

BCL6 is a zinc finger transcription factor repressor and master regulator of T follicular cells (T_{FH}) [174]. Increased expression of TH1, TH2 and TH17 cytokines were seen in BCL knock-out mice, and upon BCL over-expression, T_{FH} gene expression is induced to the detriment of TH1, TH2 or TH17 cytokines [175]. The up-regulation of BCL6 by oxycodone could favour the development of T_{FH} over other T helper cell types and the subsequent formation of germinal centres [174] and B cell memory. Interestingly, the BCL6 corepressor BCOR, thought to repress transcription of BCL6, is down-regulated in morphine, although BCL6 deregulation is not seen.

Although apoptosis processes were enriched by oxycodone, the two groups of processes in the top 20 list by p-value (Table 3.8) were lymphocyte activation and response to wounding. Lymphocyte activation showed 19 processes for oxycodone; 100 genes were represented by 70 different probes, suggesting a reliable response. Only LRRN3 and LY9 were down-regulated. No lymphocyte activation processes were enriched by the 450 genes uniquely deregulated by morphine at 2 hour; 12 processes (19 genes, 14 down-regulated) were enriched in the whole 520-gene group at 2 hours. This

breakdown suggests that processes relating to lymphocyte activation were up-regulated and particularly prevalent in the oxycodone group at 6 hr.

Several genes were found repeatedly in lymphocyte activation pathways in oxycodone, including TLR4 and TLR8. TLR4 is fundamental to innate immunity and recognises LPS in gram-negative bacteria, triggering NF-κB and MAPK signalling pathways and inducing inflammation [176]. Its up-regulation by oxycodone suggests that these patients are able to induce inflammation normally. Likewise TLR8 is involved in recognising pathogens as part of innate immunity and its up-regulation is supportive of effective inflammation and a functioning innate immune response in the oxycodone group.

Twenty-two response to wounding processes were enriched by oxycodone – 103 genes (148 probes), with only 2 down-regulated (GATA3 and LY9). This process grouping was not enriched by morphine until 6 hours, with 14 processes represented by 48 genes (67 probes), just 1 down-regulated. This suggests that response to wounding processes were up-regulated by both oxycodone and morphine at six hours, but, as before, oxycodone had a stronger response, based on the higher number of up-regulated processes and probes.

3.7 Conclusion

The study design successfully kept the 3 study analgesics distinct, and removed all confounding factors bar operation type, differently to similar previously published clinical research. Morphine induces deregulation of 450 unique genes which suggest an intraoperative reduction in immune function. The deregulation of 460 unique genes by oxycodone occurs postoperatively and suggests a possible improvement to the immune response. The scarcity of gene deregulation and statistically significant enriched biological processes by epidural bupivacaine confirms its suitability as a control group.

The main change in gene expression for morphine patients was the 2 hour down-regulation seen in genes involved in RNA transcription and translation, apoptosis and cell respiration. The down-regulation of RNA transcription- and translation-related genes implies a lower level of protein translation, concurring with the previously known suppression of lymphocyte proliferation and NKCC following morphine administration. Down-regulation of apoptosis and cell respiration pathways may reflect increased T cell anergy (see Chapter 7).

In contrast, oxycodone's effect, limited to the 6 hour timepoint, suggests a heightened immune response, based on specific gene deregulation and the enrichment of processes related to response to wounding, lymphocyte activation and apoptosis. In immunocompromised patients, oxycodone or epidural bupivacaine may therefore be considered preferable analgesics to morphine for use during the surgical period.

The deregulation of specific genes suggests suitable functional assays that may confirm the results of gene expression analysis. CD28, LCK, TRAC, AQP3

and PGLYRP1 were all uniquely deregulated by morphine and suggestive of a morphine-induced TH2 shift. ANXA3 and BACH2 were deregulated by oxycodone and suggest a TH1 shift. These potential T helper cell shifts could be confirmed by serum cytokine analysis. The down-regulations of MICB by morphine and up-regulation of STAT3 by oxycodone are consistent with morphine-induced impaired NKCC, which could be confirmed using a degranulation or ^{51}chromium-release assay. Finally, several genes deregulated in this study – GATA3, CD28 and CD163 – have been shown previously to be deregulated following cortisol administration. Measurement of serum cortisol may suggest if cortisol influenced gene deregulation in this study.

Chapter 4
Functional assays

4.1 Introduction

The analysis of gene expression data in Chapter 3 suggested that while morphine induces potentially immunosuppressive gene deregulation in lymphocytes within the intraoperative timeframe, oxycodone induces gene deregulation that may improve the immune response, postoperatively. Based on this data, we wanted to determine if the effector functions of lymphocytes were altered following analgesic administration.

Gene deregulation analysis suggested that morphine could induce a shift towards a TH2 profile whereas oxycodone could induce a shift towards a cell-mediated TH1 response. This was based on the deregulation of genes such as CD28 and AQP3 by morphine and ANXA3 and BACH2 by oxycodone, and supported by previous data [62]. Serum levels of seven TH1/2/17 cytokines were therefore compared across treatment groups using a cytometric bead array.

Cortisol is a glucocorticoid that works through the glucocorticoid receptor to coordinate inflammation, stress and immune responses, amongst other functions [177]. Cortisol levels are altered by morphine administration [178-182] and by surgery [50, 183]. Glucocorticoid receptor signalling exerts its effects in part by acting as a transcriptional regulator [184], therefore a variation in cortisol concentration may influence gene deregulation. Several deregulated genes of this study have also been shown to be deregulated by cortisol; serum cortisol levels were therefore investigated via ELISA.

Morphine is known to induce reduced NK cell cytotoxicity (NKCC), in contrast to oxycodone [29-31]; this finding is supported by gene deregulation in this study. MICB, a ligand for the NKG2D receptor needed for NKCC, was down-regulated by morphine, while STAT3 was up-regulated by oxycodone; its ablation decreases NKG2D receptor expression [161]. NKCC was therefore investigated via NK cell degranulation.

4.2 Aims

The aims of this chapter were to corroborate the gene expression analysis described in Chapter 3 using the functional assays described above.

4.3 Methods

4.3.1 Cytometric bead array

Samples were taken from non-cancer open gynaecological surgery patients recruited to this study as described in Chapters 2 and 3. Serum concentrations of 7 major cytokines expressed by TH1, TH2 and TH17 cells were assayed via cytometric bead array (CBA): IL-2, IL-4, IL-6, IL-10, IL-17a, TNFα and IFN-γ. Samples from 0 (pre-treatment) and 6 hour (postoperative) timepoints were compared across all treatment groups, using BD Biosciences kit 560484, as per protocol. The key difference from a simple ELISA is that a CBA allows simultaneous quantification of several cytokines, removing experimental variation and reducing sample volume needed. It uses different fluorescing intensities of the fluorochrome phycoerythrin (PE), attached to beads specific for each cytokine's antibody in varying intensities. Samples were run through LSR Fortessa and mean fluorescing intensities for the nine standards inputted to FCAP Array software v3, generating a dose-response curve. Sample concentrations were interpolated from the curve and averaged to take account of duplication.

Dependent-samples t-tests were performed in each treatment group, comparing changes from baseline to 6 hour for each cytokine. One-way ANOVAs were performed between treatment groups at each timepoint for each cytokine to rule out pre-existing differences. Patient samples were selected for assay based on a high sample volume in order to leave sample for future assays if needed. The number of samples assayed was limited by cost.

Table 4.1: Subject numbers of patients providing serum samples for cytometric bead array

Treatment	Subjects	N
Morphine	31 40 43 47 48 50 52 53	8
Oxycodone	33 34 44 54 56	5
Bupivacaine	32 38 39 41 46 51 57	7

4.3.2 NK cell degranulation assay

Samples were taken from non-cancer open gynaecological surgery patients recruited to this study as described in Chapters 2 and 3. NK cell cytotoxicity was measured indirectly via degranulation using CD107a, a marker of cytoplasmic granules released on cell degranulation. NK cells selected using negative magnetic separation were used for this assay. Half of each patient sample was stimulated with Staphylococcal enterotoxin B (SEB) and half was unstimulated; CD107a was captured with anti-human CD107a. NK cells were selected with anti-human antibodies for CD56 and CD3 and healthy donor PBMCs (National Blood Service) were used as compensation; three aliquots each received either PE-conjugated anti-CD56, FITC-conjugated anti-CD3 or APC-conjugated anti-CD107a antibodies. Following incubation, events were acquired through LSR Fortessa then data analysed with FloJo software.

Median and percentage change were calculated for all samples. Wilcoxon signed ranks tests were performed in each treatment group, both comparing changes from baseline to 6 hour for unstimulated and stimulated cells, and comparing within-timepoint differences for unstimulated and stimulated cells. Kruskall Wallis tests were performed between treatment groups separately at baseline and 6 hour for both unstimulated and stimulated cells. Samples were

selected for assay based on the presence of sufficient viable cells. The number of samples assayed was limited by cell viability.

Table 4.2: Subject numbers of patients providing NK cells for the NK degranulation assay

Treatment	Subjects	No per group
Morphine	1 13 45 48 50 52 53	7
Oxycodone	6 9 29 33 34 44 49	7
Bupivacaine	32 36 41 46	4

4.3.3 Cortisol ELISA

Samples were taken from non-cancer open gynaecological surgery patients recruited to this study as described in Chapters 2 and 3. Serum cortisol concentrations for samples from all treatment groups at 0 hour (pre-treatment) and 6 hour (postoperative) were assayed via ELISA using R&D Systems kit KGE008. ELISA was performed as per protocol working on the principle of competitive binding. Optical densities (ODs) were obtained using a BMG Labtech plate reader and blanked by subtracting values from non-specific binding cells. Adjusted duplicate values for standards were imported into GraphPad Prism to prepare a dose-response curve. Sample concentrations were interpolated from the curve, the mean of duplicate samples was calculated and scaled up to give serum cortisol concentration. Dependent-samples t-tests were performed in each treatment group, comparing changes from baseline to 6 hour. One-way ANOVAs were performed between treatment groups at each timepoint to rule out pre-existing differences. Samples were chosen numerically and selected for assay based on a high sample volume, in order to leave sample for future assays if needed.

Table 4.3: Subject numbers of patients providing serum samples for cortisol ELISA

Treatment	Subjects	N
Morphine	13 14 22 31 35 40 43 47 50 52 57	11
Oxycodone	5 19 23 26 29 30 33 34 44 49 56	11
Bupivacaine	24 25 32 38 39 41 46 51 54	9

Dose-response curves for each serum cortisol ELISA

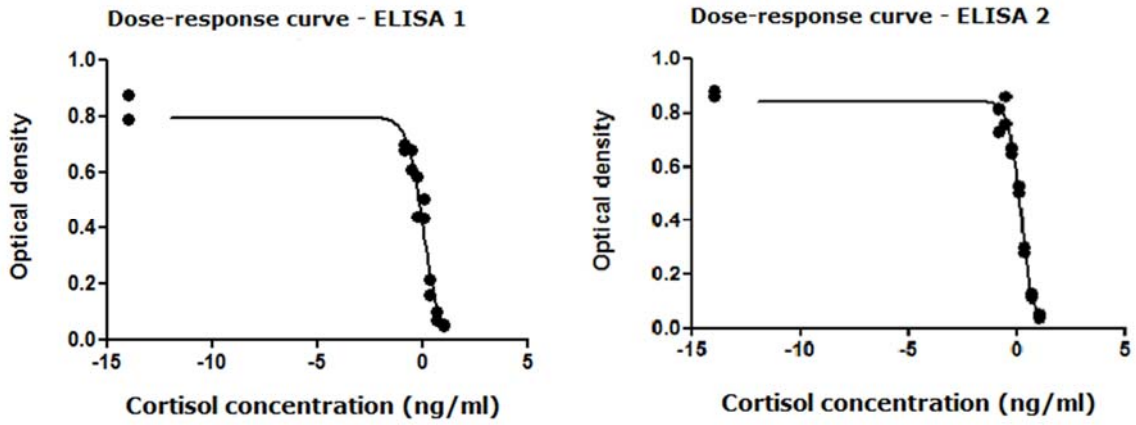

Figure 4.1: Dose-response curves were plotted for all cortisol standards separately for each ELISA. Optical densities were adjusted for non-specific binding cells and cortisol concentrations were logged.

4.4 Results

4.4.1 Cytometric bead array

The cytokine theoretical level of detection, determined from the standard curve during kit manufacture [185], provides a benchmark below which cytokine concentrations may not be accurate. Sample values for cytokines IL-2, IL-4, IFN-γ, TNFα and IL-17a were below or almost all below this level so are discounted from the analysis.

Although most baseline samples for IL-6 and IL-10 were below the level of detection, most samples at 6 hour were above, so data for these cytokines was analysed. Means were generated for IL-6 and IL-10 at both timepoints (Figure 4.2) and dependent samples t-tests were performed between timepoints for both cytokines per treatment group (SPSS v22). To investigate pre-existing differences between treatment groups at baseline or later at 6 hour, one-way ANOVA was performed at each timepoint for each cytokine.

Statistically significant increases from 0 to 6 hour were seen in IL-6 for all treatment groups. The greatest increase from baseline was seen in morphine, with mean levels increasing from 1.1 ± 0.3 to 52.9 ± 15.1pg/ml ($p=0.011$) compared to 6 hour levels of 19.4 ± 5.6pg/ml for oxycodone ($p=0.028$) and 23.0 ± 5.3pg/ml for bupivacaine ($p=0.006$). However, one-way ANOVA showed no significant difference between treatment groups at either timepoint.

Statistically significant differences between 0 and 6 hour for IL-10 were only seen in the morphine group. Mean increased from 1.0 ± 0.2 to 14.6 ± 2.6pg/ml ($p=0.001$); in oxycodone, the 6 hour mean was 12.4 ± 5.6pg/ml and in bupivacaine, 9.6 ± 4.0pg/ml, neither significant (Figure 4.2). No

difference was found in IL-10 concentration between treatment groups at either timepoint using one-way ANOVA.

Mean serum cytokine concentrations at baseline (0 hour) and 6 hour for all treatment groups

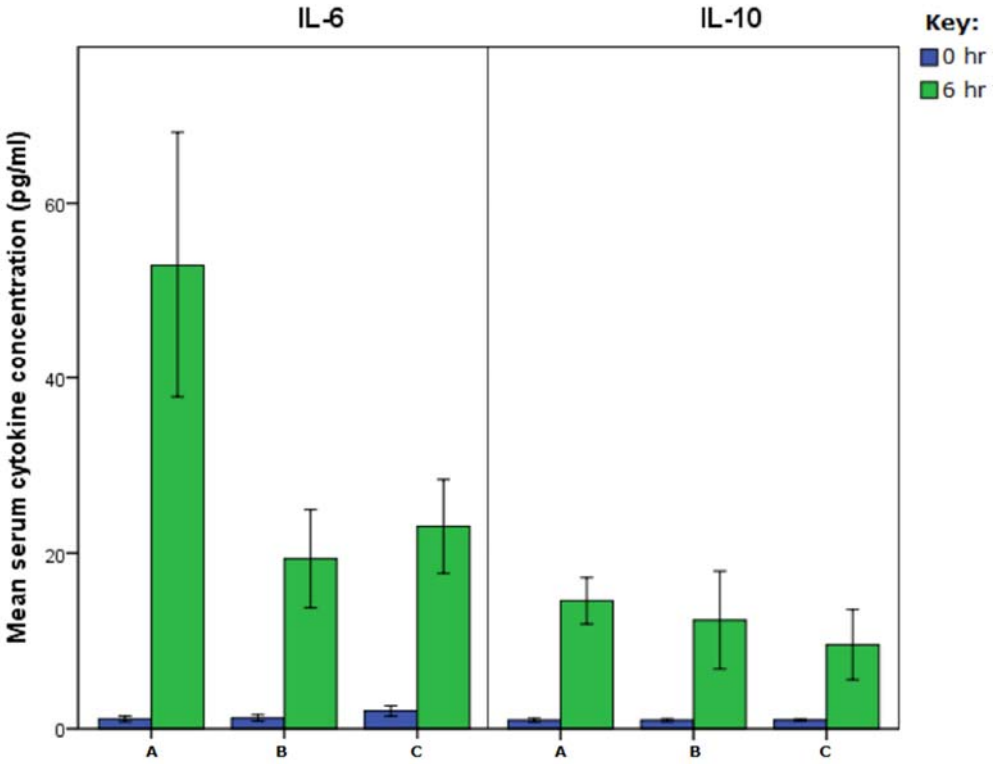

Figure 4.2: Mean serum concentrations of IL-6 and IL-10 at baseline and 6 hour for A: morphine, B: oxycodone and C: bupivacaine groups. Error bars are SEM.

4.4.2 NK degranulation assay

Box plots, median and percentage change were generated at baseline and 6 hour for unstimulated and stimulated samples in each treatment group (Figure 4.3 and Figure 4.4). Median rather than mean was used due to the small sample size and non-Gaussian distribution. Individual data is shown in Figure 4.5.

Wilcoxon signed ranks tests, suitable for small sample size or non-Gaussian distribution, were used to compare paired samples. Unstimulated versus stimulated cells at each timepoint, unstimulated cells between timepoints and stimulated cells between timepoints were compared across treatment groups. The only statistically significant change was at 6 hour in oxycodone, where median number of events increased from 392 in unstimulated cells to 2306 in stimulated cells ($Z=-1.992$; $p=0.046$). However, no statistically significant difference was found between treatment groups for any combination of datasets using Kruskal Wallis, including at 6 hour between stimulated cells.

NK cell degranulation events at baseline (0 hour) and 6 hour for both unstimulated and stimulated cells for all treatment groups

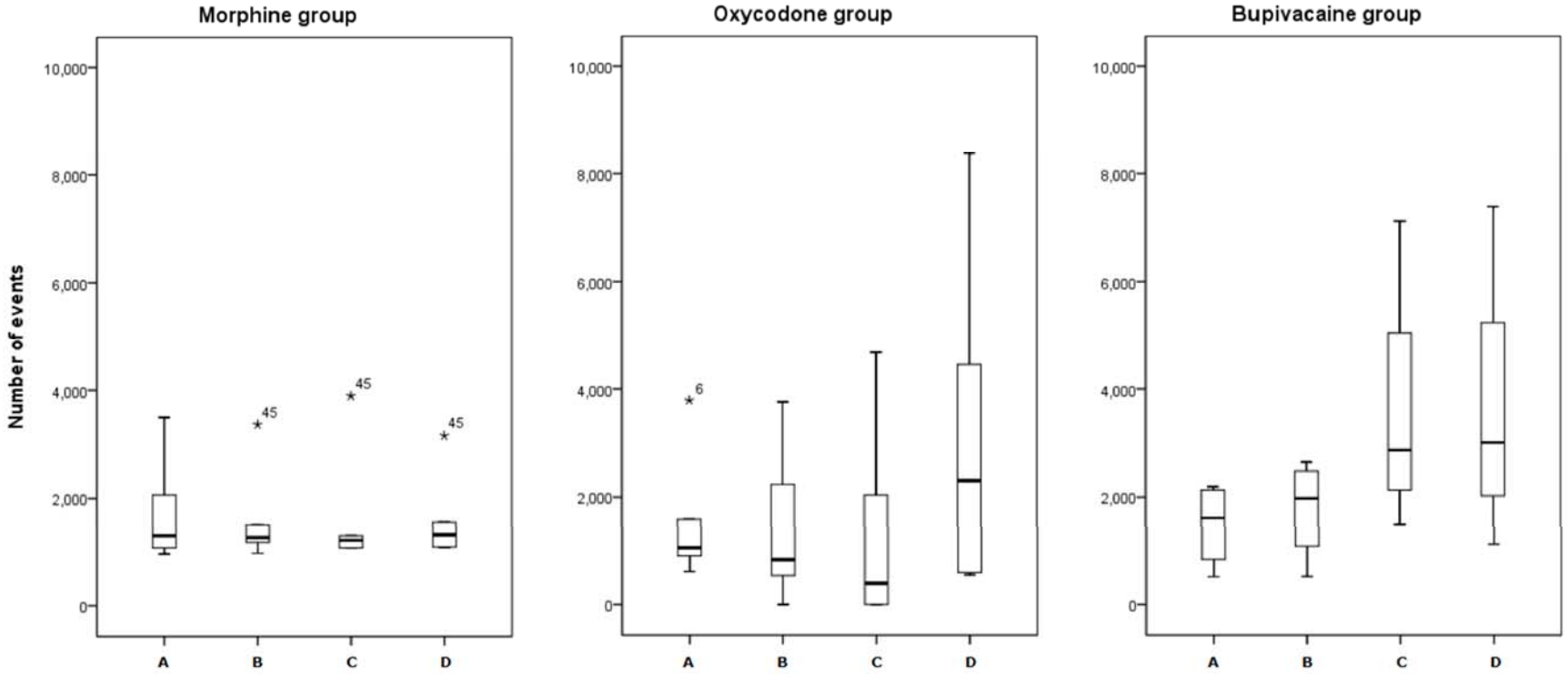

Figure 4.3: Box plots for degranulation events in all treatment groups, for A: unstimulated cells at baseline, B: stimulated cells at baseline, C: unstimulated cells at 6 hour, D: stimulated cells at 6 hour. Box plots show interquartile range with whiskers denoting largest and smallest values (excluding outliers>1.5 box lengths outside box, marked separately).

Median number of degranulation events in NK cells

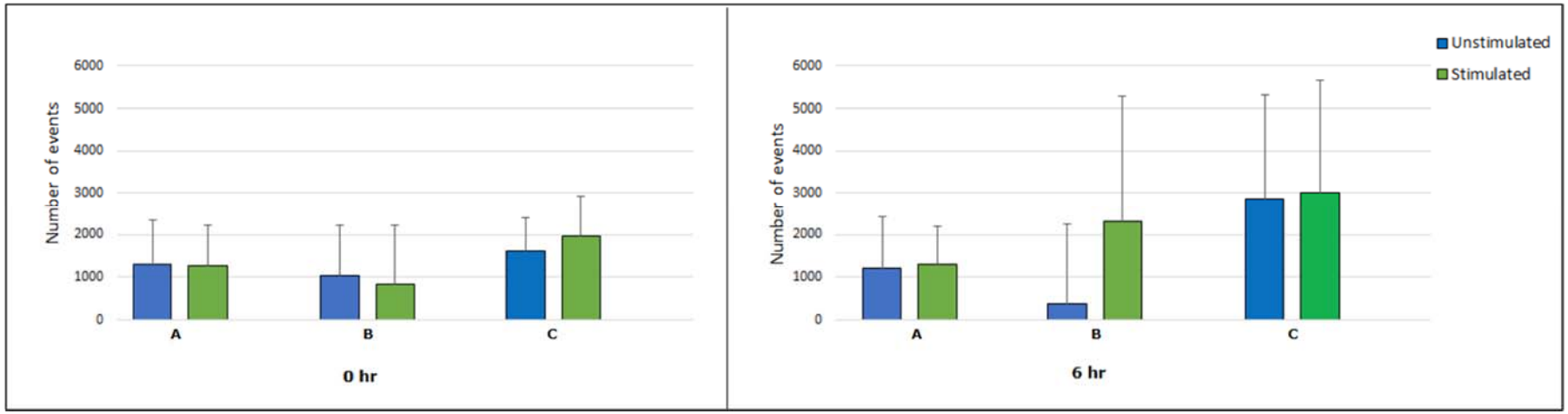

Figure 4.4: Median number of events at baseline and 6 hour in unstimulated and stimulated cells, for A: morphine, B: oxycodone and C: bupivacaine. Error bar is standard deviation.

NK degranulation events for individual patients

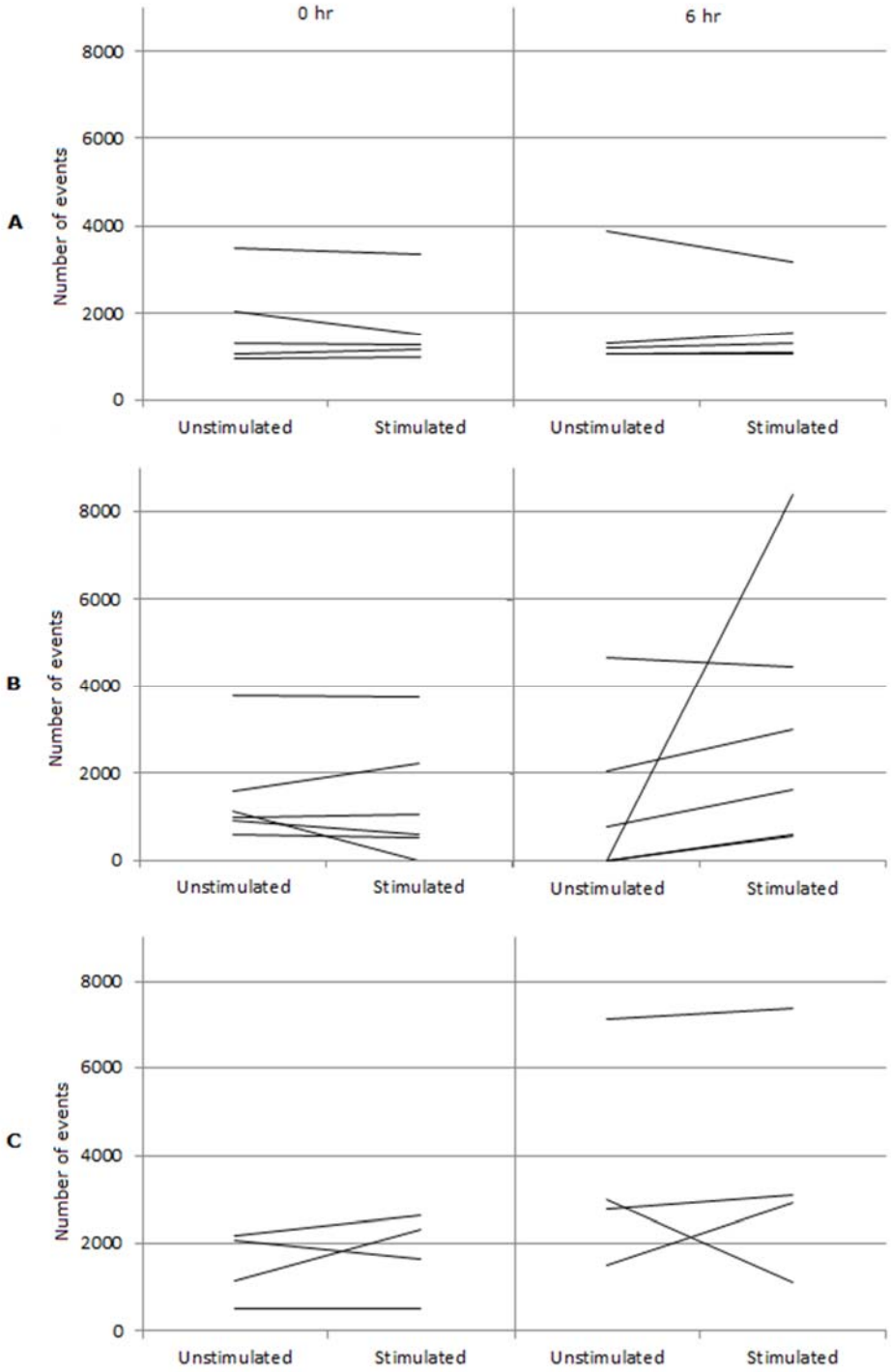

Figure 4.5: Number of degranulation events displayed for individual patients at baseline and 6 hour in A: morphine, B: oxycodone and C: bupivacaine patients

4.4.3 Cortisol ELISA

Box plots and means were generated at baseline and 6 hour for each treatment group (Figure 4.6 and Figure 4.7). Bupivacaine shows the greatest difference in mean cortisol concentration between timepoints, from 50.0 ± 8.7 to 180.4 ± 87.7 ng/ml (p=0.185), followed by morphine, from 46.9 ± 7.3 to 105.5 ± 39.6 ng/ml (p-value 0.123; Figure 4.7) and oxycodone (41.7 ± 7.7ng/ml to 50.6 ± 15.5mg/ml (p=0.607)). However, changes were not statistically significant.

To investigate pre-existing differences between treatment groups at baseline or later at 6 hour, one-way ANOVA was performed at each timepoint; again no statistically significant differences were seen. Levene's test for equality of variances showed statistically significant differences at 6 hour between morphine and oxycodone (F = 5.21; p=0.03) and bupivacaine and oxycodone (F = 6.18; p = 0.02; Figure 4.6). Individual serum cortisol concentration data and statistical results can be seen in Appendix B.

Serum cortisol concentrations at baseline (0 hour) and 6 hour for all treatment groups

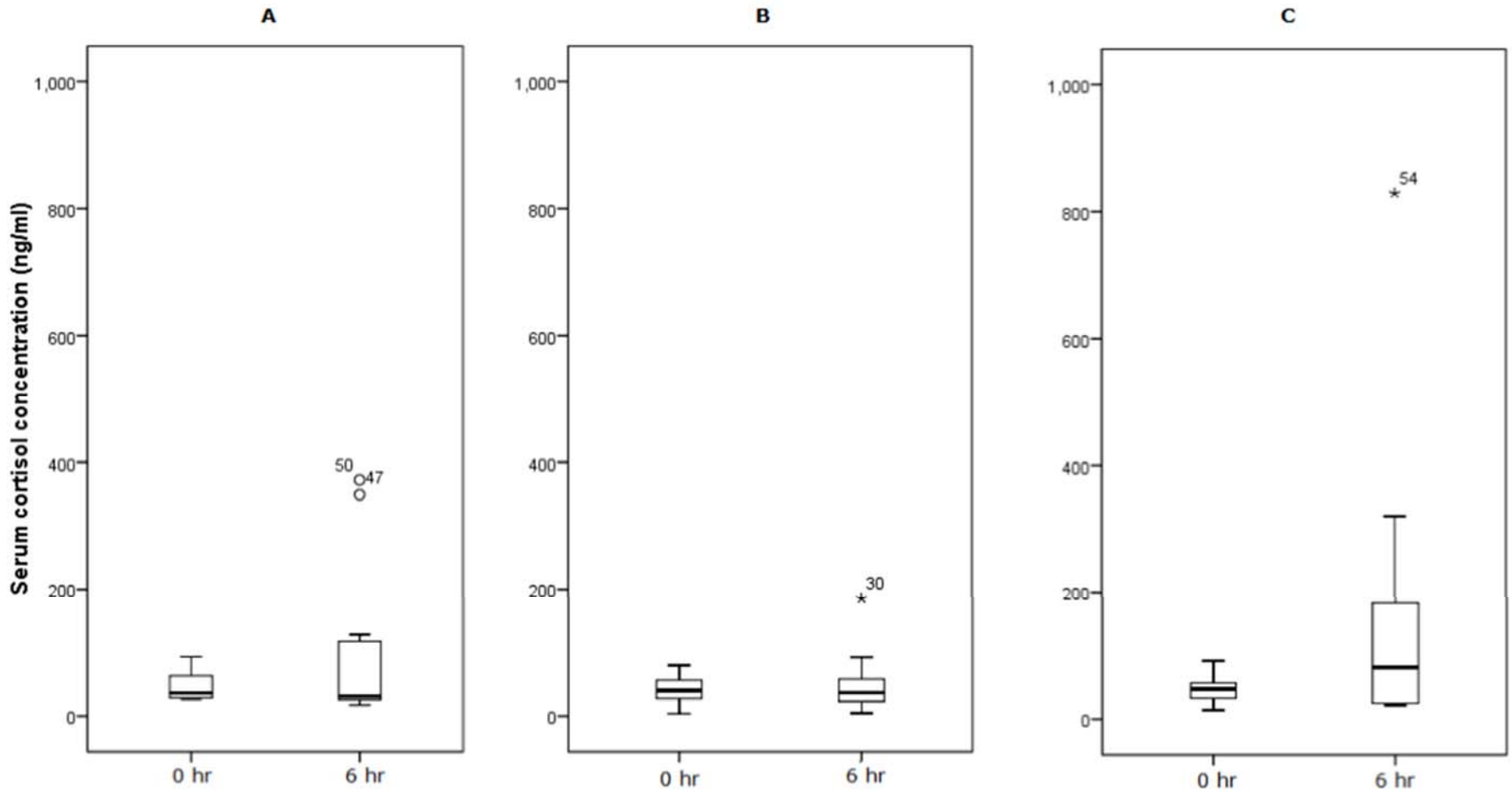

Figure 4.6: Box plots at 0 and 6 hour for serum cortisol concentrations in A: morphine, B: oxycodone and C: bupivacaine groups. Interquartile range and largest and smallest values (excluding outliers>1.5 box lengths outside box, marked separately) are shown.

Mean serum cortisol concentrations at baseline (0 hour) and 6 hour for all treatment groups

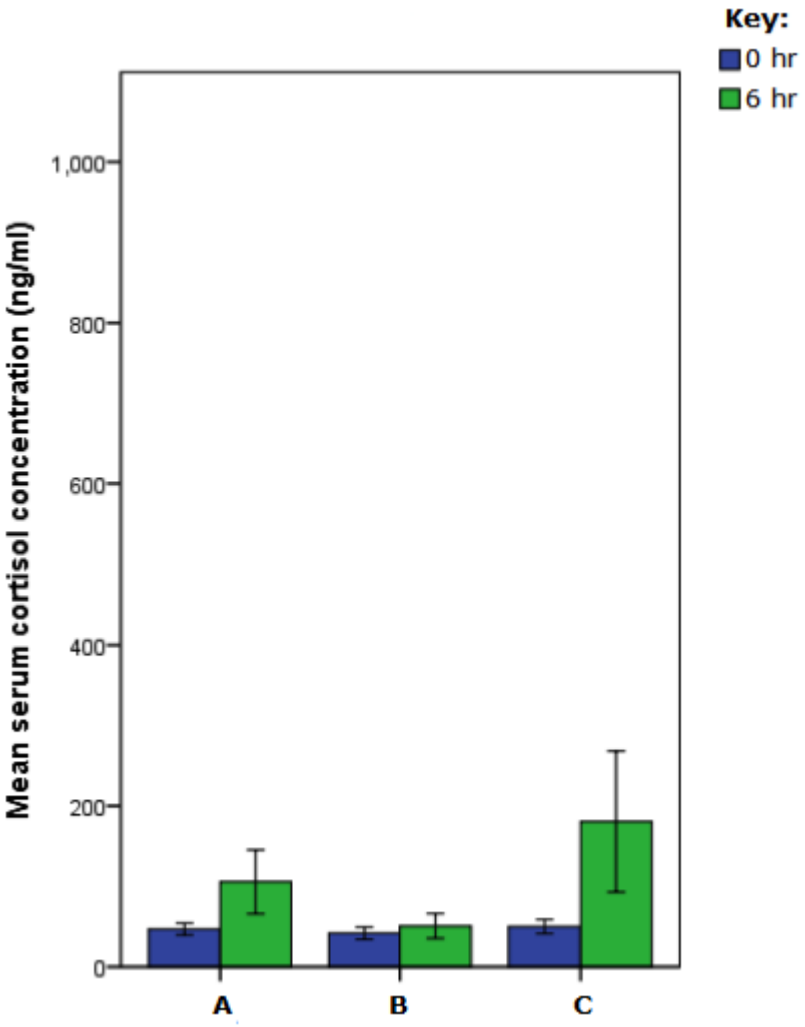

Figure 4.7: Mean cortisol concentrations for A: morphine, B: oxycodone and C: bupivacaine with SEM marked.

4.5 Discussion

This chapter aimed to use functional assays to corroborate the gene expression analysis described in Chapter 3, and to investigate a possible role for serum cortisol in influencing deregulation. A cytometric bead array (CBA) for TH1, TH2 and TH17 cytokines, an NK cell degranulation assay and a serum cortisol ELISA were all performed across treatment groups at baseline and 6 hour.

Of seven cytokines assayed with CBA, 5 (IL-2, -4, -17a, IFN-γ and TNFα) were below the detection threshold and therefore not analysed. The detection threshold for CBA is generally higher for each cytokine than for individual ELISAs; however even using a lower threshold, the samples would have remained below theoretical detection levels. Repletion of this assay in a larger sample cohort would have been desirable, however sample volume, time and cost prohibited it.

IL-6 increased significantly in all treatment groups from baseline to 6 hour, likely an effect of surgery [186, 187]. Morphine induced the greatest increase, from 1.1 to 52.9 pg/ml, compared to increases of 1.2 to 19.4 pg/ml by oxycodone and 2.0 to 23.0 pg/ml by bupivacaine. Increased IL1R2 in the blood has been associated with higher IL-6 levels in an epidemiological cardiac risk factor study [188]; IL1R2 transcript levels were increased by all analgesics at 6 hr. IL1R2 is a decoy receptor that antagonizes IL-1. Morphine induced a greater up-regulation in IL1R2 levels than oxycodone (morphine: 28.38 FC, oxycodone: 24.91 FC, bupivacaine: 30.20 FC) similarly to IL-6 levels.

However, an increase in IL-6 levels lasting over 2 hours following morphine administration in rats has also been shown, prevented by adrenal cortex removal [189], suggesting that the greater increase in IL-6 by morphine in this study may have been partially induced by morphine rather than being simply surgery-related. IL-6 shifts cells to a TH2 profile [190], as suggested by gene expression analysis in this study. Morphine has also been shown to reduce lymphocyte proliferation in rats, blocked by the MOR antagonist naltrexone [191]; as reduced lymphocyte proliferation is also seen with a TH2 shift, the morphine-induced reduced proliferation could be a result of a TH2 shift mediated through MOR.

IL-10 levels showed a statistically significant increase in response to morphine, increasing from 1.0 to 14.6 pg/ml. Levels increased from 0.9 to 12.4 pg/ml in oxycodone and 1.0 to 9.6 pg/ml in bupivacaine, neither statistically significant. IL-10 is an anti-inflammatory cytokine produced by TH2 cells and needed for a normal inflammatory response [192]. It negatively regulates the production of TH1 cytokines [193-195], consistent with a hypothesized morphine-induced shift to a TH2 profile. IL-10 also increases levels of CD163 expressed on monocytes [114]; shed CD163 can reduce T cell proliferation [196]. It has been shown to be increased 2-fold in mice following morphine administration [197] but has also been shown to be decreased [198]. As the maximal effect of morphine on lymphocyte gene deregulation was at 2 hour, it would be interesting to investigate IL-6 and IL-10 concentrations at this timepoint.

CD28, down-regulated by morphine, prevented a cortisol-induced shift to a TH2 profile following a reduction in TH1 cytokine production in naïve T cells

[123]. The down-regulation of CD28 seen in this study would therefore fail to prevent this TH2 shift, also suggested by the increases in IL-6 and IL-10 concentrations and deregulated genes. Conversely, GATA3, a transcription factor needed for notch-mediated differentiation of TH2 murine cells [166], was down-regulated by both opioids. It is a driver of TH2 differentiation and its activity, mRNA and protein levels were all repressed following glucocorticoid administration [167]. Down-regulation of GATA3 suggests a shift to a TH1 profile in both opioid groups, opposite to that suggested for the morphine group, and possibly induced by an increase in cortisol concentration.

The increase in mean serum cortisol concentration from baseline to 6 hour was not statistically significant in any treatment group. Greater increases were seen in morphine and bupivacaine groups, from 46.9 to 105.5 ng/ml and 50.0 to 180.4 ng/ml respectively, compared to that of oxycodone (41.7 to 50.6 mg/ml). However, morphine and bupivacaine had higher SEMs and statistically significant differences with oxycodone at 6 hour using Levene's test for equality of variances, suggesting greater sample spread. Bupivacaine's low sample size (n=9) contributed to this, and together these indicate that the increased (non-significant) serum cortisol concentration induced by morphine and bupivacaine at 6 hour may not translate to the whole population.

Any effect of cortisol on genes deregulated by both morphine and bupivacaine was nevertheless considered. LPL was up-regulated by both analgesics at 6 hour and has been shown to be increased by cortisol production [199]; however previous publications do not link it to morphine-induced enriched

processes such as lymphocyte activation or cell respiration. FLT3LG is down-regulated by both morphine and bupivacaine and has been shown to be up-regulated with cortisol following heavy exercise [200] but also up-regulated in PBMCs of patients with Graves' disease [201], a condition in which low cortisol can be found [202]. The down-regulation of FLT3LG in this study may be related to the small increase in cortisol level identified. FLT3LG is an essential cytokine needed for expansion of lymphoid lineages [203] therefore the gene down-regulation induced by cortisol could contribute to suppression of lymphocyte activation, also induced by cortisol in CD4+ and CD8+ lymphocytes [204] and hypothesized for morphine, although not bupivacaine.

In contrast, FLT3, the receptor for FLT3LG, was up-regulated by both analgesics; it has tyrosine kinase functions and has been shown to inhibit apoptosis and drive cellular proliferation. More importantly, it is a ligand for the glucocorticoid receptor so its up-regulation would reduce inflammation [205, 206] and suppress NKCC [207]. Cortisol is up-regulated by the HPA axis [206]; it is possible that FLT3 is similarly up-regulated, although no evidence exists for this.

NKCC was assayed indirectly via measurement of CD107a following cell degranulation. Non-stimulated and stimulated NK cells at baseline and 6 hour for all treatments were assayed. Both baseline opioid groups showed a higher

median number of events in non-stimulated compared to stimulated cells (

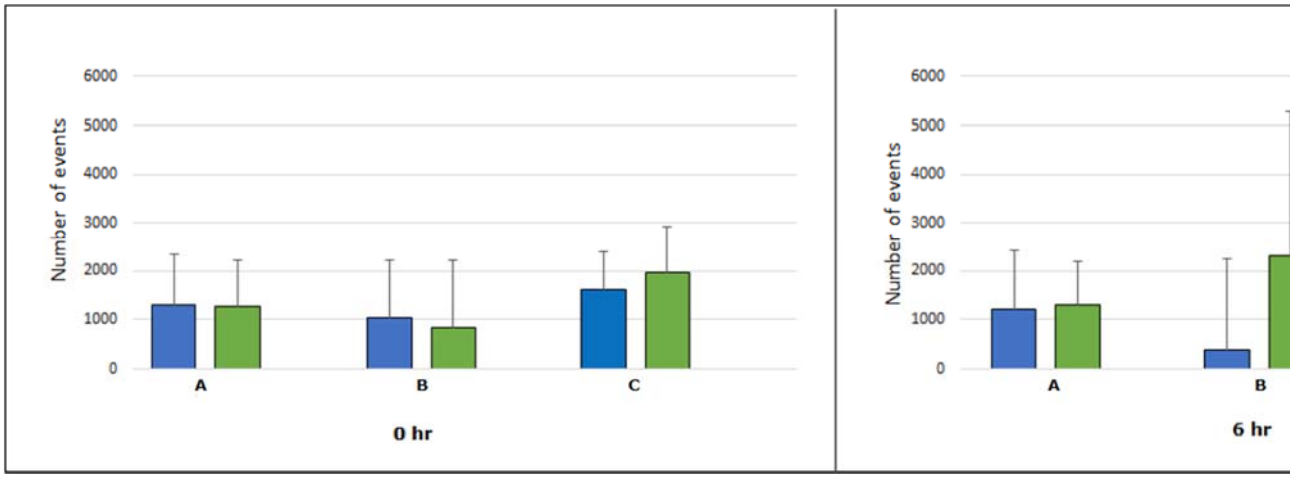

Figure 4.4) showing that stimulation unexpectedly produced reduced levels of CD107a and thus reduced degranulation. At baseline, 3/5 morphine samples and 4/6 oxycodone samples showed a lower count following stimulation. In contrast, 3/4 bupivacaine samples were successfully stimulated at baseline, shown by a 23% increase in median number of events from non-stimulated to stimulated cells. The failure to stimulate cells from opioid samples may have been due to a high number of non-viable NK cells or degraded or insufficient Staphylococcal enterotoxin B (SEB), although a problem with SEB is unlikely as bupivacaine samples were stimulated successfully. A difference in clinical characteristics of patients between treatment groups could be responsible and will be discussed in Chapter 7. Although degranulation appeared to be unsuccessful for the baseline opioid groups, this does not invalidate the 6 hour experiment; it can be viewed separately and comparisons made within the timepoint between non-stimulated and stimulated cells, and analgesic groups.

At 6 hour, median number of events was higher when stimulated were compared to non-stimulated samples, for all analgesics; 4/5 morphine samples, 5/6 oxycodone samples and 3/4 bupivacaine samples were successfully stimulated. Successful stimulation is unlikely to be due to a recovery in surgery-induced suppressed NKCC as this is thought to last for up to 28 days post-surgery [208]. Only oxycodone showed a statistically significant increase, with median events increasing from 392 to 2306 following stimulation. Although this may support the findings of the gene expression study, Figure 4.5 suggests that the significant increase is strongly influenced by 1 sample and is therefore unlikely to be representative of the whole population. When this sample is removed, the comparison is no longer statistically significant. Sample size was small (n=15 across all treatments) and the results need further validation; the degranulation assay should be repeated with more samples.

The NK cell functional degranulation assay used only NK cells, in contrast to the gene expression analysis for which mRNA from both T and NK cells were used. The data discrepancy of morphine-induced altered cell cytotoxicity suggested by gene expression analysis but not confirmed by the functional degranulation assay could be explained by the presence of cytotoxic CD8+ cells. These cells have an important role in cancer cell removal and defects in this population have been widely documented [209, 210]; CD8+ mRNA was present for the gene expression analysis but CD8 + cells were not used for the degranulation assay.

MMPs, specifically MMP1, MMP2 and MMP9, [211] mediate CD16 shedding from the NK cell surface resulting in the refractory period. MMP9 was up-

regulated by morphine at 2 hour (FC 7.2) and MMP9 and MMP25 by oxycodone at 6 hour (FCs of 17.9 and 4.4 respectively). The morphine-induced MMP9 deregulation is unlikely to have been induced by previous NK degranulation as cells failed to degranulate *in vitro* at baseline (Figure 4.4). It is more likely to have been directly induced by morphine as shown previously in humans [29] and mice [212]. Up-regulated MMP9 could then stimulate CD16 shedding, which would produce a refractory period and subsequently the expected reduced degranulation. CD16 is also present on the surface of some CD8+ cytotoxic T cells [213]; the hypothesized increased shedding could therefore also occur on CD8+ cells. It would be interesting to repeat the degranulation assay additionally using CD8+ cells.

CD16 shedding is also induced by ADAM17, a metalloprotease expressed by NK cells [214] and up-regulated, with ADAM9 and ADAM19, by oxycodone (FCs of 2.2, 3.4 and 2.8 respectively). The ADAM17 up-regulation seen may be a response to degranulation, assuming that the baseline *in vitro* degranulation was also seen *in vivo* and that the increase in degranulation in the oxycodone group is repeatable with a larger sample size. ADAM9 was up-regulated following stimulation of PBMCs with IL-10 [215] and was also up-regulated in this study by morphine at 6 hour (FC 3.4). It is a metalloproteinase disintegrin involved in leukocyte migration in inflammatory muscle conditions [215]. If it also has a role in T cell migration in healthy individuals, up-regulation of ADAM9 at 6 hour would be consistent with oxycodone's increased lymphocyte activation and morphine's recovering lymphocyte activation suggested by gene expression analysis at this timepoint. It is possible that ADAM9 up-regulation was induced by IL-10,

increased at 6 hour in all groups, and as a refractory response to NK cell degranulation.

Due to the small sample size and equivocal result, the degranulation assay should be repeated. In addition, as some publications suggest that increased degranulation exists with impaired cytotoxicity [216], direct cellular cytotoxicity could be investigated using the ^{51}chromium-release assay to further validate these findings.

4.6 Conclusion

In conclusion, all patients showed a TH2 shift, with morphine patients showing the greatest TH2 shift as demonstrated by the greatest increases in IL-6 and IL-10. The increase in IL-6 by all treatments is likely to be a surgery-induced, and, additionally in the morphine group, a morphine-induced increase. Only morphine patients showed a statistically significant increase in IL-10, strengthening the TH2 profile and possibly up-regulating ADAM9, which may be involved in CD16 shedding from NK and T cells. MMP9 was also up-regulated and has been implicated in CD16 shedding; shedding precedes the NK cell refractory period. Further work could investigate ADAM9 and MMP9 up-regulation and CD16 shedding from both NK and cytotoxic CD8+ cells in morphine and oxycodone-treated groups.

The effect of the analgesics on NK cell degranulation was equivocal and should be repeated with more samples. A ^{51}chromium-release assay could be performed to determine if target cell killing is reduced by morphine. No treatments showed a statistically significant increase in levels of serum cortisol concentration at 6 hour, suggesting that cortisol levels did not affect gene deregulation significantly. A possible influence of increased serum cortisol on deregulation of specific genes such as FLT3, FLT3LG and CD28 could be further investigated.

Chapter 5

Gene identification through statistical methods

5.1 Introduction

The analysis of gene expression data in Chapter 3 and the functional assays of Chapter 4 suggested that morphine may be immunosuppressive during the intraoperative period, while oxycodone may improve the immune response postoperatively. Morphine predominately down-regulated genes enriched in processes related to RNA transcription and translation, apoptosis and cell respiration at 2 hours. Oxycodone deregulated only 3 genes at this timepoint but induced expression of genes enriched in processes related to apoptosis and lymphocyte activation at 6 hours, suggestive of a heightened immune response.

Given that morphine is cheap and widely used for intra- and postoperative analgesia, it is not realistic or desirable to curtail its use as analgesic, particularly as pain itself is immunosuppressive [87, 89-91]. However, the identification of key genes involved in mediating the effects of analgesia on lymphocyte gene deregulation is essential to understanding the mechanisms of immunosuppression. In addition, the identification of genes indicating a baseline susceptibility to opioid-induced gene deregulation would enable analgesia to be selected appropriately in vulnerable patients.

5.2 Aims

The aims of this chapter are to use statistical methods to identify individual genes both key in mediating the effects of analgesia on gene deregulation, and those that may indicate individual susceptibility to immune modulation by opioids.

5.3 Methods

Eligible non-cancer open gynaecological patients were recruited to the study as described in Chapters 2 and 3. Following venepuncture, mononuclear cells were removed from blood samples using Ficoll-Hypaque technique then CD4+, CD8+ and NK cells separated via magnetic separation. Extracted RNA (Qiagen RNeasy kit) was hybridised to Affymetrix arrays and analysed using Partek software. ANOVA was used to generate gene lists at different time / treatment combinations which were used for the statistical analysis of this chapter.

5.3.1 Logistic regression

Binary logistic regression (LR) was performed to find genes most strongly predictive of a particular treatment. Normalised intensity values for all 40 patients for all genes deregulated by a treatment were inputted separately at each timepoint, to establish if values could predict treatment. LR was performed in SPSS v22 using forward conditional stepwise as the data entry method. Predictive genes were those with p-value ≤0.05.

5.3.2 Receiver operating characteristic (ROC) curve

ROC curves are normally used to show the accuracy of clinical prognostic testing and in this case were used to confirm LR results where possible and to evaluate the significance of genes most highly deregulated by morphine and oxycodone. Again, logged and normalised intensity values were inputted separately for each timepoint and values for all 40 patients were used. Morphine values were patient values with other treatments acting as controls, unless a gene was solely deregulated by oxycodone. ROC curves were

generated in GraphPad Prism and results were taken to be positive if AUC ≥ 0.7.

ROC curves were not generated for genes highly deregulated by bupivacaine as the low sample size of this group (n=8) compared to morphine and oxycodone groups (n=16 per group) would have conferred an inaccuracy to the test.

5.4 Results

5.4.1 Logistic regression

Genes found to be predictive of a treatment through logistic regression (LR) are shown in Table 5.1. Eight genes predicted morphine treatment and 13 (5 unannotated) predicted oxycodone treatment. Six genes predicted bupivacaine treatment and 3 predicted morphine treatment using those genes deregulated at 6 hours only. Heatmaps were drawn to show the relative position of predictive genes within the datasets with maximal effect for morphine (2 hour) and oxycodone (6 hour) (Figure 5.1 and Figure 5.2).

Table 5.1: Genes found to be predictive of analgesic use following logistic regression.

Gene group	Timepoint			
	0 hr	**2 hr**	**6 hr**	**24 hr**
Mor0-2 only 494 probes	No genes found	HSPH1 TIAM1 TPK1 AGPAT3	CH25H DAPK2 RFX7 SLC26A11	No genes found
Mor0-6 only 25 probes	No genes found	LDLRAD3	AMPH CH25H	No genes found
Oxy0-6 only 633 probes	OSCAR IL13RA1 USP15 234196_at	1559573_at C13orf18 229879_at 232958_at 234196_at	234196_at HIP1 237618_at	MCL1 ORM1/ORM2 ZNF608
Bup0-6 only 20 probes	EPHA1	C1QB STEAP3 NUDT16	MS4A4A	ARHGAP29

Supervised hierarchical clustering of probes deregulated at 2 hours exclusively by morphine (gene list Mor0-2: 450 genes / 494 probes) for all 156 samples across all 3 treatment groups.

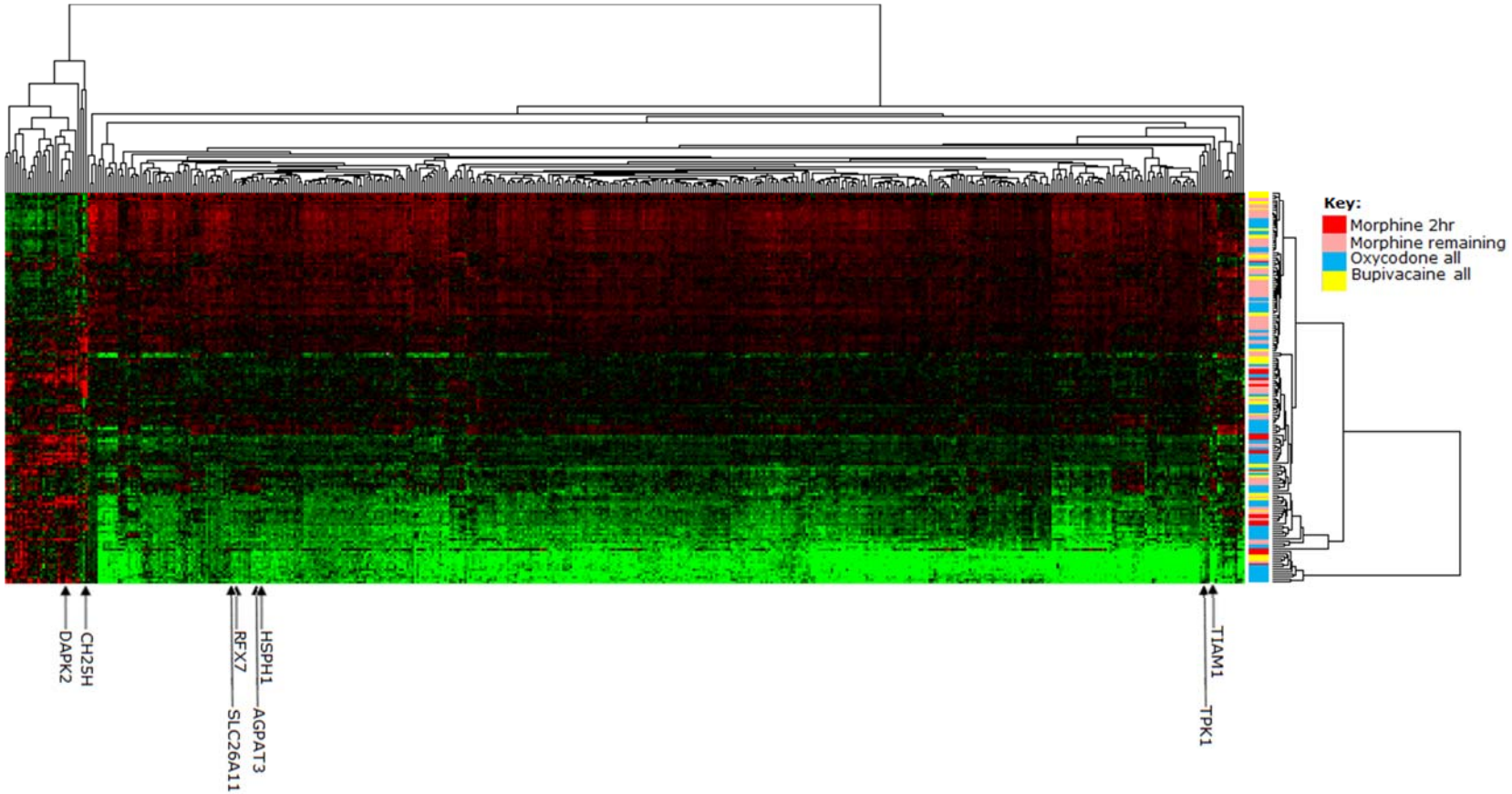

Figure 5.1: Supervised hierarchical clustering generated for all 494 probes (450 genes) deregulated by morphine only at 2 hour, for all 156 arrays. 2 hours is the timepoint at which morphine induces its maximal effect on lymphocyte gene expression. Data was correlated by Euclidean distance and average linkage was used to create the linkage tree. Genes predictive of morphine treatment following LR of this group are marked. Green pixels denote low mRNA expression and red pixels denote high mRNA expression. The key highlights samples by dataset.

Supervised hierarchical clustering of probes deregulated at 6 hours exclusively by oxycodone (gene list Oxy0-6: 460 genes / 633 probes) for all 156 samples across all 3 treatment groups.

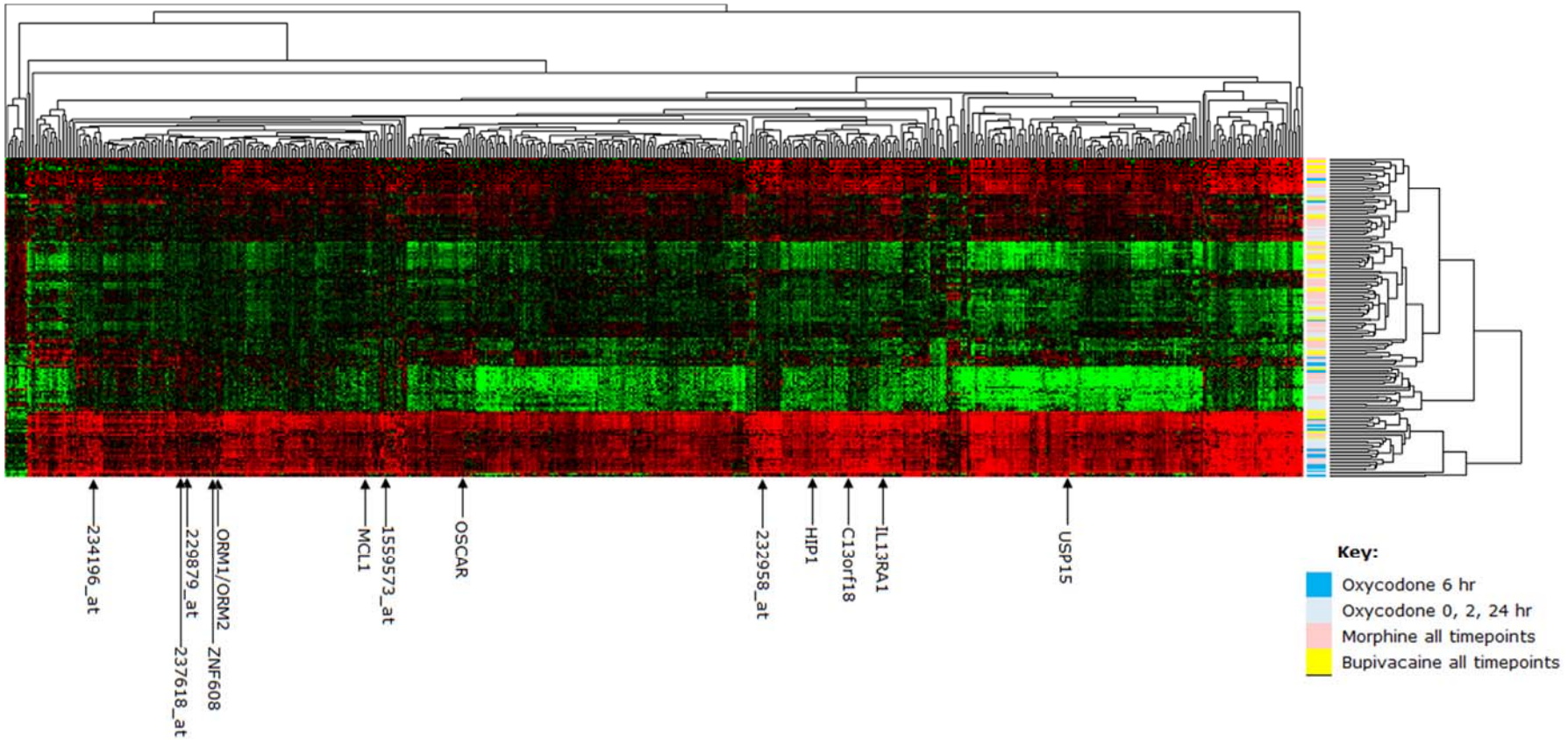

Figure 5.2: Supervised hierarchical clustering generated for all 633 probes (460 genes) deregulated by oxycodone only at 6 hour for all 156 arrays. 6 hours is the timepoint at which oxycodone induces its maximal effect on lymphocyte gene expression. Data was correlated by Euclidean distance and average linkage was used to create the linkage tree. Genes and unannotated probes predictive of oxycodone treatment following LR of this group are marked. Green pixels denote low mRNA expression and red pixels denote high mRNA expression. The key highlights samples by dataset.

5.4.2 ROC curves

ROC curves were generated for genes identified through two separate routes: those that predicted treatment through LR and those that were highly deregulated (top 10 up- and down-regulated) by morphine or oxycodone. 69 genes underwent ROC analysis in total, 10 of which had AUC values ≥ 0.7 and were therefore taken to be significant. ROC curves are shown in Figure 5.3 and Appendix B.

Table 5.2: Genes found to be significant through ROC analysis, taken from an initial pool of all genes found to predict treatment through LR and the most highly up- and down-regulated 10 genes deregulated by morphine and oxycodone. Genes were significant if AUC value ≥ 0.7. Varying patient / control numbers reflects the different group sizes and absence of some 24 hour samples.

Gene	Time-point	Group comparison	AUC	Std. Error	95% CI	P value	Controls	Patients
AGPAT3	2 hr	**M** v O+B	0.7083	0.08405	0.5436 to 0.8731	0.0272	24	16
LDLRAD3	2 hr	**M** v O+B	0.7552	0.07739	0.6035 to 0.9069	0.006842	24	16
TPK1	2 hr	**M** v O+B	0.737	0.08104	0.5781 to 0.8958	0.012	24	16
AMPH	6 hr	**M** v O+B	0.7266	0.0812	0.5674 to 0.8858	0.01635	24	16
CH25H	6 hr	**M** v O+B	0.75	0.07869	0.5957 to 0.9043	0.008066	24	16
MGST1	6 hr	**M** v O+B	0.724	0.08492	0.5575 to 0.8904	0.01762	24	16
229879_at	2 hr	**O** v M+B	0.7083	0.08697	0.5378 to 0.8788	0.02725	24	16
1559573_at	6 hr	**O** v M+B	0.7109	0.08965	0.5352 to 0.8867	0.02538	24	16
234196_at	6 hr	**O** v M+B	0.7995	0.07559	0.6513 to 0.9477	0.001508	24	16
237618_at	6 hr	**O** v M+B	0.8464	0.06512	0.7187 to 0.974	0.0002	24	16
C13orf18	6 hr	**O** v M+B	0.763	0.07591	0.6142 to 0.9118	0.005317	24	16
MCL1	6 hr	**O** v M+B	0.7656	0.07772	0.6133 to 0.918	0.0049	24	16
ORM1/ORM2	6 hr	**O** v M+B	0.7031	0.086	0.5346 to 0.8717	0.0313	24	16
SLC25A37	6 hr	**O** v M+B	0.7292	0.0844	0.5637 to 0.8946	0.01515	24	16
BACH2	24 hr	**O** v M+B	0.7563	0.08039	0.5986 to 0.9139	0.009067	20	16
GATA3	24 hr	**O** v M+B	0.7063	0.08869	0.5324 to 0.8801	0.03568	20	16
ORM1/ORM2	24 hr	**O** v M+B	0.7375	0.0821	0.5766 to 0.8984	0.0155	20	16

ROC curves for 4 of 16 genes significant for morphine and oxycodone patients following ROC analysis

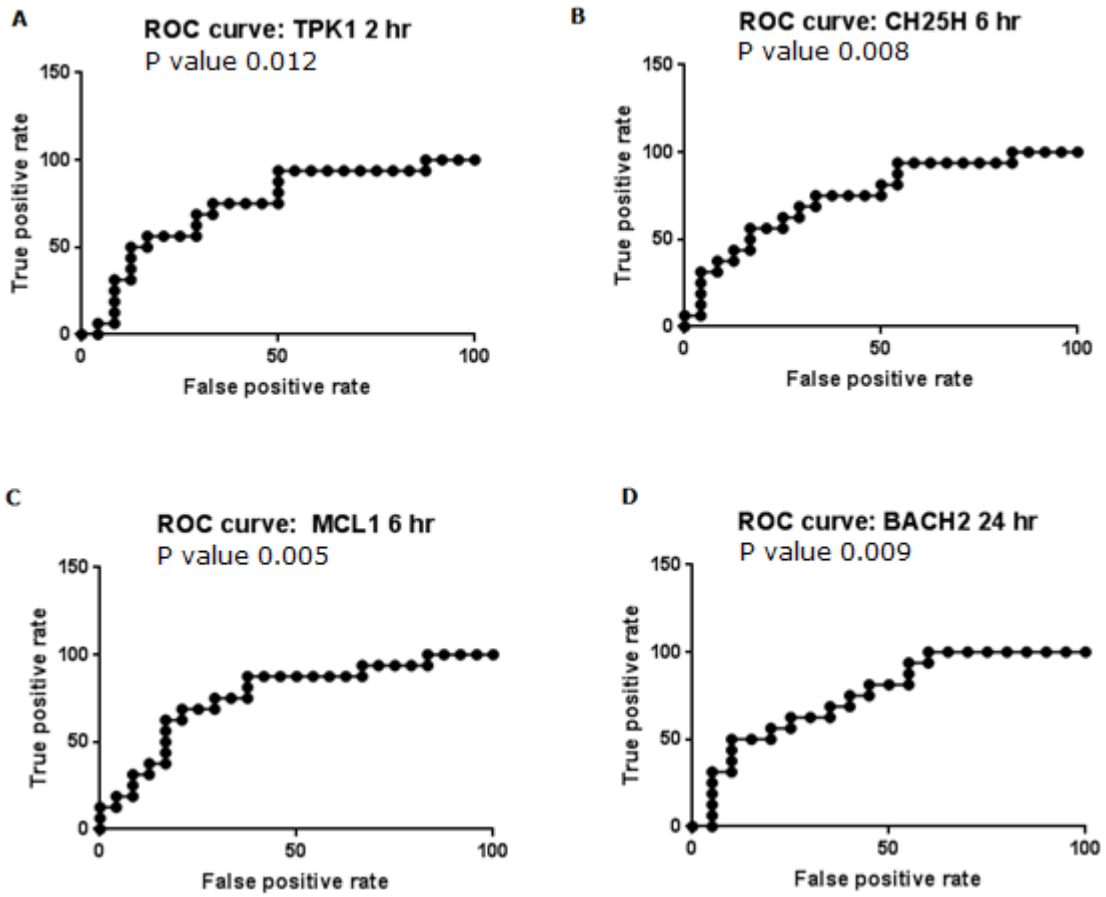

Figure 5.3: ROC curves for 4 genes found to be significant following ROC analysis. A and B are significant for morphine patients; C and D are significant for oxycodone patients. All other ROC curves are shown in Appendix B.

5.5 Discussion

5.5.1 Overview

Chapter 3 defined the general effects of the 3 study analgesics on lymphocyte gene expression, while Chapter 4 confirmed a greater TH2 shift induced by morphine and a possible reduction in NKCC. This chapter aimed to use statistical methods to both define genes that could be driving these changes, and those that could indicate individual susceptibility to the changes. Logistic regression (LR) and receiver operating characteristic (ROC) curves were used. Generally, genes predictive of a treatment at baseline might indicate a susceptibility to later opioid-induced gene deregulation, whereas genes predictive subsequently may be involved in mediating these changes.

LR of genes deregulated by morphine at 2 hour found 8 to be predictive of treatment, 5 also significant through ROC. MGST1 was highly deregulated by morphine at 6 hour and significant through ROC. Thirteen genes were found to be predictive of oxycodone treatment, 7 also significant through ROC, with a further 3 highly deregulated genes significant through ROC. Epidural bupivacaine deregulated only 20 genes exclusively at 6 hour and was predicted by 6 genes through LR.

5.5.2 Morphine

Logistic regression of the genes deregulated by morphine at 2 hour produced predictor genes that clustered together in pairs in the supervised cluster analysis (Figure 5.1). Four genes predicted morphine using 2 hour values and 4 using 6 hour values; at 2 hour all predictive genes were down-regulated.

The 4 genes predictive of treatment following LR of 2 hour values were AGPAT3, HSPH1, TIAM1 and TPK1; AGPAT3 and TPK1 were also significant

through ROC. AGPAT3 is an acyltransferase involved in the phospholipid biosynthetic pathway, converting lysophosphatidic acid (LPA) to phosphatidic acid (PA): PA is needed for lymphocyte proliferation [217]. The down-regulation of AGPAT3 would reduce levels of PA and thus T cell proliferation, in keeping with the pathway down-regulations seen. If increased LPA in turn increased levels of its precursor lysophosphatidylcholine, the suppressive qualities of TRegs could be enhanced, via increased TGF-β production [218]. TPK1 (thiamin pyrophosphokinase 1) exists as a homodimer and catalyses the conversion of thiamine to thiamine pyrophosphate (TPP). TPP is a cofactor in essential processes including oxidative degradation of sugars and mitochondrial synthesis of ATP [219]. The likely reduction of TPP following TPK1 down-regulation is in keeping with the general down-regulation of genes related to cell respiration, as discussed in Chapter 3.

HSPH1 is a heat shock protein and member of the HSP105 family [220], required for Wnt signalling and β-catenin stabilisation. Without HSP105, β-catenin is degraded and gene transcription impaired [221]; β-catenin also binds to cadherins, which influence cell adhesion and migration [222]. If HSPH1 has similar effects, its down-regulation by morphine could prevent gene transcription, influence cell adhesion and decrease IFN-β expression [223], all downstream effects of β-catenin. IFN-β has been linked with macrophage-mediated priming of NK cells, producing increased degranulation [224]; its reduction would therefore be consistent with the reduced NKCC previously induced by morphine [29-31]. TIAM1 is needed for T cell adhesion and migration [225] and was found repeatedly in pathways related to apoptosis. In T lymphocytes, it is involved in protrusion formation in the leading edge during PMA-stimulated migration [226]; knockout

produced increased tumour migration in pancreatic cancer cells [227]. The morphine-induced down-regulation is consistent with the down-regulation of processes related to lymphocyte activation and apoptosis. As a predictor gene, it may be important in mediating these changes.

Using 6 hour values, 2 up-regulated (CH25H and DAPK2) and 2 down-regulated genes (RFX7 and SLC26A11) predicted morphine treatment. CH25H (deregulated at 2 and 6 hour) is an interferon-stimulated ER-associated protein catalysing cholesterol oxidation, with antiviral effects through its 25HC production [228, 229]. It was up-regulated in LPS-stimulated murine macrophages [230], so may have a role in inflammation. If stimulation of T cells also results in CH25H up-regulation, the sustained up-regulation induced by morphine could be a sign of a normal immune response. CH25H was also significant through ROC. DAPK2 is a serine threonine protein kinase present in mitochondria and involved in apoptotic and receptor-induced cell death. Its depletion both increases intracellular reactive oxygen species (ROS), impairing mitochondrial metabolism downstream [231] and activates NF-kB by reducing the threshold for TCR activation, leading to a defect in cell survival [232]. The up-regulation of DAPK2 by morphine could produce an anti-apoptotic response and increased mitochondrial metabolism. The anti-apoptotic effect is in keeping with enriched processes seen at 2 hour, whereas increased mitochondrial metabolism is not and suggests a pro-inflammatory response.

SLC26A11 is a sulphate transporter based in the cell membrane of high endothelial venule cells; lymphocytes emigrating from blood to secondary lymphoid organs do so through these venules, whose cells contain high

sulphate levels [233]. Down-regulation by morphine could disrupt sulphate transport and subsequently lymphocyte trafficking.

LDLRAD3 was up-regulated by morphine at 6 hour but predicted morphine treatment and was significant through ROC at 2 hr. It is part of a lipoprotein receptor involved in APP processing and has a similar structure to LRP1, a protein related to the lipoprotein receptor and needed for TCR and CD28 activation [234]. The intracellular domain of LDLRAD3 has been shown to interact with several members of the NEDD4 family of E3 ubiquitin ligases, including Itch, to activate the inactive ligase via autoubiquitination; interaction subsequently increases its degradation [235]. The morphine-induced up-regulation of LDLRAD3 and initial increase in E3 ubiquitin ligase activity prior to degradation could effect regulation of immune function and cell signalling.

5.5.3 Oxycodone

Thirteen genes predicted oxycodone treatment following LR, all up-regulated in common with the majority of the group. Seven were also significant through ROC analysis. SLC25A37, BACH2 and GATA3 were highly deregulated genes significant through ROC.

OSCAR, IL13RA1 and USP15 are annotated genes that predict oxycodone response pre-treatment. OSCAR is an osteoclast-associated receptor expressed on myeloid cells, which associates with FcRγ to promote cellular activation [236] and phagocytosis of opsonised cells and microbes. A similar effect of OSCAR in T cells could increase cell activation; up-regulation of OSCAR may predict those patients more likely to experience increased lymphocyte activation or a smaller TH2 shift. IL13RA1, again a predictor gene

pre-treatment, is a subunit of IL13R, which complexes with IL4Rα to bind the TH2 cytokines IL-4 and IL-13. Up-regulation of IL13RA1 by oxycodone may increase cytokine activity and subsequent transcription and cellular immune responses via activated JAK1, STAT3 and STAT6. Its presence pre-treatment suggests a subsequent increased TH2 response.

USP15 deubiquitinates MDM2, preventing its degradation and allowing it to suppress the transcriptional activity of p53, the tumour suppressor [237] [238]. USP15 was up-regulated by oxycodone as was TP53I3, induced by P53 and thought to be involved in p53-mediated cell death. USP15 was also up-regulated following treatment of human T cells with morphine [239]; up-regulation in this study could therefore be opioid-receptor induced and part of a p53 homeostatic mechanism. However, the up-regulation of USP15 and TP5313 suggests a reduction rather than increase in p53 activity, opposite to the overall influence hypothesized for oxycodone.

Only 1 annotated gene, HIP1 (Huntingtin interacting protein 1), predicted oxycodone treatment at 6 hour. Its paralog HIP1R interacts with clathrin light chains (CLC), components of clathrin-coated vesicles, so HIP1 may be relevant for endosomal trafficking. Knockdown of CLC in HeLa cells prevented HIP1R localising correctly and caused an actin build-up [240]; if HIP1 behaved in a similar manner in lymphocytes, up-regulation by oxycodone would promote intracellular trafficking. HIP1 was predictive of oxycodone at 6 hour, the timepoint at which oxycodone exerted its maximal effect on gene deregulation.

MCL1 and ORM1/ORM2 predict oxycodone treatment at 24 hour. MCL1 was also significant through ROC and is an anti-apoptotic regulator, induced after

TCR stimulation in murine T cells [241]. Its overexpression in CD8+ cells of virally-infected mice increased differentiation of terminal effector and effector memory cells while decreasing differentiation of central memory cells [242]. Up-regulated MCL1 indicates increased TCR stimulation and an increased ability of CD8+ cells to respond quickly to antigen. ORM1/ORM2 are proteins up-regulated in the acute phase of inflammation [243] and have been shown to inhibit neutrophil migration in rats *in vivo* [244]; the up-regulation of these genes may impair T cell migration but may also be part of the inflammatory response.

BACH2 and GATA3 were highly down-regulated and significant through ROC analysis. BACH2 is a transcriptional regulator that both activates and suppresses transcription; BACH2 -/- mice showed positively regulated TReg development, repressed conventional T cells [164] and repressed lineage-specific genes, including GATA3 [165] (also down-regulated by morphine). GATA3 is a transcription factor required for notch-mediated differentiation of TH2 murine cells [166], has been called the master driver of TH2 differentiation and was repressed by glucocorticoid administration [167]. Cortisol is a glucocorticoid induced by surgery [50, 183] and morphine [178-182] which coordinates inflammation and a normal immune response [177]. An effect on cortisol levels could therefore alter the immune response. The down-regulation of BACH2 and GATA3 by oxycodone suggests T cell ratios biased towards TH1 or TRegs, possibly influenced by cortisol. The down-regulation of GATA3 by morphine suggests a TH1 rather than TH2 shift, not in keeping with functional changes hypothesized generally.

5.6 Conclusion

This chapter aimed to use statistical methods to elucidate genes key in mediating or predicting the immunomodulatory effects of morphine and oxycodone. Eight genes predicted morphine treatment and 13 predicted oxycodone treatment through logistic regression. Of these, 5 morphine and 7 oxycodone genes were also significant through ROC analysis. BACH2 and GATA3 were highly deregulated by oxycodone and also significant through ROC.

Of the genes predictive of morphine treatment, AGPAT3, TPK1 and TIAM1 have roles in lymphocytes and could be investigated further as biomarkers. AGPAT3 and TPK1 were also significant through ROC. Through altered phospholipid levels, down-regulated AGPAT3 may be key in mediating reduced T cell proliferation and increased TReg activity, while TPK1 may be important in mediating suppressed cell respiration by reducing levels of thiamine pyrophosphate, essential for ATP synthesis. TIAM1 may mediate reduced T cell trafficking by faulty leading edge formation during lymphocyte migration. LDLRAD3 is interesting as its deregulation at 6 hour, predictive ability and significance through ROC may be important in recovering lymphocyte activation.

OSCAR, BACH2 and MCL1 are relevant predictive genes induced by oxycodone. OSCAR promotes cellular activation and phagocytosis of opsonised cells, the down-regulation of BACH2 may induce a shift to a TH1 profile, and MCL1 indicates previous T cell stimulation. The deregulation of OSCAR and BACH2 are potential biomarkers for those patients who respond to oxycodone with increased lymphocyte activation or a reduced TH2 shift.

Further assays such as qRT-PCR or Western blot would be appropriate to confirm that these genes and proteins are indeed overexpressed in the relevant patient groups, with a view to considering them as biomarkers for opioid-induced lymphocyte gene deregulation. Validation in an independent cohort would be desirable to confirm the findings of this study.

Chapter 6

Dynamic changes in gene expression

6.1 Introduction

Chapter 3 reported the contrasting lymphocyte gene deregulation induced by morphine and oxycodone. Morphine induces deregulation primarily at 2 hours that, based on process enrichment, may be phenotypically immunosuppressive. The maximal effect of oxycodone on gene deregulation is at 6 hours and may be supportive of normal immune function, again based on process enrichment. The timecourse of these gene expression changes was investigated further in this chapter. Although the number of genes deregulated by each treatment at each timepoint indicates that all perturbations were brief, timepoint and treatment group overlaps were seen on supervised hierarchical clustering (Figures 16 and 17 of Chapter 3), indicating that some gene deregulation is sustained and induced by more than 1 treatment. Continued immunomodulation may produce a different phenotype to brief perturbations.

6.2 Aims

This chapter aims to investigate the duration of gene deregulation by the 3 treatment groups, and the clinical relevance of genes continually deregulated across timepoints and treatment groups.

6.3 Methods

Eligible non-cancer open gynaecological patients were recruited to the study as described in Chapters 2 and 3. Following venepuncture, mononuclear cells were removed from blood samples using Ficoll-Hypaque technique then CD4+, CD8+ and NK cells separated via magnetic separation. Extracted RNA (Qiagen RNeasy kit) was hybridised to Affymetrix arrays and analysed using Partek software. ANOVA was used to generate gene lists from different time / treatment combinations for the statistical analysis of this chapter.

6.3.1 Dynamic changes

Gene lists were compared across treatments and timepoints using Partek software and Excel, to investigate genes showing sustained versus short-lived perturbation across treatments and timepoints. Cluster 3.0, TreeView (see Chapter 2) and Excel were used to compare separation of arrays by treatment or timepoint. DAVID ontological software (Chapter 2) was used to compare process enrichment in different groups of genes.

6.4 Results

6.4.1 Overview of timepoint changes

The pattern of change by timepoint is distinctive (Figure 6.1); at 2 hours post-baseline, genes were almost exclusively deregulated by morphine, with only three (ADORA3, ANKRD22 and CHKA) induced by oxycodone treatment, and none by epidural bupivacaine. Most morphine genes (434 of 520 – those in processes relating to RNA transcription and translation, cell respiration and apoptosis as discussed in Chapter 3) were down-regulated. Genes up-regulated by morphine treatment included the three up-regulated by oxycodone.

By 6 hours, all treatments induced lymphocyte gene deregulation, but in contrast to 2 hours, oxycodone deregulated more genes than any other treatment, and almost all (540 genes) were up-regulated. These deregulated genes were represented by 810 probes, contrasting with the 520 genes deregulated by morphine at 2 hours, which were represented by only 576 probes. This may demonstrate the greater reproducibility of the oxycodone response. By 24 hours, only CCR2 was up-regulated by oxycodone and RNASE2 by morphine; neither gene was deregulated at a previous timepoint. Supervised hierarchical clustering of all deregulated genes (Figure 6.2) shows the pattern of change through the timepoints studied; the key highlights the clustering of 0 and 24 hour arrays versus 2 and 24 hour.

Dynamic gene expression changes following initiation of analgesia

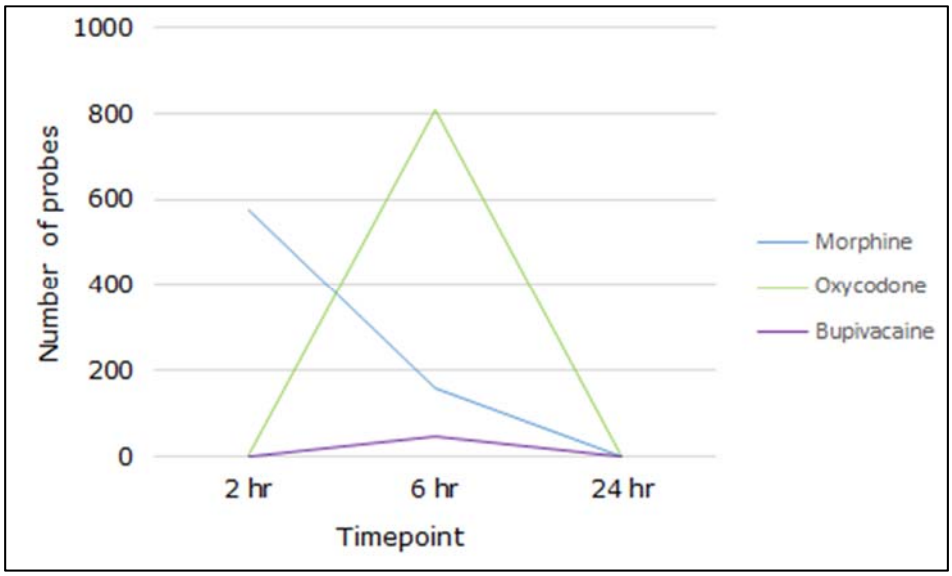

Figure 6.1: Number of probes deregulated by each treatment from 2 hour to 24 hour.

Supervised hierarchical clustering of probes deregulated by all treatments

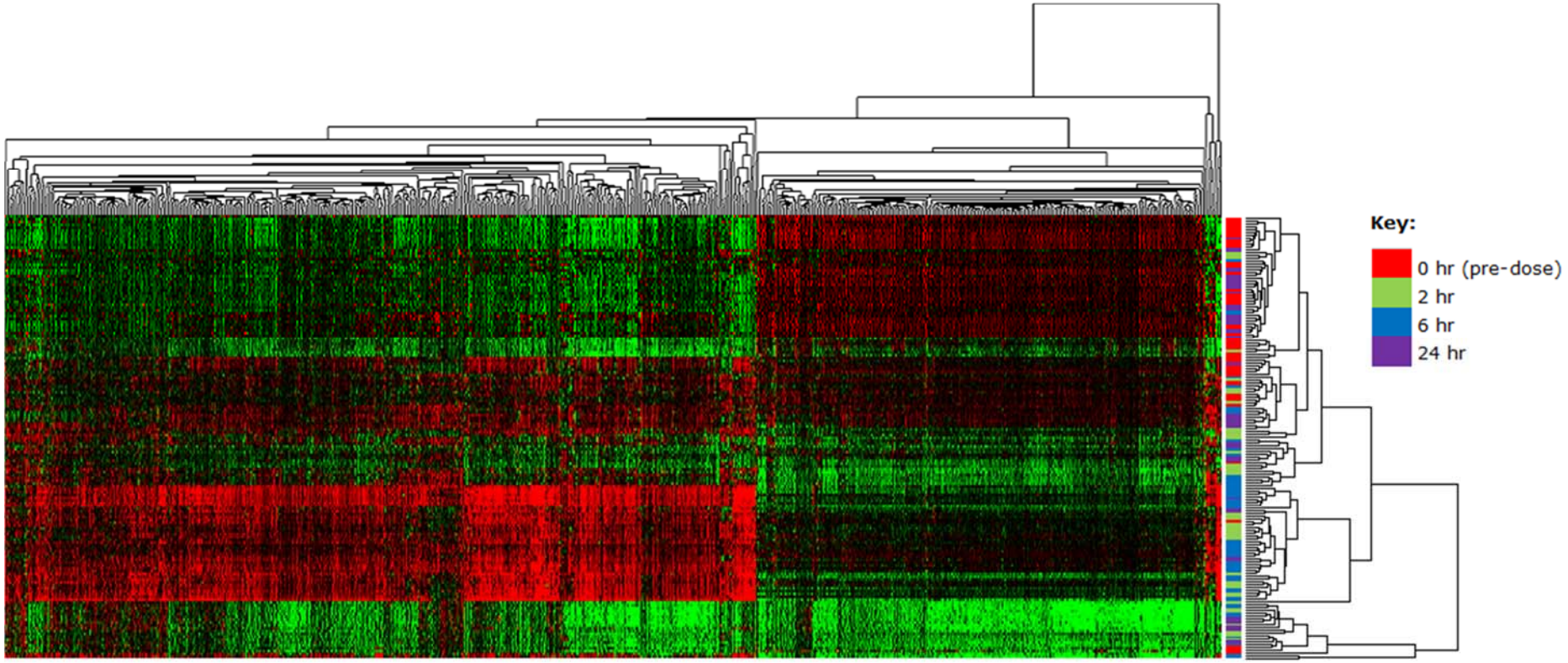

Figure 6.2: Supervised hierarchical clustering for all probes deregulated by the 3 study analgesics at 2 and 6 hour (gene groups Mor0-2, Mor0-6, Oxy0-6 and Bup0-6 – total 1485 genes) for all 156 arrays. Data was correlated by Euclidean distance and average linkage used to create the linkage tree. Green pixels denote low mRNA expression and red pixels denote high mRNA expression. The key highlights the separation of arrays by timepoint.

6.4.2 Sustained deregulation across timepoints

Within each treatment group, genes were mainly perturbed transiently (Figure 6.1 and Figure 6.3). Only small similarities were found between 2 and 6 hour gene groups deregulated by morphine and oxycodone. (No genes were differentially expressed by bupivacaine at 2 or 24 hour so the parallel comparison was not performed).

6.4.2.1 Morphine sustained response genes

In the morphine group, 495 genes deregulated at 2 hours (Mor0-2) were no longer deregulated at 6 hours (Mor0-6; Figure 6.3). The 25 genes continuously deregulated were classified as sustained response genes and considered separately, as they were continuously deregulated and mainly up-regulated (24 genes) counter to the general trend of morphine-induced genes. Sustained response (SR) genes are therefore defined as those genes deregulated by morphine at both 2 and 6 hours. They include 24 of the 86 genes up-regulated by morphine at 2 hour and just 1 down-regulated gene, FLT3LG. All SR genes have the same direction of change from baseline at both 2 and 6 hours. The only SR gene uniquely induced by morphine was CH25H.

Fold changes were compared between treatment groups for all SR genes (Figure 6.4); the most highly up-regulated gene at 6 hours for all groups was IL1R2 (28.38 FC in morphine; 24.91 FC in oxycodone; 30.20 FC in bupivacaine). In morphine and oxycodone, CLEC4D (FCs of 6.23 / 12.97 respectively) and SAMSN1 (FCs of 6.61 / 7.34 respectively) were the next highest up-regulated genes.

Supervised clustering of the 86 genes up-regulated by morphine at 2 hour (including 24 SR genes) was performed (Figure 6.5); SR genes are seen to mainly group together in the right-hand half of the heatmap, suggesting that of all up-regulated genes, SR genes resolve the array clustering by timepoint most successfully. The fold changes over time shown for SR genes in all treatment groups (Figure 6.4) demonstrates their earlier up-regulation by morphine followed by an up-regulation induced by all treatments at 6 hours, before decreasing to an insignificant FC<±2 at 24 hours. Process enrichment of SR genes only identified significant overrepresentation of processes involved in lymphocyte activation, compared to the 113-gene whole Mor0-6 group (Table 6.1).

6.4.2.2 Oxycodone early responder genes

The two genes deregulated by oxycodone at both 2 and 6 hour (Figure 6.3) were ADORA3 and ANKRD22, both up-regulated. These were defined as oxycodone early responder genes: those genes that are deregulated by oxycodone at both 2 and 6 hours. With the same pattern of sustained deregulation, ADORA3 was also a morphine SR gene (Section 6.4.2.1). Neither gene was deregulated by bupivacaine treatment.

Sustained opioid-induced gene deregulation across timepoints

Figure 6.3: The number of genes persistently deregulated following both morphine and oxycodone treatment at 2 and 6 hour. The 25 genes in the central morphine segment are defined as sustained response genes; the 2 genes in the central oxycodone segment are defined as oxycodone early responder genes.

Dynamic fold changes for morphine sustained response genes

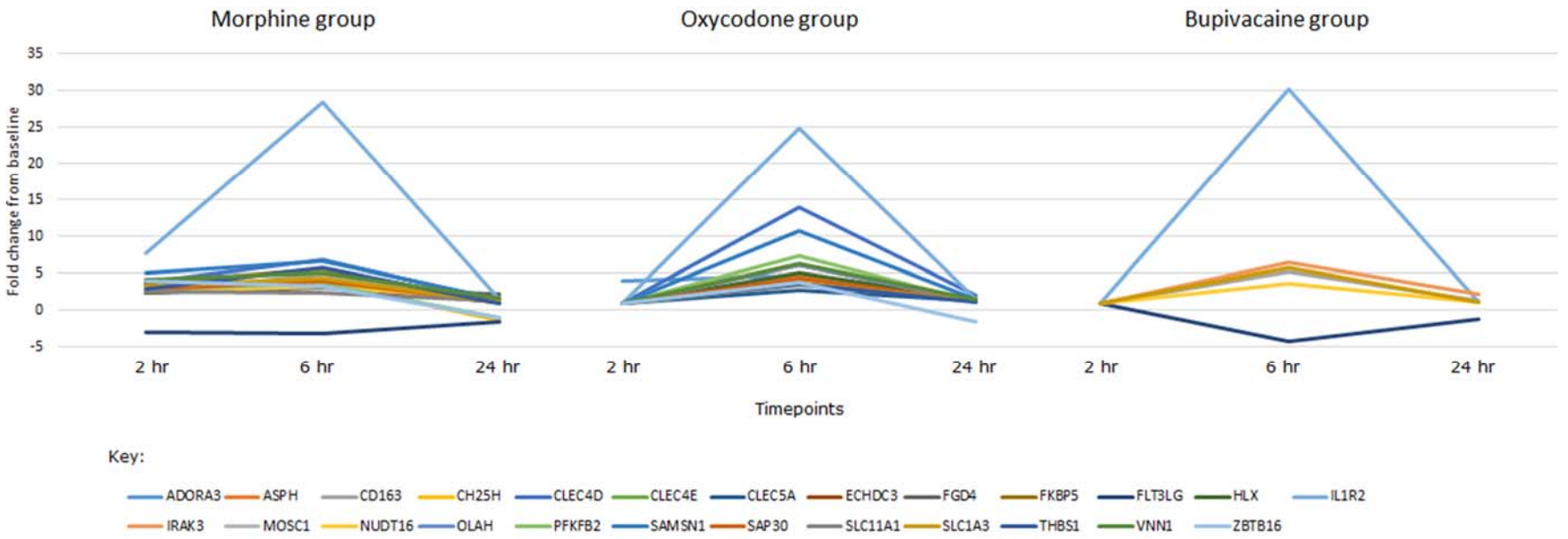

Figure 6.4: Fold changes at 2, 6 and 24 hour for morphine sustained response (SR) genes (genes deregulated by morphine at both 2 and 6 hour). The most highly up-regulated gene by all treatments is IL1R2 at 6 hour. Only one SR gene is perturbed at 2 hour by another treatment - ADORA3 by oxycodone. At 6 hour, 23 SR genes are perturbed by oxycodone and 6 SR genes by bupivacaine. FLT3LG is the only continuously down-regulated sustained response gene; this gene is also down-regulated at 6 hour by bupivacaine.

Supervised clustering of 86 genes up-regulated at 2 hour by morphine

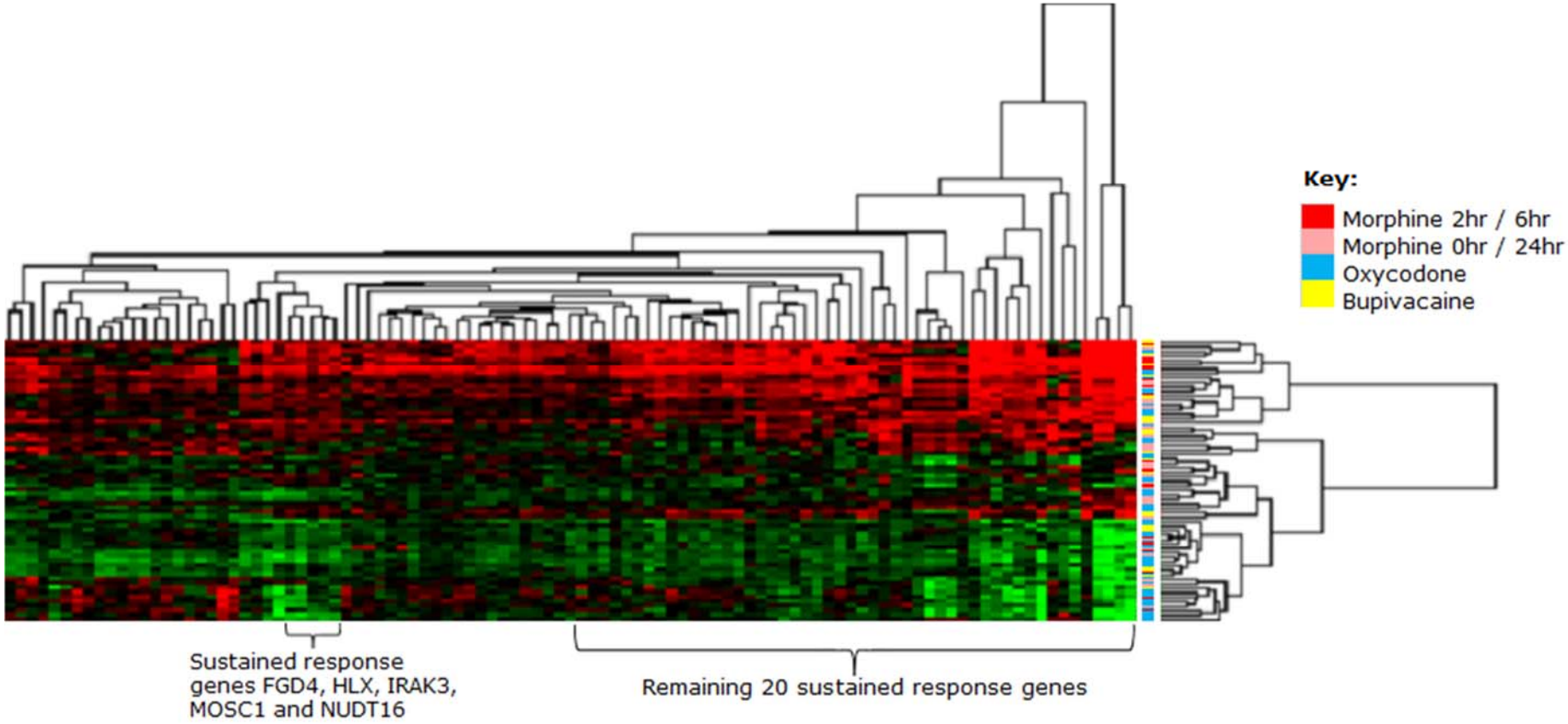

Figure 6.5: Supervised hierarchical clustering of all 86 genes up-regulated by morphine at 2 hour, for all 156 arrays. Data was correlated by Euclidean distance and average linkage used to create the linkage tree. Green pixels denote low mRNA expression and red pixels denote high mRNA expression. SR genes are annotated and the key highlights the separation of arrays by treatment.

Table 6.1: Summary of overrepresentation analysis highlighting biological processes enriched in genes significantly deregulated by A: morphine at 6 hour (113 genes / 158 probes) and B: selective enrichment for genes with sustained deregulation at 2 and 6 hour (25 SR genes / 31 SR probes). Top 20 processes by p-value are shown.

A: Biological processes - Mor0-6 (113 genes)	Genes	% of total input	p-value
response to wounding	21	19.6	2.00E-10
response to organic substance	19	17.8	9.90E-07
inflammatory response	13	12.1	1.50E-06
defense response	17	15.9	2.60E-06
innate immune response	9	8.4	3.70E-06
negative regulation of cytokine production	6	5.6	4.90E-06
immune response	7	6.5	1.20E-05
response to lipopolysaccharide	17	15.9	1.10E-05
response to molecule of bacterial origin	7	6.5	2.20E-05
response to insulin stimulus	7	6.5	5.30E-05
organic acid biosynthetic process	8	7.5	7.60E-05
carboxylic acid biosynthetic process	8	7.5	7.60E-05
positive regulation of developmental process	10	9.3	9.50E-05
positive regulation of molecular function	14	13.1	1.30E-04
fatty acid biosynthetic process	9	8.4	1.80E-04
positive regulation of immune system process	8	7.5	2.00E-04
regulation of cytokine production	6	5.6	1.80E-04
regulation of phosphorylation	12	11.2	2.60E-04
response to endogenous stimulus	12	11.2	3.60E-04
regulation of phosphate metabolic process	12	11.2	3.60E-04

B: Biological processes – SR genes (25 genes)	Genes	% of total input	p-value
positive regulation of immune system process	5	20	4.40E-04
immune response	7	28	4.80E-04
response to wounding	6	24	1.10E-03
inflammatory response	5	20	1.40E-03
negative regulation of cytokine production	3	12	1.60E-03
positive regulation of molecular function	6	24	1.70E-03
regulation of kinase activity	5	20	2.00E-03
defense response	6	24	2.10E-03
regulation of transferase activity	5	20	2.30E-03
regulation of antigen processing and presentation	2	8	3.10E-03
regulation of dendritic cell antigen processing and presentation	2	8	3.10E-03
positive regulation of kinase activity	4	16	5.20E-03
regulation of phosphorylation	5	20	5.20E-03
positive regulation of transferase activity	4	16	5.80E-03
regulation of phosphorus metabolic process	5	20	6.00E-03
regulation of phosphate metabolic process	5	20	6.00E-03
negative regulation of immune system process	3	12	7.20E-03
positive regulation of catalytic activity	5	20	7.70E-03
negative regulation of interleukin-12 production	2	8	7.70E-03
chronic inflammatory response	2	8	9.30E-03

Key:

Response to wounding
Lymphocyte activation

6.4.3 Sustained deregulation across treatment groups

6.4.3.1 All treatments at 6 hours

A number of genes were deregulated across treatments. Similarities in numbers of deregulated genes induced by treatment groups, regardless of timepoint then grouped by timepoint, are shown (Figure 6.6).

Ten genes (14 probes) were up-regulated by all treatments at 6 hour (Figure 6.6C); these genes included C19orf59/MCEMP1, CD163, CYP1B1, IL1R2, IRAK3, NUDT16, SLC1A3, SORT1 and ST6GALNAC3. The most highly up-regulated genes were IL1R2, C19orf59/MCEMP1 and CD163 (Figure 6.7); deregulation of these genes is likely to be surgery-related. The 78 genes (112 probes) deregulated by both morphine and oxycodone at 6 hours showed the same direction of change from baseline regardless of opioid and included 17 SR genes.

Numbers of genes consistently deregulated across treatment groups

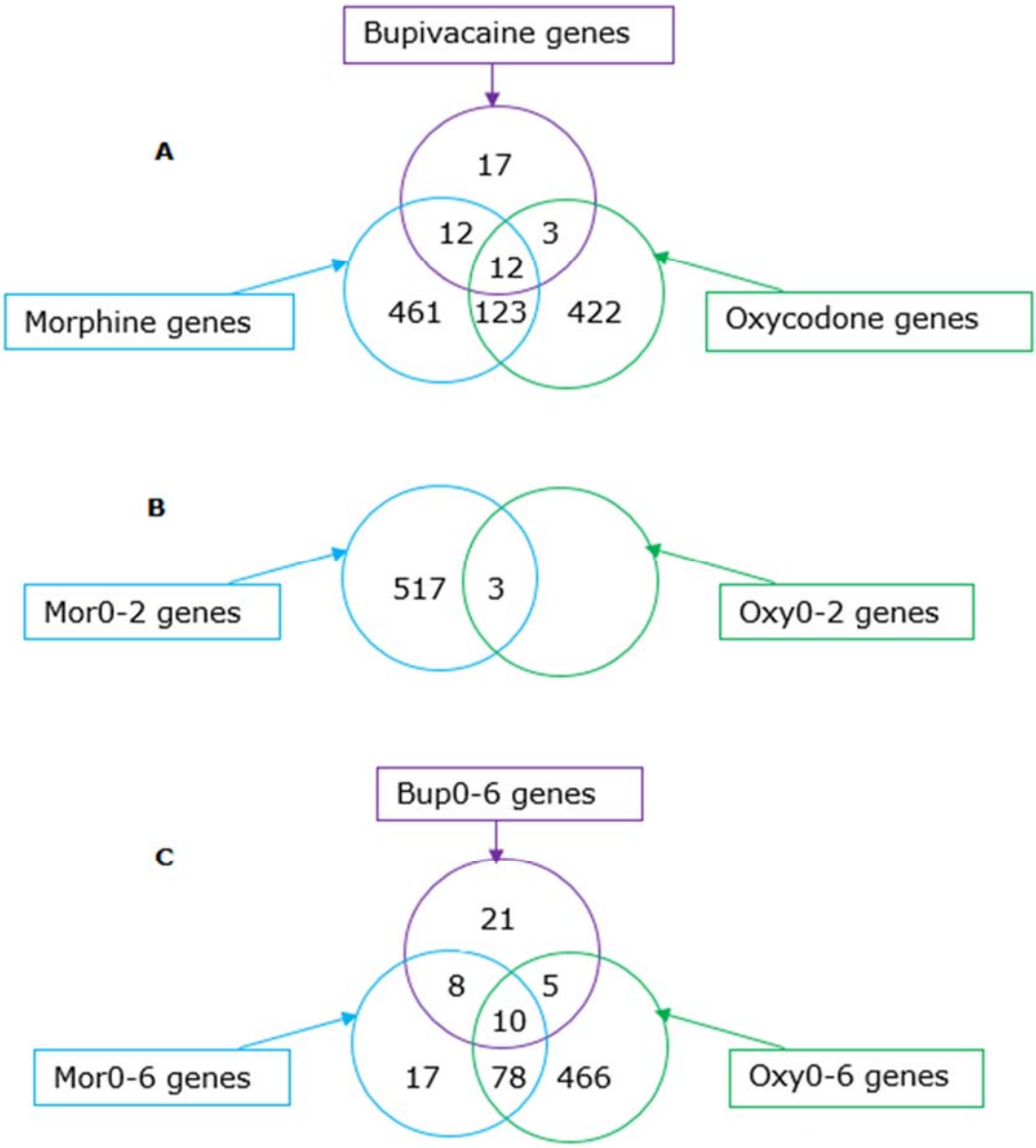

Figure 6.6: Similarities in deregulated genes A: between treatment groups, regardless of timepoint; B: between all treatment groups at 2 hours, and C: between all treatment groups at 6 hours.

Dynamic fold changes for genes deregulated by all treatments at 6 hours

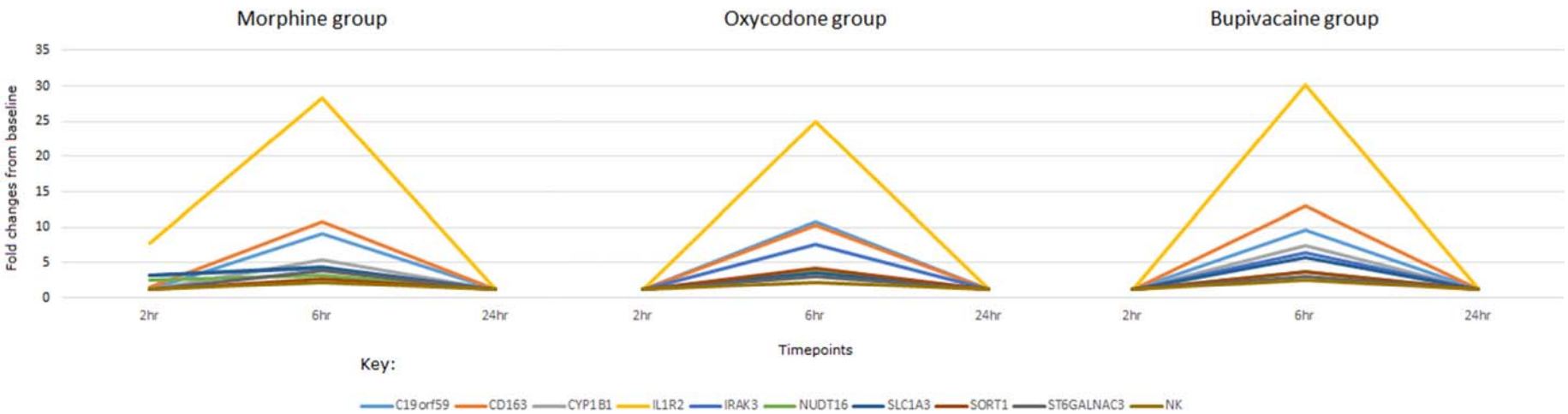

Figure 6.7: Fold changes at 2, 6 and 24 hour for the 10 genes deregulated at 6 hours by all treatments.

6.4.4 Sustained deregulation across timepoints and treatment groups

6.4.4.1 Morphine (2 hours) and oxycodone (6 hours)

66 genes (77 probes) were deregulated by both morphine at 2 hour and oxycodone at 6 hour, the timepoints where the maximal change in gene expression for these treatments was observed. All genes had the same vector of change regardless of treatment; 9 were down-regulated and 57 up-regulated. Deregulated genes were enriched in 25 processes (p-value≤0.01) related to lymphocyte activation, apoptosis and response to wounding (Table 6.2). No processes relating to RNA translation or transcription were present.

Fold changes were compared between all treatment groups for these 66 genes (Figure 6.8); the most strongly down-regulated gene in all treatment groups was NOG. The remaining 8 down-regulated genes were ADA, GATA3, IFFO2, LFNG, STRBP, TCEA3, VSIG1 and ZNF395. One of the most highly up-regulated genes in all groups was IL1R2, also deregulated by all treatments at 6 hour (Figure 6.6C). In the opioid groups, ARG1 and MMP9 were also highly up-regulated, with higher fold changes induced by oxycodone, in common with the majority of genes in this group (Figure 6.8).

Supervised hierarchical cluster analysis (Figure 6.9) highlights the separation of up- from down-regulated genes, and the clustering of morphine 2 hour and oxycodone 6 hour arrays together.

Table 6.2: Summary of overrepresentation analysis highlighting biological processes enriched in genes significantly deregulated by both morphine at 2 hour (Mor0-2) and oxycodone at 6 hour (Oxy0-6).

Biological processes – 66 genes	Genes	% of total input	p-value
positive regulation of immune system process	6	10.5	1.00E-03
immune response	9	15.8	1.50E-03
negative regulation of multicellular organismal process	5	8.8	1.90E-03
negative regulation of immune system process	4	7	2.50E-03
defense response	8	14	3.40E-03
regulation of apoptosis	9	15.8	4.00E-03
regulation of programmed cell death	9	15.8	4.20E-03
regulation of organ growth	3	5.3	4.20E-03
regulation of cell death	9	15.8	4.30E-03
positive regulation of T cell differentiation	3	5.3	4.80E-03
positive regulation of leukocyte activation	4	7	4.90E-03
positive regulation of cell activation	4	7	5.60E-03
negative regulation of signal transduction	5	8.8	5.60E-03
positive regulation of lymphocyte differentiation	3	5.3	5.70E-03
regulation of kinase activity	6	10.5	5.80E-03
regulation of dendritic cell antigen processing and presentation	2	3.5	6.50E-03
regulation of antigen processing and presentation	2	3.5	6.50E-03
negative regulation of cytokine production	3	5.3	6.70E-03
regulation of transferase activity	6	10.5	6.90E-03
response to wounding	7	12.3	7.00E-03
negative regulation of cell communication	5	8.8	8.40E-03
response to glucose stimulus	3	5.3	9.40E-03
reproductive developmental process	5	8.8	1.00E-02
response to hexose stimulus	3	5.3	1.00E-02
response to monosaccharide stimulus	3	5.3	1.00E-02

Key:

Response to wounding
Lymphocyte activation
Apoptosis

Dynamic fold changes for genes deregulated by both morphine at 2 hour (Mor0-2) and oxycodone at 6 hour (Oxy0-6)

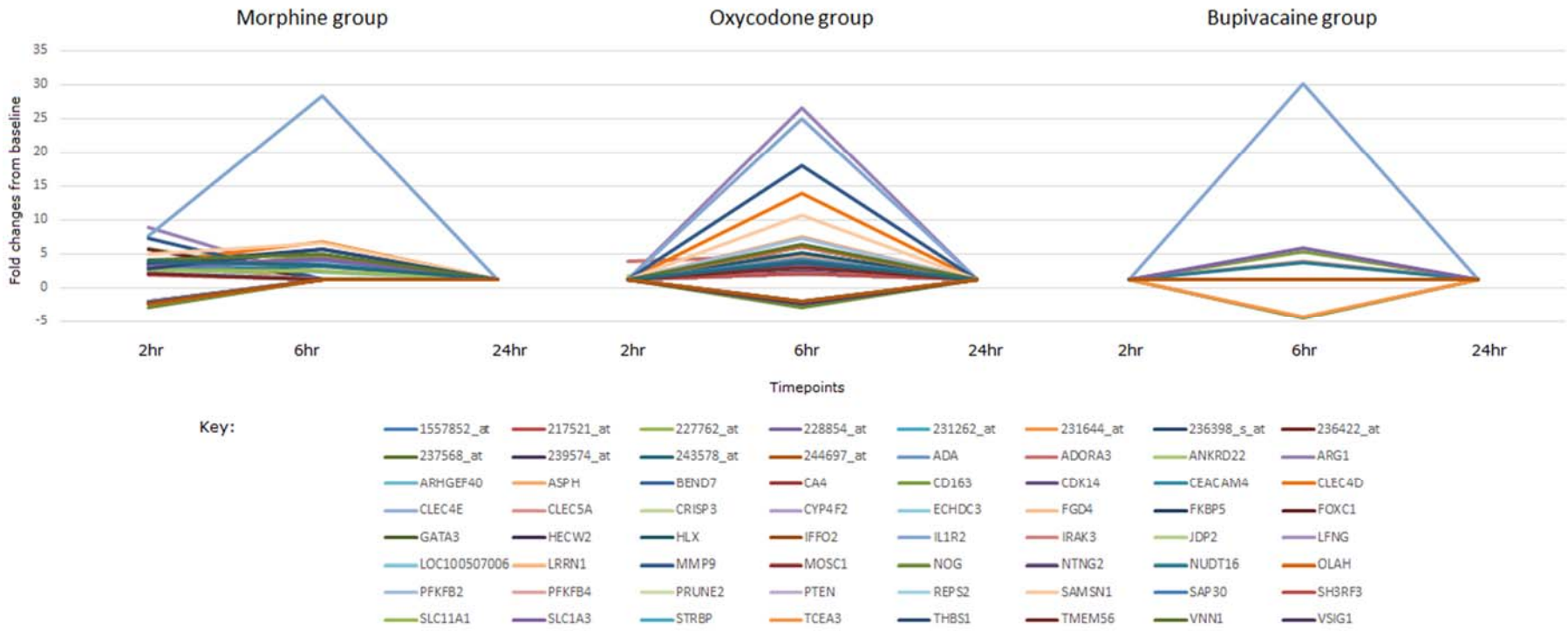

Figure 6.8: Fold changes at 2, 6 and 24 hour for the 66 genes deregulated by both morphine at 2 hour (Mor0-2) and oxycodone at 6 hour (Oxy0-6). Fold changes are shown for all treatment groups.

Supervised hierarchical clustering of all 66 genes deregulated by both morphine at 2 hour (Mor0-2) and oxycodone at 6 hour (Oxy0-6)

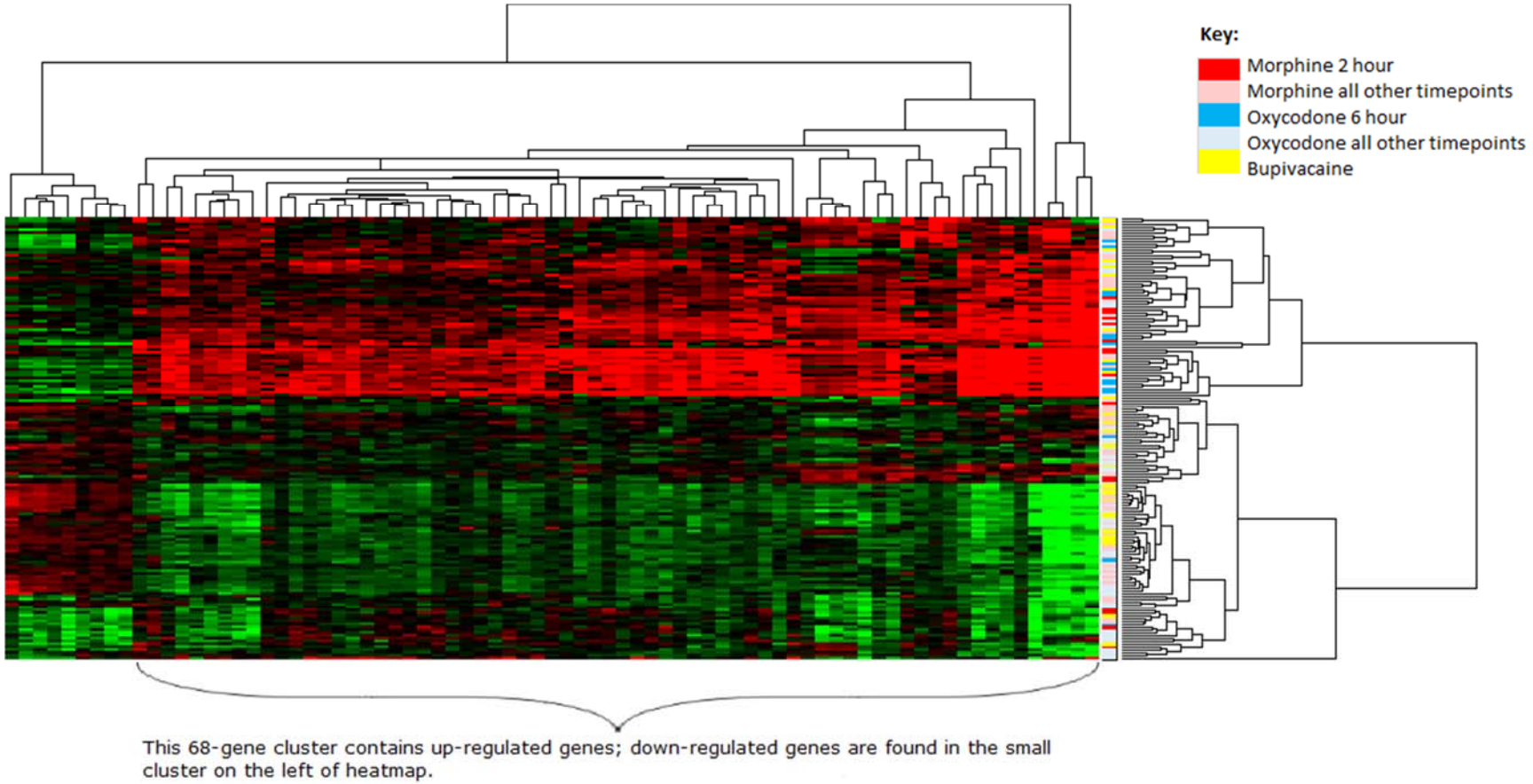

Figure 6.9: Supervised hierarchical clustering of the 66 genes deregulated by morphine at 2 hour (Mor0-2) and oxycodone at 6 hour (Oxy0-6) for all 156 arrays. Data was correlated by Euclidean distance and average linkage used to create the linkage tree. Green pixels denote low mRNA expression and red pixels denote high mRNA expression. The key highlights the separation of arrays by treatment and timepoint.

6.5 Discussion

This chapter aimed to investigate the dynamic changes in gene expression induced by all treatments, especially for the gene groups with maximal effect: those genes induced by morphine at 2 hours and oxycodone at 6 hours. It also aimed to investigate other genes deregulated by more than 1 treatment and the clinical relevance of transiently expressed genes versus those with a more sustained perturbation.

The transient nature of lymphocyte gene deregulation following initiation of analgesia can be clearly seen by the variance in numbers of probes deregulated by each treatment across timepoints (Figure 6.1). Supervised hierarchical clustering of all deregulated genes shows clear array clustering by timepoint, with 2 and 6 hour arrays clustering together, reflecting their deregulation from baseline versus the lack of deregulation seen in 0 and 24 hour arrays (Figure 6.2). Arrays that do not fit this pattern may reflect the genes deregulated from baseline at more than 1 timepoint.

The dynamics of process enrichment across timepoints also indicates that the gene deregulation seen was transient. In morphine-induced genes, processes relating to RNA transcription and translation, apoptosis and cell respiration were enriched at 2 hours, but by 6 hours only apoptosis remained enriched. The down-regulation of apoptosis processes at 2 hour may be indicative of T cell anergy [245, 246], a functional inactivation of T cells often induced by persistent antigen exposure, which leaves cells in a hyporesponsive state [247]. This is discussed further in Chapter 7. Genes in enriched processes at 2 hours were almost all down-regulated, but by 6 hours all genes bar one (FCER1A) were up-regulated.

The enrichment of processes related to lymphocyte activation, response to wounding and apoptosis by genes up-regulated by morphine at 6 hours did not seem to be immunosuppressive. However, their response was more moderate than that of oxycodone, with fewer genes present in lymphocyte activation and apoptosis processes. 28 morphine genes, 103 oxycodone genes and 13 bupivacaine genes were present in lymphocyte activation processes, suggesting that oxycodone induced lymphocyte activation more strongly than morphine, and that it did not induce anergy at any time.

Two new sub-groups of genes: Morphine sustained response (SR) and Oxycodone early responder, were introduced in this chapter based on the extended deregulation of genes across timepoints. The scarcity of genes found in each sub-group reflects the relative lack of sustained deregulation by each treatment; most deregulation was transient. 23 of the morphine SR genes were also deregulated by oxycodone, with the exception of CH25H and FLT3LG. SR genes were generally up-regulated in contrast to most Mor0-2 genes. Compared to enrichment of the full dataset of genes deregulated by morphine at 6 hours, more highly statistically significant lymphocyte activation-related processes are enriched in SR genes (Table 6.1), confirming that the SR group is well represented with lymphocyte activation-related genes. However, although 8 up-regulated SR genes were present in these processes at 2 hour, enrichment of the full dataset of Mor0-2 genes produced 19 genes, just 5 up-regulated, in lymphocyte activation processes. Without further functional assays, it is not possible to determine the lymphocyte activation phenotype induced by morphine at 2 hour.

The biological process: positive regulation of immune system process was represented in Mor0-2 by 5 up- and 11 down-regulated genes; by 6 hours, only the up-regulated probes remained deregulated, suggesting that lymphocyte activation was recovering. The enrichment by Mor0-2 genes of 16 processes involved in RNA transcription and translation (90 genes present, 2 up-regulated) not enriched by 6 hour genes also supports this. T cell activation increases protein translation [168, 169]; the reduced protein translation induced by morphine at 2 hours, evidenced by process down-regulation, may be caused by reduced T cell activation. TRAC, LCK and CD28 were all down-regulated by morphine at 2 hour and all could result in reduced T cell activation [119, 120, 124, 126].

As mentioned above, the SR genes uniquely deregulated by morphine are CH25H and FLT3LG. CH25H (cholesterol 25-hydroxylase) is an interferon-stimulated ER-associated protein catalysing the oxidation of cholesterol, and produces 25HC in human cells *in vitro*, preventing infection and replication of Hepatitis C virus [228]. It was up-regulated in murine macrophages following LPS stimulation in a TLR4-dependent manner [230]. Its sustained up-regulation by morphine is therefore counter to the general immunosuppression hypothesis. FLT3LG is the only down-regulated SR gene and acts on receptor FLT3 to activate pathways promoting proliferation of haematopoietic progenitor cells and inhibiting apoptosis. It is an essential cytokine needed for expansion of lymphoid lineages which reduced T cell dysfunction in a murine model of burn wound sepsis [203]. It primes CD8+ T cells via mobilisation of dendritic cells and subsequent production of TBet by CD8+ cells which then show increased antigen sensitivity and cytolytic ability [248, 249]. mRNA deregulation in Mor0-2 and Bup0-6 indicated ligand

down-regulation and receptor up-regulation, suggesting CD8+ cells may have lower antigen sensitivity and cytolytic ability.

Other SR genes include CLEC4D, CLEC4E and SAMSN1. CLEC4D is a constitutively expressed C-type lectin receptor up-regulated by microbial stimulation via the MyD88 pathway, which forms a trimeric receptor with CLEC4E and FCER1-γ (IgE receptor chain) to bind pathogenic ligands [250]. Binding suppresses murine TLR-4 responses *in vitro* and *in vivo*, evidenced by increased pro-inflammatory cytokines (IL-6, IFN-γ, TNF-α) in knock-out splenocytes / mice [251]. CLEC4E also transduced the loss of the transcription factor IRF1 and IL-12 following fungus binding to human dendritic cells [252]; IL-12 inhibits IL-4 synthesis and thus TH2 differentiation in T cells [183]. Up-regulation of both CLECs would therefore shift T cells away from a TH1 profile; up-regulation by oxycodone is later at 6 hour. TLR-4 was also up-regulated by both opioids at 6 hour, indicating a possible compensatory response.

SAMSN1 is an adaptor protein increased following stimulation of human CD19+ B cells with IL-4, CD40L and anti-IgM. Cluster analysis showed SAMSN1 clustering with signalling genes such as TRAF1 [253]; KO mice showed enhanced TH1 and TH2 humoural responses and increased B cell proliferation on BCR stimulation. The early up-regulation of SAMSN1 by morphine and later by oxycodone may therefore inhibit TH humoural immune responses. It is possible that the up-regulation of SR genes is an early response to counter a morphine-induced immunosuppression. This is supported by the prevalence of enrichment of lymphocyte activation-related processes in SR genes.

At 6 hour in the morphine group, enriched processes suggested that lymphocyte activation was no longer suppressed, despite continuous morphine administration via Patient-Controlled Analgesia (PCA). Patients initially received a morphine bolus in surgery at anaesthetic induction; some patients then had a second small bolus before the end of surgery (intraoperative morphine dose ranged from 10-20mg). Postoperatively, patients self-administered morphine via a PCA. The non-cumulative means of opioid dosing (Appendix A) show that no morphine patients received morphine between the intraoperative dose(s) and 2 hour timepoint, and that the mean dose at 6 hours was double that at 2 hours. Postoperatively, dosing was at maximum 1mg per 6 minutes. The half-life of morphine is 2.2 hours [254] so between 2 and 6 hours, morphine serum levels may be decreasing.

It is likely that the transient nature of the morphine-induced gene deregulation is due to the initial morphine bolus followed by slower PCA dosing. It is possible that the initial morphine (but not oxycodone) bolus induced MOR desensitisation and consequent reduced gene transcription, as seen in mice brain slices using tagged MOR [255]. Due to the timepoint spacing, the morphine-induced gene deregulation is known to be transient in nature as far fewer genes are deregulated at 6 hours. In contrast, duration of the oxycodone-induced gene deregulation is less well defined as it begins sometime between 2 and 6 hours but may last until shortly before the 24 hour timepoint.

The two oxycodone early responder genes were ADORA3 and ANKRD22. ADORA3 (adenosine A3 receptor) is coupled to a G_i receptor so inhibits adenylate cyclase; it was up-regulated in PBMCs of rheumatoid arthritis

patients [256]. In cancer, it both induced cell proliferation in a glioblastoma cell line via down-regulation of ERK1/2 [257] and inhibited colon carcinoma growth via modulation of NF-kB and GSK-3β in mice *in vivo* [258]. These divergent effects may depend on agonist concentration, with low concentrations producing proliferation in normal cells, and high concentrations producing apoptosis in normal or tumour cells [259]. Adenosine may show a surgery-induced increase in this study caused by the degradation of extracellular ATP [260] which may have caused ADORA3 up-regulation. However, adenosine levels were not measured during this study so it is not possible to ascertain the effects of increased ADORA3, up-regulated in this study by both morphine and oxycodone.

ANKRD22 (ankyrin repeat domain 22) is a transcription factor up-regulated both in pancreatic cancer [261] and following ZEB1 silencing in murine prostate tumour models. ZEB1 is a zinc finger transcription repressor critical to early T cell development [262] but was not deregulated by oxycodone. It is unlikely that the early deregulation of ANKRD22 is relevant to any putative oxycodone-induced immunomodulation.

Ten genes are perturbed by all treatments at 6 hours (Figure 6.6C); these genes are likely to represent those induced by surgery, anaesthetic or the underlying gynaecological condition. They include IL1R2, C19orf59 / MCEMP1 and CD163. IL1R2, also an SR gene, is a decoy receptor antagonising IL-1; its up-regulation would antagonise the surgery-induced increase in IL-1. It is found on immune cells only, in comparison to the ubiquitous presence of IL1R1 [116], suggesting a protective function of IL1R2 for immune cells against IL-1. IL-1 mediates inflammation in many diseases and is a key

immunosuppressive cytokine. Other genes linked to the downstream activation of IL-1 were up-regulated (IRAK3) and down-regulated (TRAF3 – morphine only); both these perturbations are in keeping with the down-regulation of IL-1 activity. IRAK3 prevents IRAK1 dissociating from IRAK4 and associating with myD88 and TRAF6 to enact TLR / IL1R signalling and pro-inflammatory response [117], providing immune homeostasis. TRAF3 was down-regulated in morphine only; it suppresses TRAF2-induced NFκB activity, associates with IRAK-1 to produce a TLR response [263] and its deficiency has been found to be present with a defective TLR3 response and HSV encephalitis [264]. The perturbation of IL1R2 and associated genes suggests a surgery-induced inflammation-modifying response, induced early in morphine.

CD163 is an acute-phase regulated receptor involved in clearance of haemoglobin complexes by macrophages, found in plasma immediately following CABG surgery [113]. It was also up-regulated (mRNA and protein) in monocytes of healthy volunteers following *in vivo* high-dose cortisol infusion [115]. Shed CD163 inhibits proliferation of T cells, possibly via cellular myosin [196] and its cell surface expression in monocytes is increased by IL-10 [114]. Its deregulation by all treatments is indicative of its role as an anti-inflammatory scavenger protein; its early up-regulation by morphine could be related to increased cortisol or IL-10 in this group. C19orf59 / MCEMP1 is a transmembrane protein expressed by mast cells [265] and macrophages [266], whose precise function is unknown, but may be involved in regulation of mast cell differentiation [266] and immune responses, due to the presence of binding motifs similar to those found in immune receptor genes in its promoter region [265].

Differentially expressed epidural bupivacaine genes (Bup0-6) were enriched in processes related to signal transduction and cell proliferation. No statistically significant processes were enriched when interrogating genes deregulated by bupivacaine only at 6 hours (23 probes). Both the deregulation of surgery- or anaesthesia-induced genes by all treatments at 6 hour, and the relative lack of an immunomodulatory effect induced by bupivacaine, are supportive of a successful study design.

One of the largest groups of genes differentially expressed across treatments was the 66-gene group consistently deregulated by morphine and oxycodone at the time of their maximal response (Mor0-2 and Oxy0-6). IL1R2, ARG1 and MMP9 were the top 3 up-regulated genes in this group, as well as the 3 most highly up-regulated genes in Mor0-2. ARG1 (Arginase 1) competes with inducible nitrous oxide (induced by IFN-γ [267]) to metabolise L-arginine, hydrolysing it to L-ornithine and urea. ARG1 was present with reduced arginine in PBMCs following injury [268] and L-arginine deficiency was linked to down-regulation of the TCR ξ chain in PBMCs and myeloid cells [268, 269]. Reduced L-arginine, increased ARG1 activity and protein expression and increased IL-10 were also seen in trauma patients [268]. ARG1 up-regulation suggests decreased T cell activation as a result of TCR ξ chain down-regulation and a shift to a TH2 profile, occurring at the earlier intraoperative timepoint in the morphine group.

MMP9 is a matrix metalloproteinase that degrades the extracellular matrix, positively contributing to wound healing as part of the surgical response. It was up-regulated in mice peripheral glial cells following morphine administration, together with glial fibrillary acidic protein and IL-1β

activation, indicating a glial cell response; these effects were blocked by naloxone, the MOR antagonist [212]. In liver cells, MMP9 is up-regulated by injury and activates TGF-β, increasing Treg numbers [270]. MMP9 also antagonised the analgesic properties of morphine in mice, shown by the increased analgesia seen in MMP9 KO mice [271]. The MMP9 up-regulation by morphine and oxycodone may therefore have been mediated through MOR, and could increase Treg numbers and patients' need for morphine during the intraoperative period.

Down-regulated genes present in both Mor0-2 and Oxy0-6 included GATA3 and NOG. GATA3 is a transcription factor pivotal in development. Notch-mediated differentiation of TH2 murine cells has been shown to depend on GATA3 [166]; it has been called the master driver of TH2 differentiation and its activity, mRNA and protein levels were repressed by glucocorticoid administration [167]. The down-regulation of GATA3 could therefore shift T cells to a TH1 profile, not in keeping with the suppressed immunity and TH2 profile hypothesized for morphine, and shown in Chapter 4. The deregulation of GATA3 may have been induced by reduced cortisol, which although not significantly increased at 6 hour, was not measured at 2 hours (Chapter 4).

NOG codes for the polypeptide noggin which binds and inactivates members of TGF-β family [272] including BMP-4, involved in CD4+ activation and proliferation [273]. Down-regulation of NOG would increase activation of BMP-4 and proliferation of CD4+ cells, counter to the immunosuppressive hypothesis of morphine. No processes involved in RNA translation or transcription were enriched in Mor0-2/Oxy0-6 genes; processes were mainly

related to lymphocyte activation, response to wounding and apoptosis, suggesting that RNA translation processes were unique to Mor0-2.

6.6 Conclusion

In conclusion, based on the consistent deregulation of surgery-related genes by all analgesics at 6 hours, the experimental design and microarray analysis were successful. This is supported by the scarcity of genes deregulated by epidural bupivacaine and the lack of enrichment of statistically significant biological processes by this group.

The morphine-induced gene deregulation discussed in Chapter 3 was transient in nature. Enrichment of processes related to RNA translation and transcription, apoptosis and cell respiration, suggestive of a morphine-induced T / NK cell anergy, were present at 2 hours but had disappeared by 6 hours. The known suppression of lymphocyte proliferation and NKCC following morphine administration suggests that the possible anergy leads to reduced effector function, as shown by the greater morphine-induced TH2 shift, and possibly by the reduced morphine-induced NK cell degranulation (Chapter 4). However, 25 sustained response genes enriched in processes involved in lymphocyte activation were up-regulated at 2 and 6 hours and their functional phenotype was not defined.

Oxycodone shows a limited effect on lymphocyte gene expression at 2 hours, and processes enriched in up-regulated genes at six hours - related to response to wounding, lymphocyte activation and apoptosis - are suggestive of an active immune response. The gene up-regulation and consequent process enrichment may be prolonged, possibly starting shortly after 2 hours post-induction and ending as late as just before 24 hours. In contrast, the timepoint design of the study confirmed that the morphine-induced gene

deregulation was mainly transient and possibly induced by receptor desensitisation as a result of the intraoperative morphine bolus.

Chapter 7
Discussion and future work

Evidence of morphine-induced immunosuppression may have been accumulating as early as the mid-16th century, following the death of a malaria patient given an experimental opium dose [7]. In the 1800s, infections linked to recreational opium use were described, while dogs given high morphine doses were seen to be susceptible to *Diplococcus lanceolatus* [7]. More recently, a plethora of animal data relating morphine to immunosuppression has been published [9, 40, 44, 55, 56, 65, 104]. However, the reliability of human *in vivo* data is limited by the difficulty of controlling for confounding factors inherently present in clinical research [37, 66, 67], which may account for the relative scarcity of prospective human clinical research. This study aimed to investigate possible morphine-induced immunosuppression by analysing gene expression of lymphocytes taken from patients undergoing gynaecological surgery. The study design limited the effect of confounding factors and the results of gene expression analysis were confirmed with functional assays.

The initial analysis of gene deregulation following ANOVA identified a maximal effect of morphine on lymphocyte gene expression 2 hours after initial analgesic administration, whereas oxycodone's maximal effect was at 6 hours. Morphine-induced genes were mainly down-regulated but those induced by oxycodone were mainly *up*-regulated. Processes categorised as RNA transcription and translation, apoptosis and cell respiration were enriched in morphine-induced genes while mitochondria were the most commonly seen enriched cellular component. In contrast, processes enriched

in oxycodone-induced genes were classified as response to wounding, lymphocyte activation and apoptosis; enriched cellular components were almost entirely restricted to the plasma-membrane. The process enrichment and vector of change of morphine-induced genes suggests reduced cellular activity, while the opposite is suggested by oxycodone-enriched processes. Reduced activity of CD4+, CD8+ and NK cells intra-operatively following morphine administration would reduce cell-based immunity, allowing tumour cells to survive, and, in tumour resection surgery, could increase the likelihood of metastatic spread due to malignant cell shedding [274].

Previous research suggests that morphine may induce an immune shift from cell-mediated (TH1) to humoural-mediated (TH2): it decreased IL-2 production and proliferation in splenocytes [31], reduced PHA-stimulated proliferation in T cells [48] and IL-2 production in T cells [56]. Several genes uniquely deregulated by morphine are indicative of a reduction in cell-based immunity: CD28, LCK and TRAC down-regulation suggest a dysfunction of the immunological synapse. CD28 is present constitutively on CD4+ and CD8+ cells and is a co-stimulant for T cell activation, enhancing TCR effects [119]. CD28-/- mice showed a lack of T cell expansion upon antigen stimulation, reduced TH cell differentiation and increased TH2 cytokine expression [120]; down-regulated CD28 may therefore induce a TH2 shift.

LCK is a tyrosine kinase that phosphorylates tyrosine in the CD28 cytoplasmic tail [124], localising with TCR or CD4+ in the central SMAC of CD8+ or CD4+ cells respectively [125, 275]. Phosphorylation initiates protein interactions and the downstream signalling cascade that result in CD28's co-stimulatory functions [276]. TRAC (T cell receptor α constant) codes for the constant part

of TCR's α subunit, an essential part of the TCR; a splicing mutation produces reduced αβ TCR chain expression causing an inherited immunodeficiency disorder [126]. The down-regulation of CD28 and LCK would therefore inhibit CD28's ability to act as a co-stimulant, while TRAC down-regulation would prevent TCR function; together these suggest a T cell immune synapse dysfunction and a reduction in cell-mediated immunity.

AQP3, a transmembrane protein transporting water and glycerol, was highly down-regulated by morphine and was expressed in activated but not inactivated T cells from healthy PBMCs [139]. It mediates H_2O_2 transport in mice, needed for activation of CDC42, essential for T cell migration towards chemokines [140]. A similar effect of AQP3 in humans may result in a shift from a TH1 profile by disrupting T cell migration and activation. PGLYRP1 (peptidoglycan recognition protein 1) was uniquely *up*-regulated by morphine and is a bacteria pattern receptor. PGLYRP1 (-/-) mice showed fewer TH2 and TH17 cells in the lungs following house dust mite sensitisation [147, 148]; a similar effect in human T cells is consistent with a TH2 shift.

A cytometric bead array, performed to confirm the possible morphine-induced TH2 shift, showed an increase from baseline for IL-6 and IL-10 [190]. The IL-6 increase was statistically significant in all treatments, suggesting a surgery-induced change [186, 187] but highest in the morphine group. Gene deregulation results supported this increase, with IL1R2 mRNA levels also increased by all analgesics at 6 hour: increased blood IL1R2 and IL-6 levels were associated in an epidemiological cardiac risk factor study [188]. As IL1R2 is a decoy receptor antagonizing IL-1 and therefore again indicative of a TH2 shift, its deregulation is consistent with the TH2 shift shown by

increased IL-6; in addition IL-6 may specifically be involved in a TH2 shift [190].

The higher IL-6 levels for morphine patients suggest an additional influence of morphine on IL-6, seen previously following morphine administration in rats [189]. IL-6 is a pleiotropic cytokine induced following infection or injury [277]; higher levels are linked to worse outcomes in burn [278] and sepsis [279, 280]. Its expression levels are also influenced by genetic diversity [281] although this was not investigated. IL-6 induces lymphocyte activation and acute phase protein synthesis when appropriately stimulated but is also a mediator of the initial systemic inflammatory response syndrome (SIRS) that can occur following acute injury or inflammation [278]. It has also been shown to increase with VEGF following colon cancer resection [282]; VEGF was not assayed but an increase, if it existed, could turn on the angiogenic switch in tumour micro-metastases [283], increasing the likelihood of tumour microfragments successfully metastasising.

A systematic review suggested that the mean IL-6 levels of this study were similar to mean peak concentrations following other moderate surgery, but also that peak levels are reached at 18-24 hours [284]. An additional measurement of IL-6 concentration at 24 hours would therefore be useful and may show an even greater increase from baseline. The lower levels of IL-6 produced following oxycodone and bupivacaine administration indicates a lesser TH2 shift, and may reduce the likelihood of patients developing SIRS and improve outcomes especially if linked with lower levels of VEGF.

IL-10 levels significantly increased only in the morphine group, to values lower than previously seen following less invasive laparoscopic

cholecystectomies [285]. IL-10 is an anti-inflammatory cytokine produced by TH2 cells and needed for a normal inflammatory response [192]. It negatively regulates the production of TH1 cytokines [193-195], consistent with a shift to a TH2 profile. Previous murine data of the effect of morphine on IL-10 both supports a morphine-induced increase [197] and is discordant with it [198]. Increased IL-10 increases CD8+ cells and their cytolytic ability *in vitro,* increases infiltration and activation of intra-tumour CD8+ cells and increases cytolytic activity of NK cells [286]. An increase in IL-10 may therefore not be consistent with the hypothesis of morphine-induced immunosuppression, although is consistent with a TH2 shift. It may be relevant that IL-10 levels were similar in all treatments at 6 hour.

Downstream, increased IL-10 could up-regulate the metalloprotease ADAM9 as shown previously in IL-10-stimulated PBMCs [215] and in this study by morphine and oxycodone gene expression data. ADAM17 induces CD16 shedding in NK cells; a similar function of ADAM9 could introduce a refractory period in NK cells [214], potentially reducing NKCC as seen previously following morphine administration [29-31, 41, 287]. The greater increase in mean IL-6 and IL-10 concentrations confirms a larger TH2 shift in morphine patients, with associated poorer prognosis due to an increased risk of SIRS and metastatic spread. It would be interesting to perform an additional CBA at 2 and 24 hours, with the addition of VEGF and other angiogenic factors, to investigate timing of the peak TH2 shift. A peak may have occurred at 2 hours - the time of morphine's maximal effect on gene deregulation, or at 24 hours as suggested by previous surgical data.

The greater morphine-induced TH2 shift would move morphine patients away from cell-mediated and towards antibody-mediated immunity. Morphine administration has also been shown to reduce NKCC, consistent with the reduced IL-2 element of a TH2 shift [288, 289]. Reduced IL-2 was not demonstrated in this study, but may have been present at the non-assayed 2 hour timepoint. Specific gene deregulation also suggests reduced NKCC induced by morphine, with the opposite effect induced by oxycodone. MICB, a ligand for the NKG2D receptor needed for NKCC, was down-regulated by morphine while STAT3, which decreases NKG2D receptor expression when ablated / mutated, was up-regulated by oxycodone [161].

The NK cell degranulation assay performed was inconclusive at baseline: opioid samples failed to degranulate effectively, and bupivacaine samples did not show a significant increase following degranulation. With the 6 hour timepoint viewed as a separate experiment, all samples degranulated effectively and oxycodone samples showed a statistically significant increase. As removal of the outlier (Figure 4.5) removed oxycodone's statistical significance due to the small sample size, the assay needs further validation and should be repeated with more numerous samples. However, the results as they stand are not discordant with the hypothesis, with morphine showing reduced NKCC compared to oxycodone. The assay could also be repeated at 2 hour – the timepoint at which morphine exerted its maximal gene deregulatory effect – to determine if reduced NK cell cytotoxicity was also seen at this timepoint.

Reduced NKCC can be indicative of anergy in NK cells [290-292]. Anergy is a functional inactivation of cells normally induced by persistent antigen

exposure, leaving cells hyporesponsive, also occurring in T cells [245-247] where it has been defined as the inability of antigen specific T cells to produce IL-2 and clonally expand [293]. Reduced IL-2 production, not demonstrated in this study, also suppresses NKCC [288, 289] and is consistent with the TH2 shift suggested here. Enriched processes in morphine-induced genes may reflect cell anergy. The down-regulation of RNA transcription and translation and cell respiration may reflect reduced T and NK cell clonal expansion; reduced cellular activity results in decreased protein translation [168]. A concomitant decrease in apoptosis is supported by previous work in which T cells activated by CTLA-4 to induce anergy also showed reduced apoptosis via the PI 3K-PKB/AKT anti-apoptotic pathway [245]. Mitochondria are the most commonly seen enriched cellular components, again supportive of a hypothesis of increased anergy. None of the above processes were enriched in genes deregulated by oxycodone, but those enriched - response to wounding, lymphocyte activation and apoptosis – are suggestive of increased cell activation rather than anergy.

Several deregulated genes are supportive of the theory of anergy. CD28 and SOCS1 were uniquely down-regulated by morphine and have previously been shown to have lower expression in anergic compared to active murine T cells [294]. LCK and TRAC, discussed above, were also uniquely down-regulated by morphine and may contribute with CD28 to a dysfunctional T cell immune synapse and reduced cellular activity. RCAN3, inhibitor of calcineurin, was one of the most strongly down-regulated genes by morphine. Sustained calcineurin activation is linked to anergy; in murine T cells, it up-regulated ubiquitin ligases and TSG101, a receptor involved in sorting monoubiquitinated proteins for degradation and producing unstable synapses

[137]. The down-regulation of RCAN3 would encourage the sustained activation of calcineurin and subsequent T cell anergy.

Functionally, increased anergy of lymphocytes in the intraoperative period would result in the reduced cytotoxic ability of CD8+ and NK cells, and a reduced ability of CD4+ cells to expand into effector cells. In vulnerable tumour resection patients, these changes could increase the likelihood of dispersed tumour microfragments, known to be disseminated after surgery [274], resulting in metastases. The increased lymphocyte activation that may be induced by oxycodone post-operatively would have the opposite effect and may protect against metastatic spread in tumour resection surgery. This is not confirmed by our data; further work could investigate reduced cytotoxic ability of CD8+ cells, reduced cytotoxic ability of NK cells in a larger sample, and any reduced expansion ability of CD4+ cells. This could be assayed in both cancer and non-cancer patients, and the 2 hour timepoint should be included.

Both immune parameter changes induced by morphine - the stronger TH2 shift and the possible decreased NKCC, are supported by previous data [29-31, 48, 56] and by pathway down-regulation in enriched morphine genes. All changes are suggestive of increased anergy. Statistical analyses, performed to evaluate the relative importance of individual genes that may mediate these parameter changes, did not find those identified previously through gene expression analysis to be predictive of treatment with either opioid. However, other relevant genes were predictive of treatment using logistic regression (LR).

AGPAT3, TIAM1 and TPK1 were predictive of morphine treatment, confirmed through ROC analysis. AGPAT3 is an acyltransferase involved in the phospholipid biosynthetic pathway. Its down-regulation would increase lysophosphatidic acid and decrease its product phosphatidic acid; the latter is needed for lymphocyte proliferation [217]. Morphine-induced down-regulation of AGPAT3 could therefore reduce T cell proliferation, consistent with increased T cell anergy and a TH2 shift. Increased lysophosphatidylcholine (lysophosphatidic's precursor) could enhance the suppressive qualities of TRegs, via increased TGF-β production, as shown previously [218]. Lipid biosynthetic pathways were enriched in unique morphine-induced genes at 6 hour so any suppression of fatty acid production induced by morphine at 2 hour may be transient.

TIAM1 is involved in protrusion formation in the leading edge of T cells with RAC1 [226]. The down-regulation of TIAM1 could reduce the ability of T cells to form a leading edge and subsequently migrate, again suggesting increased T cell anergy. TPK1 is an enzyme whose end-product, thiamine pyrophosphate, is involved in ATP synthesis; TPK1 down-regulation may therefore be involved in mediating the reduced cell respiration suggested through enriched pathways, subsequently increasing cell anergy. The down-regulation of all 3 genes is supportive of increased anergy and reduced cell respiration induced by morphine. Their ability to predict morphine treatment at 2 hours, the key timepoint for morphine-induced gene deregulation, suggests that they may be important in mediating increased anergy.

OSCAR and MCL1 predicted oxycodone treatment using LR, confirmed through ROC analysis. OSCAR is an osteoclast-associated receptor that

associates with FcRy to promote cell activation and phagocytosis of opsonized cells [236]. A similar effect of OSCAR in lymphocytes could increase T cell activation or induce increased phagocytosis by macrophages. MCL1 is an anti-apoptotic regulator, induced after TCR stimulation in murine T cells [241] whose predictive ability at 24 hour suggests successful T cell activation has occurred. Its overexpression in CD8+ cells of virally-infected mice increased differentiation of terminal effector and effector memory cells [242]; its up-regulation in this study indicates previous TCR stimulation and suggests an increased ability of CD8+ cells to respond to antigen.

GATA3 and BACH2, highly deregulated, were significant for oxycodone treatment following ROC analysis. BACH2 was uniquely down-regulated by oxycodone and may mediate a TH1 shift supportive of an improved outcome, indirectly via a decrease in GATA3 [167]. BACH2 -/- mice showed repressed lineage-specific genes, including GATA3 [165]: GATA3 drives TH2 differentiation [167] and was down-regulated not only by oxycodone but also by morphine, discordantly with the theorized morphine-induced TH2 shift.

The potential of genes as predictive biomarkers is dictated by the timepoint at which they are predictive of treatment; the 24 hour predictive ability of MCL1 precludes it as a biomarker whereas the predictive ability of OSCAR at baseline suggests it has potential. AGPAT3, TIAM1 and TPK1 are all predictive at 2 hour and therefore may not be precluded as biomarkers. OSCAR, AGPAT3, TIAM1 and TPK1 could be investigated further as biomarkers of opioid-induced gene deregulation and subsequent immunosuppression.

Cortisol is a glucocorticoid coordinating inflammation, stress and immune responses [177], whose levels are altered by morphine administration [178-

182] and by surgery [50, 183]. The glucocorticoid receptor can act as a transcriptional regulator [184]; several deregulated genes of this study (GATA3, CD28, CD163, LPL and FLT3LG) have been previously associated with changes in cortisol levels. However, the 6 hour increase in cortisol concentration seen was not significant and the largest increase was seen in bupivacaine patients, followed by morphine. It would be interesting to assay cortisol concentrations at 2 hours, as this was the time of morphine's maximal response on gene deregulation. It may also be the time of peak postoperative cortisol levels, possibly present between 0 and 4 hours (systematic review: [284]) at a higher level than measured in this study. The non-significant levels found may therefore be due to assay timing missing the peak concentration, which could potentially have influenced gene deregulation.

FLT3LG was down-regulated by both morphine and bupivacaine and is a cytokine needed for expansion of lymphoid lineages [203]. It is up-regulated in patients with Graves' disease [201], a condition in which low cortisol can be found; the down-regulation of FLT3LG could be related to the increased cortisol levels seen in these treatments. Cortisol shifts CD4+ cells to a TH2 profile in the absence of CD28 [123]; CD28 was down-regulated by morphine in this study, suggesting that cortisol could contribute to the morphine-induced TH2 shift, especially if it reached statistical significance at the non-assayed 2 hour timepoint. The degree of influence of cortisol on gene deregulation is unknown and an additional 2 hour assay should be performed. However, as the largest 6 hour cortisol increase was induced by bupivacaine, the group with the fewest deregulated genes, cortisol is unlikely to be highly influential on gene deregulation in this study.

The design of the study removed most confounding factors. Non-compliant patients administered more than 1 analgesic were withdrawn, keeping analgesic groups separated; previous studies have not done this [66, 67]. The high number of resultant withdrawals meant that mRNA of only 40 patients underwent microarray analysis. Non-cancer surgery removed immune-modulating disease processes consistently identified in many cancer types, for example changes in T cell gene expression in follicular lymphoma [109], abnormal genotype and immune synapse formation in AML [295] and features of T cell exhaustion in CLL patients [110]. All groups were BMI, age, operation duration, pain and sex-matched and opioid use was matched between opioid groups with no significant difference in mean doses. Anaesthetic was propofol-only therefore excluding those anaesthetics previously found to alter immune parameters, such as fentanyl or ketamine which reduce NKCC [68, 69] or levobupicacaine which has a different cytokine profile to sevofluorane and morphine [77].

The pattern of gene deregulation confirmed a successful study design. Ten genes were deregulated by all treatments at 6 hours. CD163 was up-regulated and is an acute-phase regulated receptor involved in macrophage haemoglobin clearance, present in plasma after surgery [113] and up-regulated in monocytes following cortisol [115] and IL-10 administration [114]. IL1R2, a decoy receptor for IL-1, was up-regulated together with related gene IRAK3. These genes all suggest an inflammation-modifying response, consistent with a surgery-induced response. Epidural bupivacaine deregulated only 20 unique genes with no statistically significant enriched processes following overrepresentation analysis, suggesting that epidural was an effective non-immunomodulatory control analgesic. These gene

deregulation changes were all indicative of a study design that successfully removed confounding factors.

However, the small number of patient samples available for gene expression limited the microarray analysis. At the time of patient recruitment, myomectomies were moving from predominately open to predominantly laparoscopic surgery, hindering recruitment. The recombination of mRNA from 3 cell sub-types for hybridisation to arrays was caused by financial constraints and prevented gene deregulation analysis assigning each deregulated gene to a specific cell type. In any future study, mRNA would ideally not be recombined, allowing mechanisms to be elucidated more easily. qRT-PCR is normally performed on highly deregulated genes to confirm the results of gene expression array; this was not performed due to time and cost constraints, but could be added in a future study.

NK cell degranulation was only performed on a small number of samples due to time and cost constraints. Some publications suggest that increased degranulation exists with impaired cytotoxicity [216] so direct cellular cytotoxicity could be investigated using the ^{51}chromium-release assay, not degranulation, with more numerous samples. The assay could be repeated with 2 and 24 hour as additional timepoints. Enriched pathways suggest that CD8+ cytotoxicity may also have been affected by morphine and therefore cytotoxicity could be measured in these cells using either the degranulation or ^{51}chromium-release assays [296].

The failure of baseline opioid samples to degranulate successfully following stimulation may be related to a difference in patients' clinical characteristics: of patients used for NK degranulation, fewer bupivacaine patients underwent

open myomectomy; remaining operation types were (sub)total hysterectomy ± BSO and debulking. Hysterectomy is usually performed to resect fibroids if preservation of fertility is not necessary [297] or if a multifibroid uterus is present (although fibroid number / size data was not collected). The higher number of TAH in bupivacaine patients therefore suggests possibly more patients with multifibroid uteri. Fibroids develop due to an abrogation of normal NKCC [298, 299] or an *in vivo* environment richer in oestrogen and therefore more suppressive to NK cells [300]; removal of NK cells from the suppressive *in vivo* environment may result in increased NKCC *in vitro*. This effect may be seen more strongly in those cells initially more strongly suppressed, ie those from patients who underwent more radical surgery due to multifibroid uteri. The successful baseline degranulation for bupivacaine samples may therefore be explained by greater initial suppression of NKCC *in vitro*, and underlines the importance of using as near-identical patients as possible for this assay. Patients were matched in all other parameters.

Five cytokines failed to reach the theoretical level of detection on CBA; an ELISA, with slightly lower cytokine detection levels, could be performed as an alternative to CBA. The later timepoint of 6 hour was chosen as previous research suggested that changes would still be present [86]; however, as with NK cell degranulation, 2 and 24 hour timepoints could be added to investigate peak TH2 shift. Additional timepoints could also be added to the cortisol ELISA to investigate the time of peak concentrations.

Although it is clear that morphine has an effect on lymphocyte gene deregulation, the mechanisms and effects of this are unknown. Morphine primarily activates the μ-opioid receptor (MOR): its metabolite morphine-6-

glucuronide (M6G) is a strong MOR agonist [301] which may be almost wholly responsible for the analgesic effects of morphine [302]. M6G may contribute to gene deregulation; it induced antinociception and reduced immune parameters (T cell proliferation, serum IgM and IgG) in patients with advanced cancer [12] and decreased NKCC, lymphocyte proliferation and IFN-γ production in rats [303]. M6G levels were not measured in this study.

The failure of oxycodone to induce immunosuppression is most likely due to a different receptor binding profile. Oxycodone, morphine and M6G all showed unique analgesia, respiratory depression and constipation activity profiles following intracerebroventricular administration in rats [93], radioligand binding studies suggest that oxycodone is a κ-opioid receptor (KOR) agonist with a weak affinity for MOR [94], and a murine bone cancer model showed reduced MOR-agonist but not oxycodone binding, suggesting that oxycodone does not bind strongly to MOR [304]. Activation of KOR by oxycodone may not cause immunosuppression, but based on the results of this study, could increase T cell activation and NKCC. The relationship of KOR versus MOR to immunosuppression could be investigated further with the use of selective antagonists in a future study.

Functional selectivity describes the ability of a ligand to induce unique intracellular responses through conformational receptor changes [18]. This has been described at various levels of activation for the MOR [305] and could explain the unique immunomodulatory profile of oxycodone, if it does primarily activate MOR. Morphine and M6G induced analgesia in mice that was blocked by a JNK inhibitor, suggesting that opioid analgesic tolerance is induced via a JNK-dependent pathway; oxycodone-induced analgesia was not

blocked in this way [19]. Morphine and fentanyl caused MOR desensitization via two separate pathways, activating JNK either without the need for arrestin, or arrestin-dependently, respectively [20], another example of functional selectivity. These suggest that even if oxycodone primarily activates MOR, not KOR, functional selectivity could enable differing immunomodulatory effects.

Opioid receptors exist on T cells [58] and opioids have been shown to induce immunomodulatory effects both *in vivo* [12, 40, 44, 55, 56, 65, 105] and *in vitro* [30] [64]. Immunomodulation could therefore be activated peripherally; if this is the case, the superior ability of oxycodone to cross the blood brain barrier [1] may produce relatively lower peripheral plasma levels of oxycodone, reducing any potential immunosuppression.

The duration of gene expression changes is relevant to the clinical translational relevance of these results. 450 mainly down-regulated unique genes were deregulated by morphine at the intraoperative 2 hour timepoint, and 113 genes (17 unique) deregulated at 6 hour. Twenty-five genes showed a sustained deregulation from 2 to 6 hour, suggestive of an early recovery of immunosuppression; 6 hour genes were almost all up-regulated and enriched in the same processes as oxycodone at 6 hour: response to wounding, lymphocyte activation and apoptosis, all suggesting increased lymphocyte activation. The shift from a total of 434 down-regulated genes at 2 hour to 2 down-regulated genes at 6 hour suggests that morphine-induced immunosuppression may be mainly transient. In contrast, the gene deregulation induced by oxycodone began at 2 hour with just 3 genes (also deregulated by morphine) then increased to deregulation of 460 unique,

mainly up-regulated, genes at 6 hour, ending with deregulation of just 1 gene at 24 hour. The absence of a venepuncture timepoint between 6 and 24 hours means that the duration of the majority of oxycodone-induced gene deregulation is unknown, but may begin between 2 and 6 hours and not end until just before 24 hours.

The difference in duration of opioid-induced gene deregulation is surprising as their half-lives are similar [1, 97] and all analgesics were administered similarly and continuously. The initial intraoperative bolus was followed by slower postoperative patient-controlled analgesia (PCA) dosing with a maximum dose of 1 mg per 6 min. There was no statistically significant difference between the means of total opioid doses. Therefore, the initial bolus may account for the morphine-induced gene deregulation at 2 hours; bolus ranges were similar but the initial oxycodone bolus induced the deregulation of only 3 non-unique genes, compared to the 450 unique genes induced by the morphine bolus. It is possible that the bolus produced MOR desensitisation and a subsequent reduction of lymphocyte gene transcription. MOR desensitisation was seen previously following morphine but not oxycodone administration using radiotagged MOR in mice brain slices [255]; desensitisation is independent of internalisation and was also seen in AtT20 tumour cells following morphine administration [306]. It is likely that oxycodone primarily activates KOR and that immunosuppression is mediated by MOR, as suggested by previous publications.

The dynamics of the gene deregulation results suggest that it may be possible to avoid morphine-induced gene deregulation by replacing the initial intraoperative morphine bolus with oxycodone or epidural bupivacaine, and

thereafter utilising the cost effectiveness of morphine via PCA. The disadvantages of morphine-induced gene deregulation were confirmed through the TH2 shift and possible reduced NKCC seen, which should be confirmed at more timepoints and, for NKCC, with more samples. A non-morphine intraoperative bolus would be particularly suitable in vulnerable patients, such as those undergoing tumour resection surgery, where reduced cell-mediated immunity should be avoided as tumour microfragments are known to be dispersed after surgery.

7.1 Future work

Additional experiments could be performed to confirm the gene expression analysis and its functional translation relevance. Gene expression analysis should initially be confirmed via qRT-PCR of the most highly deregulated genes at each timepoint. The duration of oxycodone-induced gene deregulation is not known due to venepuncture timepoint spacing, so it would be ideal to repeat the gene expression analysis with another timepoint between 6 and 24 hour.

The maximal effect of morphine on lymphocyte gene expression was at 2 hour post initial analgesia administration: cytokine and cortisol ELISAs should be performed at 2 hour to more clearly determine the functional relevance of the morphine-induced gene deregulation. Individual ELISAs rather than CBA could be performed as these have cytokine-specific theoretical levels of detection. In addition, VEGF could be assayed and a 24 hour timepoint added for all cytokines, as this may be the time of peak IL-6 concentrations.

NKCC should be investigated directly by performing a ^{51}chromium-release assay, as increased degranulation may exist with impaired NKCC. It should be investigated additionally at 2 hour as well as the original timepoints, using patients undergoing identical surgery where possible. Cytotoxic CD8+ cells were not degranulated but should be also assayed for cytotoxicity using the same ^{51}chromium-release assay.

Several genes may be key to mediating opioid-induced immunomodulation. mRNA levels may not reflect protein levels but protein levels produced by selected genes could be measured via Western blot to investigate any correlation. CD28, AGPAT3, TPK1 and TIAM1 may mediate morphine-induced

changes at 2 hour and OSCAR may mediate oxycodone-induced changes at 6 hour: gene expression results should initially be confirmed with qRT-PCR, then protein levels measured via Western blot.

An effect on the T cell immunological synapse is possible as indicated by the deregulation of srGAP2, CD28, LCK and TRAC by morphine and the increase in anergy suggested by enriched pathways. Based on the importance of the synapse, an assay could be performed to investigate the presence of an impaired immunological synapse in CD4+ and CD8+ cells treated with morphine. It is also possible that a dysfunction could produce the reduced degranulation that may be seen in NK cells treated with morphine. Morphine-treated and control lymphocytes could be incubated with target cells then live cell imaging performed using electron microscopy for 6 hours to detect synapse formation. Reduced T cell proliferation or NKCC could then be corroborated with faulty synapse formation.

The role of anergy in morphine-induced immunosuppression could be investigated by determining the cellular response of morphine- versus oxycodone-treated T cells to anti-CD3 and anti-CD28 stimulation beads, and measuring IL-2 production and proliferation using CFSE staining in conjunction with flow cytometry.

It is possible that morphine induces gene deregulation peripherally; the *in vitro* addition of morphine or oxycodone to donor lymphocytes may induce deregulation of the genes discussed above and this could be investigated via qRT-PCR. Finally, CD8+ and NK cells treated with morphine or oxycodone could be analysed via flow cytometry to investigate shedding of cell surface CD16 and concomitant deregulation of MMP or ADAM genes via qRT-PCR.

Chapter 8

Conclusion

The results of this study support the prior knowledge of morphine-induced immunosuppression, demonstrated via the intraoperative deregulation of 450 unique genes in study patients treated with morphine. In contrast, those receiving oxycodone showed a postoperative deregulation of 460 unique genes, while patients receiving epidural bupivacaine experienced deregulation of only 20 lymphocyte genes. Processes indicating a possible increase in lymphocyte anergy were transiently enriched by morphine genes at 2 hours. In contrast, processes postoperatively enriched by oxycodone genes indicated a prolonged normal inflammatory and immune response to surgery, with no change in cell anergy. Genes predictive of morphine or oxycodone were linked to decreased or increased anergy respectively and should be investigated further as possible predictive biomarkers.

Functional assays indicated that cortisol is unlikely to have influenced gene deregulation as no treatment induced a statistically significant difference in cortisol concentration from baseline. However, any influence of cortisol on gene deregulation could be further investigated at an additional 2 hour timepoint. Morphine showed the greatest increase in serum IL-6 and IL-10 concentrations from baseline, suggesting a greater morphine-induced TH2 shift that could be responsible for functional changes seen previously, such as reduced lymphocyte proliferation. This was corroborated by gene expression analysis with the unique down-regulation of genes including CD28, TRAC, LCK and AQP3. Further clarity on the degree of the TH2 shift may be obtained by additional cytokine assays at 2 and 24 hours, the

respective timepoints of morphine's maximal effect on lymphocyte gene deregulation and the possible peak postoperative IL-6 concentration. The degranulation assay of this study did not disprove the hypothesis of morphine-induced reduced NKCC but should be repeated with more samples for confirmation.

In this study, morphine induced gene deregulation suggestive of increased lymphocyte anergy in the intraoperative period, confirmed functionally via a TH2 shift. This may be a result of MOR desensitisation and subsequent decreased gene transcription induced by the intraoperative bolus. As similar gene down-regulation was not induced by intraoperative oxycodone or bupivacaine, it could be removed by using either of these analgesia as an intraoperative bolus. A non-morphine bolus would be especially beneficial for tumour resection patients, who would be vulnerable to metastatic spread if subjected to reduced cell-mediated immunity or increased lymphocyte anergy at the time of possible tumour microfragment dispersal.

References

1. Rang, H., et al., *Phamacology.* 2016(8th Edition).
2. Aggrawal, A., *Narcotic drugs.* 1995.
3. Goerig, M. and J. Schulte am Esch, *[Friedrich Wilhelm Adam Serturner-the discoverer of morphine].* Anasthesiol Intensivmed Notfallmed Schmerzther, 1991. **26**(8): p. 492-8.
4. Beeching, J., *The Chinese Opium Wars*. 1975, London: Hutchinson & Co Ltd.
5. Lawrence, G., *The hypodermic syringe.* The Lancet, 2002. **359**(1311): p. 1074.
6. Macht, D.I., *The history of intravenous and subcutaneous administration*

of drugs. JAMA, 1916. **LXVI**(12): p. 856-860.
7. Friedman, H., T.W. Klein, and S. Specter, *Drugs of abuse, immunity and infections*. 1996: CRC Press.
8. J, C., *Nouvelles recherches sur le mode de destruction des vibrions dans l'organisme.* Ann Inst Pasteur, 1898. **12**.
9. Friedman, H., C. Newton, and T.W. Klein, *Microbial infections, immunomodulation, and drugs of abuse.* Clin Microbiol Rev, 2003. **16**(2): p. 209-19.
10. Biggam, A., *Malignant malaria associated with the administration of heroin intravenously.* Trans R Soc Trop Med Hyg, 1929. **23**.
11. Kee, T., *The habitual use of opium as a factor in the production of diseases.* Philipp. J Sci, 1908. **6**: p. 63.
12. Hashiguchi, S., et al., *Effects of morphine and its metabolites on immune function in advanced cancer patients.* J Clin Anesth, 2005. **17**(8): p. 575-80.
13. McDonald, J. and D.G. Lambert, *Opioid receptors.* Continuing Education in Anaesthesia, Critical Care & Pain, 2005. **5**(1): p. 22-25.
14. Pert, C.B. and S.H. Snyder, *Opiate receptor: demonstration in nervous tissue.* Science, 1973. **179**(4077): p. 1011-4.
15. Simon, E.J., J.M. Hiller, and I. Edelman, *Stereospecific binding of the potent narcotic analgesic (3H) Etorphine to rat-brain homogenate.* Proc Natl Acad Sci U S A, 1973. **70**(7): p. 1947-9.
16. Terenius, L., *Characteristics of the "receptor" for narcotic analgesics in synaptic plasma membrane fraction from rat brain.* Acta Pharmacol Toxicol (Copenh), 1973. **33**(5): p. 377-84.
17. Snyder, S.H. and G.W. Pasternak, *Historical review: Opioid receptors.* Trends Pharmacol Sci, 2003. **24**(4): p. 198-205.
18. Kenakin, T., *Functional selectivity through protean and biased agonism: who steers the ship?* Mol Pharmacol, 2007. **72**(6): p. 1393-401.
19. Melief, E.J., et al., *Ligand-directed c-Jun N-terminal kinase activation disrupts opioid receptor signaling.* Proc Natl Acad Sci U S A, 2010. **107**(25): p. 11608-13.
20. Kuhar, J.R., et al., *Mu opioid receptor stimulation activates c-Jun N-terminal kinase 2 by distinct arrestin-dependent and independent mechanisms.* Cell Signal, 2015. **27**(9): p. 1799-806.

21. Chuang, T.K., et al., *Mu opioid receptor gene expression in immune cells.* Biochem Biophys Res Commun, 1995. **216**(3): p. 922-30.
22. Sharp, B.M., S. Roy, and J.M. Bidlack, *Evidence for opioid receptors on cells involved in host defense and the immune system.* J Neuroimmunol, 1998. **83**(1-2): p. 45-56.
23. Ninkovic, J. and S. Roy, *Role of the mu-opioid receptor in opioid modulation of immune function.* Amino Acids, 2013. **45**(1): p. 9-24.
24. Delves, P., et al., *Roitt's essential immunology.* 2006(11th Edition).
25. Yosef, N., et al., *Dynamic regulatory network controlling Th17 cell differentiation.* Nature, 2013. **496**(7446): p. 461-468.
26. Mosser, D.M. and X. Zhang, *Interleukin-10: new perspectives on an old cytokine.* Immunological reviews, 2008. **226**: p. 205-218.
27. Hsu, P., et al., *IL-10 Potentiates Differentiation of Human Induced Regulatory T Cells via STAT3 and Foxo1.* J Immunol, 2015. **195**(8): p. 3665-74.
28. Ataie-Kachoie, P., et al., *Gene of the month: Interleukin 6 (IL-6).* J Clin Pathol, 2014. **67**(11): p. 932-7.
29. Yeager, M.P., et al., *Morphine inhibits spontaneous and cytokine-enhanced natural killer cell cytotoxicity in volunteers.* Anesthesiology, 1995. **83**(3): p. 500-8.
30. Boland, J.W., et al., *A preliminary evaluation of the effects of opioids on innate and adaptive human in vitro immune function.* BMJ Support Palliat Care, 2014. **4**(4): p. 357-67.
31. Sacerdote, P., et al., *Antinociceptive and immunosuppressive effects of opiate drugs: a structure-related activity study.* Br J Pharmacol, 1997. **121**(4): p. 834-40.
32. Weber, R., et al., *Progression of HIV infection in misusers of injected drugs who stop injecting or follow a programme of maintenance treatment with methadone.* Bmj, 1990. **301**(6765): p. 1362-5.
33. Suzuki, M., et al., *Correlation between the administration of morphine or oxycodone and the development of infections in patients with cancer pain.* Am J Hosp Palliat Care, 2013. **30**(7): p. 712-6.
34. Wang, Y., et al., *Morphine suppresses IFN signaling pathway and enhances AIDS virus infection.* PLoS One, 2012. **7**(2): p. e31167.
35. Reynolds, J.L., et al., *Morphine and galectin-1 modulate HIV-1 infection of human monocyte-derived macrophages.* J Immunol, 2012. **188**(8): p. 3757-65.
36. Afsharimani, B., et al., *Comparison and analysis of the animal models used to study the effect of morphine on tumour growth and metastasis.* Br J Pharmacol, 2015. **172**(2): p. 251-9.
37. Peyton, P.J., et al., *Perioperative epidural analgesia and outcome after major abdominal surgery in high-risk patients.* Anesth Analg, 2003. **96**(2): p. 548-, table of contents.
38. Vargas-Schaffer, G., *Is the WHO analgesic ladder still valid?: Twenty-four years of experience.* Canadian Family Physician, 2010. **56**(6): p. 514-517.
39. WHO, *Scoping document for WHO guidelines for the pharmacological treatment of persisting pain in adults with medical illnesses.* 2008.
40. Breslow, J.M., et al., *Morphine, but not trauma, sensitizes to systemic Acinetobacter baumannii infection.* J Neuroimmune Pharmacol, 2011. **6**(4): p. 551-65.

41. West, J.P., D.T. Lysle, and L.A. Dykstra, *Tolerance development to morphine-induced alterations of immune status.* Drug Alcohol Depend, 1997. **46**(3): p. 147-57.
42. Nugent, A.L., R.A. Houghtling, and B.M. Bayer, *Morphine suppresses MHC-II expression on circulating B lymphocytes via activation of the HPA.* J Neuroimmune Pharmacol, 2011. **6**(1): p. 130-41.
43. Franchi, S., A.E. Panerai, and P. Sacerdote, *Buprenorphine ameliorates the effect of surgery on hypothalamus-pituitary-adrenal axis, natural killer cell activity and metastatic colonization in rats in comparison with morphine or fentanyl treatment.* Brain Behav Immun, 2007. **21**(6): p. 767-74.
44. Tubaro, E., et al., *Effect of morphine on resistance to infection.* J Infect Dis, 1983. **148**(4): p. 656-66.
45. Lamers, C.H., et al., *Optimization of culture conditions for activation and large-scale expansion of human T lymphocytes for bispecific antibody-directed cellular immunotherapy.* Int J Cancer, 1992. **51**(6): p. 973-9.
46. Kay, J.E., *Mechanisms of T lymphocyte activation.* Immunol Lett, 1991. **29**(1-2): p. 51-4.
47. O'Flynn, K., et al., *Different pathways of human T-cell activation revealed by PHA-P and PHA-M.* Immunology, 1986. **57**(1): p. 55-60.
48. Sacerdote, P., et al., *The effects of tramadol and morphine on immune responses and pain after surgery in cancer patients.* Anesth Analg, 2000. **90**(6): p. 1411-4.
49. Curran, I., K. Nye, and R. Langford, *A prospective, randomized, double-blind, crossover, placebo-controlled trial exploring intracellular phosphorylation patterns in peripheral lymphocyte preparations isolated from healthy volunteers exposed to fentanyl, buprenorphine, tramadol, and morphine.* British Journal of Anaesthesia, 2003. **90**(6): p. 828P.
50. Yokota, T., K. Uehara, and Y. Nomoto, *Intrathecal morphine suppresses NK cell activity following abdominal surgery.* Can J Anaesth, 2000. **47**(4): p. 303-8.
51. Yokota, T., K. Uehara, and Y. Nomoto, *Addition of noradrenaline to intrathecal morphine augments the postoperative suppression of natural killer cell activity.* J Anesth, 2004. **18**(3): p. 190-5.
52. Szabo, I., et al., *Suppression of peritoneal macrophage phagocytosis of Candida albicans by opioids.* J Pharmacol Exp Ther, 1993. **267**(2): p. 703-6.
53. Liu, Y., et al., *Effects of in vivo and in vitro administration of morphine sulfate upon rhesus macaque polymorphonuclear cell phagocytosis and chemotaxis.* J Pharmacol Exp Ther, 1992. **263**(2): p. 533-9.
54. Neri, S., et al., *Randomized clinical trial to compare the effects of methadone and buprenorphine on the immune system in drug abusers.* Psychopharmacology (Berl), 2005. **179**(3): p. 700-4.
55. Bhaskaran, M., et al., *Morphine-induced degradation of the host defense barrier: role of macrophage injury.* J Infect Dis, 2001. **184**(12): p. 1524-31.
56. Bokhari, S.M., et al., *Morphine potentiates neuropathogenesis of SIV infection in rhesus macaques.* Journal of Neuroimmune Pharmacology, 2011. **6**(4): p. 626-639.

57. Olin, M., K. Choi, and T.W. Molitor, *Morphine alters M. bovis infected microglia's ability to activate gammadelta T lymphocytes.* J Neuroimmune Pharmacol, 2011. **6**(4): p. 578-84.
58. Wybran, J., et al., *Suggestive evidence for receptors for morphine and methionine-enkephalin on normal human blood T lymphocytes.* J Immunol, 1979. **123**(3): p. 1068-70.
59. Paterson, S.J., L.E. Robson, and H.W. Kosterlitz, *Classification of opioid receptors.* Br Med Bull, 1983. **39**(1): p. 31-6.
60. Karaji, A.G., et al., *Influence of endogenous opioid systems on T lymphocytes as assessed by the knockout of mu, delta and kappa opioid receptors.* J Neuroimmune Pharmacol, 2011. **6**(4): p. 608-16.
61. Decker, D., et al., *Surgical stress induces a shift in the type-1/type-2 T-helper cell balance, suggesting down-regulation of cell-mediated and up-regulation of antibody-mediated immunity commensurate to the trauma.* Surgery, 1996. **119**(3): p. 316-25.
62. Le Cras, A.E., H.F. Galley, and N.R. Webster, *Spinal but not general anesthesia increases the ratio of T helper 1 to T helper 2 cell subsets in patients undergoing transurethral resection of the prostate.* Anesth Analg, 1998. **87**(6): p. 1421-5.
63. Kraus, J., et al., *Regulation of mu-opioid receptor gene transcription by interleukin-4 and influence of an allelic variation within a STAT6 transcription factor binding site.* J Biol Chem, 2001. **276**(47): p. 43901-8.
64. Börner, C., et al., *Mechanisms of opioid-mediated inhibition of human T cell receptor signaling.* J Immunol, 2009. **183**(2): p. 882-9.
65. Clark, J.D., et al., *Morphine reduces local cytokine expression and neutrophil infiltration after incision.* Mol Pain, 2007. **3**: p. 28.
66. Myles, P.S., et al., *Perioperative epidural analgesia for major abdominal surgery for cancer and recurrence-free survival: randomised trial.* Bmj, 2011. **342**: p. d1491.
67. Rigg, J.R., et al., *Epidural anaesthesia and analgesia and outcome of major surgery: a randomised trial.* Lancet, 2002. **359**(9314): p. 1276-82.
68. Beilin, B., et al., *Effects of anesthesia based on large versus small doses of fentanyl on natural killer cell cytotoxicity in the perioperative period.* Anesth Analg, 1996. **82**(3): p. 492-7.
69. Deegan, C.A., et al., *Anesthetic technique and the cytokine and matrix metalloproteinase response to primary breast cancer surgery.* Reg Anesth Pain Med, 2010. **35**(6): p. 490-5.
70. Looney, M., P. Doran, and D.J. Buggy, *Effect of anesthetic technique on serum vascular endothelial growth factor C and transforming growth factor beta in women undergoing anesthesia and surgery for breast cancer.* Anesthesiology, 2010. **113**(5): p. 1118-25.
71. Carmi, Y., et al., *The role of IL-1beta in the early tumor cell-induced angiogenic response.* J Immunol, 2013. **190**(7): p. 3500-9.
72. McCawley, L.J., et al., *Keratinocyte Expression of MMP3 Enhances Differentiation and Prevents Tumor Establishment.* The American Journal of Pathology, 2008. **173**(5): p. 1528-1539.
73. Mehner, C., et al., *Tumor cell-produced matrix metalloproteinase 9 (MMP-9) drives malignant progression and metastasis of basal-like triple negative breast cancer.* Oncotarget, 2014. **5**(9): p. 2736-49.

74. Sato, T., et al., *Interleukin 10 in the tumor microenvironment: a target for anticancer immunotherapy.* Immunol Res, 2011. **51**(2-3): p. 170-82.
75. Exadaktylos, A.K., et al., *Can anesthetic technique for primary breast cancer surgery affect recurrence or metastasis?* Anesthesiology, 2006. **105**(4): p. 660-664.
76. Lehmann, C., M. Zeis, and L. Uharek, *Activation of natural killer cells with interleukin 2 (IL-2) and IL-12 increases perforin binding and subsequent lysis of tumour cells.* Br J Haematol, 2001. **114**(3): p. 660-5.
77. Melamed, R., et al., *Suppression of natural killer cell activity and promotion of tumor metastasis by ketamine, thiopental, and halothane, but not by propofol: mediating mechanisms and prophylactic measures.* Anesth Analg, 2003. **97**(5): p. 1331-9.
78. Rogatsky, I. and L.B. Ivashkiv, *Glucocorticoid modulation of cytokine signaling.* Tissue Antigens, 2006. **68**(1): p. 1-12.
79. Agarwal, S.K. and G.D. Marshall, Jr., *Dexamethasone promotes type 2 cytokine production primarily through inhibition of type 1 cytokines.* J Interferon Cytokine Res, 2001. **21**(3): p. 147-55.
80. Chambrier, C., et al., *Cytokine and hormonal changes after cholecystectomy. Effect of ibuprofen pretreatment.* Ann Surg, 1996. **224**(2): p. 178-82.
81. Page, G.G., J.S. McDonald, and S. Ben-Eliyahu, *Pre-operative versus postoperative administration of morphine: impact on the neuroendocrine, behavioural, and metastatic-enhancing effects of surgery.* Br J Anaesth, 1998. **81**(2): p. 216-23.
82. Pollock, R.E., E. Lotzova, and S.D. Stanford, *Mechanism of surgical stress impairment of human perioperative natural killer cell cytotoxicity.* Arch Surg, 1991. **126**(3): p. 338-42.
83. Kutza, J., et al., *The effects of general anesthesia and surgery on basal and interferon stimulated natural killer cell activity of humans.* Anesth Analg, 1997. **85**(4): p. 918-23.
84. Sessler, D.I., *Temperature Monitoring and Perioperative Thermoregulation.* Anesthesiology, 2008. **109**(2): p. 318-338.
85. Róka, A., et al., *Elevated morphine concentrations in neonates treated with morphine and prolonged hypothermia for hypoxic ischemic encephalopathy.* Pediatrics, 2008. **121**(4): p. e844-9.
86. Ben-Eliyahu, S., et al., *Hypothermia in barbiturate-anesthetized rats suppresses natural killer cell activity and compromises resistance to tumor metastasis: a role for adrenergic mechanisms.* Anesthesiology, 1999. **91**(3): p. 732-40.
87. Molina, P.E., et al., *Hemodynamic and immune consequences of opiate analgesia after trauma/hemorrhage.* Shock, 2004. **21**(6): p. 526-34.
88. Page, G.G., S. Ben-Eliyahu, and J.C. Liebeskind, *The role of LGL/NK cells in surgery-induced promotion of metastasis and its attenuation by morphine.* Brain Behav Immun, 1994. **8**(3): p. 241-50.
89. Page, G.G., et al., *Morphine attenuates surgery-induced enhancement of metastatic colonization in rats.* Pain, 1993. **54**(1): p. 21-8.
90. Page, G.G., W.P. Blakely, and S. Ben-Eliyahu, *Evidence that postoperative pain is a mediator of the tumor-promoting effects of surgery in rats.* Pain, 2001. **90**(1-2): p. 191-9.

91. Page, G.G. and S. Ben-Eliyahu, *Indomethacin attenuates the immunosuppressive and tumor-promoting effects of surgery.* The Journal of Pain, 2002. **3**(4): p. 301-308.
92. Wen, K.-C., et al., *A prospective short-term evaluation of uterine leiomyomas treated by myomectomy through conventional laparotomy or ultraminilaparotomy.* Fertility and Sterility, 2008. **90**(6): p. 2361-2366.
93. Kuo, A., et al., *In vivo profiling of seven common opioids for antinociception, constipation and respiratory depression: no two opioids have the same profile.* Br J Pharmacol, 2015. **172**(2): p. 532-48.
94. Nielsen, C.K., et al., *Oxycodone and morphine have distinctly different pharmacological profiles: radioligand binding and behavioural studies in two rat models of neuropathic pain.* Pain, 2007. **132**(3): p. 289-300.
95. Bostrom, E., M. Hammarlund-Udenaes, and U.S. Simonsson, *Blood-brain barrier transport helps to explain discrepancies in in vivo potency between oxycodone and morphine.* Anesthesiology, 2008. **108**(3): p. 495-505.
96. Cahill, C.M., et al.
97. Klimas, R., et al., *Contribution of oxycodone and its metabolites to the overall analgesic effect after oxycodone administration.* Expert Opin Drug Metab Toxicol, 2013. **9**(5): p. 517-28.
98. Biotec, M., *MACS microbeads information sheet 130-042-401*. 2014.
99. Arizona, U.o., *Interpreting Nanodrop (Spectrophotometric) results.*
100. Cicinnati, V.R., et al., *Validation of putative reference genes for gene expression studies in human hepatocellular carcinoma using real-time quantitative RT-PCR.* BMC Cancer, 2008. **8**: p. 350.
101. Wilfinger, W.W., K. Mackey, and P. Chomczynski, *Effect of pH and ionic strength on the spectrophotometric assessment of nucleic acid purity.* Biotechniques, 1997. **22**(3): p. 474-6, 478-81.
102. R&DSystems, *Parameter Cortisol Assay KGE008B.* 2016.
103. Tan, Y. and Y. Liu, *Comparison of methods for identifying differentially expressed genes across multiple conditions from microarray data.* Bioinformation, 2011. **7**(8): p. 400-4.
104. Beagles, K., A. Wellstein, and B. Bayer, *Systemic morphine administration suppresses genes involved in antigen presentation.* Mol Pharmacol, 2004. **65**(2): p. 437-42.
105. Cornwell, W.D., et al., *Effect of chronic morphine administration on circulating T cell population dynamics in rhesus macaques.* J Neuroimmunol, 2013. **265**(1-2): p. 43-50.
106. Bortsov, A.V., et al., *μ-Opioid receptor gene A118G polymorphism predicts survival in patients with breast cancer.* Anesthesiology, 2012. **116**(4): p. 896-902.
107. Cronin-Fenton, D.P., et al., *Opioids and breast cancer recurrence: A Danish population-based cohort study.* Cancer, 2015. **121**(19): p. 3507-14.
108. Leuillet S, M.A., Arthaud S, Forster R, Ancian P, *Impact of RNA degradation on affymetrix gene expression profiles*.
109. Kiaii, S., et al., *Follicular lymphoma cells induce changes in T-cell gene expression and function: potential impact on survival and risk of transformation.* J Clin Oncol, 2013. **31**(21): p. 2654-61.

110. Riches, J.C., et al., *T cells from CLL patients exhibit features of T-cell exhaustion but retain capacity for cytokine production.* Blood, 2013. **121**(9): p. 1612-21.
111. Stanley, G., et al., *Dose requirements, efficacy and side effects of morphine and pethidine delivered by patient-controlled analgesia after gynaecological surgery.* Br J Anaesth, 1996. **76**(4): p. 484-6.
112. Moestrup, S.K. and H.J. Moller, *CD163: a regulated hemoglobin scavenger receptor with a role in the anti-inflammatory response.* Ann Med, 2004. **36**(5): p. 347-54.
113. Goldstein, J.I., et al., *Increase in plasma and surface CD163 levels in patients undergoing coronary artery bypass graft surgery.* Atherosclerosis, 2003. **170**(2): p. 325-32.
114. Sulahian, T.H., et al., *Human monocytes express CD163, which is upregulated by IL-10 and identical to p155.* Cytokine, 2000. **12**(9): p. 1312-21.
115. Yeager, M.P., et al., *In Vivo Exposure to High or Low Cortisol Has Biphasic Effects on Inflammatory Response Pathways of Human Monocytes.* Anesthesia and analgesia, 2008. **107**(5): p. 1726.
116. Peters, V.A., J.J. Joesting, and G.G. Freund, *IL-1 receptor 2 (IL-1R2) and its role in immune regulation.* Brain Behav Immun, 2013. **32**: p. 1-8.
117. Kobayashi, K., et al., *IRAK-M is a negative regulator of Toll-like receptor signaling.* (0092-8674 (Print)).
118. Trastulli, S., et al., *Laparoscopic vs open resection for rectal cancer: a meta-analysis of randomized clinical trials.* Colorectal Dis, 2012. **14**(6): p. e277-96.
119. Acuto, O. and F. Michel, *CD28-mediated co-stimulation: a quantitative support for TCR signalling.* Nat Rev Immunol, 2003. **3**(12): p. 939-951.
120. Howland, K.C., et al., *The roles of CD28 and CD40 ligand in T cell activation and tolerance.* J Immunol, 2000. **164**(9): p. 4465-70.
121. Fröhlich, M., et al., *Interrupting CD28 costimulation before antigen rechallenge affects CD8+ T-cell expansion and effector functions during secondary response in mice.* European Journal of Immunology, 2016. **46**(7): p. 1644-1655.
122. van der Heide, V. and D. Homann, *CD28 days later: Resurrecting costimulation for CD8+ memory T cells.* European Journal of Immunology, 2016. **46**(7): p. 1587-1591.
123. Sun, L., et al., *Effects of hydrocortisone on the differentiation of human T helper 2 cells.* Scand J Immunol, 2011. **73**(3): p. 208-14.
124. Acuto, O., V.D. Bartolo, and F. Michel, *Tailoring T-cell receptor signals by proximal negative feedback mechanisms.*
125. Dustin, M.L. and E.O. Long, *Cytotoxic immunological synapses.* Immunol Rev, 2010. **235**(1): p. 24-34.
126. Morgan, N.V., et al., *Mutation in the TCRalpha subunit constant gene (TRAC) leads to a human immunodeficiency disorder characterized by a lack of TCRalphabeta+ T cells.* J Clin Invest, 2011. **121**(2): p. 695-702.
127. Raulet, D.H., et al., *Regulation of ligands for the NKG2D activating receptor.* Annu Rev Immunol, 2013. **31**: p. 413-41.
128. Nausch, N. and A. Cerwenka, *NKG2D ligands in tumor immunity.* Oncogene, 0000. **27**(45): p. 5944-5958.

129. Tsukerman, P., et al., *MiR-10b downregulates the stress-induced cell surface molecule MICB, a critical ligand for cancer cell recognition by natural killer cells.* Cancer Res, 2012. **72**(21): p. 5463-72.
130. Holling, T.M., E. Schooten, and P.J. van Den Elsen, *Function and regulation of MHC class II molecules in T-lymphocytes: of mice and men.* Hum Immunol, 2004. **65**(4): p. 282-90.
131. Huang, X., X. Du, and Y. Li, *The role of BCL11B in hematological malignancy.* Exp Hematol Oncol, 2012. **1**(1): p. 22.
132. Li, P., et al., *Using mouse models to study function of transcriptional factors in T cell development.* Cell Regen (Lond), 2012. **1**(1): p. 8.
133. Chen, S., et al., *The role of BCL11B in regulating the proliferation of human naive T cells.* Hum Immunol, 2012. **73**(5): p. 456-64.
134. Li, P., et al., *Reprogramming of T Cells to Natural Killer–Like Cells upon Bcl11b Deletion.* Science (New York, N.Y.), 2010. **329**(5987): p. 85-89.
135. Rusnak, F. and P. Mertz, *Calcineurin: form and function.* Physiol Rev, 2000. **80**(4): p. 1483-521.
136. Mulero, M.C., et al., *RCAN3, a novel calcineurin inhibitor that down-regulates NFAT-dependent cytokine gene expression.* Biochim Biophys Acta, 2007. **1773**(3): p. 330-41.
137. Heissmeyer, V., et al., *Calcineurin imposes T cell unresponsiveness through targeted proteolysis of signaling proteins.* Nat Immunol, 2004. **5**(3): p. 255-65.
138. Zhou, X., et al., *Th17 cell differentiation increases aquaporin-3 expression, which is further increased by treatment with NaCl.* The Journal of Immunology, 2016. **196**(1 Supplement): p. 186.16-186.16.
139. Moon, C., et al., *Aquaporin expression in human lymphocytes and dendritic cells.* Am J Hematol, 2004. **75**(3): p. 128-33.
140. Hara-Chikuma, M., et al., *Chemokine-dependent T cell migration requires aquaporin-3–mediated hydrogen peroxide uptake.* The Journal of Experimental Medicine, 2012. **209**(10): p. 1743-1752.
141. Yeager, M.P., et al., *Glucocorticoids enhance the in vivo migratory response of human monocytes.* Brain Behav Immun, 2016. **54**: p. 86-94.
142. Dimitrov, S., et al., *Cortisol and epinephrine control opposing circadian rhythms in T cell subsets.* Blood, 2009. **113**(21): p. 5134-43.
143. Jin, W., et al., *TIEG1 induces apoptosis through mitochondrial apoptotic pathway and promotes apoptosis induced by homoharringtonine and velcade.* (0014-5793 (Print)).
144. Whiteside, T.L.
145. Simon, B., et al., *Death-Associated Protein Kinase Activity Is Regulated by Coupled Calcium/Calmodulin Binding to Two Distinct Sites.* Structure(London, England:1993), 2016. **24**(6): p. 851-861.
146. Schlegel, C.R., et al., *DAPK2 is a novel modulator of TRAIL-induced apoptosis.* Cell Death Differ, 2014. **21**(11): p. 1780-1791.
147. Park, S.Y., et al., *Peptidoglycan recognition protein 1 enhances experimental asthma by promoting Th2 and Th17 and limiting regulatory T cell and plasmacytoid dendritic cell responses.* J Immunol, 2013. **190**(7): p. 3480-92.
148. Yao, X., et al., *Peptidoglycan recognition protein 1 promotes house dust mite-induced airway inflammation in mice.* Am J Respir Cell Mol Biol, 2013. **49**(6): p. 902-11.

149. Fricke, R., C. Gohl, and S. Bogdan, *The F-BAR protein family.* Communicative & Integrative Biology, 2010. **3**(2): p. 89-94.
150. Guerrier, S., et al., *The F-BAR domain of srGAP2 induces membrane protrusions required for neuronal migration and morphogenesis.* Cell, 2009. **138**(5): p. 990-1004.
151. Coutinho-Budd, J., et al., *The F-BAR domains from srGAP1, srGAP2 and srGAP3 regulate membrane deformation differently.* J Cell Sci, 2012. **125**(Pt 14): p. 3390-401.
152. Fossati, M., et al., *SRGAP2 and Its Human-Specific Paralog Co-Regulate the Development of Excitatory and Inhibitory Synapses.* Neuron, 2016. **91**(2): p. 356-69.
153. Fritz, Rafael D., et al., *SrGAP2-Dependent Integration of Membrane Geometry and Slit-Robo-Repulsive Cues Regulates Fibroblast Contact Inhibition of Locomotion.* Developmental Cell, 2015. **35**(1): p. 78-92.
154. Rosenbaum, S., et al., *Identification of novel binding partners (annexins) for the cell death signal phosphatidylserine and definition of their recognition motif.* J Biol Chem, 2011. **286**(7): p. 5708-16.
155. Rogge, L., et al., *Transcript imaging of the development of human T helper cells using oligonucleotide arrays.* Nat Genet, 2000. **25**(1): p. 96-101.
156. Gross, S.R., et al., *Joining S100 proteins and migration: for better or for worse, in sickness and in health.* Cellular and Molecular Life Sciences, 2014. **71**(9): p. 1551-1579.
157. Liu, F., et al., *Characterization of murine grancalcin specifically expressed in leukocytes and its possible role in host defense against bacterial infection.* Biosci Biotechnol Biochem, 2004. **68**(4): p. 894-902.
158. Roes, J., et al., *Granulocyte function in grancalcin-deficient mice.* Mol Cell Biol, 2003. **23**(3): p. 826-30.
159. Kisseleva, T., et al.
160. Zambrano-Zaragoza, J.F., et al., *Th17 Cells in Autoimmune and Infectious Diseases.* International Journal of Inflammation, 2014. **2014**: p. 651503.
161. Zhu, S., et al., *Transcription of the activating receptor NKG2D in natural killer cells is regulated by STAT3 tyrosine phosphorylation.* Blood, 2014. **124**(3): p. 403-11.
162. Wright, M.H., et al., *Protein myristoylation in health and disease.* Journal of Chemical Biology, 2010. **3**(1): p. 19-35.
163. Selvakumar, P., et al., *N-Myristoyltransferase 2 expression in human colon cancer: Cross-talk between the calpain and caspase system.* FEBS Letters, 2006. **580**(8): p. 2021-2026.
164. Kallies, A. and A. Vasanthakumar, *Transcription factor Bach2 balances tolerance and immunity.*
165. Roychoudhuri, R., et al., *BACH2 represses effector programs to stabilize Treg-mediated immune homeostasis.*
166. Amsen, D., et al., *Direct regulation of Gata3 expression determines the T helper differentiation potential of Notch.* Immunity, 2007. **27**(1): p. 89-99.
167. Liberman, A.C., et al., *Glucocorticoids inhibit GATA-3 phosphorylation and activity in T cells.* Faseb j, 2009. **23**(5): p. 1558-71.

168. Ahern, T. and J.E. Kay, *Protein synthesis and ribosome activation during the early stages of phytohemagglutinin lymphocyte stimulation.* Exp Cell Res, 1975. **92**(2): p. 513-5.
169. Seedhom, M.O., et al., *Protein Translation Activity: A New Measure of Host Immune Cell Activation.* 2016. **197**(4): p. 1498-506.
170. Quidville, V., et al., *Targeting the Deregulated Spliceosome Core Machinery in Cancer Cells Triggers mTOR Blockade and Autophagy.* Cancer Research, 2013. **73**(7): p. 2247-2258.
171. Taira, N., et al., *DYRK2 priming phosphorylation of c-Jun and c-Myc modulates cell cycle progression in human cancer cells.* The Journal of Clinical Investigation. **122**(3): p. 859-872.
172. Roa, I., et al., *Inactivation of tumor suppressor gene pten in early and advanced gallbladder cancer.* Diagnostic Pathology, 2015. **10**(1): p. 1-5.
173. Hawse, W.F., et al., *Cutting Edge: Differential Regulation of PTEN by TCR, Akt, and FoxO1 Controls CD4+ T Cell Fate Decisions.* 2015. **194**(10): p. 4615-9.
174. Crotty, S., *Follicular helper CD4 T cells (TFH).* Annu Rev Immunol, 2011. **29**: p. 621-63.
175. Nurieva, R.I., et al., *Bcl6 Mediates the Development of T Follicular Helper Cells.* Science, 2009. **325**(5943): p. 1001-1005.
176. Yan, Z.Q., *Regulation of TLR4 expression is a tale about tail.* Arterioscler Thromb Vasc Biol, 2006. **26**(12): p. 2582-4.
177. Caratti, G., et al., *Glucocorticoid receptor function in health and disease.* Clin Endocrinol (Oxf), 2015. **83**(4): p. 441-8.
178. Adamson, W.T., et al., *Ontogeny of mu- and kappa-opiate receptor control of the hypothalamo-pituitary-adrenal axis in rats.* Endocrinology, 1991. **129**(2): p. 959-64.
179. Coventry, T.L., et al., *Endomorphins and activation of the hypothalamo-pituitary-adrenal axis.* J Endocrinol, 2001. **169**(1): p. 185-93.
180. Flores, L.R., M.C. Hernandez, and B.M. Bayer, *Acute immunosuppressive effects of morphine: lack of involvement of pituitary and adrenal factors.* J Pharmacol Exp Ther, 1994. **268**(3): p. 1129-34.
181. Mellon, R.D. and B.M. Bayer, *The effects of morphine, nicotine and epibatidine on lymphocyte activity and hypothalamic-pituitary-adrenal axis responses.* J Pharmacol Exp Ther, 1999. **288**(2): p. 635-42.
182. Nikolarakis, K.E., et al., *Facilitation of ACTH secretion by morphine is mediated by activation of CRF releasing neurons and sympathetic neuronal pathways.* Brain Res, 1989. **498**(2): p. 385-8.
183. Marik, P.E. and M. Flemmer, *The immune response to surgery and trauma: Implications for treatment.* J Trauma Acute Care Surg, 2012. **73**(4): p. 801-8.
184. Rose, A.J., A. Vegiopoulos, and S. Herzig, *Role of glucocorticoids and the glucocorticoid receptor in metabolism: insights from genetic manipulations.* J Steroid Biochem Mol Biol, 2010. **122**(1-3): p. 10-20.
185. Biosciences, B., *BD™ Cytometric Bead Array (CBA) Human Th1/Th2/Th17 Cytokine Kit.* 2014.
186. Kashiwabara, M., et al., *Surgical trauma-induced adrenal insufficiency is associated with postoperative inflammatory responses.* J Nippon Med Sch, 2007. **74**(4): p. 274-83.

187. Yahara, N., et al., *Comparison of interleukin-6, interleukin-8, and granulocyte colony-stimulating factor production by the peritoneum in laparoscopic and open surgery.* Surg Endosc, 2002. **16**(11): p. 1615-9.
188. Lin, H., et al., *Whole blood gene expression and interleukin-6 levels.* Genomics, 2014. **104**(6 Pt B): p. 490-5.
189. Houghtling, R.A. and B.M. Bayer, *Rapid elevation of plasma interleukin-6 by morphine is dependent on autonomic stimulation of adrenal gland.* J Pharmacol Exp Ther, 2002. **300**(1): p. 213-9.
190. Diehl, S. and M. Rincon, *The two faces of IL-6 on Th1/Th2 differentiation.* Mol Immunol, 2002. **39**(9): p. 531-6.
191. Houghtling, R.A., et al., *Acute effects of morphine on blood lymphocyte proliferation and plasma IL-6 levels.* Ann N Y Acad Sci, 2000. **917**: p. 771-7.
192. Hutchins, A.P., D. Diez, and D. Miranda-Saavedra, *The IL-10/STAT3-mediated anti-inflammatory response: recent developments and future challenges.* Brief Funct Genomics, 2013. **12**(6): p. 489-98.
193. Grunig, G., et al., *Interleukin-10 is a natural suppressor of cytokine production and inflammation in a murine model of allergic bronchopulmonary aspergillosis.* J Exp Med, 1997. **185**(6): p. 1089-99.
194. Hawrylowicz, C.M. and A. O'Garra, *Potential role of interleukin-10-secreting regulatory T cells in allergy and asthma.* Nat Rev Immunol, 2005. **5**(4): p. 271-83.
195. Fiorentino, D.F., M.W. Bond, and T.R. Mosmann, *Two types of mouse T helper cell. IV. Th2 clones secrete a factor that inhibits cytokine production by Th1 clones.* J Exp Med, 1989. **170**(6): p. 2081-95.
196. Timmermann, M., et al., *Interaction of soluble CD163 with activated T lymphocytes involves its association with non-muscle myosin heavy chain type A.* Immunol Cell Biol, 2004. **82**(5): p. 479-87.
197. Pacifici, R., et al., *Pharmacokinetics and cytokine production in heroin and morphine-treated mice.* Int J Immunopharmacol, 2000. **22**(8): p. 603-14.
198. Holan, V., et al., *Augmented production of proinflammatory cytokines and accelerated allotransplantation reactions in heroin-treated mice.* Clin Exp Immunol, 2003. **132**(1): p. 40-5.
199. Ottosson, M., et al., *The effects of cortisol on the regulation of lipoprotein lipase activity in human adipose tissue.* J Clin Endocrinol Metab, 1994. **79**(3): p. 820-5.
200. Morici, G., et al., *Supramaximal exercise mobilizes hematopoietic progenitors and reticulocytes in athletes.* Am J Physiol Regul Integr Comp Physiol, 2005. **289**(5): p. R1496-503.
201. Danilovic, D., et al., *Differential inflammatory gene expression profile in Graves' disease.* Endocrine Reviews, Supplement 1, 2010. **31**(3): p. S993.
202. Karl, M., et al., *Hypocortisolemia in Graves hyperthyroidism.* Endocr Pract, 2009. **15**(3): p. 220-4.
203. Patil, N.K., et al., *FLT3 Ligand Treatment Attenuates T Cell Dysfunction and Improves Survival in A Murine Model of Burn Wound Sepsis.* Shock, 2016.

204. Choi, J., S.R. Fauce, and R.B. Effros, *Reduced telomerase activity in human T lymphocytes exposed to cortisol.* Brain Behav Immun, 2008. **22**(4): p. 600-5.
205. Asadi, A., et al., *FMS-like tyrosine kinase 3 interacts with the glucocorticoid receptor complex and affects glucocorticoid dependent signaling.* Biochem Biophys Res Commun, 2008. **368**(3): p. 569-74.
206. Desborough, J.P., *The stress response to trauma and surgery.* Br J Anaesth, 2000. **85**(1): p. 109-17.
207. Rosenne, E., et al., *In vivo suppression of NK cell cytotoxicity by stress and surgery: glucocorticoids have a minor role compared to catecholamines and prostaglandins.* Brain Behav Immun, 2014. **37**: p. 207-19.
208. Tai, L.H., et al., *Preventing postoperative metastatic disease by inhibiting surgery-induced dysfunction in natural killer cells.* Cancer Res, 2013. **73**(1): p. 97-107.
209. Blohm, U., et al., *Solid tumors "melt" from the inside after successful CD8 T cell attack.* Eur J Immunol, 2006. **36**(2): p. 468-77.
210. Russell, J.H. and T.J. Ley, *Lymphocyte-mediated cytotoxicity.* Annu Rev Immunol, 2002. **20**: p. 323-70.
211. Liu, Q., et al., *Matrix metalloprotease inhibitors restore impaired NK cell-mediated antibody-dependent cellular cytotoxicity in human immunodeficiency virus type 1 infection.* J Virol, 2009. **83**(17): p. 8705-12.
212. Berta, T., et al., *Acute morphine activates satellite glial cells and up-regulates IL-1beta in dorsal root ganglia in mice via matrix metalloprotease-9.* Mol Pain, 2012. **8**: p. 18.
213. Bjorkstrom, N.K., et al., *Elevated numbers of Fc gamma RIIIA+ (CD16+) effector CD8 T cells with NK cell-like function in chronic hepatitis C virus infection.* J Immunol, 2008. **181**(6): p. 4219-28.
214. Romee, R., et al., *NK cell CD16 surface expression and function is regulated by a disintegrin and metalloprotease-17 (ADAM17).* Blood, 2013. **121**(18): p. 3599-608.
215. Dehmel, T., et al., *The cell-specific expression of metalloproteinase-disintegrins (ADAMs) in inflammatory myopathies*, in *Neurobiol Dis*. 2007: United States. p. 665-74.
216. Brenu, E.W., et al., *Role of adaptive and innate immune cells in chronic fatigue syndrome/myalgic encephalomyelitis.* Int Immunol, 2014. **26**(4): p. 233-42.
217. Flores, I., et al., *Phosphatidic acid generation through interleukin 2 (IL-2)-induced alpha-diacylglycerol kinase activation is an essential step in IL-2-mediated lymphocyte proliferation.* J Biol Chem, 1996. **271**(17): p. 10334-40.
218. Hasegawa, H., et al., *Lysophosphatidylcholine enhances the suppressive function of human naturally occurring regulatory T cells through TGF-beta production.* Biochem Biophys Res Commun, 2011. **415**(3): p. 526-31.
219. Gangolf, M., et al., *Thiamine Status in Humans and Content of Phosphorylated Thiamine Derivatives in Biopsies and Cultured Cells.* PLoS ONE, 2010. **5**(10): p. e13616.
220. Buttner, P., et al., *Exercise affects the gene expression profiles of human white blood cells.* J Appl Physiol (1985), 2007. **102**(1): p. 26-36.

221. Yu, N., et al., *HSP105 recruits protein phosphatase 2A to dephosphorylate beta-catenin.* Mol Cell Biol, 2015. **35**(8): p. 1390-400.
222. Nelson, W.J. and R. Nusse, *Convergence of Wnt, beta-catenin, and cadherin pathways.* Science, 2004. **303**(5663): p. 1483-7.
223. Marcato, V., et al., *beta-Catenin Upregulates the Constitutive and Virus-Induced Transcriptional Capacity of the Interferon Beta Promoter through T-Cell Factor Binding Sites.* Mol Cell Biol, 2016. **36**(1): p. 13-29.
224. Mattiola, I., et al., *Priming of Human Resting NK Cells by Autologous M1 Macrophages via the Engagement of IL-1beta, IFN-beta, and IL-15 Pathways.* 2015. **195**(6): p. 2818-28.
225. Gerard, A., et al., *The Rac activator Tiam1 controls efficient T-cell trafficking and route of transendothelial migration.* Blood, 2009. **113**(24): p. 6138-47.
226. Wei, S.Y., et al., *Protein kinase C-delta and -beta coordinate flow-induced directionality and deformation of migratory human blood T-lymphocytes.* J Mol Cell Biol, 2014. **6**(6): p. 458-72.
227. Guo, X., et al., *Balanced Tiam1-rac1 and RhoA drives proliferation and invasion of pancreatic cancer cells.* Mol Cancer Res, 2013. **11**(3): p. 230-9.
228. Chen, Y., et al., *Interferon-inducible cholesterol-25-hydroxylase inhibits hepatitis C virus replication via distinct mechanisms.* Sci Rep, 2014. **4**: p. 7242.
229. Xiang, Y., et al., *Identification of Cholesterol 25-Hydroxylase as a Novel Host Restriction Factor and a Part of the Primary Innate Immune Responses against Hepatitis C Virus Infection.* J Virol, 2015. **89**(13): p. 6805-16.
230. Diczfalusy, U., et al., *Marked upregulation of cholesterol 25-hydroxylase expression by lipopolysaccharide.* J Lipid Res, 2009. **50**(11): p. 2258-64.
231. Schlegel, C.R., et al., *DAPK2 regulates oxidative stress in cancer cells by preserving mitochondrial function.* Cell Death Dis, 2015. **6**: p. e1671.
232. Newton, R.H., et al., *Protein kinase D orchestrates the activation of DRAK2 in response to TCR-induced Ca2+ influx and mitochondrial reactive oxygen generation.* J Immunol, 2011. **186**(2): p. 940-50.
233. Vincourt, J.B., et al., *Molecular and functional characterization of SLC26A11, a sodium-independent sulfate transporter from high endothelial venules.* Faseb j, 2003. **17**(8): p. 890-2.
234. Bergstrom, S.E., et al., *Antigen-induced regulation of T-cell motility, interaction with antigen-presenting cells and activation through endogenous thrombospondin-1 and its receptors.* Immunology, 2015. **144**(4): p. 687-703.
235. Noyes, N.C., et al., *Regulation of Itch and Nedd4 E3 Ligase Activity and Degradation by LRAD3.* Biochemistry, 2016. **55**(8): p. 1204-13.
236. Merck, E., et al., *OSCAR is an FcRgamma-associated receptor that is expressed by myeloid cells and is involved in antigen presentation and activation of human dendritic cells.* Blood, 2004. **104**(5): p. 1386-95.
237. Zou, Q., et al., *USP15 stabilizes MDM2 to mediate cancer-cell survival and inhibit antitumor T cell responses.* Nat Immunol, 2014. **15**(6): p. 562-70.

238. Zou, Q., et al., *T Cell Intrinsic USP15 Deficiency Promotes Excessive IFN-gamma Production and an Immunosuppressive Tumor Microenvironment in MCA-Induced Fibrosarcoma.* Cell Rep, 2015. **13**(11): p. 2470-9.
239. Borner, C. and J. Kraus, *Inhibition of NF-kappaB by opioids in T cells.* J Immunol, 2013. **191**(9): p. 4640-7.
240. Poupon, V., et al., *Clathrin light chains function in mannose phosphate receptor trafficking via regulation of actin assembly.* Proc Natl Acad Sci U S A, 2008. **105**(1): p. 168-73.
241. Dunkle, A., I. Dzhagalov, and Y.W. He, *Cytokine-dependent and cytokine-independent roles for Mcl-1: genetic evidence for multiple mechanisms by which Mcl-1 promotes survival in primary T lymphocytes.* Cell Death and Dis, 2011. **2**: p. e214.
242. Kim, E.H., et al., *Mcl-1 regulates effector and memory CD8 T-cell differentiation during acute viral infection.* Virology, 2016. **490**: p. 75-82.
243. Luo, Z., et al., *Orosomucoid, an acute response protein with multiple modulating activities.* J Physiol Biochem, 2015. **71**(2): p. 329-40.
244. Mestriner, F.L., et al., *Acute-phase protein alpha-1-acid glycoprotein mediates neutrophil migration failure in sepsis by a nitric oxide-dependent mechanism.* Proc Natl Acad Sci U S A, 2007. **104**(49): p. 19595-600.
245. Schneider, H., et al., *CTLA-4 activation of phosphatidylinositol 3-kinase (PI 3-K) and protein kinase B (PKB/AKT) sustains T-cell anergy without cell death.* PLoS One, 2008. **3**(12): p. e3842.
246. Boussiotis, V.A., et al., *Induction of T cell clonal anergy results in resistance, whereas CD28-mediated costimulation primes for susceptibility to Fas- and Bax-mediated programmed cell death.* J Immunol, 1997. **159**(7): p. 3156-67.
247. Schwartz, R.H., *T cell anergy.* Annu Rev Immunol, 2003. **21**: p. 305-34.
248. Lissina, A., et al., *Priming of Qualitatively Superior Human Effector CD8+ T Cells Using TLR8 Ligand Combined with FLT3 Ligand.* 2016. **196**(1): p. 256-63.
249. Guermonprez, P., et al., *Inflammatory Flt3L is essential to mobilize dendritic cells and for T cell responses during Plasmodium infection.* Nature medicine, 2013. **19**(6): p. 730-738.
250. Kerscher, B., et al., *Signalling through MyD88 drives surface expression of the mycobacterial receptors MCL (Clecsf8, Clec4d) and Mincle (Clec4e) following microbial stimulation.* Microbes and Infection.
251. Greco, S.H., et al., *Mincle suppresses Toll-like receptor 4 activation.* J Leukoc Biol, 2016. **100**(1): p. 185-94.
252. Wevers, B.A., et al., *Fungal engagement of the C-type lectin mincle suppresses dectin-1-induced antifungal immunity.* Cell Host Microbe, 2014. **15**(4): p. 494-505.
253. Zhu, Y.X., et al., *The SH3-SAM adaptor HACS1 is up-regulated in B cell activation signaling cascades.* J Exp Med, 2004. **200**(6): p. 737-47.
254. drugs.com, *Morphine injection*.
255. Arttamangkul, S., et al., *Differential activation and trafficking of micro-opioid receptors in brain slices.* Mol Pharmacol, 2008. **74**(4): p. 972-9.

256. Madi, L., et al., *Overexpression of A3 adenosine receptor in peripheral blood mononuclear cells in rheumatoid arthritis: involvement of nuclear factor-kappaB in mediating receptor level.* J Rheumatol, 2007. **34**(1): p. 20-6.
257. Taliani, S., et al., *Novel N2-substituted pyrazolo[3,4-d]pyrimidine adenosine A3 receptor antagonists: inhibition of A3-mediated human glioblastoma cell proliferation.* J Med Chem, 2010. **53**(10): p. 3954-63.
258. Fishman, P., et al., *An agonist to the A3 adenosine receptor inhibits colon carcinoma growth in mice via modulation of GSK-3[beta] and NF-[kappa]B.* Oncogene, 0000. **23**(14): p. 2465-2471.
259. Ohana, G., et al., *Differential effect of adenosine on tumor and normal cell growth: focus on the A3 adenosine receptor.* J Cell Physiol, 2001. **186**(1): p. 19-23.
260. Wall, M. and N. Dale, *Activity-Dependent Release of Adenosine: A Critical Re-Evaluation of Mechanism.* Current Neuropharmacology, 2008. **6**(4): p. 329-337.
261. Baine, M.J., et al., *Transcriptional profiling of peripheral blood mononuclear cells in pancreatic cancer patients identifies novel genes with potential diagnostic utility.* PLoS One, 2011. **6**(2): p. e17014.
262. Higashi, Y., et al., *Impairment of T cell development in deltaEF1 mutant mice.* J Exp Med, 1997. **185**(8): p. 1467-79.
263. Oganesyan, G., et al., *Critical role of TRAF3 in the Toll-like receptor-dependent and -independent antiviral response.* Nature, 2006. **439**(7073): p. 208-211.
264. de Diego, R.P., et al., *Human TRAF3 adaptor molecule deficiency leads to impaired Toll-like receptor 3 response and susceptibility to herpes simplex encephalitis.* Immunity, 2010. **33**(3): p. 400-411.
265. Li, K., et al., *Identification and expression of a new type II transmembrane protein in human mast cells.* Genomics, 2005. **86**(1): p. 68-75.
266. Andersson, S., et al., *The transcriptomic and proteomic landscapes of bone marrow and secondary lymphoid tissues.* PLoS One, 2014. **9**(12): p. e115911.
267. Munder, M., *Arginase: an emerging key player in the mammalian immune system.* Br J Pharmacol, 2009. **158**(3): p. 638-51.
268. Ochoa, J.B., et al., *Arginase I Expression and Activity in Human Mononuclear Cells After Injury.* Annals of Surgery, 2001. **233**(3): p. 393-399.
269. Rodriguez, P.C., et al., *Arginase I production in the tumor microenvironment by mature myeloid cells inhibits T-cell receptor expression and antigen-specific T-cell responses.* Cancer Res, 2004. **64**(16): p. 5839-49.
270. Lu, L., et al., *Restoration of intrahepatic regulatory T cells through MMP-9/13-dependent activation of TGF-beta is critical for immune homeostasis following acute liver injury.* J Mol Cell Biol, 2013. **5**(6): p. 369-79.
271. Liu, Y.C., et al., *Acute morphine induces matrix metalloproteinase-9 up-regulation in primary sensory neurons to mask opioid-induced analgesia in mice.* Mol Pain, 2012. **8**: p. 19.

272. Brunet, L.J., et al., *Noggin, cartilage morphogenesis, and joint formation in the mammalian skeleton.* Science, 1998. **280**(5368): p. 1455-7.
273. Martínez, V.G., et al., *The BMP Pathway Participates in Human Naive CD4(+) T Cell Activation and Homeostasis.* PLoS ONE, 2015. **10**(6): p. e0131453.
274. Yamaguchi, K., et al., *Significant detection of circulating cancer cells in the blood by reverse transcriptase-polymerase chain reaction during colorectal cancer resection.* Ann Surg, 2000. **232**(1): p. 58-65.
275. Roh, K.H., et al., *The coreceptor CD4 is expressed in distinct nanoclusters and does not colocalize with T-cell receptor and active protein tyrosine kinase p56lck.* Proc Natl Acad Sci U S A, 2015. **112**(13): p. E1604-13.
276. Boomer, J.S. and J.M. Green, *An enigmatic tail of CD28 signaling.* Cold Spring Harb Perspect Biol, 2010. **2**(8): p. a002436.
277. Biffl, W.L., et al., *Interleukin-6 in the injured patient. Marker of injury or mediator of inflammation?* Ann Surg, 1996. **224**(5): p. 647-64.
278. Hager, S., et al., *Interleukin-6 Serum Levels Correlate With Severity of Burn Injury but Not With Gender.* J Burn Care Res, 2017.
279. Ricarte-Bratti, J.P., et al., *IL-6, MMP 3 and prognosis in previously healthy sepsis patients.* Rev Fac Cien Med Univ Nac Cordoba, 2017. **74**(2): p. 99-106.
280. Waage, A., et al., *The complex pattern of cytokines in serum from patients with meningococcal septic shock. Association between interleukin 6, interleukin 1, and fatal outcome.* J Exp Med, 1989. **169**(1): p. 333-8.
281. Fairfax, B.P., et al., *An integrated expression phenotype mapping approach defines common variants in LEP, ALOX15 and CAPNS1 associated with induction of IL-6.* Hum Mol Genet, 2010. **19**(4): p. 720-30.
282. Pascual, M., et al., *Randomized clinical trial comparing inflammatory and angiogenic response after open versus laparoscopic curative resection for colonic cancer.* Br J Surg, 2011. **98**(1): p. 50-9.
283. Neeman, E. and S. Ben-Eliyahu.
284. Watt, D.G., P.G. Horgan, and D.C. McMillan, *Routine clinical markers of the magnitude of the systemic inflammatory response after elective operation: a systematic review.* Surgery, 2015. **157**(2): p. 362-80.
285. Ozcan, S., et al., *Effects of combined general anesthesia and thoracic epidural analgesia on cytokine response in patients undergoing laparoscopic cholecystectomy.* Niger J Clin Pract, 2016. **19**(4): p. 436-42.
286. Dennis, K.L., et al., *Current status of interleukin-10 and regulatory T-cells in cancer.* Curr Opin Oncol, 2013. **25**(6): p. 637-45.
287. Oliviero, B., et al., *Hepatitis C virus-Induced NK Cell Activation Causes Metzincin-Mediated CD16 Cleavage and Impaired Antibody-Dependent Cytotoxicity.* J Hepatol, 2017.
288. Rosenberg, S.A., et al., *Observations on the systemic administration of autologous lymphokine-activated killer cells and recombinant interleukin-2 to patients with metastatic cancer.* N Engl J Med, 1985. **313**(23): p. 1485-92.

289. Ochoa, M.C., et al., *Antibody-dependent cell cytotoxicity: immunotherapy strategies enhancing effector NK cells.* Immunol Cell Biol, 2017. **95**(4): p. 347-355.
290. Vredevoe, D.L., et al., *Natural killer cell anergy to cytokine stimulants in a subgroup of patients with heart failure: relationship to norepinephrine.* Neuroimmunomodulation, 1995. **2**(1): p. 16-24.
291. Ardolino, M., et al., *Cytokine therapy reverses NK cell anergy in MHC-deficient tumors.* J Clin Invest, 2014. **124**(11): p. 4781-94.
292. Shifrin, N., D.H. Raulet, and M. Ardolino, *NK cell self tolerance, responsiveness and missing self recognition.* Semin Immunol, 2014. **26**(2): p. 138-44.
293. Schwartz, R.H., *Models of T cell anergy: is there a common molecular mechanism?* J Exp Med, 1996. **184**(1): p. 1-8.
294. Lechner, O., et al., *Fingerprints of anergic T cells.* Current Biology. **11**(8): p. 587-595.
295. Le Dieu, R., et al., *Peripheral blood T cells in acute myeloid leukemia (AML) patients at diagnosis have abnormal phenotype and genotype and form defective immune synapses with AML blasts.* Blood, 2009. **114**(18): p. 3909-16.
296. Brunner, K.T., et al., *Quantitative assay of the lytic action of immune lymphoid cells on 51-Cr-labelled allogeneic target cells in vitro; inhibition by isoantibody and by drugs.* Immunology, 1968. **14**(2): p. 181-96.
297. Kim, D.H., et al., *Is myomectomy in women aged 45 years and older an effective option?* Eur J Obstet Gynecol Reprod Biol, 2014. **177**: p. 57-60.
298. Commandeur, A.E., A.K. Styer, and J.M. Teixeira, *Epidemiological and genetic clues for molecular mechanisms involved in uterine leiomyoma development and growth.* Hum Reprod Update, 2015. **21**(5): p. 593-615.
299. Roszkowski, P.I., A. Hyc, and J. Malejczyk, *Natural killer cell activity in patients with ovarian tumors and uterine myomas.* Eur J Gynaecol Oncol, 1993. **14 Suppl**: p. 114-7.
300. Ben-Eliyahu, S., et al., *Timing within the oestrous cycle modulates adrenergic suppression of NK activity and resistance to metastasis: possible clinical implications.* Br J Cancer, 2000. **83**(12): p. 1747-54.
301. Ulens, C., et al., *Morphine-6beta-glucuronide and morphine-3-glucuronide, opioid receptor agonists with different potencies.* Biochem Pharmacol, 2001. **62**(9): p. 1273-82.
302. Klimas, R. and G. Mikus, *Morphine-6-glucuronide is responsible for the analgesic effect after morphine administration: a quantitative review of morphine, morphine-6-glucuronide, and morphine-3-glucuronide.* Br J Anaesth, 2014. **113**(6): p. 935-44.
303. Carrigan, K.A. and D.T. Lysle, *Morphine-6 beta-glucuronide induces potent immunomodulation.* Int Immunopharmacol, 2001. **1**(5): p. 821-31.
304. Nakamura, A., et al., *Differential activation of the mu-opioid receptor by oxycodone and morphine in pain-related brain regions in a bone cancer pain model.* Br J Pharmacol, 2013. **168**(2): p. 375-88.
305. Raehal, K.M., et al., *Functional selectivity at the mu-opioid receptor: implications for understanding opioid analgesia and tolerance.* Pharmacol Rev, 2011. **63**(4): p. 1001-19.

306. Borgland, S.L., et al., *Opioid agonists have different efficacy profiles for G protein activation, rapid desensitization, and endocytosis of mu-opioid receptors.* J Biol Chem, 2003. **278**(21): p. 18776-84.

Appendix A

Table 9.1: Demographic data for all patients at the time of study enrolment

Subject No	BMI	Age	Ethnicity	Treatment	Surgery duration (hh:mm)	Surgery performed	Opioid dose (mg)
1	24	43	Caucasian	Morphine	02:15	Open myomectomy	27
2	24	45	Other	Morphine	03:50	Open myomectomy and hysteroscopy	34
3	25	34	Black	Oxycodone	02:35	Open myomectomy + right partial salpingectomy for adhesions on tube	33
4	19	49	Caucasian	Morphine	02:15		25
5	24	43	Asian	Oxycodone	01:50		25
6	22	32		Oxycodone		Open myomectomy	29.2
7	26	41	Black	Morphine	02:50		
8	32	40	Black	Oxycodone			
9	25	38	Asian	Oxycodone	01:40	myomectomy and laparatomy	21
10	28	35	Asian		01:55		28
11	34	33	Black		03:00		
12	34	37	Black				
13	20	36	Black	Morphine	03:01	Open myomectomy	21
14	20	37	Caucasian	Morphine	02:40		31
15	21	37	Black	Oxycodone		open myomectomy	15
16	36	58	Black		05:00		
17		29	Asian		02:00		
18	24	41	Black	Oxycodone	03:04	open myomectomy	17
19	22	49	Caucasian	Oxycodone	02:50	Right salpingo-oophorectomy	20
20	42	33	Black	Bupivacaine	02:15		
21		40	Asian	Morphine	02:30	open myomectomy	15
22	27	35	Black	Morphine	03:15	open myomectomy	23
23	27	45	Black	Oxycodone	02:30	open myomectomy	31
24	32	43	Black	Bupivacaine	02:00		
25	24	34	Asian	Bupivacaine	02:30		
26		38	Asian	Oxycodone	02:20	open myomectomy	23
27	35	45	Caucasian	Morphine	03:10		
28	21	30	Black	Bupivacaine	01:30		
29	18	38	Asian	Oxycodone	02:10	open myomectomy	14
30	32	48	Other	Oxycodone	02:20	Total abdominal hysterectomy (non-Pfannenstiel incision)	23
31	26	40	Black	Morphine	02:15	Total abdominal hysterectomy	66

32	40	50	Other	Bupivacaine	03:00	Subtotal hysterectomy and bilateral salpingo-oophorectomy	
33	40	33	Caucasian	Oxycodone	02:00	Open myomectomy	20
34	27	41	Black	Oxycodone		Open myomectomy	24
35	29	41	Caucasian	Morphine	02:00	Total abdominal hysterectomy with conservation of ovaries	41.4
36	26	47	Caucasian	Bupivacaine	01:25	Open subtotal hysterectomy	
37	30	43	Black	Bupivacaine			
38		33	Asian	Bupivacaine			
39	23	45	Black	Bupivacaine	02:00	Subtotal hysterectomy	
40	26	44	Asian	Morphine	02:00	Open myomectomy	10
41	37	43	Caucasian	Bupivacaine	02:25	Total abdominal hysterectomy and bilateral salpingo-oophorectomy	
42	21			Morphine			
43	29	34	Black	Morphine			24
44	32	34	Caucasian	Oxycodone	02:00	Open myomectomy	18
45				Morphine			
46	23	40		Bupivacaine	01:50	Open myomectomy	
47	25	72	Asian	Morphine		Total abdominal hysterectomy and bilateral salpingo-oophorectomy	17
48	31	37	Caucasian	Morphine	02:00	Open myomectomy	30
49	42	44	Black	Oxycodone	01:40	Open myomectomy	30
50	33	70	Caucasian	Morphine		Hysterectomy	24
51	30	36	Caucasian	Bupivacaine	01:30	Open salpingo-oophorectomy and appendectomy	
52	25	35	Caucasian	Morphine	02:30	Open myomectomy	23
53	32	55	Caucasian	Morphine	02:30	Laparotomy – frozen section and debulking	24
54	36	60	Caucasian	Bupivacaine	03:45	Total abdominal hysterectomy, bilateral salpingo-oophorectomy and appendectomy	
55	22	38	Caucasian	Oxycodone	01:35	Right salpingo-oophorectomy and appendectomy	27
56	22	33	Caucasian	Oxycodone	02:30	Open myomectomy	20
57	23	43	Asian	Morphine	01:45	Open myomectomy	23

Table 9.2: Consented versus completed microarray cohort patients for each surgical procedure.

Surgery performed	Consented patients	Completed patients
Open myomectomy	24	22
Total abdominal hysterectomy +/- bilateral salpingo-oophorectomy	6	6
Subtotal abdominal hysterectomy +/- salpingo-oophorectomy	4	3
Open myomectomy + partial salpingectomy for tubal adhesions	1	1
Right salpingo-oophorectomy	1	1
Laparotomy – frozen section and debulking	1	1
Salpingo-oophorectomy + appendectomy	2	2
Total abdominal hysterectomy + appendectomy	1	1

Table 9.3: Mean age, BMI, operation duration and modal ethnicity for each treatment group in microarray patient cohort.

Treatment group	N	Mean age	Mean BMI	Operation duration (min)	Modal ethnicity
Morphine	16	44.9	26.1	151	Caucasian
Oxycodone	16	38.9	26.7	135	Black
Bupivacaine	8	45.5	31.1	134	Caucasian

Table 9.4: Distribution of ethnicity for each treatment group in microarray patient cohort.

Treatment group	N	Black	Caucasian	Asian	Other	Unknown
Morphine	16	3	7	4	1	1
Oxycodone	16	6	5	3	1	1
Bupivacaine	8	2	4	0	1	1

Table 9.5: Ethnicity for all patients enrolled into the study.

Ethnicity	Number of patients
Caucasian	18
Black	20
Asian	12
Other	3

Table 9.6: Age for all patients enrolled in the study.

Age range	Number of patients
18-29	1
30-39	24
40-49	24
50-59	3
60-69	1
70+	2

Table 9.7: BMI for all patients enrolled in the study.

BMI range	Number of patients
<20	2
20-24	17
25-29	14
30-34	11
35-39	4
40+	4

Table 9.8: Statistical data for differences in age, BMI and operation duration for all treatment groups in microarray patient cohort.

	Treatment group	N	Mean	SD	Median	25 %	75 %	ANOVA	KW
Age	Morphine	15	44.9	11.8	41.0	37.0	45	0.11	0.09
	Oxycodone	16	38.9	5.4	38.0	34.0	43.3		
	Bupivacaine	8	45.5	7.2	44.0	40.8	49.3		
BMI	Morphine	15	26.1	4.1	25.4	23.5	29.8	0.15	0.21
	Oxycodone	16	26.7	7.0	24.7	21.6	31.6		
	Bupivacaine	8	31.1	6.3	31.1	24.2	36.9		
Op duration	Morphine	15	150.0	34.9	150.0	120.0	170.0	0.49	0.38
	Oxycodone	16	134.9	27.5	140.0	110.0	152.5		
	Bupivacaine	8	134.4	47.5	120.0	95.0	171.3		

Table 9.9: Pain scores for all patients enrolled in the study. *Where mild was recorded in error rather than a numerical rating, a score of 3 was allocated to enable statistical analysis. NK = not known.

Subject No	0 hr	2 hr	6 hr	24 hr	Treatment
1	0	0	4	4	Morphine
2	0	0	5	4	Morphine
3	0	0	2	1	Oxycodone
4	0	0	2	1	Morphine
5	0	0	2	2	Oxycodone
6	0	0	1	3	Oxycodone
7	0	0	WD	WD	Morphine
8	0	WD	WD	WD	Oxycodone
9	0	8	6	4	Oxycodone
10	0	0	5	2	Morphine
11	0	0	5	WD	Epidural
12	0	WD	WD	WD	Oxycodone
13	0	0	8	1	Morphine
14	0	0	6	3	Morphine
15	0	0	1	6	Oxycodone
16	0	WD	WD	WD	Not treated
17	0	WD	WD	WD	Oxycodone
18	0	0	5	2	Oxycodone
19	0	1	1	1	Oxycodone
20	0	4	WD	WD	Epidural
21	0	0	1	1	Morphine
22	0	0	0	0	Morphine
23	0	0	5	5	Oxycodone
24	2	0	2	WD	Epidural
25	0	0	1	1	Epidural
26	0	0	3	4	Oxycodone
27	0	0	WD	WD	Morphine
28	0	0	WD	WD	Epidural
29	0	0	0	1	Oxycodone
30	0	0	8	8	Oxycodone
31	0	0	7	7	Morphine
32	0	0	3	4	Epidural
33	0	0	3	1	Oxycodone
34	0	0	2	2	Oxycodone
35	0	5	1	0	Morphine
36	0	5	7	5	Epidural
37	0	0	9	WD	Epidural
38	0	0	1	5	Epidural
39	0	0	2	1	Epidural

40	0	0	NK	7.5	Morphine
41	0	0	8	WD	Epidural
42	0	WD	WD	WD	Morphine
43	0	0	1	1	Morphine
44	0	0	2	2	Oxycodone
45	NK	NK	NK	NK	Morphine
46	0	0	0	2	Epidural
47	0	0	2	0	Morphine
48	0	0	0	0	Morphine
49	0	0	5	2	Oxycodone
50	0	0	Mild*	5	Morphine
51	0	0	0	4	Epidural
52	0	0	3	3	Morphine
53	0	NK	4	3	Morphine
54	0	0	7	2	Epidural
55	0	8	0	5	Oxycodone
56	0	0	3	0	Oxycodone
57	0	Mild*	Mild*	0	Morphine

Table 9.10: Statistical data for differences in pain for all treatment groups in microarray patient cohort. (Mor = morphine group, oxy = oxycodone group; bup = bupivacaine group)

Time point	Treatment group	N	Mean	SD	Median	25 %	75 %	ANOVA	KW
0 hr	Mor	15	0	0	0	0	0	0.14	0.14
	Oxy	16	0	0	0	0	0		
	Bup	8	0.25	0.71	0.00	0	0		
2 hr	Mor	14	0.57	1.50	0	0	0	0.801	0.89
	Oxy	16	1.06	2.72	0	0	0		
	Bup	8	0.63	1.77	0	0	0		
6 hr	Mor	14	3.36	2.50	3.00	1.00	5.25	0.81	0.87
	Oxy	16	2.94	2.29	2.50	1.10	5.00		
	Bup	8	3.63	3.25	2.50	0.50	7.00		
24 hr	Mor	15	2.57	2.57	0	3.00	4.00	0.88	0.67
	Oxy	16	2.94	2.21	1.00	2.00	4.75		
	Bup	6	3.00	1.55	3.00	1.75	4.25		

Table 9.11: Cumulative opioid doses for morphine and opioid patients of microarray patient cohort.

Subject number	Treatment	Cumulative opioid dose			
		Intraoperative	By 2 hr	By 6 hr	By 24 hr
1	Morphine	12	12	27	47
2	Morphine	20	20	34	44
13	Morphine	10	10	21	30
14	Morphine	10	10	31	81
21	Morphine	15	15	15	59
22	Morphine	12	12	23	44
31	Morphine	15	15	66	111.4
35	Morphine	15	15	41.4	56.4
40	Morphine	10	10	10	12
47	Morphine	10	10	17	32
48	Morphine	15	15	30	62
50	Morphine	10	10	24	56
52	Morphine	18	18	23	43
53	Morphine	0	0	24	29
57	Morphine	16	16	23	25
3	Oxycodone	15	15	33	42
6	Oxycodone	10	10	29.2	42.2
9	Oxycodone	13	20	21	21
15	Oxycodone	10	10	15	73
18	Oxycodone	12	12	17	25
19	Oxycodone	10	10	20	37
23	Oxycodone	20	20	31	37
26	Oxycodone	12	12	23	35
29	Oxycodone	10	10	14	70
30	Oxycodone	10	10	23	76
33	Oxycodone	15	15	20	62
34	Oxycodone	10	10	24	50
44	Oxycodone	10	10	18	30
49	Oxycodone	15	15	30	61
55	Oxycodone	10	10	27	44
56	Oxycodone	9	9	20	68

Table 9.12: Statistical data for differences in cumulative opioid doses between morphine and oxycodone groups, for microarray patient cohort.

	Treatment								
	Morphine				Oxycodone				Statistics
Dose	**N**	**Mean**	**SD**	**SEM**	**N**	**Mean**	**SD**	**SEM**	**Sig. (2-tailed)**
Intra-op	15	12.53	4.72	1.22	16	11.94	2.98	0.74	0.68
By 2 hr	15	12.53	4.72	1.22	16	12.38	3.59	0.90	0.92
By 6 hr	15	27.29	13.19	3.41	16	22.82	5.80	1.45	0.23
By 24 hr	15	48.79	24.46	6.32	16	48.33	17.77	4.44	0.95

Table 9.13: Non-cumulative opioid doses for morphine and opioid patients of microarray patient cohort.

Subject number	Treatment	Non-cumulative opioid doses			
		Intraoperative	By 2 hr	By 6 hr	By 24 hr
1	Morphine	12	0	15	20
2	Morphine	20	0	14	10
13	Morphine	10	0	11	9
14	Morphine	10	0	21	50
21	Morphine	15	0	0	44
22	Morphine	12	0	11	21
31	Morphine	15	0	51	45.4
35	Morphine	15	0	26.4	15
40	Morphine	10	0	0	2
47	Morphine	10	0	7	15
48	Morphine	15	0	15	32
50	Morphine	10	0	14	32
52	Morphine	18	0	5	20
53	Morphine	0	0	24	5
57	Morphine	16	0	7	2
3	Oxycodone	15	0	18	9
6	Oxycodone	10	0	19.2	13
9	Oxycodone	13	7	1	0
15	Oxycodone	10	0	5	58
18	Oxycodone	12	0	5	8
19	Oxycodone	10	0	10	17
23	Oxycodone	20	0	11	6
26	Oxycodone	12	0	11	12
29	Oxycodone	10	0	4	56
30	Oxycodone	10	0	13	53
33	Oxycodone	15	0	5	42
34	Oxycodone	10	0	14	26
44	Oxycodone	10	0	8	12
49	Oxycodone	15	0	15	31
55	Oxycodone	10	0	17	17
56	Oxycodone	9	0	11	48

Table 9.14: Statistical data for differences in non-cumulative opioid doses between morphine and oxycodone groups, for microarray patient cohort.

	Treatment								
	Morphine				Oxycodone				Statistics
Dose	**N**	**Mean**	**SD**	**SEM**	**N**	**Mean**	**SD**	**SEM**	**Sig. (2-tailed)**
Intra-op	15	12.53	4.72	1.22	16	11.94	2.98	0.74	0.68
By 2 hr	15	0	0	0	16	0.44	1.75	0.44	0.34
By 6 hr	15	14.76	12.69	3.28	16	10.45	5.44	1.36	0.22
By 24 hr	15	21.49	15.86	4.09	16	25.50	19.71	4.93	0.54

Appendix B

Table 10.1: RNA quantity and absorbance measured on the Nanodrop 1000 for all subjects, pre-amplification and pre-fragmentation of RNA.

			Pre-amplification		Pre-fragmentation	
Subject	Time-point	Cell type	RNA quantity (ng/µl)	Absorbance (260/280)	RNA quantity (ng/µl)	Absorbance (260/280)
1	0	CD4	79.5	2	1193.97	2.13
1	0	CD8	324.9	1.95		
1	0	NK	72.6	1.99		
1	2	CD4	20.7	1.97	419.70	2.10
1	2	CD8	37.7	1.94		
1	2	NK	241	1.84		
1	6	CD4	16.7	1.85	691.30	2.11
1	6	CD8	11.6	1.96		
1	6	NK	125.6	1.93		
1	24	CD4	132.5	2.04	822.70	2.15
1	24	CD8	78	1.98		
1	24	NK	68.2	1.94		
2	0	CD4	59.4	2.1	795.60	2.15
2	0	CD8	24.7	2.02		
2	0	NK	19.8	2.05		
2	2	CD4	35	2.02	669.70	2.09
2	2	CD8	19.8	1.97		
2	2	NK	10.2	2.23		
2	6	CD4	22.6	1.98	1049.10	2.16
2	6	CD8	5.7	1.7		
2	6	NK	nk	nk		
2	24	CD4	122.9	1.98	876.20	2.15
2	24	CD8	33.4	2		
2	24	NK	3.30	3.94		
3	0	CD4	15.9	1.73	2220.70	2.01
3	0	CD8	43.2	2.08		
3	0	NK	12.9	2.68		
3	2	CD4	6.6	2.04	2262.70	2.00
3	2	CD8	52.3	1.89		
3	2	NK	47.5	1.9		
3	6	CD4	91.2	1.98	2419.80	1.98
3	6	CD8	34.5	1.98		
3	6	NK	52.5	2		

3	24	CD4	234.7	2.06	2768.30	1.94
3	24	CD8	82.6	1.96		
3	24	NK	23.1	2.19		
5	0	CD4	11.2	2.12	247.80	1.74
5	0	CD8	-0.9	1.63		
5	0	NK	-1.5	1.48		
5	2	CD4	2.8	1.55	597.20	2.14
5	2	CD8	-1.48	1.07		
5	2	NK	2.4	1.54		
5	6	CD4	10.1	1.87	273.90	2.03
5	6	CD8	-0.8	1.26		
5	6	NK	-0.3	-0.25		
5	24	CD4	nk		403.40	2.06
5	24	CD8	-0.4	0.68		
5	24	NK	0.2	0.32		
6	0	CD4	63.5	2.06	1707.50	2.08
6	0	CD8	32.6	1.92		
6	0	NK	63.6	16.58		
6	2	CD4	22.9	2.09	977.90	2.11
6	2	CD8	14.1	2.23		
6	2	NK	51.9	5.53		
6	6	CD4	8.9	2.31	1127.50	2.09
6	6	CD8	7	2.18		
6	6	NK	20.7	6.69		
6	24	CD4	150.5	2.08	2331.10	2.00
6	24	CD8	40.4	2.03		
6	24	NK	18.1	11.08		
9	0	CD4	24.4	1.8	1016.44	2.08
9	0	CD8				
9	0	NK				
9	2	CD4	44.76	2.13	2503.93	1.97
9	2	CD8				
9	2	NK				
9	6	CD4	33.85	2.43	2238.35	1.99
9	6	CD8				
9	6	NK				
9	24	CD4	62.62	2.21	1723.40	2.01
9	24	CD8				
9	24	NK				
13	0	CD4	61.17	5.9	1113.20	2.16
13	0	CD8	21.88	2.96		
13	0	NK	20.35	3.13		

13	2	CD4	14.51	6.15	1315.63	2.14
13	2	CD8	15.82	3.15		
13	2	NK	30.09	2.38		
13	6	CD4	21.6	3.12	974.68	2.20
13	6	CD8	34.08	8.72		
13	6	NK	56.24	4.11		
13	24	CD4	39.13	2.5	2156.56	2.10
13	24	CD8	132.8	8.43		
13	24	NK	109.9	8.99		
14	0	CD4	104.34	1.98	1606.30	2.09
14	0	CD8	77.2	2.02		
14	0	NK	19	3.44		
14	2	CD4	82.2	2.21	416.50	1.99
14	2	CD8	516.7	2.89		
14	2	NK				
14	6	CD4	63.1	5.58	563.00	2.12
14	6	CD8	70.6	12.05		
14	6	NK	112.9	8.23		
14	24	CD4	87.5	9.61	394.00	2.02
14	24	CD8	113.5	7.45		
14	24	NK				
15	0	CD4	108.56	8.42	1614.73	2.15
15	0	CD8	32.31	2.16		
15	0	NK	33.07	2.67		
15	2	CD4	49.13	3.11	1901.14	2.10
15	2	CD8	29.18	2.24		
15	2	NK	118.44	5.1		
15	6	CD4	17.35	1.73	1217.81	2.18
15	6	CD8	12.31	1.61		
15	6	NK	1.85	0.44		
15	24	CD4	4.41	1.16	931.53	2.19
15	24	CD8	2.4	1.76		
15	24	NK	21.56	1.67		
18	0	CD4	44.1	1.98	940.80	2.12
18	0	CD8	20	2.11		
18	0	NK	29.4	2.11		
18	2	CD4	14.6	2.25	1139.20	2.10
18	2	CD8	12.3	2.21		
18	2	NK	30.4	2.1		
18	6	CD4	6.2	2.52	1276.80	2.11
18	6	CD8	6.4	1.88		
18	6	NK	14.6	2.05		

18	24	CD4	19.8	2.37	1163.50	2.12
18	24	CD8	25.3	2.22		
18	24	NK	3.1	1.56		
19	0	CD4	32	2.04	1855.30	2.07
19	0	CD8	14.7	2.35		
19	0	NK	24.1	1.98		
19	2	CD4	13.5	2.41	1987.60	2.07
19	2	CD8	29	1.9		
19	2	NK	13.7	2.12		
19	6	CD4	11.8	2.22	1586.00	2.12
19	6	CD8	9	2.56		
19	6	NK	19.7	2.31		
19	24	CD4	38.4	2.11	2441.10	2.02
19	24	CD8	13.1	1.93		
19	24	NK	31.3	2.17		
21	0	CD4	28.2	2.03	1569.80	2.11
21	0	CD8	11.8	2.35		
21	0	NK	13.1	1.46		
21	2	CD4	5.1	2.07	1234.90	2.10
21	2	CD8	2.8	6.45		
21	2	NK	11.6	1.77		
21	6	CD4	6.8	2.85	886.40	2.07
21	6	CD8	13.2	2.61		
21	6	NK	2.2	7.01		
21	24	CD4	26.2	2.05	1174.70	2.09
21	24	CD8	14.2	2.49		
21	24	NK	24.3	2.07		
22	0	CD4	19.8	2.88	1097.40	2.10
22	0	CD8	19.3	2.05		
22	0	NK	16	1.68		
22	2	CD4	3.9	7.15	590.50	2.17
22	2	CD8	18.2	2.25		
22	2	NK	8.9	2.23		
22	6	CD4	-1.3	0.65	965.70	2.12
22	6	CD8	0.8	-2.36		
22	6	NK	4.8	4.61		
22	24	CD4	1.7	-20.8	1024.70	2.12
22	24	CD8	5.6	2.92		
22	24	NK	1.1	-2.14		
23	0	CD4	46.8	1.97	1732.50	2.09
23	0	CD8	8.5	2.12		
23	0	NK	14.7	1.77		

23	2	CD4	19.7	1.86	899.30	2.13
23	2	CD8		2.01		
23	2	NK	9	1.54		
23	6	CD4	13.4	1.9	1851.80	2.08
23	6	CD8	19.8	1.91		
23	6	NK	24.2	1.96		
23	24	CD4	25	1.97	2140.70	2.05
23	24	CD8	31.6	1.75		
23	24	NK	116.3	1.96		
24	0	CD4	17.1	2.23	1040.40	2.15
24	0	CD8	40.1	2.1		
24	0	NK	29.3	2.08		
24	2	CD4	5.4	2.55	1288.60	2.14
24	2	CD8	16.1	2.28		
24	2	NK	4.3	2.59		
24	6	CD4	-0.2	0.23	679.50	2.18
24	6	CD8	2.9	1.78		
24	6	NK	12.2	2.92		
control					3029.90	1.86
24	24	CD8				
24	24	NK				
26	0	CD4	48.4	1.98	516.90	2.10
26	0	CD8	31	1.98		
26	0	NK	0.6	1.12		
26	2	CD4	13.4	1.86	667.60	2.15
26	2	CD8	13.9	7.88		
26	2	NK	8.45	2.22		
26	6	CD4	20.7	1.68	1593.10	2.08
26	6	CD8	22.4	1.95		
26	6	NK	24.6	1.83		
26	24	CD4	28.9	1.81	1948.90	2.06
26	24	CD8	14.1	1.98		
26	24	NK	24.4	1.9		
29	0	CD4	2.27	0.72	517.82	2.42
29	0	CD8	2.28	0.95		
29	0	NK	16.3	1.73		
29	2	CD4	1.93	0.77	628.57	2.27
29	2	CD8	4.21	1.21		
29	2	NK	67.12	1.82		
29	6	CD4	3.42	1.26	335.16	2.22
29	6	CD8	0.11	0.14		
29	6	NK	27.91	1.75		

29	24	CD4	2.16	0.94	224.39	2.31
29	24	CD8	11.94	1.24		
29	24	NK	3.91	1.35		
30	0	CD4	39.4	1.8	2422.50	1.99
30	0	CD8	27.8	2.09		
30	0	NK	0.6	0.27		
30	2	CD4	14.7	1.85	1661.70	2.08
30	2	CD8	25.9	2.38		
30	2	NK	24.2	1.59		
30	6	CD4	20	2.67	2308.20	1.99
30	6	CD8	18.4	2.06		
30	6	NK	29.6	1.84		
30	24	CD4	29.6	1.91	2360.90	1.99
30	24	CD8	12.6	1.99		
30	24	NK	5.8	1.55		
31	0	CD4	150.7	1.94	2092.10	2.04
31	0	CD8	35.2	1.96		
31	0	NK	3.8	1.33		
31	2	CD4	47.5	1.99	1831.00	2.07
31	2	CD8	15	1.75		
31	2	NK	28.3	2.04		
31	6	CD4	79	1.95	2753.90	1.97
31	6	CD8	40.8	1.97		
31	6	NK	33.7	1.91		
31	24	CD4	20.9	1.9	2311.60	2.01
31	24	CD8	60.8	2.04		
31	24	NK	1.4	1.26		
32	0	CD4	18.92	1.68	1584.75	2.18
32	0	CD8	13.71	1.42		
32	0	NK	11.12	1.52		
32	2	CD4	18.94	2.05	1833.04	2.16
32	2	CD8	12.38	1.53		
32	2	NK	7.51	1.43		
32	6	CD4	85.84	1.92	2358.47	2.03
32	6	CD8	15.99	1.64		
32	6	NK	4.92	1.44		
32	24	CD4	110.86	2	2323.62	2.05
32	24	CD8				
32	24	NK	31.78	1.71		
33	0	CD4	56.7	1.97	2613.60	1.93
33	0	CD8	65.2	1.94		
33	0	NK	1.6	0.7		

33	2	CD4	80.3	1.95	2524.30	1.95
33	2	CD8	16.4	1.73		
33	2	NK	18.1	1.66		
33	6	CD4	13.2	1.73	1381.50	2.10
33	6	CD8	16.5	1.71		
33	6	NK	6.7	1.46		
33	24	CD4	116.9	2.72	671.30	2.06
33	24	CD8	70.2	1.99		
33	24	NK	17.5	1.87		
34	0	CD4	46.72	1.98	2247.74	1.94
34	0	CD8	41.2	2.02		
34	0	NK	22.73	2.3		
34	2	CD4	29.62	2.18	1324.83	2.08
34	2	CD8	37.7	1.93		
34	2	NK	16.66	2.08		
34	6	CD4	5.17	2.07	1471.69	2.00
34	6	CD8	8.88	1.86		
34	6	NK	24.16	2.19		
34	24	CD4	52.7	1.94	1931.56	2.03
34	24	CD8	41.92	2.65		
34	24	NK	-2.18	14.75		
35	0	CD4	86.5	2.05	2103.30	2.04
35	0	CD8	37	1.93		
35	0	NK	1.7	1.34		
35	2	CD4	100	3.06	289.00	1.95
35	2	CD8	8.5	1.81		
35	2	NK	25.6	2.14		
35	6	CD4	33.3	1.94	1977.00	2.04
35	6	CD8	6.5	1.64		
35	6	NK	33.9	2.02		
35	24	CD4	43.6	1.96	1668.50	2.07
35	24	CD8	22.1	1.96		
35	24	NK	1.4	1.77		
36	0	CD4	129.7	2.02	2558.80	1.98
36	0	CD8	50.2	2.03		
36	0	NK	2.4	4.04		
36	2	CD4	88.1	2.05	2386.30	2.00
36	2	CD8	75.9	2.06		
36	2	NK	37.7	2.19		
36	6	CD4	101.8	2.09	1387.40	2.02
36	6	CD8	60.9	2.09		
36	6	NK	26.5	2.25		

36	24	CD4	16.1	3.18	1497.20	2.02
36	24	CD8	214.2	2.01		
36	24	NK	40.3	2.03		
38	6	CD4				
38	6	CD8				
38	6	NK				
38	24	CD4				
38	24	CD8				
38	24	NK				
39	0	CD4	49.8	1.99	1689.20	2.09
39	0	CD8	24.5	2		
39	0	NK	11.3	1.66		
39	2	CD4	50.4	1.8	1171.80	2.14
39	2	CD8	44.5	1.88		
39	2	NK	39	1.81		
39	6	CD4	62.5	1.84	1353.60	2.10
39	6	CD8	29.9	1.93		
39	6	NK	1.6	0.91		
39	24	CD4	40	1.97	2267.20	2.08
39	24	CD8	30.6	1.84		
39	24	NK	35.5	1.72		
40	0	CD4	73.73	2.1	1841.37	1.92
40	0	CD8	75.29	1.95		
40	0	NK	2.84	1.27		
40	2	CD4	40.1	1.96	1962.94	1.99
40	2	CD8	93.09	1.91		
40	2	NK	79.79	1.73		
40	6	CD4	17.29	1.81	2017.23	1.98
40	6	CD8	21.36	1.82		
40	6	NK	5.32	1.38		
40	24	CD4	23.03	1.98	2182.53	1.95
40	24	CD8	24.47	2.16		
40	24	NK	3.58	1.2		
41	0	CD4	52.25	2.1	1163.60	1.99
41	0	CD8	29.97	1.85		
41	0	NK	11.07	1.49		
41	2	CD4	11.25	1.74	2140.82	1.95
41	2	CD8	11	1.61		
41	2	NK	493.93	2.11		
41	6	CD4	12.17	1.81	2959.71	1.90
41	6	CD8	12.12	1.87		
41	6	NK	96.48	1.99		

41	24	CD4				
41	24	CD8				
41	24	NK				
43	0	CD4				
43	0	CD8				
43	0	NK				
43	2	CD4				
43	2	CD8				
43	2	NK				
43	6	CD4				
43	6	CD8				
43	6	NK				
43	24	CD4				
43	24	CD8				
43	24	NK				
44	0	CD4	4.7	2.63		
44	0	CD8	-94.1	2.1	2261.90	1.97
44	0	NK	-7.2	2.94		
44	2	CD4	2.7	2.03		
44	2	CD8	0.5	-1.21	227.00	1.97
44	2	NK	0.8	-1.48		
44	6	CD4	-0.5	1.22		
44	6	CD8	1.1	5.25	970.90	2.13
44	6	NK	0.9	-3.68		
44	24	CD4	34.1	1.94		
44	24	CD8	7.5	1.65	1409.70	2.11
44	24	NK	2.7	1.18		
45	0	CD4	38.2	2.02		
45	0	CD8	4.1	1.52	2060.30	2.01
45	0	NK	3.5	1.43		
45	2	CD4	29.8	1.98		
45	2	CD8	16.3	1.69	1526.50	2.04
45	2	NK	36.1	1.8		
45	6	CD4	10.5	2.19		
45	6	CD8	10.1	1.64	1307.10	2.02
45	6	NK	2.2	1.09		
45	24	CD4	20.1	1.74		
45	24	CD8	15.5	1.64	1981.40	2.00
45	24	NK	3.3	1.18		
46	0	CD4	14.8	1.09		
46	0	CD8	13.7	1.1	1586.30	2.05
46	0	NK	21.4	1.03		

46	2	CD4	8	0.93	1272.60	2.09
46	2	CD8	9.3	0.93		
46	2	NK	2	0.65		
46	6	CD4	1.1	0.25	971.70	2.10
46	6	CD8	2.2	0.3		
46	6	NK	-0.12	-0.05		
46	24	CD4	20	1.35	1779.80	2.05
46	24	CD8	17.3	1.19		
46	24	NK	7.5	0.97		
47	0	CD4	104.56	2.18	2433.67	1.95
47	0	CD8	33.62	1.71		
47	0	NK	17.85	1.55		
47	2	CD4	32.41	1.78	2043.63	1.97
47	2	CD8	19.68	1.67		
47	2	NK	17.94	2.15		
47	6	CD4	2.92	1.26	1548.52	2.01
47	6	CD8	4.04	2.03		
47	6	NK	2.13	7.59		
47	24	CD4	44	1.92	1945.57	1.97
47	24	CD8	23.58	1.8		
47	24	NK	-0.11	-0.15		
48	0		113.4	1.99	2532.50	1.97
48	0		62.1	2.06		
48	0		10.4	1.51		
48	2	CD4	19.2	1.84	475.80	2.03
48	2	CD8	24	1.7		
48	2	NK	14.6	1.48		
48	6	CD4	7.9	1.21	351.30	2.01
48	6	CD8	7	1.43		
48	6	NK	9.1	1.15		
48	24	CD4	19	1.65	1454.30	2.09
48	24	CD8	45.4	1.9		
48	24	NK	4.3	1		
49	0	CD4	60.6	1.96	1509.10	2.05
49	0	CD8	36.6	1.83		
49	0	NK	18.1	1.72		
49	2	CD4	30.5	1.88	1573.50	2.06
49	2	CD8	30	1.85		
49	2	NK	24.3	1.78		
49	6	CD4	3.2	1.35	1138.10	2.11
49	6	CD8	4.4	1.79		
49	6	NK	14	1.73		

49	24	CD4	4.5	0.7	753.60	2.12
49	24	CD8	51.8	1.91		
49	24	NK	11.5	1.4		
50	0	CD4	43.7	1.93	982.40	2.10
50	0	CD8	28.2	1.89		
50	0	NK	14.8	1.75		
50	2	CD4	45.8	1.86	1395.30	2.09
50	2	CD8	37.1	1.93		
50	2	NK	19.9	1.84		
50	6	CD4	17.2	1.68	1405.60	2.11
50	6	CD8	9.5	1.49		
50	6	NK	17.2	1.62		
50	24	CD4	13.2	1.81	1483.34	2.07
50	24	CD8	16.8	2		
50	24	NK	3.4	1.38		
52	0	CD4	52.23	1.95	2337.02	2.06
52	0	CD8	22.4	1.77		
52	0	NK	6.75	1.51		
52	2	CD4	8.16	1.75	1694.02	2.15
52	2	CD8	10.47	1.79		
52	2	NK	25.33	1.61		
52	6	CD4	5.54	1.46	888.28	2.27
52	6	CD8	8.25	1.39		
52	6	NK	3.43	1.5		
52	24	CD4	19.9	2	1543.48	2.24
52	24	CD8	24.16	1.81		
52	24	NK	22.37	1.52		
53	0	CD4	25.9	1.46	1761.23	2.19
53	0	CD8	17.11	1.47		
53	0	NK	5.99	14.1		
53	2	CD4	11.59	0.94	1947.53	2.15
53	2	CD8	13.3	1.41		
53	2	NK	7.11	1.96		
53	6	CD4	5.67	1.42	1479.49	2.23
53	6	CD8	4.87	4.37		
53	6	NK	1.8	20.43		
53	24	CD4	6.97	2.04	1018.77	2.43
53	24	CD8	2.63	1.6		
53	24	NK				
54	0	CD4	20.31	1.85	1289.85	2.31
54	0	CD8	3.88	0.67		
54	0	NK	1.63	1.14		

54	2	CD4	16.82	2.28	1764.23	2.16
54	2	CD8	6.14	1.63		
54	2	NK	17.06	1.85		
54	6	CD4	4.44	0.87	2017.17	2.15
54	6	CD8	8.14	1.95		
54	6	NK	22.13	1.94		
55	0	CD4	21.2	1.81	1886.72	2.14
55	0	CD8	22.7	1.58		
55	0	NK	16.3	2.72		
55	2	CD4	12.09	1.15	1504.10	2.23
55	2	CD8	1.89	0.49		
55	2	NK	28.76	1.92		
55	6	CD4	8.58	1.52	1104.75	2.30
55	6	CD8	2.23	3.09		
55	6	NK	15.28	1.61		
55	24	CD4	21.83	1.86	462.41	2.00
55	24	CD8	13.13	1.78		
55	24	NK	2.77	0.81		
56	0	CD4	8.96	-3.85	1480.92	2.20
56	0	CD8	21.88	1.88		
56	0	NK	5.1	1.09		
56	2	CD4	19.37	1.96	1462.90	2.21
56	2	CD8	11.07	1.62		
56	2	NK	8.94	1.24		
56	6	CD4	24.06	1.7	2176.21	2.13
56	6	CD8	26.15	1.74		
56	6	NK	3.58	1.13		
56	24	CD4	25.02	2.35	1847.29	2.17
56	24	CD8	24.75	1.67		
56	24	NK	7.34	0.83		
57	0	CD4	15.2	1.09	1579.80	2.04
57	0	CD8	4.7	0.74		
57	0	NK	3.12	0.42		
57	2	CD4	-0.1	-0.02	1164.10	2.06
57	2	CD8	9.3	0.91		
57	2	NK	10.2	0.97		
57	6	CD4	2.7	0.76	647.80	2.00
57	6	CD8	-0.8	0.23		
57	6	NK	0.6	0.12		

Table 10.2: RNA integrity numbers for microarray patient cohort measured on Agilent Bioanalyzer pre-amplification of combined cell sub-types.

Subject	Treatment	0 hr	2 hr	6 hr	24 hr
1	Morphine	3.8	3.1	3	4.6
2	Morphine	7.6	6.3	7.3	6.8
3	Oxycodone	8	7.5	6.6	8.2
6	Oxycodone	5.3	2.7	2.8	9.4
9	Oxycodone	7.2	7.8	6.6	5.9
13	Morphine	5.8	3.8	6.3	2.7
14	Morphine	4.3	2.7	6	4
15	Oxycodone	N/A	2.8	5.6	2.6
18	Oxycodone	4.7	2.5	2.3	4
19	Oxycodone	6.9	5.5	7.2	6.7
21	Morphine	5.8	5.7	N/A	5.4
22	Morphine	4.4	2.1	2.7	N/A
23	Oxycodone	2.5	5.5	4.5	3.9
24	Epidural	5.9	6.4	N/A	N/A
26	Oxycodone	8.9	2.4	5.3	8.7
29	Oxycodone	1.1	2.3	2.2	1.1
30	Oxycodone	8.3	2.7	2.6	5.8
31	Morphine	5.9	8.8	6.3	N/A
32	Epidural	6.8	6.3	5.3	7.2
33	Oxycodone	8.5	N/A	3.2	5.9
34	Oxycodone	3.7	2.6	2.3	7.6
35	Morphine	9.2	5.7	6.7	9.4
36	Epidural	3.5	5.4	4	6
39	Epidural	3.7	3.8	2.9	2.9
40	Morphine	2.5	2.6	2.8	4.2
41	Epidural	3.5	2.7	3.8	N/A
44	Oxycodone	8.7	1.3	N/A	5.1
45	Morphine	8.8	5.2	3.8	5.3
46	Epidural	2.8	2.3	N/A	2.2
47	Morphine	4.4	6.7	1.2	5.6
48	Morphine	7.2	4.1	N/A	N/A
49	Oxycodone	2.3	3	3.2	2.9
50	Morphine	2.6	2.5	2.6	7
51	Epidural	2.2	N/A	2.4	2.5
52	Morphine	8.7	7.2	N/A	2.8
53	Morphine	4.2	5.4	2.6	3
54	Epidural	6.5	5.4	2.6	N/A
55	Oxycodone	2.7	3	N/A	N/A
56	Oxycodone	1.8	2.1	5.1	3.5
57	Morphine	1.6	2.7	N/A	N/A

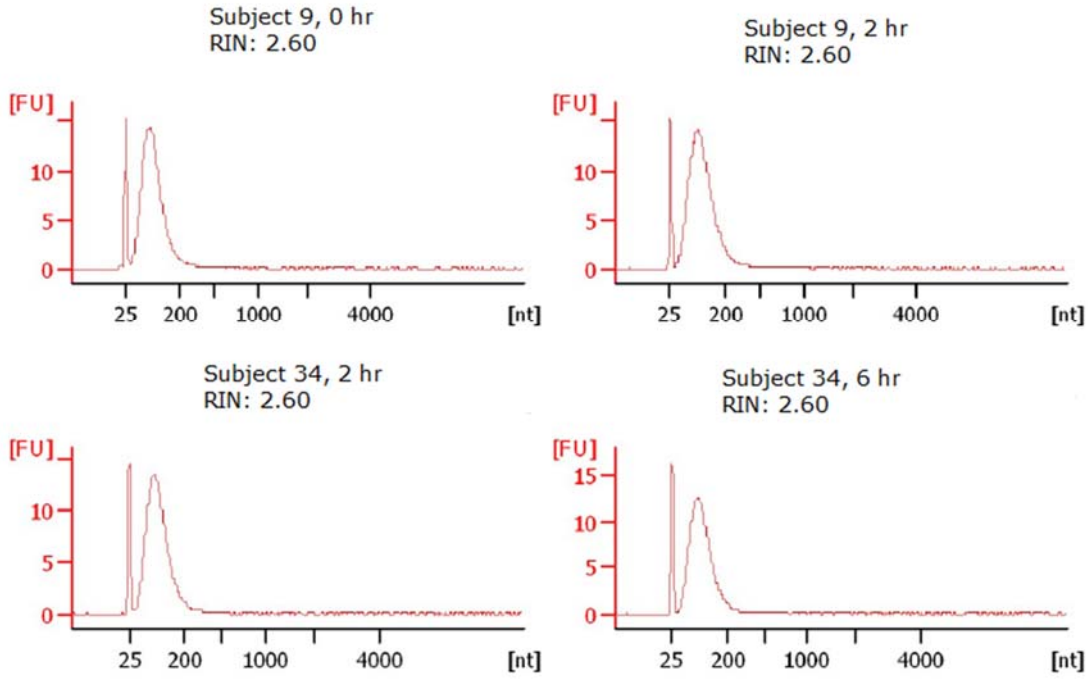

Figure 10.1: Spectrophotograms of fragmented RNA. RNA was analysed on the Bioanalyzer to determine that fragmentation had occurred, which was confirmed by the distinctive shape of the spectrophotogram.

Table 10.3: Statistical data for differences in RIN for all treatment groups at each timepoint, for microarray patient cohort only.

Time-point	Treatment group	N	Mean	SD	Median	25 %	75 %	ANOVA	KW
0 hr	Mor	16	5.42	2.35	5.10	3.90	7.43	0.64	0.56
	Oxy	15	5.37	2.85	5.30	2.50	8.30		
	Bup	8	4.36	1.77	3.60	2.98	6.35		
2 hr	Mor	16	4.66	2.00	4.65	2.70	6.15	0.23	0.21
	Oxy	15	3.58	1.20	2.70	2.40	5.50		
	Bup	7	4.61	1.68	5.40	2.70	6.30		
6 hr	Mor	12	4.28	2.08	3.40	2.63	6.30	0.55	0.66
	Oxy	14	4.25	1.80	3.85	2.53	5.85		
	Bup	6	3.50	1.09	3.35	2.55	4.33		
24 hr	Mor	12	5.07	1.98	4.95	3.25	6.50	0.54	0.56
	Oxy	15	5.42	2.43	5.80	3.50	7.60		
	Bup	5	4.16	2.28	2.90	2.35	6.60		

Table 10.4: Statistical data for differences in RIN between all timepoints for each treatment group, for microarray patient cohort only.

Treatment group	Time-point	N	Mean	SD	Med-ian	25 %	75 %	ANOVA	KW
Mor	0 hr	16	5.43	2.36	5.10	3.90	7.50	0.08	0.17
	2 hr	16	4.66	2.00	4.65	2.70	6.15		
	6 hr	16	3.21	2.62	2.75	0.30	6.23		
	24 hr	15	4.05	2.73	4.20	2.70	5.60		
Oxy	0 hr	16	5.04	3.06	5.00	2.35	8.22	0.13	0.14
	2 hr	16	3.36	2.13	2.70	2.33	4.88		
	6 hr	16	3.72	2.22	3.20	2.30	5.53		
	24 hr	16	5.08	2.71	5.45	3.05	7.38		
Bup	0 hr	8	4.36	1.77	3.60	2.98	6.35	0.34	0.49
	2 hr	8	4.04	2.25	4.60	2.40	6.08		
	6 hr	8	2.63	1.86	2.75	0.60	4.33		
	24 hr	5	4.16	2.28	2.90	2.35	6.60		

Table 10.5: Biological pathways enriched in genes deregulated by morphine at 2 hour (Mor0-2: 520 genes / 576 probes), identified using DAVID ontological software (p≤0.01).

Biological processes	Genes	% of total input	p value
translation	28	5.7	7.80E-07
ribonucleoprotein complex biogenesis	18	3.6	1.40E-05
regulation of apoptosis	45	9.1	1.90E-05
regulation of programmed cell death	45	9.1	2.40E-05
regulation of cell death	45	9.1	2.60E-05
RNA processing	32	6.5	1.80E-04
cellular macromolecular complex assembly	22	4.4	2.80E-04
cellular macromolecular complex subunit organization	23	4.6	5.10E-04
positive regulation of apoptosis	26	5.3	5.20E-04
positive regulation of programmed cell death	26	5.3	5.80E-04
positive regulation of cell death	26	5.3	6.30E-04
mRNA metabolic process	23	4.6	8.40E-04
apoptosis	32	6.5	9.30E-04
programmed cell death	32	6.5	1.20E-03
cell death	36	7.3	1.20E-03
death	36	7.3	1.30E-03
RNA splicing, via transesterification reactions with bulged adenosine as nucleophile	13	2.6	1.30E-03
RNA splicing, via transesterification reactions	13	2.6	1.30E-03
nuclear mRNA splicing, via spliceosome	13	2.6	1.30E-03
electron transport chain	11	2.2	1.40E-03
cellular respiration	10	2	1.70E-03
induction of apoptosis	20	4	1.90E-03
induction of programmed cell death	20	4	2.00E-03
ncRNA metabolic process	16	3.2	2.30E-03
macromolecular complex assembly	33	6.7	2.30E-03
regulation of T cell receptor signaling pathway	4	0.8	2.30E-03
ribosome biogenesis	11	2.2	2.40E-03
regulation of leukocyte activation	13	2.6	2.70E-03
positive regulation of leukocyte activation	10	2	3.10E-03
positive regulation of immune system process	16	3.2	3.20E-03
regulation of lymphocyte activation	12	2.4	3.20E-03
macromolecular complex subunit organization	34	6.9	3.40E-03
generation of precursor metabolites and energy	19	3.8	3.50E-03
activation of caspase activity	7	1.4	4.00E-03
regulation of antigen receptor-mediated signaling pathway	4	0.8	4.10E-03
regulation of cell activation	13	2.6	4.10E-03
positive regulation of cell activation	10	2	4.20E-03
positive regulation of T cell activation	8	1.6	5.60E-03
negative regulation of apoptosis	20	4	5.70E-03

mitochondrion organization	11	2.2	5.80E-03
regulation of T cell activation	10	2	5.90E-03
positive regulation of lymphocyte activation	9	1.8	6.10E-03
positive regulation of peptidase activity	7	1.4	6.20E-03
positive regulation of caspase activity	7	1.4	6.20E-03
negative regulation of programmed cell death	20	4	6.60E-03
negative regulation of cell death	20	4	6.80E-03
positive regulation of catalytic activity	26	5.3	6.80E-03
ncRNA processing	13	2.6	6.90E-03
spliceosomal snRNP biogenesis	5	1	7.50E-03
energy derivation by oxidation of organic compounds	11	2.2	7.70E-03
cellular macromolecule catabolic process	33	6.7	8.40E-03
mitotic cell cycle	20	4	9.00E-03
respiratory electron transport chain	7	1.4	9.20E-03
positive regulation of adaptive immune response based on somatic recombination of immune receptors built from immunoglobulin superfamily domains	5	1	9.60E-03
mRNA processing	18	3.6	9.90E-03
interphase	9	1.8	1.00E-02

Table 10.6: Biological pathways enriched in genes deregulated by morphine at 6 hour (Mor0-6: 113 genes / 149 probes), identified using DAVID ontological software (p≤0.01).

GOTERM_BP_FAT

Biological processes	Genes	% of total input	p value
response to wounding	21	19.6	2.00E-10
response to organic substance	19	17.8	9.90E-07
inflammatory response	13	12.1	1.50E-06
defense response	17	15.9	2.60E-06
innate immune response	9	8.4	3.70E-06
negative regulation of cytokine production	6	5.6	4.90E-06
immune response	7	6.5	1.20E-05
response to lipopolysaccharide	17	15.9	1.10E-05
response to molecule of bacterial origin	7	6.5	2.20E-05
response to insulin stimulus	7	6.5	5.30E-05
organic acid biosynthetic process	8	7.5	7.60E-05
carboxylic acid biosynthetic process	8	7.5	7.60E-05
positive regulation of developmental process	10	9.3	9.50E-05
positive regulation of molecular function	14	13.1	1.30E-04
fatty acid biosynthetic process	9	8.4	1.80E-04
positive regulation of immune system process	8	7.5	2.00E-04
regulation of cytokine production	6	5.6	1.80E-04
regulation of phosphorylation	12	11.2	2.60E-04
response to endogenous stimulus	12	11.2	3.60E-04
regulation of phosphate metabolic process	12	11.2	3.60E-04
regulation of phosphorus metabolic process	11	10.3	3.50E-04
response to peptide hormone stimulus	7	6.5	5.60E-04
positive regulation of fat cell differentiation	12	11.2	6.50E-04
positive regulation of catalytic activity	15	14	8.10E-04
response to hormone stimulus	3	2.8	6.50E-04
negative regulation of multicellular organismal process	15	14	9.00E-04
protein kinase cascade	15	14	9.30E-04
regulation of transferase activity	8	7.5	8.70E-04
regulation of apoptosis	10	9.3	8.10E-04
positive regulation of kinase activity	10	9.3	7.80E-04
regulation of programmed cell death	8	7.5	9.80E-04
regulation of cell death	10	9.3	7.40E-04
positive regulation of response to stimulus	7	6.5	7.80E-04
positive regulation of transferase activity	7	6.5	1.10E-03
regulation of cell activation	8	7.5	1.10E-03
lipid biosynthetic process	9	8.4	1.40E-03
response to steroid hormone stimulus	7	6.5	1.80E-03
response to bacterium	7	6.5	1.80E-03
response to cytokine stimulus	5	4.7	1.90E-03
fatty acid metabolic process	7	6.5	2.00E-03
activation of MAPK activity	5	4.7	2.20E-03

negative regulation of immune system process	5	4.7	2.30E-03
regulation of MAP kinase activity	7	6.5	2.50E-03
anti-apoptosis	9	8.4	2.60E-03
regulation of kinase activity	6	5.6	2.50E-03
positive regulation of immune response	6	5.6	2.80E-03
membrane invagination	7	6.5	3.50E-03
endocytosis	7	6.5	3.50E-03
positive regulation of protein kinase activity	7	6.5	3.70E-03
phagocytosis	4	3.7	4.00E-03
acute inflammatory response	5	4.7	4.10E-03
positive regulation of cell differentiation	7	6.5	4.20E-03
positive regulation of MAP kinase activity	5	4.7	4.70E-03
regulation of fat cell differentiation	6	5.6	5.00E-03
regulation of leukocyte activation	3	2.8	4.90E-03
fat cell differentiation	4	3.7	5.20E-03
regulation of interleukin-12 production	3	2.8	5.60E-03
positive regulation of multicellular organismal process	7	6.5	5.70E-03
regulation of protein amino acid phosphorylation	6	5.6	5.90E-03
positive regulation of cell activation	5	4.7	6.40E-03
leukotriene biosynthetic process	3	2.8	7.00E-03
alkene biosynthetic process	3	2.8	7.00E-03
sulfur metabolic process	5	4.7	7.20E-03
MAPKKK cascade	6	5.6	7.60E-03
regulation of protein kinase activity	8	7.5	8.10E-03
positive regulation of response to external stimulus	4	3.7	8.90E-03
negative regulation of apoptosis	3	2.8	9.30E-03
leukotriene metabolic process	8	7.5	9.20E-03
negative regulation of programmed cell death	8	7.5	1.00E-02
negative regulation of cell death	3	2.8	1.00E-02
response to nutrient levels	6	5.6	1.00E-02
cellular alkene metabolic process	8	7.5	1.00E-02
negative regulation of cell proliferation	8	7.5	9.90E-03

Table 10.7: Biological pathways enriched in genes deregulated by oxycodone at 6 hour (Oxy0-6: 559 genes / 810 probes), identified using DAVID ontological software (p≤0.01).

Biological processes	Genes	% of total input	p value
response to wounding	53	11	1.60E-15
defense response	54	11.2	1.80E-13
inflammatory response	37	7.6	1.50E-12
immune response	48	9.9	1.30E-08
innate immune response	18	3.7	3.00E-07
positive regulation of immune system process	23	4.8	9.00E-07
protein kinase cascade	28	5.8	5.40E-06
positive regulation of cytokine production	13	2.7	7.30E-06
negative regulation of cytokine production	9	1.9	8.10E-06
regulation of cytokine production	18	3.7	1.30E-05
positive regulation of multicellular organismal process	21	4.3	1.70E-05
regulation of programmed cell death	45	9.3	1.80E-05
regulation of cell death	45	9.3	2.00E-05
response to molecule of bacterial origin	12	2.5	2.60E-05
response to bacterium	18	3.7	3.00E-05
regulation of apoptosis	44	9.1	3.10E-05
positive regulation of response to stimulus	20	4.1	3.60E-05
response to lipopolysaccharide	11	2.3	5.30E-05
positive regulation of immune response	15	3.1	5.50E-05
response to organic substance	40	8.3	5.80E-05
detection of biotic stimulus	6	1.2	1.10E-04
anti-apoptosis	17	3.5	2.20E-04
positive regulation of cell activation	12	2.5	2.70E-04
adaptive immune response based on somatic recombination of immune receptors built from immunoglobulin superfamily domains	10	2.1	2.80E-04
adaptive immune response	10	2.1	2.80E-04
immune effector process	13	2.7	3.70E-04
regulation of T-helper 2 cell differentiation	4	0.8	4.10E-04
leukocyte mediated immunity	10	2.1	6.50E-04
JAK-STAT cascade	7	1.4	6.80E-04
regulation of adaptive immune response based on somatic recombination of immune receptors built from immunoglobulin superfamily domains	8	1.7	8.00E-04
regulation of adaptive immune response	8	1.7	9.00E-04
intracellular signalling cascade	55	11.4	9.00E-04
positive regulation of defense response	9	1.9	9.50E-04
negative regulation of apoptosis	22	4.5	9.90E-04
membrane organization	23	4.8	1.10E-03
negative regulation of programmed cell death	22	4.5	1.20E-03
negative regulation of cell death	22	4.5	1.20E-03
activation of immune response	10	2.1	1.20E-03

regulation of cell activation	14	2.9	1.30E-03
regulation of interferon-gamma production	6	1.2	1.30E-03
regulation of erythrocyte differentiation	5	1	1.30E-03
regulation of tumor necrosis factor production	6	1.2	1.50E-03
response to cytokine stimulus	9	1.9	1.60E-03
acute inflammatory response	10	2.1	1.70E-03
positive regulation of cell motion	10	2.1	1.70E-03
positive regulation of T cell differentiation	6	1.2	1.80E-03
regulation of lymphocyte differentiation	8	1.7	1.80E-03
negative regulation of multicellular organismal process	13	2.7	2.20E-03
regulation of T-helper cell differentiation	4	0.8	2.20E-03
regulation of T-helper 2 type immune response	4	0.8	2.20E-03
positive regulation of lymphocyte differentiation	6	1.2	2.70E-03
regulation of T cell differentiation	7	1.4	2.80E-03
positive regulation of leukocyte activation	10	2.1	2.90E-03
hexose metabolic process	14	2.9	2.90E-03
response to steroid hormone stimulus	14	2.9	2.90E-03
cell activation	18	3.7	3.00E-03
regulation of cell motion	14	2.9	3.10E-03
cell activation during immune response	6	1.2	3.10E-03
leukocyte activation during immune response	6	1.2	3.10E-03
regulation of myeloid cell differentiation	8	1.7	3.30E-03
lymphocyte mediated immunity	8	1.7	3.30E-03
leukocyte activation	16	3.3	3.40E-03
immunoglobulin mediated immune response	7	1.4	3.80E-03
neuron projection regeneration	4	0.8	3.90E-03
defense response to bacterium	10	2.1	4.10E-03
fructose 2,6-bisphosphate metabolic process	3	0.6	4.50E-03
JAK-STAT cascade involved in growth hormone signalling pathway	3	0.6	4.50E-03
B cell mediated immunity	7	1.4	4.60E-03
negative regulation of transport	11	2.3	4.60E-03
regulation of alpha-beta T cell differentiation	5	1	4.80E-03
positive regulation of programmed cell death	23	4.8	5.10E-03
positive regulation of cell death	23	4.8	5.50E-03
positive regulation of lymphocyte activation	9	1.9	5.70E-03
positive regulation of interleukin-1 beta production	4	0.8	6.30E-03
regulation of leukocyte activation	12	2.5	7.00E-03
negative regulation of CD4-positive, alpha beta T cell differentiation	3	0.6	7.40E-03
negative regulation of T-helper cell differentiation	3	0.6	7.40E-03
detection of molecule of bacterial origin	3	0.6	7.40E-03
regulation of germinal center formation	3	0.6	7.40E-03
negative regulation of interleukin-12 production	3	0.6	7.40E-03
positive regulation of molecular function	28	5.8	7.60E-03
regulation of interleukin-8 production	4	0.8	7.70E-03

macrophage activation	4	0.8	7.70E-03
regulation of CD4-positive, alpha beta T cell differentiation	4	0.8	7.70E-03
enzyme linked receptor protein signalling pathway	19	3.9	7.80E-03
regulation of cell migration	12	2.5	7.90E-03
activation of MAPK activity	8	1.7	7.90E-03
I-kappaB kinase/NF-kappaB cascade	7	1.4	8.10E-03
negative regulation of immune system process	8	1.7	8.50E-03
regulation of lymphocyte activation	11	2.3	8.70E-03
positive regulation of response to external stimulus	7	1.4	8.80E-03
myeloid leukocyte activation	6	1.2	8.90E-03
cytokine production	6	1.2	8.90E-03
positive regulation of innate immune response	6	1.2	8.90E-03
endocytosis	14	2.9	9.00E-03
membrane invagination	14	2.9	9.00E-03
response to vitamin D	4	0.8	9.20E-03
positive regulation of inflammatory response	5	1	9.30E-03
positive regulation of apoptosis	22	4.5	9.50E-03
lipid biosynthetic process	18	3.7	9.50E-03
regulation of phosphate metabolic process	24	5	9.60E-03
regulation of phosphorus metabolic process	24	5	9.60E-03
monosaccharide metabolic process	14	2.9	9.70E-03
icosanoid metabolic process	6	1.2	9.70E-03

Table 10.8: Biological pathways enriched in genes deregulated by bupivacaine at 6 hour (Bup0-6: 44 genes / 49 probes), identified using DAVID ontological software (p≤0.01).

Biological processes	**Genes**	**% of total input**	**p value**
enzyme linked receptor protein signaling pathway	5	12.8	5.10E-03
positive regulation of cell proliferation	5	12.8	9.90E-03
negative regulation of signal transduction	4	10.3	1.00E-02

Table 10.9: Pre- and post-surgical serum cortisol concentrations for all patient samples used for cortisol ELISA.

	Cortisol concentration (ng/ml)		
Subject	**0 hr**	**6 hr**	**Treatment**
13	29.58	106.19	Morphine
14	27.65	30.43	Morphine
22	35.49	128.05	Morphine
31	28.75	30.63	Morphine
35	45.44	29.90	Morphine
40	27.12	17.38	Morphine
43	26.62	19.77	Morphine
47	77.76	349.24	Morphine
50	92.51	372.39	Morphine
52	48.16	55.58	Morphine
57	77.21	20.63	Morphine
19	57.69	28.88	Oxycodone
23	21.22	40.71	Oxycodone
26	79.44	53.24	Oxycodone
29	32.51	61.84	Oxycodone
30	33.17	185.63	Oxycodone
33	78.06	27.54	Oxycodone
34	6.93	8.30	Oxycodone
44	53.10	17.60	Oxycodone
49	53.79	92.00	Oxycodone
56	39.53	36.23	Oxycodone
5	3.78	4.47	Oxycodone
24	27.48	27.30	Bupivacaine
25	14.11	112.66	Bupivacaine
32	31.87	182.90	Bupivacaine
38	91.24	21.73	Bupivacaine
39	46.83	25.11	Bupivacaine
41	48.16	320.28	Bupivacaine
45	56.25	80.85	Bupivacaine
51	89.76	22.83	Bupivacaine
54	44.29	830.07	Bupivacaine

Table 10.10: Statistical data for differences in serum cortisol concentration between timepoints and treatment groups.

	0 hr				6 hr				
Treatment	**N**	**Mean**	**SD**	**SEM**	**N**	**Mean**	**SD**	**SEM**	**Sig. (2-tailed)**
Mor	11	46.94	24.26	7.32	11	105.47	131.50	39.65	0.12
Oxy	11	41.75	25.51	7.69	11	50.58	51.37	15.49	0.61
Bup	9	50.00	26.20	8.72	9	180.42	263.08	87.69	0.19
All	**ANOVA**				**ANOVA**				
	0.76				0.23				
	Levene's test				**Levene's test**				
Mor v oxy	0.86				0.03				
Mor v bup	0.97				0.22				
Oxy v bup	0.86				0.02				

Table 10.11: Serum IL-2 concentration measured using cytometric bead array (CBA). Data is given for each treatment group at each timepoint and paired per subject. Shaded cells indicate values below theoretical level of significance.

	Morphine		**Oxycodone**		**Bupivacaine**	
	0 hr	**6 hr**	**0 hr**	**6 hr**	**0 hr**	**6 hr**
	0	0	0.16	0.08	0	0.60
	0	0	0.51	0.06	0	0
	0.03	0.11	0.21	0.18	0	0.03
	0.03	0.24	0.24	0.26	0	0
	0.06	0.06	0.03	0.26	0.11	0.11
	0	0.08			0.46	0.24
	0.11	0.11			0.16	0.06
	0.26	0.03				
Mean	0.06	0.08	0.23	0.17	0.10	0.15
StDev	0.08	0.07	0.16	0.09	0.16	0.20

Table 10.12: Serum IL-4 concentration measured using cytometric bead array (CBA). Data is given for each treatment group at each timepoint and paired per subject. Shaded cells indicate values below theoretical level of significance.

	Morphine		Oxycodone		Bupivacaine	
	0 hr	**6 hr**	**0 hr**	**6 hr**	**0 hr**	**6 hr**
	0.15	0	0.31	0.5	0	0
	0	0	0.47	0.04	0	0
	0.01	0.23	0.31	0.26	0.18	0
	0.04	0.15	0.2	0.04	0.34	0
	0.23	0.31	0.12	0.2	0.18	0.31
	0.42	0.04			0.36	0.15
	0.12	0.45			0.36	0.42
	0.28	0.23				
Mean	0.16	0.18	0.28	0.21	0.20	0.13
StDev	0.14	0.15	0.12	0.17	0.15	0.16

Table 10.13: Serum IL-6 concentration measured using cytometric bead array (CBA). Data is given for each treatment group at each timepoint and paired per subject. Shaded cells indicate values below theoretical level of significance.

	Morphine		Oxycodone		Bupivacaine	
	0 hr	**6 hr**	**0 hr**	**6 hr**	**0 hr**	**6 hr**
	0.3	95.2	1.51	25.15	1.63	22.62
	1.57	33.61	0.33	0.11	1.36	12.67
	0.43	16.5	1.78	14.96	0.93	12.52
	2.92	30.03	2.11	32.93	3.21	50.21
	1.06	16.26	0.39	23.64	5.1	26.57
	1.63	89.6			1.1	8.75
	0.73	18.79			0.81	27.88
	0.2	123.31				
Mean	1.11	52.91	1.22	19.36	2.02	23.03
StDev	0.86	40.03	0.73	11.19	1.46	13.08

Table 10.14: Serum IL-10 concentration measured using cytometric bead array (CBA). Data is given for each treatment group at each timepoint and paired per subject. Shaded cells indicate values below theoretical level of significance.

	Morphine		Oxycodone		Bupivacaine	
	0 hr	**6 hr**	**0 hr**	**6 hr**	**0 hr**	**6 hr**
	2.10	22.45	1.32	13.62	1.26	5.54
	0.83	6.52	0.51	0.24	1.01	5.41
	0.57	16.36	0.98	30.97	0.67	5.44
	0.79	13.87	1.38	15.42	1.35	13.69
	0.92	8.42	0.61	1.62	1.32	31.9
	0.83	27.7			0.44	1.44
	1.65	7.62			0.86	3.59
	0.06	13.72				
Mean	0.97	14.58	0.96	12.37	0.99	9.57
StDev	0.59	6.98	0.36	11.13	0.32	9.77

Table 10.15: Serum IL-17a concentration measured using cytometric bead array (CBA). Data is given for each treatment group at each timepoint and paired per subject. Shaded cells indicate values below theoretical level of significance.

	Morphine		Oxycodone		Bupivacaine	
	0 hr	**6 hr**	**0 hr**	**6 hr**	**0 hr**	**6 hr**
	9.06	10.75	12.85	10.75	20.54	8.22
	9.90	12.01	45.47	19.68	11.59	10.32
	7.38	15.82	13.28	14.55	12.85	10.32
	10.75	12.01	16.25	12.01	15.4	17.10
	14.97	12.43	9.06	12.85	10.75	12.85
	9.90	14.12			13.28	9.06
	13.70	13.28			12.01	10.32
	18.39	13.70				
Mean	11.76	13.02	19.38	13.97	13.77	11.17
StDev	3.40	1.46	13.24	3.11	3.08	2.76

Table 10.16: Serum IFN-γ concentration measured using cytometric bead array (CBA). Data is given for each treatment group at each timepoint and paired per subject. Shaded cells indicate values below theoretical level of significance.

	Morphine		Oxycodone		Bupivacaine	
	0 hr	**6 hr**	**0 hr**	**6 hr**	**0 hr**	**6 hr**
	0.10	0	0.19	0.04	0.19	0.06
	0.08	0.06	0.40	0	0.1	0
	0	0.08	0.19	0.26	0	0.01
	0.10	0.15	0.21	0.08	0.10	0.04
	0.15	0.35	0	0.21	0.37	0.17
	0.01	0.06			0.17	0.10
	0.17	0.01			0.24	0.19
	0.06	0.10				
Mean	0.084	0.10	0.20	0.12	0.17	0.08
StDev	0.06	0.10	0.13	0.10	0.11	0.07

Table 10.17: Serum TNFα concentration measured using cytometric bead array (CBA). Data is given for each treatment group at each timepoint and paired per subject. Shaded cells indicate values below theoretical level of significance.

	Morphine		Oxycodone		Bupivacaine	
	0 hr	**6 hr**	**0 hr**	**6 hr**	**0 hr**	**6 hr**
	0.13	0.44	0.65	7.39	0.13	0.27
	0.33	0.20	0.81	0	0.13	0.13
	0.20	0.38	0.76	0.55	0.13	0
	0.27	0.06	0.33	0.20	0.13	0.27
	0.33	0.60	1.89	0.60	0.33	0.20
	0.06	0.44			0.33	0.65
	0.60	0.20			0.27	0.33
	0.27	0.38				
Mean	0.27	0.34	0.89	1.75	0.21	0.26
StDev	0.15	0.16	0.53	2.83	0.09	0.19

Table 10.18: P-values for dependent-samples t-tests performed across timepoints for each cytokine per treatment group. Shaded numbers are statistically insignificant.

Treatment	N	IL-2	IL-4	IL-6	1L-10	IL-17a	IFNγ	TNFα
Morphine	8	0.70	0.81	0.01	0.001	0.41	0.67	0.54
Oxycodone	5	0.60	0.53	0.03	0.11	0.36	0.49	0.59
Bupivacaine	7	0.67	0.27	0.01	0.07	0.20	0.01	0.39

Table 10.19: Results for ANOVA performed across treatment groups at each timepoint for all 7 cytokines. Shaded numbers are statistically insignificant.

Treatment	IL-2	IL-4	IL-6	1L-10	IL-17a	IFNγ	TNFα
0 hr	0.15	0.35	0.31	1	0.25	0.15	0.003
6 hr	0.50	0.71	0.09	0.63	0.20	0.82	0.22

Table 10.20: Statistical data from ROC curve analysis, for all genes analysed

Probeset ID	Gene	Time-point	Group comparison	AUC	Std. Error	95% CI	P value	Controls	Patients
1554503_a_at	OSCAR	0 hr	O v M+B	0.5026	0.09554	0.3153 to 0.6899	0.978	24	16
1554503_a_at	OSCAR	2 hr	O v M+B	0.5703	0.09087	0.3922 to 0.7485	0.4561	24	16
1554503_a_at	OSCAR	6 hr	O v M+B	0.5547	0.09221	0.3739 to 0.7355	0.5621	24	16
1554503_a_at	OSCAR	24 hr	O v M+B	0.5281	0.1036	0.3250 to 0.7313	0.7745	20	16
201887	il13ra1	0 hr	O v M+B	0.5443	0.09697	0.3542 to 0.7344	0.6389	24	16
201887	il13ra2	2 hr	O v M+B	0.5938	0.0968	0.4040 to 0.7835	0.3203	24	16
201887	il13ra3	6 hr	O v M+B	0.6563	0.08877	0.4822 to 0.8303	0.09769	24	16
201887	il13ra4	24 hr	O v M+B	0.5375	0.1046	0.3325 to 0.7425	0.7025	20	16
201888	il13ra1	0 hr	O v M+B	0.5521	0.0994	0.3572 to 0.7470	0.5809	24	16
201888	il13ra2	2 hr	O v M+B	0.6146	0.09283	0.4326 to 0.7966	0.2245	24	16
201888	il13ra3	6 hr	O v M+B	0.6615	0.09071	0.4836 to 0.8393	0.08702	24	16
201888	il13ra4	24 hr	O v M+B	0.5063	0.1028	0.3048 to 0.7077	0.9492	20	16
211612	il13ra1	0 hr	O v M+B	0.5443	0.09781	0.3525 to 0.7360	0.6389	24	16
211612	il13ra2	2 hr	O v M+B	0.6276	0.09451	0.4423 to 0.8129	0.1762	24	16
211612	il13ra3	6 hr	O v M+B	0.6484	0.09076	0.4705 to 0.8264	0.1156	24	16
211612	il13ra4	24 hr	O v M+B	0.5	0.1031	0.2980 to 0.7020	1	20	16
231990	USP15	0 hr	O v M+B	0.625	0.09775	0.4334 to 0.8166	0.1852	24	16
231990	USP16	2 hr	O v M+B	0.5391	0.09537	0.3521 to 0.7260	0.6788	24	16
231990	USP17	6 hr	O v M+B	0.6302	0.09529	0.4434 to 0.8170	0.1675	24	16
231990	USP18	24 hr	O v M+B	0.6313	0.09741	0.4403 to 0.8222	0.1813	20	16
219471	C13orf18	0 hr	O v M+B	0.6068	0.0925	0.4254 to 0.7881	0.2577	24	16
219471	C13orf18	2 hr	O v M+B	0.5859	0.09014	0.4092 to 0.7627	0.3623	24	16
219471	C13orf18	6 hr	O v M+B	0.763	0.07591	0.6142 to 0.9118	0.005317	24	16
219471	C13orf18	24 hr	O v M+B	0.55	0.09767	0.3585 to 0.7415	0.6105	20	16
44790	C13orf18	0 hr	O v M+B	0.5729	0.09327	0.3901 to 0.7558	0.4395	24	16
44790	C13orf18	2 hr	O v M+B	0.5313	0.09256	0.3498 to 0.7127	0.7404	24	16
44790	C13orf18	6 hr	O v M+B	0.7188	0.08246	0.5571 to 0.8804	0.02043	24	16
44790	C13orf18	24 hr	O v M+B	0.5563	0.09926	0.3616 to 0.7509	0.5666	20	16
1559573_at	C13orf18	0 hr	O v M+B	0.5573	0.09589	0.3693 to 0.7453	0.5436	24	16
1559573_at	C13orf18	2 hr	O v M+B	0.5964	0.09259	0.4148 to 0.7779	0.3071	24	16

1559573_at	C13orf18	6 hr	O v M+B	0.7109	0.08965	0.5352 to 0.8867	0.02538	24	16
1559573_at	C13orf18	24 hr	O v M+B	0.5719	0.09684	0.3820 to 0.7617	0.4641	20	16
229879_at	C13orf18	0 hr	O v M+B	0.5078	0.09925	0.3132 to 0.7024	0.934	24	16
229879_at	C13orf18	2 hr	O v M+B	0.7083	0.08697	0.5378 to 0.8788	0.02725	24	16
229879_at	C13orf18	6 hr	O v M+B	0.6797	0.08854	0.5061 to 0.8533	0.05684	24	16
229879_at	C13orf18	24 hr	O v M+B	0.5031	0.1002	0.3067 to 0.6995	0.9746	20	16
232958_at	C13orf18	0 hr	O v M+B	0.6224	0.08862	0.4487 to 0.7961	0.1945	24	16
232958_at	C13orf18	2 hr	O v M+B	0.5339	0.09442	0.3488 to 0.7190	0.7197	24	16
232958_at	C13orf18	6 hr	O v M+B	0.5651	0.1077	0.3539 to 0.7763	0.4901	24	16
232958_at	C13orf18	24 hr	O v M+B	0.5594	0.09921	0.3649 to 0.7539	0.5453	20	16
234196_at	C13orf18	0 hr	O v M+B	0.6875	0.08461	0.5216 to 0.8534	0.04689	24	16
234196_at	C13orf18	2 hr	O v M+B	0.5677	0.09526	0.3809 to 0.7545	0.4729	24	16
234196_at	C13orf18	6 hr	O v M+B	0.7995	0.07559	0.6513 to 0.9477	0.001508	24	16
234196_at	C13orf18	24 hr	O v M+B	0.575	0.09879	0.3813 to 0.7687	0.4449	20	16
226364	HIP1	0 hr	O v M+B	0.526	0.09483	0.3401 to 0.7120	0.7825	24	16
226364	HIP1	2 hr	O v M+B	0.5078	0.09714	0.3174 to 0.6983	0.934	24	16
226364	HIP1	6 hr	O v M+B	0.5365	0.09962	0.3412 to 0.7318	0.6991	24	16
226364	HIP1	24 hr	O v M+B	0.5594	0.1004	0.3625 to 0.7562	0.5453	20	16
222630	RFX7	0 hr	M v O+B	0.5026	0.09505	0.3163 to 0.6890	0.978	24	16
222630	RFX7	2 hr	M v O+B	0.6354	0.09378	0.4516 to 0.8193	0.1512	24	16
222630	RFX7	6 hr	M v O+B	0.5313	0.09262	0.3497 to 0.7128	0.7404	24	16
222630	RFX7	24 hr	M v O+B	0.5587	0.09764	0.3673 to 0.7501	0.5528	21	15
226679	SLC26A11	0 hr	M v O+B	0.5182	0.09503	0.3319 to 0.7045	0.8468	24	16
226679	SLC26A11	2 hr	M v O+B	0.6042	0.09291	0.4220 to 0.7863	0.2695	24	16
226679	SLC26A11	6 hr	M v O+B	0.6536	0.09101	0.4752 to 0.8321	0.1034	24	16
226679	SLC26A11	24 hr	M v O+B	0.6063	0.0946	0.4209 to 0.7918	0.2825	21	15
226272	RCAN3	0 hr	M v O+B	0.6107	0.09023	0.4338 to 0.7876	0.2407	24	16
226272	RCAN3	2 hr	M v O+B	0.5729	0.09329	0.3900 to 0.7558	0.4395	24	16
226272	RCAN3	6 hr	M v O+B	0.6615	0.09247	0.4802 to 0.8427	0.08702	24	16
226272	RCAN3	24 hr	M v O+B	0.527	0.09731	0.3362 to 0.7178	0.7851	21	15
39248	AQP3	0 hr	M v O+B	0.5521	0.09514	0.3656 to 0.7386	0.5809	24	16
39248	AQP3	2 hr	M v O+B	0.6536	0.08683	0.4834 to 0.8239	0.1034	24	16
39248	AQP3	6 hr	M v O+B	0.6302	0.09655	0.4409 to 0.8195	0.1675	24	16
39248	AQP3	24 hr	M v O+B	0.5111	0.09868	0.3176 to 0.7046	0.9106	21	15

205898	CX3CR1	0 hr	M v O+B	0.5234	0.09412	0.3389 to 0.7080	0.8038	24	16
205898	CX3CR1	2 hr	M v O+B	0.6927	0.08551	0.5251 to 0.8604	0.04111	24	16
205898	CX3CR1	6 hr	M v O+B	0.612	0.09062	0.4343 to 0.7896	0.2352	24	16
205898	CX3CR1	24 hr	M v O+B	0.5524	0.0965	0.3632 to 0.7416	0.5965	21	15
201990	CREBL2	0 hr	M v O+B	0.526	0.09272	0.3443 to 0.7078	0.7825	24	16
201990	CREBL2	2 hr	M v O+B	0.638	0.08885	0.4638 to 0.8122	0.1435	24	16
201990	CREBL2	6 hr	M v O+B	0.5885	0.09392	0.4044 to 0.7727	0.3479	24	16
201990	CREBL2	24 hr	M v O+B	0.546	0.09714	0.3556 to 0.7365	0.6418	21	15
209670	TRAC	0 hr	M v O+B	0.5417	0.09419	0.3570 to 0.7263	0.6587	24	16
209670	TRAC	2 hr	M v O+B	0.6354	0.08847	0.4620 to 0.8089	0.1512	24	16
209670	TRAC	6 hr	M v O+B	0.6094	0.09207	0.4289 to 0.7899	0.2463	24	16
209670	TRAC	24 hr	M v O+B	0.5524	0.09731	0.3616 to 0.7432	0.5965	21	15
202393	KLF10	0 hr	M v O+B	0.6068	0.09071	0.4289 to 0.7846	0.2577	24	16
202393	KLF10	2 hr	M v O+B	0.5521	0.09521	0.3654 to 0.7387	0.5809	24	16
202393	KLF10	6 hr	M v O+B	0.6276	0.0919	0.4474 to 0.8078	0.1762	24	16
202393	KLF10	24 hr	M v O+B	0.5841	0.09794	0.3921 to 0.7761	0.3952	21	15
219528	BCL11B	0 hr	M v O+B	0.5182	0.09414	0.3337 to 0.7028	0.8468	24	16
219528	BCL11B	2 hr	M v O+B	0.6042	0.08996	0.4278 to 0.7805	0.2695	24	16
219528	BCL11B	6 hr	M v O+B	0.625	0.09522	0.4383 to 0.8117	0.1852	24	16
219528	BCL11B	24 hr	M v O+B	0.5492	0.09799	0.3571 to 0.7413	0.619	21	15
206545	CD28	0 hr	M v O+B	0.5521	0.09738	0.3612 to 0.7430	0.5809	24	16
206545	CD28	2 hr	M v O+B	0.5599	0.09332	0.3770 to 0.7428	0.5255	24	16
206545	CD28	6 hr	M v O+B	0.6328	0.09346	0.4496 to 0.8160	0.1592	24	16
206545	CD28	24 hr	M v O+B	0.5238	0.09841	0.3309 to 0.7167	0.8098	21	15
223244	NDUFA12	0 hr	M v O+B	0.5885	0.09182	0.4085 to 0.7685	0.3479	24	16
223244	NDUFA12	2 hr	M v O+B	0.5599	0.09345	0.3767 to 0.7431	0.5255	24	16
223244	NDUFA12	6 hr	M v O+B	0.6432	0.0917	0.4635 to 0.8230	0.129	24	16
223244	NDUFA12	24 hr	M v O+B	0.5619	0.09688	0.3720 to 0.7518	0.5315	21	15
229629	229629	0 hr	M v O+B	0.5208	0.09262	0.3393 to 0.7024	0.8252	24	16
229629	229629	2 hr	M v O+B	0.638	0.09205	0.4576 to 0.8185	0.1435	24	16
229629	229629	6 hr	M v O+B	0.5286	0.09391	0.3445 to 0.7127	0.7614	24	16
229629	229629	24 hr	M v O+B	0.5841	0.09603	0.3959 to 0.7724	0.3952	21	15
1562255_at	SYTL3	0 hr	M v O+B	0.5703	0.09746	0.3793 to 0.7614	0.4561	24	16
1562255_at	SYTL3	2 hr	M v O+B	0.5313	0.09815	0.3388 to 0.7237	0.7404	24	16

1562255_at	SYTL3	6 hr	M v O+B	0.5365	0.09334	0.3535 to 0.7195	0.6991	24	16
1562255_at	SYTL3	24 hr	M v O+B	0.5524	0.09738	0.3615 to 0.7433	0.5965	21	15
204266	CHKA	0 hr	M v O+B	0.5938	0.09301	0.4114 to 0.7761	0.3203	24	16
204266	CHKA	2 hr	M v O+B	0.6406	0.08942	0.4653 to 0.8159	0.1361	24	16
204266	CHKA	6 hr	M v O+B	0.5677	0.09153	0.3883 to 0.7471	0.4729	24	16
204266	CHKA	24 hr	M v O+B	0.6794	0.09068	0.5016 to 0.8571	0.0699	21	15
210244	CAMP	0 hr	M v O+B	0.5208	0.09546	0.3337 to 0.7080	0.8252	24	16
210244	CAMP	2 hr	M v O+B	0.513	0.1002	0.3166 to 0.7095	0.8902	24	16
210244	CAMP	6 hr	M v O+B	0.5833	0.093	0.4010 to 0.7657	0.377	24	16
210244	CAMP	24 hr	M v O+B	0.5556	0.09899	0.3615 to 0.7496	0.5745	21	15
1556202_at	SRGAP2	0 hr	M v O+B	0.5286	0.09541	0.3416 to 0.7157	0.7614	24	16
1556202_at	SRGAP2	2 hr	M v O+B	0.5547	0.09157	0.3752 to 0.7342	0.5621	24	16
1556202_at	SRGAP2	6 hr	M v O+B	0.5234	0.09339	0.3403 to 0.7065	0.8038	24	16
1556202_at	SRGAP2	24 hr	M v O+B	0.5429	0.09835	0.3500 to 0.7357	0.6649	21	15
240038_at	240038_at	0 hr	M v O+B	0.5521	0.09631	0.3633 to 0.7409	0.5809	24	16
240038_at	240038_at	2 hr	M v O+B	0.5911	0.09051	0.4137 to 0.7686	0.334	24	16
240038_at	240038_at	6 hr	M v O+B	0.5078	0.0925	0.3265 to 0.6892	0.934	24	16
240038_at	240038_at	24 hr	M v O+B	0.5143	0.09783	0.3225 to 0.7061	0.8852	21	15
235592_at	235592_at	0 hr	M v O+B	0.5547	0.09651	0.3655 to 0.7439	0.5621	24	16
235592_at	235592_at	2 hr	M v O+B	0.6302	0.09044	0.4529 to 0.8075	0.1675	24	16
235592_at	235592_at	6 hr	M v O+B	0.5833	0.0936	0.3998 to 0.7668	0.377	24	16
235592_at	235592_at	24 hr	M v O+B	0.6222	0.09422	0.4375 to 0.8069	0.2168	21	15
207384	PGLYRP1	0 hr	M v O+B	0.5964	0.0919	0.4162 to 0.7765	0.3071	24	16
207384	PGLYRP2	2 hr	M v O+B	0.5651	0.09737	0.3742 to 0.7560	0.4901	24	16
207384	PGLYRP3	6 hr	M v O+B	0.5885	0.09294	0.4063 to 0.7707	0.3479	24	16
207384	PGLYRP4	24 hr	M v O+B	0.5651	0.1001	0.3689 to 0.7613	0.5107	21	15
205239	AREG	0 hr	M v O+B	0.5729	0.09364	0.3893 to 0.7565	0.4395	24	16
205239	AREG	2 hr	M v O+B	0.5573	0.09499	0.3711 to 0.7435	0.5436	24	16
205239	AREG	6 hr	M v O+B	0.5703	0.09478	0.3845 to 0.7561	0.4561	24	16
205239	AREG	24 hr	M v O+B	0.5683	0.09974	0.3727 to 0.7638	0.4903	21	15
237618_at	237618_at	0 hr	O v M+B	0.5313	0.1003	0.3347 to 0.7278	0.7404	24	16
237618_at	237618_at	2 hr	O v M+B	0.5677	0.09159	0.3882 to 0.7472	0.4729	24	16
237618_at	237618_at	6 hr	O v M+B	0.8464	0.06512	0.7187 to 0.974	0.0002	24	16
237618_at	237618_at	24 hr	O v M+B	0.5719	0.09848	0.3789 to 0.7649	0.464	20	16

200796	MCL1	0 hr	O v M+B	0.6094	0.0945	0.4242 to 0.7946	0.2462	24	16
200796	MCL1	2 hr	O v M+B	0.6875	0.0867	0.5176 to 0.8574	0.0468	24	16
200796	MCL1	6 hr	O v M+B	0.7656	0.07772	0.6133 to 0.918	0.0049	24	16
200796	MCL1	24 hr	O v M+B	0.6938	0.09072	0.5159 to 0.8716	0.0484	20	16
214465	ORM1/ORM2	0 hr	O v M+B	0.5339	0.1	0.3378 to 0.7299	0.7197	24	16
214465	ORM1/ORM2	2 hr	O v M+B	0.5313	0.09331	0.3484 to 0.7141	0.7404	24	16
214465	ORM1/ORM2	6 hr	O v M+B	0.7031	0.086	0.5346 to 0.8717	0.0313	24	16
214465	ORM1/ORM2	24 hr	O v M+B	0.7375	0.0821	0.5766 to 0.8984	0.0155	20	16
229817	ZNF608	0 hr	O v M+B	0.5521	0.09219	0.3714 to 0.7328	0.5808	24	16
229817	ZNF608	2 hr	O v M+B	0.5443	0.09513	0.3578 to 0.7307	0.6388	24	16
229817	ZNF608	6 hr	O v M+B	0.6979	0.08842	0.5246 to 0.8712	0.0359	24	16
229817	ZNF608	24 hr	O v M+B	0.5625	0.09994	0.3666 to 0.7584	0.5243	20	16
209840	LRRN3	0 hr	O v M+B	0.6406	0.09408	0.4562 to 0.825	0.136	24	16
209840	LRRN3	2 hr	O v M+B	0.5703	0.09209	0.3898 to 0.7508	0.456	24	16
209840	LRRN3	6 hr	O v M+B	0.599	0.09194	0.4188 to 0.7792	0.2941	24	16
209840	LRRN3	24 hr	O v M+B	0.5875	0.1011	0.3893 to 0.7857	0.3727	20	16
212414	GLYR1 /// SEPT6	0 hr	O v M+B	0.5807	0.09706	0.3904 to 0.7710	0.3921	24	16
212414	GLYR1 /// SEPT6	2 hr	O v M+B	0.5677	0.09534	0.3808 to 0.7546	0.4729	24	16
212414	GLYR1 /// SEPT6	6 hr	O v M+B	0.6276	0.09114	0.4489 to 0.8063	0.1762	24	16
212414	GLYR1 /// SEPT6	24 hr	O v M+B	0.6406	0.0995	0.4456 to 0.8357	0.152	20	16
205006	NMT2	0 hr	O v M+B	0.5651	0.09241	0.3839 to 0.7463	0.4901	24	16
205006	NMT2	2 hr	O v M+B	0.5885	0.09187	0.4084 to 0.7687	0.3479	24	16
205006	NMT2	6 hr	O v M+B	0.5781	0.09307	0.3957 to 0.7606	0.4076	24	16
205006	NMT2	24 hr	O v M+B	0.6313	0.09639	0.4423 to 0.8202	0.1813	20	16
209604	GATA3	0 hr	O v M+B	0.5104	0.09658	0.3211 to 0.6998	0.9121	24	16
209604	GATA3	2 hr	O v M+B	0.6146	0.09504	0.4283 to 0.8009	0.2245	24	16
209604	GATA3	6 hr	O v M+B	0.5807	0.09272	0.3989 to 0.7625	0.3921	24	16
209604	GATA3	24 hr	O v M+B	0.7063	0.08869	0.5324 to 0.8801	0.03568	20	16
236796	BACH2	0 hr	O v M+B	0.5234	0.09383	0.3395 to 0.7074	0.8038	24	16
236796	BACH2	2 hr	O v M+B	0.5	0.09407	0.3156 to 0.6844	1	24	16

236796	BACH2	6 hr	O v M+B	0.5599	0.09553	0.3726 to 0.7472	0.5255	24	16
236796	BACH2	24 hr	O v M+B	0.7563	0.08039	0.5986 to 0.9139	0.009067	20	16
231124_x_at	LY9	0 hr	O v M+B	0.6458	0.08896	0.4714 to 0.8202	0.1222	24	16
231124_x_at	LY9	2 hr	O v M+B	0.5807	0.09534	0.3938 to 0.7676	0.3921	24	16
231124_x_at	LY9	6 hr	O v M+B	0.612	0.09507	0.4256 to 0.7984	0.2352	24	16
231124_x_at	LY9	24 hr	O v M+B	0.6594	0.09659	0.4700 to 0.8487	0.1045	20	16
235122_at	HIVEP3	0 hr	O v M+B	0.5521	0.1045	0.3473 to 0.7569	0.5809	24	16
235122_at	HIVEP3	2 hr	O v M+B	0.638	0.09164	0.4584 to 0.8177	0.1435	24	16
235122_at	HIVEP3	6 hr	O v M+B	0.6068	0.09666	0.4173 to 0.7963	0.2577	24	16
235122_at	HIVEP3	24 hr	O v M+B	0.5438	0.1013	0.3452 to 0.7423	0.6558	20	16
242761_s_at	ZNF420	0 hr	O v M+B	0.5755	0.09267	0.3938 to 0.7572	0.4234	24	16
242761_s_at	ZNF420	2 hr	O v M+B	0.6224	0.09391	0.4383 to 0.8065	0.1945	24	16
242761_s_at	ZNF420	6 hr	O v M+B	0.6198	0.09561	0.4324 to 0.8072	0.2042	24	16
242761_s_at	ZNF420	24 hr	O v M+B	0.6031	0.1033	0.4006 to 0.8057	0.2935	20	16
213164_at	SLC5A3	0 hr	O v M+B	0.526	0.1044	0.3213 to 0.7308	0.7825	24	16
213164_at	SLC5A3	2 hr	O v M+B	0.5755	0.09444	0.3904 to 0.7607	0.4234	24	16
213164_at	SLC5A3	6 hr	O v M+B	0.6146	0.09528	0.4278 to 0.8014	0.2245	24	16
213164_at	SLC5A3	24 hr	O v M+B	0.6875	0.09453	0.5022 to 0.8728	0.05617	20	16
228320_x_at	CCDC64	0 hr	O v M+B	0.6458	0.09287	0.4638 to 0.8279	0.1222	24	16
228320_x_at	CCDC64	2 hr	O v M+B	0.5208	0.09955	0.3257 to 0.7160	0.8252	24	16
228320_x_at	CCDC64	6 hr	O v M+B	0.5208	0.6563	0.08856	0.4826 to 0.8299		24
228320_x_at	CCDC64	24 hr	O v M+B	0.6156	0.1018	0.4160 to 0.8152	0.2389	20	16
225612_s_at	B3GNT5	0 hr	O v M+B	0.5182	0.09694	0.3282 to 0.7083	0.8468	24	16
225612_s_at	B3GNT5	2 hr	O v M+B	0.5729	0.0983	0.3802 to 0.7656	0.4395	24	16
225612_s_at	B3GNT5	6 hr	O v M+B	0.6641	0.08987	0.4879 to 0.8403	0.08204	24	16
225612_s_at	B3GNT5	24 hr	O v M+B	0.5156	0.09786	0.3238 to 0.7075	0.8735	20	16
222528	SLC25A37	0 hr	O v M+B	0.5547	0.097	0.3645 to 0.7449	0.5621	24	16
222528	SLC25A37	2 hr	O v M+B	0.6042	0.09389	0.4201 to 0.7882	0.2695	24	16
222528	SLC25A37	6 hr	O v M+B	0.7292	0.0844	0.5637 to 0.8946	0.01515	24	16
222528	SLC25A37	24 hr	O v M+B	0.5188	0.1005	0.3216 to 0.7159	0.8485	20	16
219669_at	CD177	0 hr	O v M+B	0.5182	0.09468	0.3326 to 0.7038	0.8468	24	16
219669_at	CD177	2 hr	O v M+B	0.5	0.09342	0.3169 to 0.6831	1	24	16
219669_at	CD177	6 hr	O v M+B	0.638	0.09466	0.4524 to 0.8236	0.1435	24	16

219669_at	CD177	24 hr	O v M+B	0.5875	0.09803	0.3953 to 0.7797	0.3728	20	16
203765_at	GCA	0 hr	O v M+B	0.5365	0.09493	0.3503 to 0.7226	0.6991	24	16
203765_at	GCA	2 hr	O v M+B	0.5599	0.09649	0.3707 to 0.7491	0.5255	24	16
203765_at	GCA	6 hr	O v M+B	0.6029	0.09359	0.4194 to 0.7863	0.2755	24	16
203765_at	GCA	24 hr	O v M+B	0.5438	0.09988	0.3479 to 0.7396	0.6558	20	16
204351_at	S100P	0 hr	O v M+B	0.5182	0.09521	0.3316 to 0.7049	0.8468	24	16
204351_at	S100P	2 hr	O v M+B	0.5313	0.09384	0.3473 to 0.7152	0.7404	24	16
204351_at	S100P	6 hr	O v M+B	0.6224	0.09913	0.4281 to 0.8167	0.1945	24	16
204351_at	S100P	24 hr	O v M+B	0.5469	0.09934	0.3521 to 0.7416	0.633	20	16
205863_at	S100A12	0 hr	O v M+B	0.5547	0.09294	0.3725 to 0.7369	0.5621	24	16
205863_at	S100A12	2 hr	O v M+B	0.5339	0.09258	0.3524 to 0.7154	0.7197	24	16
205863_at	S100A12	6 hr	O v M+B	0.5729	0.09369	0.3893 to 0.7566	0.4395	24	16
205863_at	S100A12	24 hr	O v M+B	0.525	0.09961	0.3297 to 0.7203	0.799	20	16
205041_s_at	ORM1/ORM2	0 hr	O v M+B	0.5833	0.09109	0.4048 to 0.7619	0.377	24	16
205041_s_at	ORM1/ORM2	2 hr	O v M+B	0.5521	0.09448	0.3669 to 0.7373	0.5809	24	16
205041_s_at	ORM1/ORM2	6 hr	O v M+B	0.6667	0.0936	0.4832 to 0.8502	0.07731	24	16
205041_s_at	ORM1/ORM2	24 hr	O v M+B	0.6719	0.09185	0.4918 to 0.8519	0.08001	20	16
206522_at	MGAM	0 hr	O v M+B	0.526	0.09377	0.3422 to 0.7099	0.7825	24	16
206522_at	MGAM	2 hr	O v M+B	0.5026	0.09421	0.3179 to 0.6873	0.978	24	16
206522_at	MGAM	6 hr	O v M+B	0.6536	0.09347	0.4704 to 0.8369	0.1034	24	16
206522_at	MGAM	24 hr	O v M+B	0.5188	0.1022	0.3184 to 0.7191	0.8485	20	16
201963	ACSL1	0 hr	O v M+B	0.5495	0.09614	0.3610 to 0.7380	0.5999	24	16
201963	ACSL1	2 hr	O v M+B	0.5391	0.09351	0.3557 to 0.7224	0.6788	24	16
201963	ACSL1	6 hr	O v M+B	0.6146	0.09533	0.4277 to 0.8015	0.2245	24	16
201963	ACSL1	24 hr	O v M+B	0.5125	0.1005	0.3154 to 0.7096	0.8987	20	16
209369_at	ANXA3	0 hr	O v M+B	0.5339	0.09298	0.3516 to 0.7161	0.7197	24	16
209369_at	ANXA3	2 hr	O v M+B	0.5469	0.0937	0.3632 to 0.7306	0.6193	24	16
209369_at	ANXA3	6 hr	O v M+B	0.6302	0.09205	0.4497 to 0.8107	0.1675	24	16
209369_at	ANXA3	24 hr	O v M+B	0.5344	0.09802	0.3422 to 0.7265	0.7262	20	16
210640_s_at	GPER	0 hr	B v O+B	0.6992	0.08652	0.5296 to 0.8688	0.08469	32	8
210640_s_at	GPER	2 hr	B v O+B	0.5156	0.123	0.2745 to 0.7568	0.8924	32	8
210640_s_at	GPER	6 hr	B v O+B	0.5391	0.1364	0.2717 to 0.8064	0.7353	32	8
210640_s_at	GPER	24 hr	B v O+B	0.7935	0.08286	0.6311 to 0.9560	0.03746	31	5
227984_at	LMF1	0 hr	B v O+B	0.7188	0.1244	0.4748 to 0.9627	0.05835	32	8

227984_at	LMF1	2 hr	B v O+B	0.5039	0.1198	0.2691 to 0.7387	0.973	32	8
227984_at	LMF1	6 hr	B v O+B	0.625	0.118	0.3938 to 0.8562	0.2793	32	8
227984_at	LMF1	24 hr	B v O+B	0.7226	0.1608	0.4074 to 1.038	0.1146	31	5
1562731_s_at	MDS2	0 hr	B v O+B	0.7969	0.1026	0.5958 to 0.9980	0.01021	32	8
1562731_s_at	MDS2	2 hr	B v O+B	0.5938	0.1248	0.3490 to 0.8385	0.4171	32	8
1562731_s_at	MDS2	6 hr	B v O+B	0.5547	0.1187	0.3221 to 0.7873	0.636	32	8
1562731_s_at	MDS2	24 hr	B v O+B	0.729	0.1189	0.4959 to 0.9622	0.1045	31	5
244798	LOC100507492	0 hr	B v O+B	0.5391	0.14	0.2646 to 0.8135	0.7353	32	8
244798	LOC100507492	2 hr	B v O+B	0.5508	0.1205	0.3145 to 0.7870	0.6603	32	8
244798	LOC100507492	6 hr	B v O+B	0.6602	0.1253	0.4145 to 0.9058	0.1657	32	8
244798	LOC100507492	24 hr	B v O+B	0.5032	0.09299	0.3209 to 0.6855	0.9818	31	5
221221	KLHL3	0 hr	B v O+B	0.7148	0.1087	0.5017 to 0.9280	0.06299	32	8
221221	KLHL3	2 hr	B v O+B	0.5195	0.1245	0.2754 to 0.7637	0.8658	32	8
221221	KLHL3	6 hr	B v O+B	0.5508	0.1193	0.3168 to 0.7847	0.6603	32	8
221221	KLHL3	24 hr	B v O+B	0.7742	0.1301	0.5191 to 1.029	0.05194	31	5
219671	HPCAL4	0 hr	B v O+B	0.6445	0.1146	0.4199 to 0.8691	0.211	32	8
219671	HPCAL4	2 hr	B v O+B	0.5391	0.1209	0.3020 to 0.7762	0.7353	32	8
219671	HPCAL4	6 hr	B v O+B	0.6914	0.09265	0.5098 to 0.8730	0.09762	32	8
219671	HPCAL4	24 hr	B v O+B	0.6516	0.1114	0.4333 to 0.8699	0.2824	31	5
1555883_s_at	SPIN3	0 hr	B v O+B	0.6406	0.1393	0.3675 to 0.9137	0.2236	32	8
1555883_s_at	SPIN3	2 hr	B v O+B	0.625	0.1268	0.3764 to 0.8736	0.2793	32	8
1555883_s_at	SPIN3	6 hr	B v O+B	0.6367	0.1319	0.3782 to 0.8952	0.2367	32	8
1555883_s_at	SPIN3	24 hr	B v O+B	0.671	0.1332	0.4099 to 0.9321	0.2255	31	5
40837_at	TLE2	0 hr	B v O+B	0.6563	0.1197	0.4217 to 0.8908	0.1763	32	8
40837_at	TLE2	2 hr	B v O+B	0.5078	0.1285	0.2558 to 0.7598	0.9461	32	8
40837_at	TLE2	6 hr	B v O+B	0.5	0.1155	0.2735 to 0.7265	1	32	8
40837_at	TLE2	24 hr	B v O+B	0.729	0.1384	0.4577 to 1.000	0.1045	31	5
219308_s_at	AK5	0 hr	B v O+B	0.6758	0.1138	0.4526 to 0.8990	0.1282	32	8
219308_s_at	AK5	2 hr	B v O+B	0.5469	0.1223	0.3072 to 0.7866	0.6849	32	8
219308_s_at	AK5	6 hr	B v O+B	0.6523	0.09769	0.4608 to 0.8439	0.1873	32	8
219308_s_at	AK5	24 hr	B v O+B	0.6387	0.1402	0.3638 to 0.9136	0.3254	31	5
1564155_x_at	1564155_x_at	0 hr	B v O+B	0.6367	0.1083	0.4243 to 0.8491	0.2367	32	8
1564155_x_at	1564155_x_at	2 hr	B v O+B	0.5156	0.1083	0.3033 to 0.7280	0.8924	32	8
1564155_x_at	1564155_x_at	6 hr	B v O+B	0.6719	0.1068	0.4626 to 0.8812	0.1369	32	8

1564155_x_at	1564155_x_at	24 hr	B v O+B	0.6774	0.1122	0.4575 to 0.8974	0.2085	31	5
203184_at	FBN2	0 hr	M v O+B	0.5443	0.09349	0.3610 to 0.7276	0.6389	24	16
203184_at	FBN2	2 hr	M v O+B	0.6797	0.0891	0.5050 to 0.8544	0.05684	24	16
203184_at	FBN2	6 hr	M v O+B	0.6615	0.08937	0.4862 to 0.8367	0.08702	24	16
203184_at	FBN2	24 hr	M v O+B	0.6	0.1008	0.4024 to 0.7976	0.3122	21	15
227038_at	SGMS2	0 hr	M v O+B	0.5625	0.09169	0.3827 to 0.7423	0.5076	24	16
227038_at	SGMS2	2 hr	M v O+B	0.5052	0.09529	0.3184 to 0.6920	0.956	24	16
227038_at	SGMS2	6 hr	M v O+B	0.599	0.09201	0.4186 to 0.7793	0.2942	24	16
227038_at	SGMS2	24 hr	M v O+B	0.5937	0.1001	0.3974 to 0.7899	0.3439	21	15
228285_at	TDRD9	0 hr	M v O+B	0.5443	0.09711	0.3539 to 0.7346	0.6389	24	16
228285_at	TDRD9	2 hr	M v O+B	0.5234	0.09362	0.3399 to 0.7070	0.8038	24	16
228285_at	TDRD9	6 hr	M v O+B	0.6953	0.08537	0.5280 to 0.8627	0.03845	24	16
228285_at	TDRD9	24 hr	M v O+B	0.5905	0.1014	0.3916 to 0.7893	0.3605	21	15
1565162_s_at	MGST1	0 hr	M v O+B	0.6172	0.08872	0.4432 to 0.7911	0.2142	24	16
1565162_s_at	MGST1	2 hr	M v O+B	0.6146	0.0897	0.4387 to 0.7904	0.2245	24	16
1565162_s_at	MGST1	6 hr	M v O+B	0.724	0.08492	0.5575 to 0.8904	0.01762	24	16
1565162_s_at	MGST1	24 hr	M v O+B	0.6095	0.09634	0.4206 to 0.7984	0.2683	21	15
226517_at	BCAT1	0 hr	M v O+B	0.5599	0.09537	0.3729 to 0.7469	0.5255	24	16
226517_at	BCAT1	2 hr	M v O+B	0.5938	0.09374	0.4100 to 0.7775	0.3203	24	16
226517_at	BCAT1	6 hr	M v O+B	0.6432	0.08992	0.4669 to 0.8195	0.129	24	16
226517_at	BCAT1	24 hr	M v O+B	0.6571	0.09428	0.4723 to 0.8420	0.1123	21	15
235019_at	CPM	0 hr	M v O+B	0.599	0.09535	0.4120 to 0.7859	0.2942	24	16
235019_at	CPM	2 hr	M v O+B	0.6042	0.0893	0.4291 to 0.7792	0.2695	24	16
235019_at	CPM	6 hr	M v O+B	0.6745	0.08743	0.5031 to 0.8459	0.06441	24	16
235019_at	CPM	24 hr	M v O+B	0.6032	0.09597	0.4150 to 0.7913	0.2971	21	15
211734_s_at	FCER1A	0 hr	M v O+B	0.5781	0.09042	0.4009 to 0.7554	0.4076	24	16
211734_s_at	FCER1A	2 hr	M v O+B	0.5651	0.0949	0.3791 to 0.7511	0.4901	24	16
211734_s_at	FCER1A	6 hr	M v O+B	0.5078	0.09382	0.3239 to 0.6917	0.934	24	16
211734_s_at	FCER1A	24 hr	M v O+B	0.5714	0.09711	0.3810 to 0.7618	0.4703	21	15
234985_at	LDLRAD3	0 hr	M v O+B	0.5677	0.09028	0.3907 to 0.7447	0.4729	24	16
234985_at	LDLRAD3	2 hr	M v O+B	0.7552	0.07739	0.6035 to 0.9069	0.006842	24	16
234985_at	LDLRAD3	6 hr	M v O+B	0.6693	0.08559	0.5015 to 0.8371	0.07279	24	16
234985_at	LDLRAD3	24 hr	M v O+B	0.6063	0.1001	0.4101 to 0.8026	0.2825	21	15
234985_at	LDLRAD3	0 hr	M v O+B	0.5846	0.09086	0.4065 to 0.7628	0.3696	24	16

234985_at	LDLRAD3	2 hr	M v O+B	0.6615	0.08824	0.4885 to 0.8344	0.08702	24	16
205257	AMPH	6 hr	M v O+B	0.7266	0.0812	0.5674 to 0.8858	0.01635	24	16
205257	AMPH	24 hr	M v O+B	0.5079	0.101	0.3099 to 0.7060	0.9361	21	15
206932_at	CH25H	0 hr	M v O+B	0.5547	0.09436	0.3697 to 0.7397	0.5621	24	16
206932_at	CH25H	2 hr	M v O+B	0.5911	0.09397	0.4069 to 0.7754	0.334	24	16
206932_at	CH25H	6 hr	M v O+B	0.75	0.07869	0.5957 to 0.9043	0.008066	24	16
206932_at	CH25H	24 hr	M v O+B	0.5556	0.1004	0.3588 to 0.7523	0.5745	21	15
205977_s_at	EPHA1	0 hr	B v O+B	0.8281	0.09538	0.6412 to 1.015	0.0045	32	8
205977_s_at	EPHA1	2 hr	B v O+B	0.5781	0.1053	0.3717 to 0.7846	0.4989	32	8
205977_s_at	EPHA1	6 hr	B v O+B	0.5664	0.1286	0.3144 to 0.8184	0.5654	32	8
205977_s_at	EPHA1	24 hr	B v O+B	0.6323	0.1126	0.4115 to 0.853	0.3484	31	5
202953_at	C1QB	0 hr	B v O+B	0.5898	0.1203	0.3541 to 0.8256	0.4368	32	8
202953_at	C1QB	2 hr	B v O+B	0.7305	0.105	0.5246 to 0.9363	0.046	32	8
202953_at	C1QB	6 hr	B v O+B	0.668	0.121	0.4309 to 0.9051	0.146	32	8
202953_at	C1QB	24 hr	B v O+B	0.5742	0.1414	0.297 to 0.8514	0.5989	31	5
218424_s_at	STEAP3	0 hr	B v O+B	0.5742	0.104	0.3704 to 0.778	0.5206	32	8
218424_s_at	STEAP3	2 hr	B v O+B	0.6992	0.1004	0.5024 to 0.896	0.0846	32	8
218424_s_at	STEAP3	6 hr	B v O+B	0.6094	0.1114	0.3909 to 0.8278	0.3438	32	8
218424_s_at	STEAP3	24 hr	B v O+B	0.8129	0.09711	0.6226 to 1.003	0.0265	31	5
238515	NUDT16	0 hr	B v O+B	0.5156	0.1165	0.2873 to 0.744	0.8924	32	8
238515	NUDT16	2 hr	B v O+B	0.668	0.123	0.4269 to 0.909	0.146	32	8
238515	NUDT16	6 hr	B v O+B	0.6563	0.1195	0.4221 to 0.8904	0.1762	32	8
238515	NUDT16	24 hr	B v O+B	0.7355	0.09415	0.551 to 0.92	0.095	31	5
224357_s_at	MS4A4A	0 hr	B v O+B	0.5586	0.1186	0.3262 to 0.7909	0.612	32	8
224357_s_at	MS4A4A	2 hr	B v O+B	0.6172	0.1086	0.4044 to 0.83	0.3104	32	8
224357_s_at	MS4A4A	6 hr	B v O+B	0.7695	0.07918	0.6143 to 0.9247	0.0196	32	8
224357_s_at	MS4A4A	24 hr	B v O+B	0.6194	0.1238	0.3767 to 0.862	0.3974	31	5
203910_at	ARHGAP29	0 hr	B v O+B	0.6367	0.1109	0.4194 to 0.854	0.2366	32	8
203910_at	ARHGAP29	2 hr	B v O+B	0.5586	0.1264	0.311 to 0.8062	0.612	32	8
203910_at	ARHGAP29	6 hr	B v O+B	0.6719	0.1164	0.4438 to 0.9	0.1368	32	8
203910_at	ARHGAP29	24 hr	B v O+B	0.8194	0.08423	0.6543 to 0.9844	0.0236	31	5
206976	HSPH1	0 hr	M v O+B	0.5286	0.0936	0.3452 to 0.7121	0.7614	24	16
206976	HSPH1	2 hr	M v O+B	0.6016	0.09315	0.419 to 0.7841	0.2816	24	16
206976	HSPH1	6 hr	M v O+B	0.612	0.08964	0.4363 to 0.7877	0.2352	24	16

206976	HSPH1	24 hr	M v O+B	0.5079	0.09718	0.3175 to 0.6984	0.9361	21	15
213135	TIAM1	0 hr	M v O+B	0.5807	0.09136	0.4017 to 0.7598	0.3921	24	16
213135	TIAM1	2 hr	M v O+B	0.5677	0.09368	0.3841 to 0.7513	0.4729	24	16
213135	TIAM1	6 hr	M v O+B	0.6172	0.0949	0.4312 to 0.8032	0.2141	24	16
213135	TIAM1	24 hr	M v O+B	0.5032	0.0984	0.3103 to 0.696	0.9744	21	15
221218	TPK1	0 hr	M v O+B	0.5339	0.094	0.3496 to 0.7181	0.7197	24	16
221218	TPK1	2 hr	M v O+B	0.737	0.08104	0.5781 to 0.8958	0.012	24	16
221218	TPK1	6 hr	M v O+B	0.5026	0.09283	0.3207 to 0.6845	0.978	24	16
221218	TPK1	24 hr	M v O+B	0.5492	0.09883	0.3555 to 0.7429	0.6189	21	15
223182	AGPAT3	0 hr	M v O+B	0.5182	0.09626	0.3296 to 0.7069	0.8468	24	16
223182	AGPAT3	2 hr	M v O+B	0.7083	0.08405	0.5436 to 0.8731	0.0272	24	16
223182	AGPAT3	6 hr	M v O+B	0.5313	0.09311	0.3488 to 0.7137	0.7404	24	16
223182	AGPAT3	24 hr	M v O+B	0.5048	0.09765	0.3134 to 0.6962	0.9616	21	15

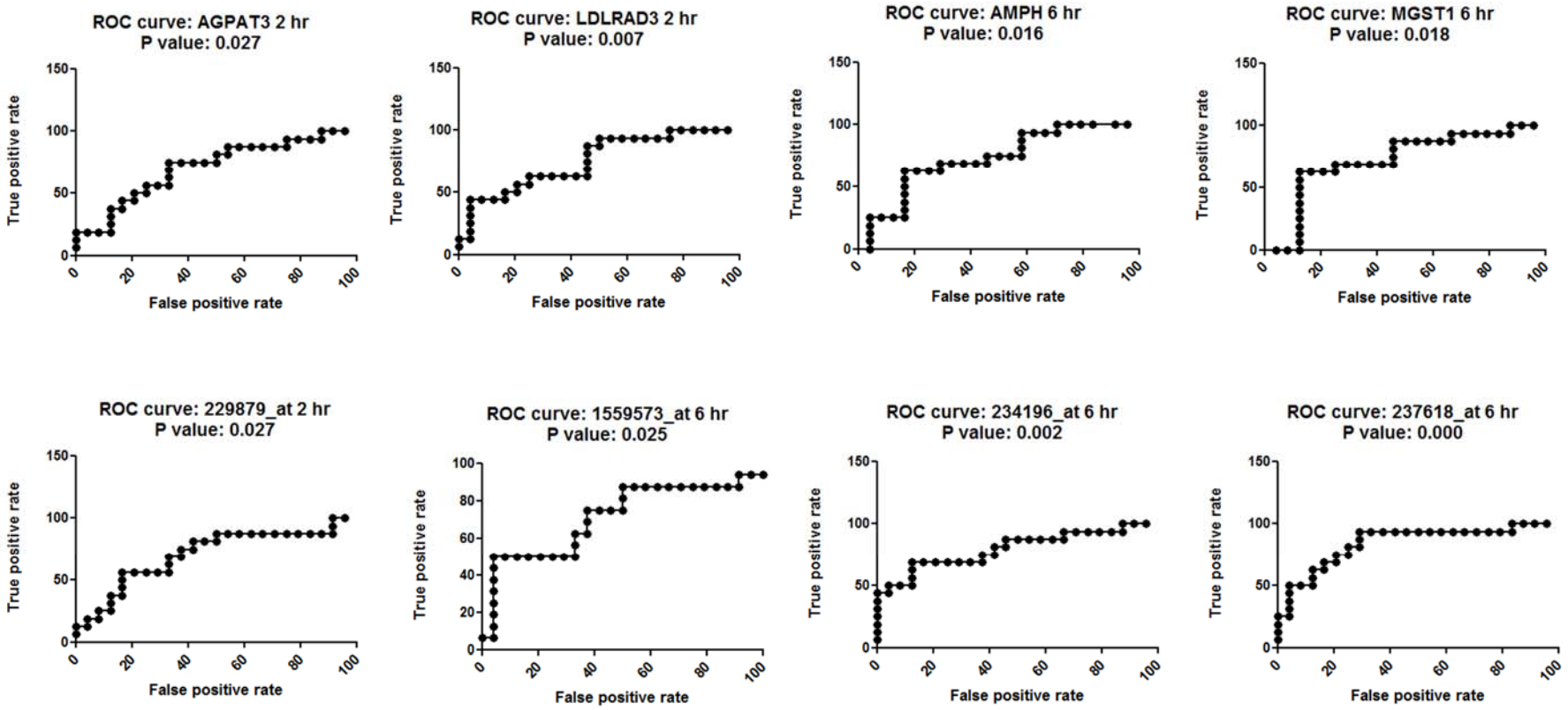

Figure 10.2: ROC curves for genes found to be significant through ROC analysis.

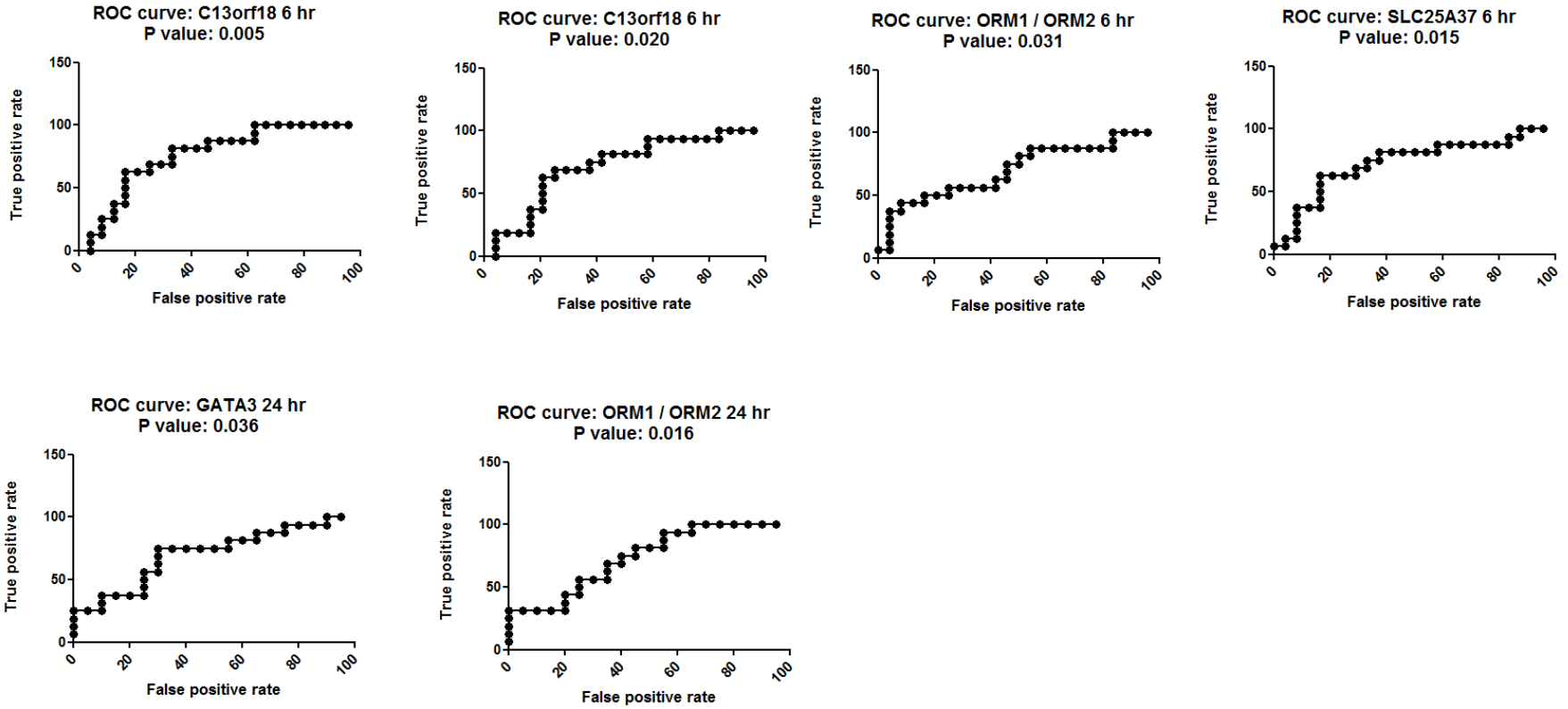

Figure 10.3: ROC curves for genes found to be significant through ROC analysis.

Table 10.21: Number of degranulation events for morphine group NK cell samples degranulated through CD107a assay.

Morphine group				
	0 hr		6 hr	
Subject No	**Unstimulated**	**Stimulated**	**Unstimulated**	**Stimulated**
48	2063	1513	1067	1087
50	959	974	1210	1313
52	1294	1260	1294	1563
53	1068	1174	1068	1071
45	3500	3366	3895	3162
Median	1294	1260	1210	1313
% change between timepoints	-0.03		0.09	

Table 10.22: Number of degranulation events for oxycodone group NK cell samples degranulated through CD107a assay

Oxycodone group				
	0 hr		6 hr	
Subject No	**Unstimulated**	**Stimulated**	**Unstimulated**	**Stimulated**
9	611	535	1.1	593
44	1591	2236	0	545
34	1110	0	0	8378
33	984	1056	2041	2988
49	899	599	783	1624
6	3789	3762	4681	4457
Median	1047	828	392	2306
% change between timepoints	-0.21		4.88	

Table 10.23: Number of degranulation events for bupivacaine group NK cell samples degranulated through CD107a assay

Bupivacaine group				
	0 hr		6 hr	
Subject No	**Unstimulated**	**Stimulated**	**Unstimulated**	**Stimulated**
32	517	518	1497	2932
41	1149	2315	2978	1115
46	2189	2648	2767	3087
36	2077	1641	7123	7392
Median	1613	1978	2873	3010
% change between timepoints	0.23		0.05	

Table 10.24: Results of Wilcoxon signed ranks test for NK cell degranulation data

	0 hr				6 hr			
Treat-ment	**N**	**Median Unstim**	**Median Stim**	**Asymp sig**	**N**	**Median Unstim**	**Median Stim**	**Asymp sig**
M	5	1294	1260	0.35	5	1210	1313	0.50
O	6	1047	828	0.46	6	392	2306	0.05
B	4	1613	1978	0.27	4	2872	3010	0.72

Table 10.25: Results of Kruskal Wallis test for NK cell degranulation data

	Statistics
Group	**Asymp sig**
0 hr unstim	0.78
0 hr stim	0.63
6 hr unstim	0.11
6 hr stim	0.53

